DISSERTATION

IMPLICATIONS OF DIET-INDUCED OBESITY ON METABOLIC AND IMMUNE HOMEOSTASIS: THE ROLE OF THE MESENTERIC LYMPH NODES

Submitted by

Jessica Lynn Hill

Department of Food Science and Human Nutrition

In partial fulfillment of the requirements

For the Degree of Doctor of Philosophy

Colorado State University

Fort Collins, Colorado

Summer 2020

Doctoral Committee:

Advisor: Michelle T Foster

Tiffany L Weir
Christopher L Gentile
Alan Schenkel

ABSTRACT

IMPLICATIONS OF DIET-INDUCED OBESITY ON METABOLIC AND IMMUNE HOMEOSTASIS: THE ROLE OF THE MESENTERIC LYMPH NODES

Obesity is a major public health crisis among adolescents and adults. The development of obesity is associated with several comorbidities as a result of underlying systemic chronic inflammation, the culmination of which increases one's risk for chronic and infectious disease. Excessive accumulation of visceral adipose tissue is shown to confer the greatest disease risk. This is primarily due to inherent depot differences, namely proximity to and a shared blood supply with the liver and gastrointestinal (GI) tract. Recent work demonstrates the considerable influence gut physiology has over both local and systemic homeostasis, as GI diseases such as inflammatory bowel disease are associated with metabolic derangements characteristic of obesity. While the mechanisms that mediate this inter-organ crosstalk continue to be elucidated, several studies suggest that inflammation originating from the gut triggers these broad metabolic and immunologic changes found in obesity. Previous work from our lab has demonstrated that high-fat diet (HFD) induced obesity results in mesenteric lymph node (MLN) fibrosis, which was associated with a localized impairment in immune function. MLNs, located within mesenteric adipose tissue (MAT) surrounding the GI tract, constitutively monitor the mesenteric adipose depot and draining sections of the small and large intestines, serving as critical inductive sites for adaptive immune responses. Subsequently, they are essential for overall tissue maintenance and protection. Hence, further study into the role of the MLNs in obesity-associated pathology is an important area of research.

The goals of this dissertation research were to 1) examine the relationship between MLNs and GI inflammation on metabolic outcomes, and 2) characterize immunologic changes associated with models of chronic inflammation. To investigate the above-mentioned, we conducted four separate preclinical studies utilizing mouse models of diet-induced obesity, MLN cauterization, and dextran sulfate sodium (DSS) induced GI inflammation.

In the first study (Chapter 2), we examined the contribution of the MLNs on disease pathology associated with HFD-induced obesity. We found that MLN dysfunction, either as a result of surgical manipulation or obesity-induced fibrosis, led to metabolic dysfunction. Furthermore, that functional MLNs are needed for the full restorative effects of Pirfenidone treatment. In the second study (Chapter 3), we examined the effect of chronic low-dose DSS-induced GI inflammation, independent of diet and obesity, on metabolic and immune function. We found that non-obese mice treated with DSS had a modest reduction in total body weight and MAT mass yet showed substantial alterations in tissue immune cell populations and frequencies. These adaptations occurred without a concurrent change in glucose homeostasis. Finally, in the third study (Chapter 4) we characterized immunologic parameters within a normal weight and obese human population, free of disease, through the *ex vivo* challenge of peripheral blood mononuclear cells (PBMCs) with the T lymphocyte mitogen Concanavalin A (ConA). We found that PBMCs isolated from obese adults had a modest increase in cell proliferation and IFNγ secretion upon stimulation within ConA relative to their normal weight controls. Additionally, we found a distinct expansion of $CD4^{+}CD8^{+}$ T cells, $CD16^{+}$ monocytes, and NK cells within ConA stimulated PBMCs from obese donors.

Collectively, these studies provide evidence that 1) the MLNs are critical for metabolic homeostasis as their dysfunction exacerbates features of HFD-induced obesity; 2) chronic GI

inflammation, independent of diet and obesity, can reshape the immune milieu without altering glucose homeostasis; and 3) obesity distinctly alters the PBMC response to acute *ex vivo* challenge as compared to that of normal weight individuals. Future studies should further elucidate mechanisms of crosstalk between the immune system, MLNs, and GI tract on metabolic homeostasis in models of obesity.

DEDICATION

To my husband, Rasean Sr., my kids, Rasean Jr. and Parker, my parents, Robin and Robert, my in-laws, Iristeine and Holly, for their unwavering support, encouragement, and love. Furthermore, to those that have played significant roles as mentors in my professional and academic career.

TABLE OF CONTENTS

CHAPTER 1: OBESITY ASSOCIATED DISEASE RISK: THE ROLE OF INHERENT DIFFERENCES AND LOCATION OF ADIPOSE DEPOTS[1]

Overview

Obesity and associated metabolic co-morbidities are a worldwide public health problem. Negative health outcomes associated with obesity, however, don't arise from excessive adiposity alone. Rather, deleterious outcomes of adipose tissue accumulation are a result of how adipocytes are distributed to individual regions in the body. Due to our increased understanding of the dynamic relationship that exists between specific adipose depots and disease risk, an accurate characterization of total body adiposity, as well as location, is required to properly evaluate a population's disease risk. Specifically, distinctive tissue depots within the body include the lower body, upper body, and abdominal (deep and superficial) subcutaneous regions, as well as visceral (mesenteric and omental) regions. Upper body and visceral adipose tissues are highly associated with metabolic dysfunction and chronic disease development, whereas lower body gluteofemoral subcutaneous adipose tissue imparts protection against diet-induced metabolic derangement. Each adipose depot functions distinctly as an endocrine organ hence has a different level of impact on health outcomes. Effluent from adipose tissue can modulate the functions of other tissues, whilst receiving differential communication from the rest of the body via central nervous system innervation, metabolites and other signaling molecules. More so, adipose depots contain a diverse reservoir of tissue-resident immune cells that play an integral

[1]This is the peer reviewed but unedited manuscript version of the following article: Hill JH, Solt C, Foster MT. Obesity associated disease risk: the role of inherent differences and location of adipose depots. Horm Mol Biol Clin Investig. 2018 Mar 16;33(2). doi: 10.1515/hmbci-2018-0012. Review. PubMed PMID: 29547393.

part in maintaining tissue homeostasis, as well as propagating metabolically induced inflammation. Overall, the conceptualization of obesity and associated risks needs updating to reflect the complexities of obesity. We review adipose tissue characteristics that are linked to deleterious or beneficial adipose tissue distributions.

Obesity Trends

Obesity and associated comorbidities continue to demand high resources and attention from health care. Deleterious outcomes of obesity, however, are preventable and reversible, hence public health efforts to decrease obesity is a major worldwide focus. Environmental and modifiable factors such as poor dietary habits, excessive energy intake, and a sedentary lifestyle contribute to weight gain and the development of obesity (1, 2). However, obesity is a multifactorial and complex disease state, driven by both genetic (3) and environmental factors (1), with much biologic variability (2). The prevalence of obesity among youth (16.9%) and adults (34.9%) in the U.S. has remained relatively stable over the past decade, according to current 2011-2012 and past 2003-2004 NHANES (National Health and Nutrition Examination Survey) data (4). Figures from other countries, such as Australia, China, England, France, Netherlands, New Zealand, Sweden, and Switzerland, also appear to show a decline or stabilization of obesity prevalence (5). Yet, subgroup level analysis of 2011-2012 statistics depicts increases in obesity prevalence in American women aged 60 and older from ~31.5% to ~38%, and a decrease ~14% to ~8% among American children aged 2 to 5 years old (4). Further analysis of 2011-2014 NHANES data by the CDC (Centers of Disease Control) showed a link in the prevalence of obesity among lower income and less educated women. Whereas, in men (6) and children (7) high obesity occurred in those classified as racial and ethnic minorities.

Although obesity trends tend to change, the overall occurrence among adults is still alarmingly high and should remain a focus of public health efforts.

BMI

In the assessment of weight and classification of obesity the most commonly used anthropometric tool is body mass index (BMI) (4, 8-10), expressing the weight-for-height relationship written as [weight (in kilograms)]/[height (in meters)]^2. Most traditional studies utilize body mass index (BMI) to characterize excessive weight defined by NHANES as a BMI of $\geq$25 kg/m^2 for overweight (11) and $\geq$30 kg/m^2 for obese (6). High BMI is associated with several chronic health problems (12, 13), such as type 2 diabetes mellitus (T2DM), cancer, non-alcoholic fatty liver disease (NAFLD) (14), cardiovascular disease (CVD) (8), stroke (15), and kidney disease (16) in both men and women. It also is linked to higher rates of mortality. Some studies, however, demonstrate this relation between BMI and disease to be controversial (11). Specifically, several show an inverse relation between metabolic diseases, such as CVD and coronary heart disease (CHD) with BMI, describing it as the "Obesity Paradox" (2, 17). This paradox implies that a higher BMI might actually be protective or less harmful when compared to individuals with a lower BMI and the same chronic health conditions (i.e. CVD) (2, 17). This suggests that although BMI can be used as an indicator of obesity, it may not necessarily relate well with all co-morbidities linked with excessive adipose tissue deposition (2). Indeed, while correlated to fat mass, it is well known that BMI alone cannot distinguish between body weight due to fat mass or fat free (lean) mass (4, 8, 10, 11).

Misconceptions of BMI and Alternative Methods

In adults, BMI is the preferred method over other indices of relative weight, as it has a low correlation to height, a high correlation with body fat, is simple to calculate, and is applicable to every population at all times (11). To date, BMI is still a central aspect in the weight-for-height guidelines for the World Health Organization and U.S. National Heart, Lung, and Blood Institute (11). However, BMI defines weight status based on statistical criteria, and it represents only a score, making it of somewhat limited value (11). More so, as it is does not accurately reflect an individual's body composition, it can provide only limited insight into obesity and obesity-associated co-morbidities.

The phenomenon known as "normal weight" obesity is described as an individual with normal body weight, as defined by BMI criteria, a high body fat percentage and a high degree of metabolic dysfunction (18). "Normal weight" obesity is associated with a higher risk of developing metabolic syndrome, cardiometabolic dysfunction, and subsequently mortality (18, 19). Thus, an updated definition for obesity based on characteristics of adiposity, rather than body weight, is needed. Additionally, a better adiposity-based risk stratification that reflects the gradations and location of fat distribution is necessary to accurately recognize high-risk groups. On the contrary, a subset of the obese population, ~29.2% of men and ~35.4% of women within the U.S. (19), present as metabolically healthy individuals, similar to that of lean counterparts (20-23). This subset displays resistance to the development of obesity-associated complications and has lower cardiometabolic risk factors (i.e. waist circumference) than those non-metabolically healthy obese individuals (19). Overall, excessive adipose tissue frequently results in the promotion of metabolic abnormalities and inflammation, yet in some can be protective. It is difficult to determine adiposity, good or bad, by way of solely measuring BMI. Thus,

understanding the complexities of body fat composition, distribution, type of fat, and function is necessary in interpreting the relationship between BMI, adiposity, morbidity, and mortality (2).

Dual-energy X-ray absorptiometry (DEXA) is considered a gold standard for measuring body composition. In a comparison of BMI against percent body fat (determined by DEXA), one study found that almost half of obese individuals (as determined by BMI criteria) were considered metabolically healthy using the percent body fat index (20). This discrepancy between BMI and percent body fat, however, did not occur when assessing normal weight or overweight individuals (20). This, nevertheless, is controversial because a separate paper from this group identified significant differences in the discrepancies between percent body fat and BMI for both overweight men and women (24). These studies support and extend that BMI in not a reliable measure to link adiposity with health outcomes.

BMI alone is a poor indicator of disease risk associated with dysfunctional adipose tissue, due in part to its poor estimation of percent body fat (25). Therefore, utilizing BMI in combination with other metrics might prove more useful. In elderly men age 60-79 BMI in combination with waist circumference best associated with metabolic abnormalities, such as metabolic syndrome and insulin resistance (26). The authors propose that waist circumference should be utilized to assess normal-weight and over-weight individuals (26). In support of this, others demonstrate that waist circumference index was the most uniform predictive power in assessment of intraperitoneal and posterior subcutaneous adipose tissue mass (27). The strong association between obesity and chronic diseases necessitates the accurate characterization of adiposity in the assessment of disease risk. Waist circumference is one measure to evaluate the level of abdominal obesity, and is shown to strongly predict risk for T2DM (28). However, a more precise measure of body composition by way of DEXA or computed tomography (CT)

would allow for a more accurate description of anatomical adipose deposition, and thus level of disease risk (29). Despite these supporting studies and drawbacks that accompany BMI as a measure for adiposity, BMI still remains a vital tool in assessment of individuals within a clinical setting. Additionally, several expert and advisory groups maintain their recommendation for the primary use of BMI in the assessment of weight status in children and adolescents aged 2-19 (30). However, understanding its limitations and maintaining a level of skepticism will provide clinicians and researchers with better accuracy in interpreting data.

Adipose Specific Accumulation Links to Disease Risk

Adipose tissue expansion can be broadly categorized as either healthy or unhealthy, depending on the depot location and nature of expansion (31). Accumulating adipose tissue can occur in different anatomical locations within the body and varies among individuals (32). In general, adipose tissue distribution can occur in the lower body, upper body, abdominal subcutaneous (underneath the skin), and/or visceral cavity (located on the abdominal cavity among organs) (32). However, obesity-related co-morbidities associate better with adipose accumulation in the upper body, visceral depot, rather than total body adiposity (16, 32). Conversely, accumulation of lower body subcutaneous adipose tissue is considered protective against metabolic dysfunction (33). This has led to the labeling of "good fat", referring to lower body and superficial abdominal subcutaneous regions (34), and "bad fat" which refers to upper body and visceral regions (35, 36). Metabolic derangements associated with visceral adipose accumulation "bad fat" include, but are not limited to dyslipidemia, hypertension, insulin resistance and T2DM insulin resistance, hypertension, atherogenic dyslipidemia, abdominal obesity, inflammation and thrombotic prevalence (15, 32, 37, 38). The previous constellation of metabolic abnormalities are core components in the development of the metabolic syndrome

(15), a precursor to chronic diseases like cardiovascular disease and cancer (38, 39). The pathogenesis of metabolic syndrome is thought to have etiological origins in disorders of adipose tissue, *i.e.* insulin resistance, and a grouping of independent factors originating from liver, vasculature, and/or immune cells (37). Other factors such as aging, a pro-inflammatory state, and hormonal changes are also implicated in metabolic syndrome development (37). Furthermore, depending on the combination of core components, metabolic syndrome can present differently among individuals with varying levels of severity (39).

Whether lean or obese, total adipose tissue mass on average is made up of ~85% subcutaneous and ~15% intra-abdominal adipose tissue (32). Interestingly, visceral adipose depots, mesenteric and omental, make up only 10% of total body fat yet have the highest associated risk for metabolic dysfunction (16, 32). Inherent characteristics are demonstrated to link visceral obesity to health risk (40), as well as its close proximity and venous drainage to the liver (32, 41). Specifically, adipose location next to the liver directly exposes insulin-sensitive hepatocytes to depot effluent containing metabolites and secreted products from both visceral adipocytes and other visceral depot resident cells via the portal vein (32, 41, 42). Hence, there is a complex relation between adipose tissue locations, inherent cell characteristics with whole-body homeostasis

Adipose Tissue: An Endocrine Organ with Immune Cells

Traditionally, adipose tissue characterized for being an energy repository, important for organism survival and metabolic regulation as well as insulation. Adipose tissue is now also defined as a multicellular endocrine organ system with central nervous system innervation (43) and lymphatic tissue (44, 45). During energy surplus adipocyte storage capabilities increase while endocrine and immune functions fluctuate in response to the new expanding environment

(31, 36, 46, 47). A role of healthy adipose tissue is to expand and accommodate energy excess as well as prevent lipotoxicity of other organs and tissues (48). Expansion occurs through two distinct mechanisms, either an increase in adipocyte size (hypertrophy) or adipocyte number (hyperplasia) through the process of adipogenesis (31, 49). As mature adipocytes are post-mitotic, new mature adipocytes are generated from pre-adipocytes within the stromal vascular fraction (48, 49). Not all adipose depot expansion is healthy, and this is proposed to be the basis for many metabolic co-morbidities. As changes in the number and size of adipocytes modulate the microenvironment within adipose tissue, concomitant alterations in its endocrine secretory products are also observed. This can communicate adipose tissue metabolism, as well as dysfunction, with the rest of the body and transform the systemic response.

Adipokines

The adipose tissue secretome, which differs between depots (50), is dictated by the various tissue resident cell types and surrounding environment (51, 52). In general, adipose tissue contains adipocytes, immune cells, endothelial cells, pre-adipocytes, and fibroblasts (51, 53, 54). Signaling factors that are produced and released from adipose tissue are generally referred to as adipokines or adipocytokines (52, 55-57), however there is disagreement with this definition (53, 54, 58). Some literature makes the distinction between signaling molecules that are released solely from adipocytes vs a whole adipose depot, referring to those molecules unique to adipocytes only, as adipokines. However, only a small portion of "adipokines" are produced exclusively by adipocytes or even adipose tissue, with many now being identified within other tissues due to advancements in technology. Hence, for the purpose of this review we will refer to secretory products of the collective adipose depot as adipokines. Under normal physiologic conditions adipokines serve to regulate numerous processes such as appetite, energy

stores and expenditure (54), glucose and insulin homeostasis (57, 58), cell growth (50), inflammation (51, 59), angiogenesis (60), and reproduction (61). Below we briefly review recent literature of adipokines proposed to differ between adipose depots that may drive differential metabolic outcomes within specific types of adipose tissue distributions.

Omentin

Omentin (or intelectin) is a more recently identified signaling molecule that is differentially released among adipose depots (59). Although a specific receptor has not yet been identified, omentin has two highly homologous isoforms: omentin-1 and -2 (59). Omentin-1 has been more extensively studied and is identified as the major circulating isoform. Omentin-1 has been characterized to be released from visceral adipose tissue (62), but not subcutaneous adipose tissue (63). Omentin-1 release decreases as visceral adipose mass increases, exhibiting an inverse relationship. Proposed mechanisms of action include omentin-1 activation of adenosine 5'-monophosphate (AMP)-activated protein kinase (AMPK), phosphatidylinositol 3 kinase (PI3K), and inhibition of NADPH oxidase (NOX) (59). These actions ultimately result in insulin sensitization, a reduction in inflammation and cardioprotection (59, 62).

WISP1

WISP1 is a novel adipokine described as an extracellular matrix associated protein (54, 64). It is primarily expressed during organ development (i.e. neuronal and skeletal muscle) (65, 66) and under diseased conditions such as inflammation, cancer, and fibrosis (64). It is characterized in both visceral and subcutaneous adipose depots and released by mature adipocytes (54, 64). WISP1 oversees many cellular mechanisms such as apoptosis, autophagy, cell migration, stem cell proliferation, angiogenesis, tumorigenesis, and immune cell modulation

(65, 67). Recently, plasma WISP1 levels were found to increase during obesity; and correlate with visceral adipose tissue mass, C-X-C motif chemokine ligand 8 [CXCL8 (formally known as IL-8)], and lower adiponectin levels (64). CXCL8 is a chemoattractant and activation factor for neutrophils, as well as T cells and basophils during inflammation (68).

Resistin

Resistin and its functions are best characterized during obesity where it plays a fundamental role in promoting inflammation and insulin resistance (51, 69, 70), although there are slight differences in the regulatory mechanisms between models and humans (57). Peripheral blood mononuclear cells (PBMCs) and adipose tissue resident macrophages appear to be the main producers of resistin (57, 61). Pro-inflammatory cytokines, such as IL-1β, IL-6, and TNF induce the expression of resistin within human macrophages (51) and resistin stimulates PBMCs to express IL-6 and TNF through NF-κB signaling (51, 69). One mode of action, proposed from rodent adipocytes, involves activation of SOCS3, results in the suppression of insulin mediated signaling (51, 69). However, the physiologic role of resistin and its mechanisms of action within humans remains to be fully elucidated.

NAMPT

Nicotinamide phosphoribosyl transferase (NAMPT) (a.k.a. Visfatin) in humans is released from PBMCs, resident tissue macrophages, and mature white adipocytes (54, 71, 72). NAMPT is distinguished into intracellular (iNAMPT) and extracellular (eNAMPT) forms, with the iNAMPT form acting as the rate-limiting enzyme in the NAD biosynthetic pathway from nicotinamide (73). The eNAMPT form has been reported to function as a cytokine named pre-B cell colony-enhancing factor (PBEF), which is proposed to enhance the maturation of B cell

precursors in the presence of IL-7 and stem cell factor (56, 73, 74). Although this has not been explicitly confirmed, other groups have corroborated its cytokine functionality (75-78). Primary mechanisms include signaling through p38 mitogen-activated protein kinase (p38 mAPK) and extracellular signal-regulated kinase (ERK) pathways, which lead to the production of IL-1β, TNF, and IL-6 (56, 76). These in turn enhance monocyte chemotactic activity which has led NAMPT to be characterized as pro-inflammatory (56). The eNAMPT form has also been reported to act as an insulin-mimetic hormone (Visfatin), however this physiologic role remains controversial (56, 72, 79). Recent data show that NAMPT does not exert insulin-memetic effects *in vitro* or *in vivo*, rather as previously stated exhibits NAD biosynthetic activity (73). Specifically, haplodeficiency and chemical inhibition of NAMPT attenuates NAD biosynthesis and glucose-stimulated insulin secretion in pancreatic islets *in vivo* and *in vitro* (73), yet nicotinamide mononucleotide (NMN) administration reveres it (73). Overall, NAMPT-mediated systemic NAD biosynthesis (through iNAMPT and eNAMPT) is critical for β cell function and glucose homeostasis (73). Within mice, iNAMPT protein expression is shown to be highest within brown adipose tissue, liver, kidney, and heart, whereas very low within white adipose tissue, lung, spleen, testis, and muscle (73).

Leptin

Leptin is primarily, but not solely, produced by adipocytes. It plays a fundamental role in regulating food intake as a satiety hormone that signals in the hypothalamus to suppress hunger (51, 52, 54, 57, 61). In concordance with its anorexogenic effects, it is a factor in energy expenditure homeostasis (54, 57, 80). Leptin is also considered pro-inflammatory as its chemical structure resembles that of other inflammatory cytokines (i.e. IL-2, IL-6, granulocyte-colony stimulating factor). Pro-inflammatory signaling during obesity is also prompted by

hyperleptinemia caused by leptin resistance (51, 56, 81). Leptin activates monocytes and macrophages, inducing inflammation and pro-inflammatory cytokine production (IL-6, TNF, and IL-12) by the long isoform of the leptin receptor b ($LepR_b$) through proximal Janus kinase 2 (JAK2)/signal transducer and activator of transcription 3 (STAT3) pathways (51, 56).

Adiponectin

Adiponectin is primarily released by adipocytes and is best characterized to induce insulin sensitization (52, 57, 63, 82, 83). This occurs mainly through glucose and lipid regulation within insulin sensitive tissues. Activation and signaling through AMPK is likely the main mechanism of action for this sensitization (51, 52, 57). Additionally, adiponectin can impart its insulin sensitizing effects through inhibition of growth factor activity (i.e. platelet-derived growth factor, fibroblast growth factor, and heparin-binding epidermal growth factor-like growth factor) by preventing their ligation with membrane receptors (52, 84). Additionally, adiponectin reduces inflammatory signaling which oppose insulins action (81). One mechanism for adiponectin-mediated reduction in inflammation occurs through an associated increase in ceramidase activity within the liver, which reduces the buildup of harmful ceramides (52). A second mechanism includes augmentation of immune cell activity (NK cells, T cells, Macrophages) and thus their cytokine release, ultimately biasing cells towards a more tolerogenic state (51, 57, 85).

Tumor Necrosis Factor (TNF)

Sometimes considered pseudo-adipokines, classical cytokines like TNF are also produced from resident immune cells within adipose tissue (58). The role of TNF in inflammation and pathology has been extensively studied (86-88). Within adipose tissue, macrophages account for

nearly all of the TNF produced (89). Local TNF protein and transcript expression are shown to be elevated during obesity (89, 90), specifically visceral (91), and positively correlate with insulin resistance. However, discrepancies still remain between *in vivo* and *in vitro* studies from human and rodent subjects as to specific depot contributions of circulating TNF (89, 92). More so, the importance of systemic TNF levels in the contribution to metabolic dysfunction remains unclear as there has been wide variability in reported levels, however the local paracrine and autocrine effects of TNF remain central in metabolically-driven inflammation (89). TNF propagates insulin resistance within adipocytes in part through its TNF receptor serine kinase activity (93), increased lipolysis (94), as well as via downstream intracellular signaling through NF-κB and JNK (89, 95, 96). Additionally, macrophage derived TNF acts locally in a dose and time dependent manor to stimulate lipolysis (97, 98) in part through a reduction in cell death-inducing DFF45-like effector C (CIDEC) and perilipin (as well as its phosphorylation) (99).

Interleukin 6 (IL-6)

IL-6 is produced by both adipocytes and macrophages (100), with a reported ~30% of total circulating IL-6 levels coming from adipose tissue (101). IL-6 concentrations increase in proportion with adiposity (89) and with greater production from SAT depots than visceral (101-103). Although IL-6 is often categorized as a pro-inflammatory cytokine, it is highly pleiotropic (104) and can impart anti-inflammatory effects as well (105-107). In concordance with this, IL-6 can induce the expression of *IL-4ra*, which permits anti-inflammatory macrophage polarization (106). This has even been demonstrated to occur during obesity (107). IL-6 contributes to the initiation of hepatic acute phase response (injury response) through induction of acute phase protein expression (i.e. c-reactive protein, serum amyloid a) both *in vitro* and *in vivo* (104). IL-6 also reduces food intake and increase energy expenditure via signaling in the CNS (108). Hence,

some propose that obesity-induced IL-6 increases occur as an attempt to regulate and restrain obesity driven dysfunction (89, 105-107) through enhance energy expenditure. Together this demonstrates that IL-6 may play a homeostatic role in limiting inflammation within adipose tissue.

Monocyte Chemoattractant Protein 1 (MCP-1)

MCP-1, otherwise known as CCL2, is produced primarily by macrophages, endothelial cells (56, 109) and adipocytes (58, 110). It is a potent chemotactic factor for monocytes (56, 109) that increases during obesity and contributes to adipose tissue macrophage infiltration (111). MCP-1 contributes to the development of insulin resistance (58) and hepatic steatosis in mice (109). Adipose tissue increases in MCP-1 increase pro-inflammatory macrophage accumulation, and TNF and IL-6 release (111). Indeed, macrophages exacerbate inflammation by also releasing MCP-1, TNF, IL-6, IL-1β, and IL-12 (112). This occurs in part through NF-κB signaling (55, 110) and continues the inflammatory cycle. These events are associated with profound systemic insulin resistance due to decreases in insulin-stimulated phosphorylation of AKT in both skeletal muscle and the liver (111). MCP-1 is higher in visceral adipose tissue compared with subcutaneous (113).

Adipose Tissue Immune Milieu

Healthy adipose tissue contains various immune cells (114, 115) that primarily include macrophages, eosinophils, natural killer T (NKT) cells, and various T cell subsets (58, 110, 112, 116). T cell subsets include $CD4^+$, which predominate, and $CD8^+$ T cells. Of the $CD4^+$ cells present, ~50% of them constitute regulatory T cells which are responsible for suppressing the immune response (117). Other $CD4^+$ cells represent effector T helpers, which are polarized

between anti- or pro-inflammatory depending on the milieu of the tissue. In adipose tissue, immune cells produce a range of cytokines such as IL-4, IL-13, IL-10, and IL-1Ra that act to maintain a homeostatic and tolerogenic environment (56, 110, 112, 116). Eosinophils and Th2 polarized T helper cells work to reduce adipose tissue pro-inflammation through IL-4, IL-13 and IL-10 dependent anti-inflammatory macrophage polarization (56, 110, 112, 118). Regulatory T cells also aid in the maintenance of adipose tissue homeostasis, in part through the production of IL-10 and IL-10-mediated suppression of proliferation of other T cell subsets (112, 117). Although controversial (112, 119, 120), the role of NKT cells, specifically adipose resident invariant NKT (iNKT) cells, is thought to help maintain adipose tissue homeostasis (121-124) through a unique cytokine profile including production of IL-4 and IL-10 (115, 121).

An inflammatory response produced to fight and contain infections, cellular injury, and/or death is standard in the maintenance of homeostasis. It encompasses both the innate (non-specific, first responders) and adaptive (specific, humoral and cellular) arms of the immune system. Inflammation is intended to be acute with resolution of the insult (i.e. antigen or cell clearance) and promotion of healing. When chronic, inflammation can lead to deleterious outcomes (55, 88), hence inflammation plays a fundamental role in the development and progression of many diseases (55, 88, 98, 125). This is the suggested link between obesity-induced inflammation and subsequent prevalence of associated co-morbidities. As stated previously, visceral adiposity, but not general adiposity, is highly associated with obesity related co-morbidities such as hypertension, dyslipidemia, and insulin resistance. This would suggest an inherent difference of the visceral adipose tissue depot from other adipose depots within the body.

Visceral Adipose Tissue

Excess adipose tissue within the visceral cavity, whether overweight or lean, is associated with an in increased prevalence of high disease risk (18). Location of this adipose tissue among the organs in the abdominal cavity plays a fundamental role in this outcome (33, 42, 126). However, the inherent characteristics of this depot also play a chief role (41). Adipose depots differ in several ways including nerve innervation, drainage, metabolism, immune response and angiogenesis (33, 41, 126). These characteristics play a large role in how an adipose depot may respond to injury, pathogens, lipolysis, lipid storage and growth.

Upper body adipocytes differ from lower body adipocytes in numerous ways. First, upper body fat has a higher triglyceride turnover than lower body fat (127, 128). Specifically, visceral adipocytes have a higher lipid turnover due to increased lipolysis and decreased sensitivity to the antilipolytic effect of insulin (128). In comparison to subcutaneous, visceral adipocytes have a higher lipolytic rate (129) because of higher of beta-1, -2 and -3 adrenergic receptors (130, 131) and decreased response to alpha-adrenergic agonists (132). Taken together this higher rate of lipolysis and lack of sensitivity to insulin promote lipid flux to the liver in individuals with visceral obesity, leading to NAFLD (32, 133-136). Visceral adipocytes also differ from subcutaneous in rate of apoptosis and differentiation capacity of adipocyte precursor cells (126). Visceral adipocytes, *in vitro,* are highly susceptible to tumor necrosis factor (TNF), an apoptotic stimulus, compared with subcutaneous adipocytes (137). Yet, *in vivo* inhibition of TNF mediated cell death is greater in the visceral adipocytes than in subcutaneous (138). On the other hand, subcutaneous adipocytes have greater differentiation capacity than those from the visceral depot; (126, 139), this is mediated by proliferator-activated receptor-γ (PPAR-γ) (140). Differentiation capacity and growth capacity of adipose tissue depots, however, are also dictated by their inherent ability to grow new vasculature (31, 141-143). Compared with the subcutaneous depot,

the visceral has a lower capacity to expand its capillary network (144). The lack of supporting vasculature during rapid adipose depot expansion can lead to the release of chemical mediators that cause a pro-inflammatory response (31, 143).

Compared with other adipose depots, for example lower body subcutaneous, the visceral depot is characterized to be more pro-inflammatory. This propensity towards inflammation, in part, originates from how cells within the visceral depot recognize cellular injury (either from the damaged cell, surrounding cells, or tissue resident immune cells) (55, 88, 145) and the release of subsequent chemical mediators (146). Ensuing mediators involved in the response to noxious stimulus recruit phagocytic cells to the site of injury (55, 146), which function to contain the insult and recruit additional immune cells to assist in the removal of debris and tissue repair (88). This is the sort of response that occurs during obesity; however, the harmful stimulus is long lasting, hence the term "chronic state of low-grade inflammation".

In the visceral depot, compared with subcutaneous, the microenvironment and resident cells all change dynamically during obesity (114, 116, 146, 147). Although the order of events, which contribute, to adipose tissue dysfunction and inflammation are not fully understood, several key steps have been identified. First, nutrient excess promotes adipocyte and adipose tissue expansion, which can lead to adipocyte dysfunction (110, 112, 148). Then, dysfunctional adipocytes release adipokines such as TNF, leptin, resistin, IL-6, RANTES, and MCP-1, which induce the infiltration of immune cells promote a pro-inflammatory phenotype (110, 112, 125). Moreover, released pro-inflammatory mediators can activate pathways like IKKβ/NF-κB, JNKs, and inflammasomes, which negatively regulate insulin signaling in adipocytes (55, 112). Last, infiltrating immune cells exacerbate and propagate adipose tissue inflammation, as well as facilitate the development of systemic inflammation (55, 110). It is predicted that these previous

events precipitate from a combination of cellular stress, unrestrained lipolysis and free fatty acid release, an abundance of reactive oxygen species and toxic lipids, as well as poor blood flow and hypoxia (55, 116, 125). These processes are characterized to occur to a greater extent within the visceral depot than in the subcutaneous (41, 134, 149). As such, resident immune cells such as macrophages (150-152) become activated and can be characterized by their expression of CD11c, inducible nitric oxide synthase (iNOS), TNF, IL-6, MCP-1, IL-1β, and IL-12 (112, 153-155). In fact, the degree of macrophage infiltration correlates with the level of insulin resistance and tissue fibrosis, due to the pro-inflammatory cytokine output of macrophages (56, 110). During obesity, the presence of macrophages can range from 40-70% of total cells within the stromal vascular fraction (55, 112). A limited number of neutrophils also become recruited in response to weight gain (156) hampering insulin signaling and propagating macrophage activation (110). Meanwhile, mast cells enter and secrete IL-6 and interferon γ (IFNγ) (157). Also, during obesity the number of $CD4^+$ (158) and $CD8^+$ T cells increase (159, 160), while regulatory T cell numbers decrease (161), this change is in part mediated by the expression of STAT3 (55, 110). $CD4^+$ cells now present in obesity appear to be primarily Th1 polarized, which play a fundamental role in pro-inflammatory macrophage recruitment through the expression of IFNγ (110, 162). While characterization of the role dendritic cells play within obesity-induced inflammation has yet to be fully elucidated, their importance in the development of cellular immunity and macrophage activation is key (163). Additionally, B cells increase early in obesity. Although their role is still being defined, studies thus far suggest that B cell depletion during obesity is associated with better glucose tolerance (112, 164, 165). Natural Killer (NK) cells have also been associated with an increase in presence and activation during obesity, playing a role in the development of inflammation (166-168). Overall, during the progression of obesity

and inflammation, the populations and activities of immune cells present within adipose tissue shift dynamically (110). This shift occurs in response to the adipose tissue milieu, which includes, but is not limited to adipokine profile, adipocyte metabolism, adipocyte growth, response to insulin, angiogenic capacity, cytokine release and immune cells (55, 112). The visceral depot is dispositioned, especially with obesity, to result in a pro-inflammatory response.

Subcutaneous Adipose Tissue

Subcutaneous adipose tissue (SAT) depots, located under the epidermis, comprise roughly 85% of the total adipose tissue mass in humans (169). Distinct adipose depots that are well characterized include the gluteofemoral subcutaneous adipose tissue (GSAT; lower body regions among the thighs, hips, and buttocks), upper body subcutaneous adipose tissue (arms, trunk and abdomen) (170) and abdominal subcutaneous adipose tissue (ASAT). ASAT includes the superficial subcutaneous adipose tissue (sSAT) (laying superficial to the Scarpa's fascia) and the deep subcutaneous adipose tissue (dSAT) which lies beneath in the posterior half of the abdomen (171).

In mice, the two primary SAT depots are located anteriorly and posteriorly. The former, found between the scapulae, descends from the neck to the axillae. The latter, located in the inguinal area, spans the dorsolumbar to gluteal region. Analogous to GSAT in humans, the inguinal fat pad is the most commonly analyzed SAT in rodents. These individual adipose regions have distinctive contributions to metabolism and abilities to adapt to energy flux.

Lower Body Subcutaneous: The "Protective Depot"

Lower body obesity is associated with less metabolic disease risk than central obesity (172, 173). Large hip and thigh circumferences of both men and women are related to a

decreased risk of T2D, independent of BMI, age, and waist circumference (174). In opposition, a greater waist circumference is linked to larger risk (174). Low levels of GSAT are associated with unfavorable glucose and lipid levels, and greater ASAT mass with higher LDL and total cholesterol levels, as well as lowered HDL (175, 176). Contributing factors associated with variant disease risk among adipose depots are intrinsic differences in energy uptake, storage, and turnover rates. Studies indicate reduced lipolysis in the GSAT results in appropriation of lipids typically directed to non-adipose tissues. A greater lipid buffering ability and storage capacity, allows the GSAT to act as a protective "metabolic sink" and defend tissues that are insulin sensitive from ectopic lipidation and lipotoxicity (172, 177).

Rodent transplantation studies emphasize that inherent differences among adipose depots play a fundamental role in the association between adipose tissue distribution and disease susceptibility. Specifically, improvements in glucose tolerance and decreases in circulating lipids occur in mice with auto-transplantation of inguinal SAT into the visceral cavity (136). More so, SAT auto-transplantation into the visceral cavity enhances hepatic insulin sensitivity and reduces liver and portal vein lipid concentrations. Notably, these improvements occurred without an increase in the mass of the transplanted tissue, which indicates that the protective benefits of SAT are not only a product of its lipid storing capacity, but also its distinct adipokine secretome. Factors released from SAT transplanted into the visceral depot, which have yet to be identified, drove the improvement in hepatic lipid and glucose regulation (178).

The reduced risk of co-morbidity development associated with GSAT is also attributed to its lower pro-inflammatory profile. A study of 729 older obese women and men correlated metabolic syndrome with a higher deposition of VAT to GSAT. Those affected by metabolic syndrome also had significantly increased level of adipokines associated with insulin resistance:

IL-6, TNF, and PAI-1 (179). Additional *in vivo* investigations determined that the release of IL-6 is lower from GSAT than ASAT (180), however this is controversial. More so, macrophage infiltration, a hallmark of visceral adipose tissue accumulation, was lower in GSAT (181). Researchers propose that these regional variations in adipocyte function can be attributed to their inherent developmental variances (180).

Abdominal Subcutaneous is Not Protective

While GSAT imparts protective benefits, research has found that the inverse is true for ASAT. A greater accumulation of ASAT corresponds to insulin resistance, similar to that of VAT (182). Additionally, ASAT mass has a stronger correlation with insulin resistance than intraperitoneal and retroperitoneal adipose tissue (183). Consistent with this, adipocyte hypertrophy within ASAT positively correlates to insulin resistance, hyperinsulinemia, and glucose intolerance (184-187). ASAT size, independent of insulin sensitivity, is also a predictor of T2D (188). However, of the ASAT regions sSAT typically exhibits a profile similar to GSAT, while dSAT, analogous to VAT, plays an autonomous role in obesity-driven complications (189). A cross-sectional study of men and women with T2D quantified ASAT distribution into sSAT and dSAT sub-depots. A distinct advantage between the sSAT region and cardiometabolic health was proposed due to observed improvements, such as increased heart rate variability, reduced blood pressure, and improved glycemic control. The inverse relation was correlated with dSAT. Additional exploration, however, is essential to determine causality due to several study limitations, principally the failure to measure GSAT and a low representation of women (190).

Recent investigations into the structural and functional roles of sSAT and dSAT propose differences in gene expression play a critical role in metabolic disease risk. Increases of dSAT highly associate with metabolic risk factors in both men and women (191). In support of this, a

higher expression of lipogenic and lipolytic genes have been attributed to dSAT and associated with increased insulin resistance (34). Analysis of biopsied ASAT tissue in obese women revealed that dSAT displays a significantly distinct pattern of pro-inflammatory gene expression, while sSAT is characterized by beneficial genes, including adiponectin (189).

Subcutaneous Dysregulation Leads to Visceral Accumulation

As our understanding into the importance of anatomical fat deposition has become clearer, many groups have begun unraveling the roles that specific adipose tissue depots play in disease development and progression (33, 178). Indeed, it is evident that intra-abdominal or visceral adipose tissue accumulation is strongly associated with dyslipidemia, insulin resistance and T2D (33, 35, 136, 178), as well as cardiovascular dysfunction (134, 192, 193). Whereas a greater percentage of total body fat consisting of lower body adiposity, GSAT, exerts protection against inflammation, dyslipidemia, insulin resistance and glucose intolerance. Studies now propose an association between the visceral to subcutaneous adipose tissue ratio and cardiovascular disease risk factors, with an increased ratio correlating to a greater risk for cardiovascular disease (194-198). This ratio, however, is distinct to relative amounts of GSAT, not sSAT or dSAT.

During caloric excess adipose tissue undergoes hypertrophy of adipocytes, adipogenesis, and extracellular matrix remodeling to accommodate expansion. In addition, there are changes in the amount and type of cells within the stromal vascular fraction, angiogenesis, and alterations in the adipose tissue secretome (142, 199-201). Remodeling is a continuous process that can become pathological, as in obesity (100, 141, 143, 202). Excess fatty acids are thought to store preferentially within subcutaneous adipose tissue depots (38, 199). However, when adipose tissue reaches a maximum threshold, lipid spill over into ectopic locations can occur (203). A

reduction in SAT expansion or general dysfunction, can lead to ectopic fat deposition and VAT accumulation. This is postulated to result from a combination of poor blood flow, inflammation, tissue fibrosis, stress, and altered lipid metabolism within GSAT (199, 204, 205). For example, chronic stress mediates a reduction in the ability of SAT to take up circulating lipids, this promotes VAT tissue deposition (204) and hence plays a role in belly fat accumulation associated with stress.

Conclusions

In conclusion, distinct adipose tissue depots are inherently different in numerous ways. These inherent characteristics drive the differential health outcomes reported among divergent adipose tissue distributions. It is well established that visceral adiposity is strongly associated with metabolic co-morbidities, hence most current studies strive to investigate deleterious mechanisms within the visceral cavity. However, reversal or treatment mechanisms can also be discovered from investigating inherent characteristics of adipose tissue depots that can accumulate without metabolic risk. As research now indicates, visceral adiposity “bad fat” may predominantly be an outcome exacerbated by the lack or dysregulation of subcutaneous depots “good fat”. Numerous chronic diseases are associated with redistribution of adipose depots. Perhaps these types of studies can give future insight into mechanisms that drive good fat to become bad.

REFERENCES

1. Kumar S, Kelly AS. Review of Childhood Obesity: From Epidemiology, Etiology, and Comorbidities to Clinical Assessment and Treatment. Mayo Clin Proc. 2017 Feb;92:251-65.
2. Goyal A, Nimmakayala KR, Zonszein J. Is there a paradox in obesity? Cardiol Rev. 2014 Jul-Aug;22:163-70.
3. Sun X, Li P, Yang X, Li W, Qiu X, Zhu S. From genetics and epigenetics to the future of precision treatment for obesity. Gastroenterol Rep (Oxf). 2017 Nov;5:266-70.
4. Ogden CL, Carroll MD, Kit BK, Flegal KM. Prevalence of childhood and adult obesity in the United States, 2011-2012. JAMA. 2014 Feb 26;311:806-14.
5. Olds T, Maher C, Zumin S, Peneau S, Lioret S, Castetbon K, Bellisle, de Wilde J, Hohepa M, et al. Evidence that the prevalence of childhood overweight is plateauing: data from nine countries. Int J Pediatr Obes. 2011 Oct;6:342-60.
6. Ogden CL, Fakhouri TH, Carroll MD, Hales CM, Fryar CD, Li X, Freedman DS. Prevalence of Obesity Among Adults, by Household Income and Education - United States, 2011-2014. MMWR Morb Mortal Wkly Rep. 2017 Dec 22;66:1369-73.
7. Isong IA, Rao SR, Bind MA, Avendano M, Kawachi I, Richmond TK. Racial and Ethnic Disparities in Early Childhood Obesity. Pediatrics. 2018 Jan;141.
8. Bastien M, Poirier P, Lemieux I, Despres JP. Overview of epidemiology and contribution of obesity to cardiovascular disease. Prog Cardiovasc Dis. 2014 Jan-Feb;56:369-81.
9. Hales CM, Carroll MD, Fryar CD, Ogden CL. Prevalence of Obesity Among Adults and Youth: United States, 2015-2016. NCHS Data Brief. 2017 Oct:1-8.
10. Ogden CL, Carroll MD, Flegal KM. Prevalence of obesity in the United States. JAMA. 2014 Jul;312:189-90.
11. Muller MJ, Braun W, Enderle J, Bosy-Westphal A. Beyond BMI: Conceptual Issues Related to Overweight and Obese Patients. Obes Facts. 2016;9:193-205.
12. Zamboni M, Mazzali G, Zoico E, Harris TB, Meigs JB, Di Francesco V, Fantin F, Bissoli L, Bosello O. Health consequences of obesity in the elderly: a review of four unresolved questions. Int J Obes (Lond). 2005 Sep;29:1011-29.
13. Cordain L, Eaton SB, Sebastian A, Mann N, Lindeberg S, Watkins BA, O'Keefe JH, Brand-Miller J. Origins and evolution of the Western diet: health implications for the 21st century. Am J Clin Nutr. 2005 Feb;81:341-54.
14. Said A, Ghufran A. Epidemic of non-alcoholic fatty liver disease and hepatocellular carcinoma. World J Clin Oncol. 2017 Dec 10;8:429-36.
15. Frasca D, Blomberg BB, Paganelli R. Aging, Obesity, and Inflammatory Age-Related Diseases. Front Immunol. 2017;8:1745.
16. Tchernof A, Despres JP. Pathophysiology of human visceral obesity: an update. Physiol Rev. 2013 Jan;93:359-404.
17. Lavie CJ, Schutter AD, Archer E, McAuley PA, Blair SN. Obesity and prognosis in chronic diseases--impact of cardiorespiratory fitness in the obesity paradox. Curr Sports Med Rep. 2014 Jul-Aug;13:240-5.

18. Oliveros E, Somers VK, Sochor O, Goel K, Lopez-Jimenez F. The concept of normal weight obesity. Prog Cardiovasc Dis. 2014 Jan-Feb;56:426-33.
19. Wildman RP, Muntner P, Reynolds K, McGinn AP, Rajpathak S, Wylie-Rosett J, Sowers MR. The obese without cardiometabolic risk factor clustering and the normal weight with cardiometabolic risk factor clustering: prevalence and correlates of 2 phenotypes among the US population (NHANES 1999-2004). Arch Intern Med. 2008 Aug 11;168:1617-24.
20. Shea JL, Randell EW, Sun G. The prevalence of metabolically healthy obese subjects defined by BMI and dual-energy X-ray absorptiometry. Obesity (Silver Spring). 2011 Mar;19:624-30.
21. Stefan N, Kantartzis K, Machann J, Schick F, Thamer C, Rittig K, Balletshofer B, Machicao F, Fritsche A, Haring HU. Identification and characterization of metabolically benign obesity in humans. Arch Intern Med. 2008 Aug 11;168:1609-16.
22. Karelis AD, St-Pierre DH, Conus F, Rabasa-Lhoret R, Poehlman ET. Metabolic and body composition factors in subgroups of obesity: what do we know? J Clin Endocrinol Metab. 2004 Jun;89:2569-75.
23. Sims EA. Are there persons who are obese, but metabolically healthy? Metabolism. 2001 Dec;50:1499-504.
24. Kennedy AP, Shea JL, Sun G. Comparison of the classification of obesity by BMI vs. dual-energy X-ray absorptiometry in the Newfoundland population. Obesity (Silver Spring). 2009 Nov;17:2094-9.
25. Gomez-Ambrosi J, Silva C, Galofre JC, Escalada J, Santos S, Millan D, Vila N, Ibanez P, Gil MJ, et al. Body mass index classification misses subjects with increased cardiometabolic risk factors related to elevated adiposity. Int J Obes (Lond). 2012 Feb;36:286-94.
26. Wannamethee SG, Shaper AG, Morris RW, Whincup PH. Measures of adiposity in the identification of metabolic abnormalities in elderly men. Am J Clin Nutr. 2005 Jun;81:1313-21.
27. Chan DC, Watts GF, Barrett PH, Burke V. Waist circumference, waist-to-hip ratio and body mass index as predictors of adipose tissue compartments in men. QJM. 2003 Jun;96:441-7.
28. Wang Y, Rimm EB, Stampfer MJ, Willett WC, Hu FB. Comparison of abdominal adiposity and overall obesity in predicting risk of type 2 diabetes among men. Am J Clin Nutr. 2005 Mar;81:555-63.
29. Shea JL, King MT, Yi Y, Gulliver W, Sun G. Body fat percentage is associated with cardiometabolic dysregulation in BMI-defined normal weight subjects. Nutrition, metabolism, and cardiovascular diseases : NMCD. 2012 Sep;22:741-7.
30. Krebs NF, Himes JH, Jacobson D, Nicklas TA, Guilday P, Styne D. Assessment of child and adolescent overweight and obesity. Pediatrics. 2007 Dec;120 Suppl 4:S193-228.
31. Choe SS, Huh JY, Hwang IJ, Kim JI, Kim JB. Adipose Tissue Remodeling: Its Role in Energy Metabolism and Metabolic Disorders. Front Endocrinol (Lausanne). 2016;7:30.
32. Foster MT, Pagliassotti MJ. Metabolic alterations following visceral fat removal and expansion: Beyond anatomic location. Adipocyte. 2012 Oct 1;1:192-9.
33. Harris RB, Leibel RL. Location, location, location. Cell Metab. 2008 May;7:359-61.
34. Marinou K, Hodson L, Vasan SK, Fielding BA, Banerjee R, Brismar K, Koutsilieris M, Clark A, Neville MJ, Karpe F. Structural and functional properties of deep abdominal subcutaneous adipose tissue explain its association with insulin resistance and cardiovascular risk in men. Diabetes Care. 2014 Mar;37:821-9.
35. Kwon H, Kim D, Kim JS. Body Fat Distribution and the Risk of Incident Metabolic Syndrome: A Longitudinal Cohort Study. Sci Rep. 2017 Sep 8;7:10955.

36. Pellegrinelli V, Carobbio S, Vidal-Puig A. Adipose tissue plasticity: how fat depots respond differently to pathophysiological cues. Diabetologia. 2016 Jun;59:1075-88.
37. Grundy SM, Brewer HB, Jr., Cleeman JI, Smith SC, Jr., Lenfant C, American Heart A, National Heart L, Blood I. Definition of metabolic syndrome: Report of the National Heart, Lung, and Blood Institute/American Heart Association conference on scientific issues related to definition. Circulation. 2004 Jan 27;109:433-8.
38. Despres JP, Lemieux I. Abdominal obesity and metabolic syndrome. Nature. 2006 Dec 14;444:881-7.
39. Monteiro R, Azevedo I. Chronic inflammation in obesity and the metabolic syndrome. Mediators of inflammation. 2010;2010.
40. Guglielmi V, Sbraccia P. Obesity phenotypes: depot-differences in adipose tissue and their clinical implications. Eat Weight Disord. 2017 Dec 11.
41. Booth A, Magnuson A, Foster M. Detrimental and protective fat: body fat distribution and its relation to metabolic disease. Horm Mol Biol Clin Investig. 2014 Jan;17:13-27.
42. Rytka JM, Wueest S, Schoenle EJ, Konrad D. The portal theory supported by venous drainage-selective fat transplantation. Diabetes. 2011 Jan;60:56-63.
43. Tozzi M, Novak I. Purinergic Receptors in Adipose Tissue As Potential Targets in Metabolic Disorders. Front Pharmacol. 2017;8:878.
44. Kim CS, Lee SC, Kim YM, Kim BS, Choi HS, Kawada T, Kwon BS, Yu R. Visceral fat accumulation induced by a high-fat diet causes the atrophy of mesenteric lymph nodes in obese mice. Obesity (Silver Spring). 2008 Jun;16:1261-9.
45. Pond CM, Mattacks CA. In vivo evidence for the involvement of the adipose tissue surrounding lymph nodes in immune responses. Immunol Lett. 1998 Oct;63:159-67.
46. Corvera S, Gealekman O. Adipose tissue angiogenesis: impact on obesity and type-2 diabetes. Biochim Biophys Acta. 2014 Mar;1842:463-72.
47. Gregor MF, Hotamisligil GS. Thematic review series: Adipocyte Biology. Adipocyte stress: the endoplasmic reticulum and metabolic disease. J Lipid Res. 2007 Sep;48:1905-14.
48. Kwok KH, Lam KS, Xu A. Heterogeneity of white adipose tissue: molecular basis and clinical implications. Exp Mol Med. 2016 Mar 11;48:e215.
49. Jeffery E, Wing A, Holtrup B, Sebo Z, Kaplan JL, Saavedra-Pena R, Church CD, Colman L, Berry R, Rodeheffer MS. The Adipose Tissue Microenvironment Regulates Depot-Specific Adipogenesis in Obesity. Cell Metab. 2016 Jul 12;24:142-50.
50. Opatrilova R, Caprnda M, Kubatka P, Valentova V, Uramova S, Nosal V, Gaspar L, Zachar L, Mozos I, et al. Adipokines in neurovascular diseases. Biomed Pharmacother. 2017 Dec 23;98:424-32.
51. Kwon H, Pessin JE. Adipokines mediate inflammation and insulin resistance. Front Endocrinol (Lausanne). 2013;4:71.
52. Luo L, Liu M. Adipose tissue in control of metabolism. J Endocrinol. 2016 Dec;231:R77-R99.
53. Smekal A, Vaclavik J. Adipokines and cardiovascular disease: A comprehensive review. Biomed Pap Med Fac Univ Palacky Olomouc Czech Repub. 2017 Mar;161:31-40.
54. Booth A, Magnuson A, Fouts J, Foster MT. Adipose tissue: an endocrine organ playing a role in metabolic regulation. Horm Mol Biol Clin Investig. 2016 Apr 1;26:25-42.
55. Lee BC, Lee J. Cellular and molecular players in adipose tissue inflammation in the development of obesity-induced insulin resistance. Biochim Biophys Acta. 2014 Mar;1842:446-62.

56. Ouchi N, Parker JL, Lugus JJ, Walsh K. Adipokines in inflammation and metabolic disease. Nat Rev Immunol. 2011 Feb;11:85-97.
57. Kocot J, Dziemidok P, Kielczykowska M, Hordyjewska A, Szczesniak G, Musik I. Adipokine Profile in Patients with Type 2 Diabetes Depends on Degree of Obesity. Med Sci Monit. 2017 Oct 19;23:4995-5004.
58. Esteve Rafols M. Adipose tissue: cell heterogeneity and functional diversity. Endocrinol Nutr. 2014 Feb;61:100-12.
59. Zhou Y, Zhang B, Hao C, Huang X, Li X, Huang Y, Luo Z. Omentin-A Novel Adipokine in Respiratory Diseases. Int J Mol Sci. 2017 Dec 28;19.
60. Chung HS, Choi KM. Adipokines and Myokines: A Pivotal Role in Metabolic and Cardiovascular Disorders. Curr Med Chem. 2017 Dec 5.
61. Booth A, Magnuson A, Fouts J, Foster M. Adipose tissue, obesity and adipokines: role in cancer promotion. Horm Mol Biol Clin Investig. 2015 Jan;21:57-74.
62. Zhou JY, Chan L, Zhou SW. Omentin: linking metabolic syndrome and cardiovascular disease. Curr Vasc Pharmacol. 2014 Jan;12:136-43.
63. Sitticharoon C, Nway NC, Chatree S, Churintaraphan M, Boonpuan P, Maikaew P. Interactions between adiponectin, visfatin, and omentin in subcutaneous and visceral adipose tissues and serum, and correlations with clinical and peripheral metabolic factors. Peptides. 2014 Dec;62:164-75.
64. Barchetta I, Cimini FA, Capoccia D, De Gioannis R, Porzia A, Mainiero F, Di Martino M, Bertoccini L, De Bernardinis M, et al. WISP1 Is a Marker of Systemic and Adipose Tissue Inflammation in Dysmetabolic Subjects With or Without Type 2 Diabetes. J Endocr Soc. 2017 Jun 1;1:660-70.
65. Maiese K, Chong ZZ, Shang YC, Wang S. Targeting disease through novel pathways of apoptosis and autophagy. Expert Opin Ther Targets. 2012 Dec;16:1203-14.
66. Berschneider B, Konigshoff M. WNT1 inducible signaling pathway protein 1 (WISP1): a novel mediator linking development and disease. Int J Biochem Cell Biol. 2011 Mar;43:306-9.
67. Maiese K. WISP1: Clinical insights for a proliferative and restorative member of the CCN family. Curr Neurovasc Res. 2014;11:378-89.
68. Belchamber KBR, Donnelly LE. Macrophage Dysfunction in Respiratory Disease. Results Probl Cell Differ. 2017;62:299-313.
69. Huang X, Yang Z. Resistin's, obesity and insulin resistance: the continuing disconnect between rodents and humans. J Endocrinol Invest. 2016 Jun;39:607-15.
70. Jonas MI, Kurylowicz A, Bartoszewicz Z, Lisik W, Jonas M, Domienik-Karlowicz J, Puzianowska-Kuznicka M. Adiponectin/resistin interplay in serum and in adipose tissue of obese and normal-weight individuals. Diabetol Metab Syndr. 2017;9:95.
71. Curat CA, Wegner V, Sengenes C, Miranville A, Tonus C, Busse R, Bouloumie A. Macrophages in human visceral adipose tissue: increased accumulation in obesity and a source of resistin and visfatin. Diabetologia. 2006 Apr;49:744-7.
72. Fukuhara A, Matsuda M, Nishizawa M, Segawa K, Tanaka M, Kishimoto K, Matsuki Y, Murakami M, Ichisaka T, et al. Visfatin: a protein secreted by visceral fat that mimics the effects of insulin. Science. 2005 Jan 21;307:426-30.
73. Revollo JR, Korner A, Mills KF, Satoh A, Wang T, Garten A, Dasgupta B, Sasaki Y, Wolberger C, et al. Nampt/PBEF/Visfatin regulates insulin secretion in beta cells as a systemic NAD biosynthetic enzyme. Cell Metab. 2007 Nov;6:363-75.

74. Samal B, Sun Y, Stearns G, Xie C, Suggs S, McNiece I. Cloning and characterization of the cDNA encoding a novel human pre-B-cell colony-enhancing factor. Molecular and cellular biology. 1994 Feb;14:1431-7.
75. Jia SH, Li Y, Parodo J, Kapus A, Fan L, Rotstein OD, Marshall JC. Pre-B cell colony-enhancing factor inhibits neutrophil apoptosis in experimental inflammation and clinical sepsis. J Clin Invest. 2004 May;113:1318-27.
76. Moschen AR, Kaser A, Enrich B, Mosheimer B, Theurl M, Niederegger H, Tilg H. Visfatin, an adipocytokine with proinflammatory and immunomodulating properties. Journal of immunology. 2007 Feb 1;178:1748-58.
77. Ognjanovic S, Bryant-Greenwood GD. Pre-B-cell colony-enhancing factor, a novel cytokine of human fetal membranes. Am J Obstet Gynecol. 2002 Oct;187:1051-8.
78. Ye SQ, Simon BA, Maloney JP, Zambelli-Weiner A, Gao L, Grant A, Easley RB, McVerry BJ, Tuder RM, et al. Pre-B-cell colony-enhancing factor as a potential novel biomarker in acute lung injury. Am J Respir Crit Care Med. 2005 Feb 15;171:361-70.
79. Oki K, Yamane K, Kamei N, Nojima H, Kohno N. Circulating visfatin level is correlated with inflammation, but not with insulin resistance. Clin Endocrinol (Oxf). 2007 Nov;67:796-800.
80. Houde AA, Legare C, Biron S, Lescelleur O, Biertho L, Marceau S, Tchernof A, Vohl MC, Hivert MF, Bouchard L. Leptin and adiponectin DNA methylation levels in adipose tissues and blood cells are associated with BMI, waist girth and LDL-cholesterol levels in severely obese men and women. BMC Med Genet. 2015 May 1;16:29.
81. Fantuzzi G. Adiponectin in inflammatory and immune-mediated diseases. Cytokine. 2013 Oct;64:1-10.
82. Xia JY, Sun K, Hepler C, Ghaben AL, Gupta RK, An YA, Holland WL, Morley TS, Adams AC, et al. Acute loss of adipose tissue-derived adiponectin triggers immediate metabolic deterioration in mice. Diabetologia. 2017 Dec 9.
83. Nway NC, Sitticharoon C, Chatree S, Maikaew P. Correlations between the expression of the insulin sensitizing hormones, adiponectin, visfatin, and omentin, and the appetite regulatory hormone, neuropeptide Y and its receptors in subcutaneous and visceral adipose tissues. Obes Res Clin Pract. 2016 May-Jun;10:256-63.
84. Wang Y, Lam KS, Xu JY, Lu G, Xu LY, Cooper GJ, Xu A. Adiponectin inhibits cell proliferation by interacting with several growth factors in an oligomerization-dependent manner. J Biol Chem. 2005 May 6;280:18341-7.
85. Ge Q, Ryken L, Noel L, Maury E, Brichard SM. Adipokines identified as new downstream targets for adiponectin: lessons from adiponectin-overexpressing or -deficient mice. Am J Physiol Endocrinol Metab. 2011 Aug;301:E326-35.
86. Brenner D, Blaser H, Mak TW. Regulation of tumour necrosis factor signalling: live or let die. Nat Rev Immunol. 2015 Jun;15:362-74.
87. Huber R, Bikker R, Welz B, Christmann M, Brand K. TNF Tolerance in Monocytes and Macrophages: Characteristics and Molecular Mechanisms. J Immunol Res. 2017;2017:9570129.
88. Chen GY, Nunez G. Sterile inflammation: sensing and reacting to damage. Nat Rev Immunol. 2010 Dec;10:826-37.
89. Wisse BE. The inflammatory syndrome: the role of adipose tissue cytokines in metabolic disorders linked to obesity. J Am Soc Nephrol. 2004 Nov;15:2792-800.
90. Hotamisligil GS, Arner P, Caro JF, Atkinson RL, Spiegelman BM. Increased adipose tissue expression of tumor necrosis factor-alpha in human obesity and insulin resistance. J Clin Invest. 1995 May;95:2409-15.

91. Tsigos C, Kyrou I, Chala E, Tsapogas P, Stavridis JC, Raptis SA, Katsilambros N. Circulating tumor necrosis factor alpha concentrations are higher in abdominal versus peripheral obesity. Metabolism. 1999 Oct;48:1332-5.
92. Winkler G, Kiss S, Keszthelyi L, Sapi Z, Ory I, Salamon F, Kovacs M, Vargha P, Szekeres O, et al. Expression of tumor necrosis factor (TNF)-alpha protein in the subcutaneous and visceral adipose tissue in correlation with adipocyte cell volume, serum TNF-alpha, soluble serum TNF-receptor-2 concentrations and C-peptide level. Eur J Endocrinol. 2003 Aug;149:129-35.
93. Hotamisligil GS, Murray DL, Choy LN, Spiegelman BM. Tumor necrosis factor alpha inhibits signaling from the insulin receptor. Proc Natl Acad Sci U S A. 1994 May 24;91:4854-8.
94. Grunfeld C, Feingold KR. The metabolic effects of tumor necrosis factor and other cytokines. Biotherapy. 1991;3:143-58.
95. Hotamisligil GS. Inflammatory pathways and insulin action. Int J Obes Relat Metab Disord. 2003 Dec;27 Suppl 3:S53-5.
96. Hirosumi J, Tuncman G, Chang L, Gorgun CZ, Uysal KT, Maeda K, Karin M, Hotamisligil GS. A central role for JNK in obesity and insulin resistance. Nature. 2002 Nov 21;420:333-6.
97. Jin D, Sun J, Huang J, He Y, Yu A, Yu X, Yang Z. TNF-alpha reduces g0s2 expression and stimulates lipolysis through PPAR-gamma inhibition in 3T3-L1 adipocytes. Cytokine. 2014 Oct;69:196-205.
98. Chen Z, Yu R, Xiong Y, Du F, Zhu S. A vicious circle between insulin resistance and inflammation in nonalcoholic fatty liver disease. Lipids Health Dis. 2017 Oct 16;16:203.
99. Tan X, Cao Z, Li M, Xu E, Wang J, Xiao Y. TNF-alpha downregulates CIDEC via MEK/ERK pathway in human adipocytes. Obesity (Silver Spring). 2016 May;24:1070-80.
100. Weisberg SP, McCann D, Desai M, Rosenbaum M, Leibel RL, Ferrante AW, Jr. Obesity is associated with macrophage accumulation in adipose tissue. J Clin Invest. 2003 Dec;112:1796-808.
101. Mohamed-Ali V, Goodrick S, Rawesh A, Katz DR, Miles JM, Yudkin JS, Klein S, Coppack SW. Subcutaneous adipose tissue releases interleukin-6, but not tumor necrosis factor-alpha, in vivo. J Clin Endocrinol Metab. 1997 Dec;82:4196-200.
102. Fried SK, Bunkin DA, Greenberg AS. Omental and subcutaneous adipose tissues of obese subjects release interleukin-6: depot difference and regulation by glucocorticoid. J Clin Endocrinol Metab. 1998 Mar;83:847-50.
103. Bastard JP, Jardel C, Bruckert E, Blondy P, Capeau J, Laville M, Vidal H, Hainque B. Elevated levels of interleukin 6 are reduced in serum and subcutaneous adipose tissue of obese women after weight loss. J Clin Endocrinol Metab. 2000 Sep;85:3338-42.
104. Heinrich PC, Castell JV, Andus T. Interleukin-6 and the acute phase response. Biochem J. 1990 Feb 1;265:621-36.
105. Covarrubias AJ, Horng T. IL-6 strikes a balance in metabolic inflammation. Cell Metab. 2014 Jun 3;19:898-9.
106. Mauer J, Chaurasia B, Goldau J, Vogt MC, Ruud J, Nguyen KD, Theurich S, Hausen AC, Schmitz J, et al. Signaling by IL-6 promotes alternative activation of macrophages to limit endotoxemia and obesity-associated resistance to insulin. Nat Immunol. 2014 May;15:423-30.
107. Braune J, Weyer U, Hobusch C, Mauer J, Bruning JC, Bechmann I, Gericke M. IL-6 Regulates M2 Polarization and Local Proliferation of Adipose Tissue Macrophages in Obesity. J Immunol. 2017 Apr 01;198:2927-34.

108. Plata-Salaman CR. Immunoregulators in the nervous system. Neurosci Biobehav Rev. 1991 Summer;15:185-215.
109. Kanda H, Tateya S, Tamori Y, Kotani K, Hiasa K, Kitazawa R, Kitazawa S, Miyachi H, Maeda S, et al. MCP-1 contributes to macrophage infiltration into adipose tissue, insulin resistance, and hepatic steatosis in obesity. J Clin Invest. 2006 Jun;116:1494-505.
110. Seijkens T, Kusters P, Chatzigeorgiou A, Chavakis T, Lutgens E. Immune cell crosstalk in obesity: a key role for costimulation? Diabetes. 2014 Dec;63:3982-91.
111. Kamei N, Tobe K, Suzuki R, Ohsugi M, Watanabe T, Kubota N, Ohtsuka-Kowatari N, Kumagai K, Sakamoto K, et al. Overexpression of monocyte chemoattractant protein-1 in adipose tissues causes macrophage recruitment and insulin resistance. J Biol Chem. 2006 Sep 8;281:26602-14.
112. Huh JY, Park YJ, Ham M, Kim JB. Crosstalk between adipocytes and immune cells in adipose tissue inflammation and metabolic dysregulation in obesity. Mol Cells. 2014 May;37:365-71.
113. Bruun JM, Lihn AS, Pedersen SB, Richelsen B. Monocyte chemoattractant protein-1 release is higher in visceral than subcutaneous human adipose tissue (AT): implication of macrophages resident in the AT. J Clin Endocrinol Metab. 2005 Apr;90:2282-9.
114. Guzman-Flores JM, Lopez-Briones S. [Cells of innate and adaptive immunity in type 2 diabetes and obesity]. Gac Med Mex. 2012 Jul-Aug;148:381-9.
115. Lynch L. Adipose invariant natural killer T cells. Immunology. 2014 Jul;142:337-46.
116. Ferrante AW, Jr. The immune cells in adipose tissue. Diabetes Obes Metab. 2013 Sep;15 Suppl 3:34-8.
117. Feuerer M, Herrero L, Cipolletta D, Naaz A, Wong J, Nayer A, Lee J, Goldfine AB, Benoist C, et al. Lean, but not obese, fat is enriched for a unique population of regulatory T cells that affect metabolic parameters. Nat Med. 2009 Aug;15:930-9.
118. Wu D, Molofsky AB, Liang HE, Ricardo-Gonzalez RR, Jouihan HA, Bando JK, Chawla A, Locksley RM. Eosinophils sustain adipose alternatively activated macrophages associated with glucose homeostasis. Science. 2011 Apr 08;332:243-7.
119. Wu L, Parekh VV, Gabriel CL, Bracy DP, Marks-Shulman PA, Tamboli RA, Kim S, Mendez-Fernandez YV, Besra GS, et al. Activation of invariant natural killer T cells by lipid excess promotes tissue inflammation, insulin resistance, and hepatic steatosis in obese mice. Proc Natl Acad Sci U S A. 2012 May 8;109:E1143-52.
120. Ohmura K, Ishimori N, Ohmura Y, Tokuhara S, Nozawa A, Horii S, Andoh Y, Fujii S, Iwabuchi K, et al. Natural killer T cells are involved in adipose tissues inflammation and glucose intolerance in diet-induced obese mice. Arterioscler Thromb Vasc Biol. 2010 Feb;30:193-9.
121. Lynch L, Nowak M, Varghese B, Clark J, Hogan AE, Toxavidis V, Balk SP, O'Shea D, O'Farrelly C, Exley MA. Adipose tissue invariant NKT cells protect against diet-induced obesity and metabolic disorder through regulatory cytokine production. Immunity. 2012 Sep 21;37:574-87.
122. Ji Y, Sun S, Xia S, Yang L, Li X, Qi L. Short term high fat diet challenge promotes alternative macrophage polarization in adipose tissue via natural killer T cells and interleukin-4. J Biol Chem. 2012 Jul 13;287:24378-86.
123. Schipper HS, Rakhshandehroo M, van de Graaf SF, Venken K, Koppen A, Stienstra R, Prop S, Meerding J, Hamers N, et al. Natural killer T cells in adipose tissue prevent insulin resistance. J Clin Invest. 2012 Sep;122:3343-54.

124. Ji Y, Sun S, Xu A, Bhargava P, Yang L, Lam KS, Gao B, Lee CH, Kersten S, Qi L. Activation of natural killer T cells promotes M2 Macrophage polarization in adipose tissue and improves systemic glucose tolerance via interleukin-4 (IL-4)/STAT6 protein signaling axis in obesity. J Biol Chem. 2012 Apr 20;287:13561-71.
125. de Heredia FP, Gomez-Martinez S, Marcos A. Obesity, inflammation and the immune system. Proc Nutr Soc. 2012 May;71:332-8.
126. Wajchenberg BL, Giannella-Neto D, da Silva ME, Santos RF. Depot-specific hormonal characteristics of subcutaneous and visceral adipose tissue and their relation to the metabolic syndrome. Horm Metab Res. 2002 Nov-Dec;34:616-21.
127. Jensen MD. Health consequences of fat distribution. Horm Res. 1997;48 Suppl 5:88-92.
128. Ostman J, Arner P, Engfeldt P, Kager L. Regional differences in the control of lipolysis in human adipose tissue. Metabolism. 1979 Dec;28:1198-205.
129. Rebuffe-Scrive M, Andersson B, Olbe L, Bjorntorp P. Metabolism of adipose tissue in intraabdominal depots of nonobese men and women. Metabolism. 1989 May;38:453-8.
130. Hellmer J, Marcus C, Sonnenfeld T, Arner P. Mechanisms for differences in lipolysis between human subcutaneous and omental fat cells. J Clin Endocrinol Metab. 1992 Jul;75:15-20.
131. Arner P, Hellstrom L, Wahrenberg H, Bronnegard M. Beta-adrenoceptor expression in human fat cells from different regions. J Clin Invest. 1990 Nov;86:1595-600.
132. Vikman HL, Savola JM, Raasmaja A, Ohisalo JJ. Alpha 2A-adrenergic regulation of cyclic AMP accumulation and lipolysis in human omental and subcutaneous adipocytes. Int J Obes Relat Metab Disord. 1996 Feb;20:185-9.
133. Bergman RN. Non-esterified fatty acids and the liver: why is insulin secreted into the portal vein? Diabetologia. 2000 Jul;43:946-52.
134. Bjorntorp P. Metabolic implications of body fat distribution. Diabetes Care. 1991 Dec;14:1132-43.
135. Foster MT, Shi H, Seeley RJ, Woods SC. Removal of intra-abdominal visceral adipose tissue improves glucose tolerance in rats: role of hepatic triglyceride storage. Physiol Behav. 2011 Oct 24;104:845-54.
136. Foster MT, Shi H, Softic S, Kohli R, Seeley RJ, Woods SC. Transplantation of non-visceral fat to the visceral cavity improves glucose tolerance in mice: investigation of hepatic lipids and insulin sensitivity. Diabetologia. 2011 Nov;54:2890-9.
137. Niesler CU, Siddle K, Prins JB. Human preadipocytes display a depot-specific susceptibility to apoptosis. Diabetes. 1998 Aug;47:1365-8.
138. Montague CT, Prins JB, Sanders L, Zhang J, Sewter CP, Digby J, Byrne CD, O'Rahilly S. Depot-related gene expression in human subcutaneous and omental adipocytes. Diabetes. 1998 Sep;47:1384-91.
139. Hauner H, Wabitsch M, Pfeiffer EF. Differentiation of adipocyte precursor cells from obese and nonobese adult women and from different adipose tissue sites. Horm Metab Res Suppl. 1988;19:35-9.
140. Tontonoz P, Hu E, Spiegelman BM. Stimulation of adipogenesis in fibroblasts by PPAR gamma 2, a lipid-activated transcription factor. Cell. 1994 Dec 30;79:1147-56.
141. Pasarica M, Sereda OR, Redman LM, Albarado DC, Hymel DT, Roan LE, Rood JC, Burk DH, Smith SR. Reduced adipose tissue oxygenation in human obesity: evidence for rarefaction, macrophage chemotaxis, and inflammation without an angiogenic response. Diabetes. 2009 Mar;58:718-25.

142. Sun K, Kusminski CM, Scherer PE. Adipose tissue remodeling and obesity. J Clin Invest. 2011 Jun;121:2094-101.
143. Farb MG, Ganley-Leal L, Mott M, Liang Y, Ercan B, Widlansky ME, Bigornia SJ, Fiscale AJ, Apovian CM, et al. Arteriolar function in visceral adipose tissue is impaired in human obesity. Arterioscler Thromb Vasc Biol. 2012 Feb;32:467-73.
144. Gealekman O, Guseva N, Hartigan C, Apotheker S, Gorgoglione M, Gurav K, Tran KV, Straubhaar J, Nicoloro S, et al. Depot-specific differences and insufficient subcutaneous adipose tissue angiogenesis in human obesity. Circulation. 2011 Jan 18;123:186-94.
145. Fresno M, Alvarez R, Cuesta N. Toll-like receptors, inflammation, metabolism and obesity. Arch Physiol Biochem. 2011 Jul;117:151-64.
146. Magnuson AM, Regan DP, Fouts JK, Booth AD, Dow SW, Foster MT. Diet-induced obesity causes visceral, but not subcutaneous, lymph node hyperplasia via increases in specific immune cell populations. Cell Prolif. 2017 Oct;50.
147. Kumari M, Heeren J, Scheja L. Regulation of immunometabolism in adipose tissue. Semin Immunopathol. 2017 Dec 5.
148. Despres JP. Abdominal obesity and cardiovascular disease: is inflammation the missing link? Can J Cardiol. 2012 Nov-Dec;28:642-52.
149. Lopes HF, Correa-Giannella ML, Consolim-Colombo FM, Egan BM. Visceral adiposity syndrome. Diabetol Metab Syndr. 2016;8:40.
150. McNelis JC, Olefsky JM. Macrophages, immunity, and metabolic disease. Immunity. 2014 Jul 17;41:36-48.
151. Li C, Xu MM, Wang K, Adler AJ, Vella AT, Zhou B. Macrophage polarization and meta-inflammation. Transl Res. 2018 Jan;191:29-44.
152. McGillicuddy FC, Harford KA, Reynolds CM, Oliver E, Claessens M, Mills KH, Roche HM. Lack of interleukin-1 receptor I (IL-1RI) protects mice from high-fat diet-induced adipose tissue inflammation coincident with improved glucose homeostasis. Diabetes. 2011 Jun;60:1688-98.
153. Finucane OM, Reynolds CM, McGillicuddy FC, Harford KA, Morrison M, Baugh J, Roche HM. Macrophage migration inhibitory factor deficiency ameliorates high-fat diet induced insulin resistance in mice with reduced adipose inflammation and hepatic steatosis. PLoS One. 2014;9:e113369.
154. Finucane OM, Reynolds CM, McGillicuddy FC, Roche HM. Insights into the role of macrophage migration inhibitory factor in obesity and insulin resistance. Proc Nutr Soc. 2012 Nov;71:622-33.
155. Suganami T, Ogawa Y. Adipose tissue macrophages: their role in adipose tissue remodeling. J Leukoc Biol. 2010 Jul;88:33-9.
156. Talukdar S, Oh DY, Bandyopadhyay G, Li D, Xu J, McNelis J, Lu M, Li P, Yan Q, et al. Neutrophils mediate insulin resistance in mice fed a high-fat diet through secreted elastase. Nat Med. 2012 Sep;18:1407-12.
157. Liu J, Divoux A, Sun J, Zhang J, Clement K, Glickman JN, Sukhova GK, Wolters PJ, Du J, et al. Genetic deficiency and pharmacological stabilization of mast cells reduce diet-induced obesity and diabetes in mice. Nat Med. 2009 Aug;15:940-5.
158. Sell H, Habich C, Eckel J. Adaptive immunity in obesity and insulin resistance. Nat Rev Endocrinol. 2012 Dec;8:709-16.

159. Nishimura S, Manabe I, Nagasaki M, Eto K, Yamashita H, Ohsugi M, Otsu M, Hara K, Ueki K, et al. CD8+ effector T cells contribute to macrophage recruitment and adipose tissue inflammation in obesity. Nat Med. 2009 Aug;15:914-20.
160. Harford KA, Reynolds CM, McGillicuddy FC, Roche HM. Fats, inflammation and insulin resistance: insights to the role of macrophage and T-cell accumulation in adipose tissue. Proc Nutr Soc. 2011 Nov;70:408-17.
161. Becker M, Levings MK, Daniel C. Adipose-tissue regulatory T cells: Critical players in adipose-immune crosstalk. Eur J Immunol. 2017 Nov;47:1867-74.
162. Rocha VZ, Folco EJ, Sukhova G, Shimizu K, Gotsman I, Vernon AH, Libby P. Interferon-gamma, a Th1 cytokine, regulates fat inflammation: a role for adaptive immunity in obesity. Circ Res. 2008 Aug 29;103:467-76.
163. Stefanovic-Racic M, Yang X, Turner MS, Mantell BS, Stolz DB, Sumpter TL, Sipula IJ, Dedousis N, Scott DK, et al. Dendritic cells promote macrophage infiltration and comprise a substantial proportion of obesity-associated increases in CD11c+ cells in adipose tissue and liver. Diabetes. 2012 Sep;61:2330-9.
164. Winer DA, Winer S, Shen L, Wadia PP, Yantha J, Paltser G, Tsui H, Wu P, Davidson MG, et al. B cells promote insulin resistance through modulation of T cells and production of pathogenic IgG antibodies. Nat Med. 2011 May;17:610-7.
165. DeFuria J, Belkina AC, Jagannathan-Bogdan M, Snyder-Cappione J, Carr JD, Nersesova YR, Markham D, Strissel KJ, Watkins AA, et al. B cells promote inflammation in obesity and type 2 diabetes through regulation of T-cell function and an inflammatory cytokine profile. Proc Natl Acad Sci U S A. 2013 Mar 26;110:5133-8.
166. Tobin LM, Mavinkurve M, Carolan E, Kinlen D, O'Brien EC, Little MA, Finlay DK, Cody D, Hogan AE, O'Shea D. NK cells in childhood obesity are activated, metabolically stressed, and functionally deficient. JCI Insight. 2017 Dec 21;2.
167. Viel S, Besson L, Charrier E, Marcais A, Disse E, Bienvenu J, Walzer T, Dumontet C. Alteration of Natural Killer cell phenotype and function in obese individuals. Clin Immunol. 2017 Apr;177:12-7.
168. Campbell KS, Hasegawa J. Natural killer cell biology: an update and future directions. J Allergy Clin Immunol. 2013 Sep;132:536-44.
169. Klein S, Allison DB, Heymsfield SB, Kelley DE, Leibel RL, Nonas C, Kahn R, Association for Weight M, Obesity P, et al. Waist circumference and cardiometabolic risk: a consensus statement from shaping America's health: Association for Weight Management and Obesity Prevention; NAASO, the Obesity Society; the American Society for Nutrition; and the American Diabetes Association. Diabetes Care. 2007 Jun;30:1647-52.
170. Tchkonia T, Thomou T, Zhu Y, Karagiannides I, Pothoulakis C, Jensen MD, Kirkland JL. Mechanisms and metabolic implications of regional differences among fat depots. Cell Metab. 2013 May 7;17:644-56.
171. Kelley DE, Thaete FL, Troost F, Huwe T, Goodpaster BH. Subdivisions of subcutaneous abdominal adipose tissue and insulin resistance. Am J Physiol Endocrinol Metab. 2000 May;278:E941-8.
172. Karpe F, Pinnick KE. Biology of upper-body and lower-body adipose tissue--link to whole-body phenotypes. Nat Rev Endocrinol. 2015 Feb;11:90-100.
173. Manolopoulos KN, Karpe F, Frayn KN. Gluteofemoral body fat as a determinant of metabolic health. Int J Obes (Lond). 2010 Jun;34:949-59.

174. Snijder MB, Dekker JM, Visser M, Bouter LM, Stehouwer CD, Kostense PJ, Yudkin JS, Heine RJ, Nijpels G, Seidell JC. Associations of hip and thigh circumferences independent of waist circumference with the incidence of type 2 diabetes: the Hoorn Study. Am J Clin Nutr. 2003 May;77:1192-7.
175. Snijder MB, Visser M, Dekker JM, Goodpaster BH, Harris TB, Kritchevsky SB, De Rekeneire N, Kanaya AM, Newman AB, et al. Low subcutaneous thigh fat is a risk factor for unfavourable glucose and lipid levels, independently of high abdominal fat. The Health ABC Study. Diabetologia. 2005 Feb;48:301-8.
176. Terry RB, Stefanick ML, Haskell WL, Wood PD. Contributions of regional adipose tissue depots to plasma lipoprotein concentrations in overweight men and women: possible protective effects of thigh fat. Metabolism. 1991 Jul;40:733-40.
177. Frayn KN. Adipose tissue as a buffer for daily lipid flux. Diabetologia. 2002 Sep;45:1201-10.
178. Foster MT, Softic S, Caldwell J, Kohli R, de Kloet AD, Seeley RJ. Subcutaneous Adipose Tissue Transplantation in Diet-Induced Obese Mice Attenuates Metabolic Dysregulation While Removal Exacerbates It. Physiological reports. 2013 Aug;1.
179. Koster A, Stenholm S, Alley DE, Kim LJ, Simonsick EM, Kanaya AM, Visser M, Houston DK, Nicklas BJ, et al. Body fat distribution and inflammation among obese older adults with and without metabolic syndrome. Obesity (Silver Spring). 2010 Dec;18:2354-61.
180. Pinnick KE, Nicholson G, Manolopoulos KN, McQuaid SE, Valet P, Frayn KN, Denton N, Min JL, Zondervan KT, et al. Distinct developmental profile of lower-body adipose tissue defines resistance against obesity-associated metabolic complications. Diabetes. 2014 Nov;63:3785-97.
181. Xu H, Barnes GT, Yang Q, Tan G, Yang D, Chou CJ, Sole J, Nichols A, Ross JS, et al. Chronic inflammation in fat plays a crucial role in the development of obesity-related insulin resistance. J Clin Invest. 2003 Dec;112:1821-30.
182. Goodpaster BH, Thaete FL, Simoneau JA, Kelley DE. Subcutaneous abdominal fat and thigh muscle composition predict insulin sensitivity independently of visceral fat. Diabetes. 1997 Oct;46:1579-85.
183. Abate N, Garg A, Peshock RM, Stray-Gundersen J, Grundy SM. Relationships of generalized and regional adiposity to insulin sensitivity in men. J Clin Invest. 1995 Jul;96:88-98.
184. Kissebah AH, Vydelingum N, Murray R, Evans DJ, Hartz AJ, Kalkhoff RK, Adams PW. Relation of body fat distribution to metabolic complications of obesity. J Clin Endocrinol Metab. 1982 Feb;54:254-60.
185. Krotkiewski M, Bjorntorp P, Sjostrom L, Smith U. Impact of obesity on metabolism in men and women. Importance of regional adipose tissue distribution. J Clin Invest. 1983 Sep;72:1150-62.
186. Salans LB, Knittle JL, Hirsch J. The role of adipose cell size and adipose tissue insulin sensitivity in the carbohydrate intolerance of human obesity. J Clin Invest. 1968 Jan;47:153-65.
187. Salans LB, Cushman SW, Weismann RE. Studies of human adipose tissue. Adipose cell size and number in nonobese and obese patients. J Clin Invest. 1973 Apr;52:929-41.
188. Weyer C, Foley JE, Bogardus C, Tataranni PA, Pratley RE. Enlarged subcutaneous abdominal adipocyte size, but not obesity itself, predicts type II diabetes independent of insulin resistance. Diabetologia. 2000 Dec;43:1498-506.
189. Cancello R, Zulian A, Gentilini D, Maestrini S, Della Barba A, Invitti C, Cora D, Caselle M, Liuzzi A, Di Blasio AM. Molecular and morphologic characterization of superficial- and

deep-subcutaneous adipose tissue subdivisions in human obesity. Obesity (Silver Spring). 2013 Dec;21:2562-70.
190. Golan R, Shelef I, Rudich A, Gepner Y, Shemesh E, Chassidim Y, Harman-Boehm I, Henkin Y, Schwarzfuchs D, et al. Abdominal superficial subcutaneous fat: a putative distinct protective fat subdepot in type 2 diabetes. Diabetes Care. 2012 Mar;35:640-7.
191. Kim SH, Chung JH, Song SW, Jung WS, Lee YA, Kim HN. Relationship between deep subcutaneous abdominal adipose tissue and metabolic syndrome: a case control study. Diabetol Metab Syndr. 2016;8:10.
192. Cox-York K, Wei Y, Wang D, Pagliassotti MJ, Foster MT. Lower body adipose tissue removal decreases glucose tolerance and insulin sensitivity in mice with exposure to high fat diet. Adipocyte. 2015 Jan-Mar;4:32-43.
193. Kissebah AH, Krakower GR. Regional adiposity and morbidity. Physiol Rev. 1994 Oct;74:761-811.
194. Miyazaki Y, DeFronzo RA. Visceral fat dominant distribution in male type 2 diabetic patients is closely related to hepatic insulin resistance, irrespective of body type. Cardiovasc Diabetol. 2009 Aug 5;8:44.
195. Gastaldelli A, Sironi AM, Ciociaro D, Positano V, Buzzigoli E, Giannessi D, Lombardi M, Mari A, Ferrannini E. Visceral fat and beta cell function in non-diabetic humans. Diabetologia. 2005 Oct;48:2090-6.
196. Kim S, Cho B, Lee H, Choi K, Hwang SS, Kim D, Kim K, Kwon H. Distribution of abdominal visceral and subcutaneous adipose tissue and metabolic syndrome in a Korean population. Diabetes Care. 2011 Feb;34:504-6.
197. Kaess BM, Pedley A, Massaro JM, Murabito J, Hoffmann U, Fox CS. The ratio of visceral to subcutaneous fat, a metric of body fat distribution, is a unique correlate of cardiometabolic risk. Diabetologia. 2012 Oct;55:2622-30.
198. He H, Ni Y, Chen J, Zhao Z, Zhong J, Liu D, Yan Z, Zhang W, Zhu Z. Sex difference in cardiometabolic risk profile and adiponectin expression in subjects with visceral fat obesity. Transl Res. 2010 Feb;155:71-7.
199. Yeoh AJ, Pedley A, Rosenquist KJ, Hoffmann U, Fox CS. The Association Between Subcutaneous Fat Density and the Propensity to Store Fat Viscerally. J Clin Endocrinol Metab. 2015 Aug;100:E1056-64.
200. Pessin JE, Kwon H. How does high-fat diet induce adipose tissue fibrosis? J Investig Med. 2012 Dec;60:1147-50.
201. Suganami T, Tanaka M, Ogawa Y. Adipose tissue inflammation and ectopic lipid accumulation. Endocr J. 2012;59:849-57.
202. Hotamisligil GS, Shargill NS, Spiegelman BM. Adipose expression of tumor necrosis factor-alpha: direct role in obesity-linked insulin resistance. Science. 1993 Jan 1;259:87-91.
203. Gray SL, Vidal-Puig AJ. Adipose tissue expandability in the maintenance of metabolic homeostasis. Nutr Rev. 2007 Jun;65:S7-12.
204. Foster MT. So as we worry we weigh: Visible burrow system stress and visceral adiposity. Physiol Behav. 2017 Sep 1;178:151-6.
205. Weber RV, Buckley MC, Fried SK, Kral JG. Subcutaneous lipectomy causes a metabolic syndrome in hamsters. Am J Physiol Regul Integr Comp Physiol. 2000 Sep;279:R936-43.

CHAPTER 2: ROLE OF THE MESENTERIC LYMPH NODES IN METABOLIC AND IMMUNE HOMEOSTASIS

Overview

Background: Our lab has recently reported that diet-induced obesity causes mesenteric lymph node (MLN) fibrosis, resulting in localized immunologic dysfunction. However, our understanding of how the MLNs may contribute to obesity-associated pathophysiology is unclear. We hypothesized that MLN dysfunction would contribute to metabolic derangements associated with obesity and that without functional MLNs obesity-associated disease reversal would not occur. To investigate this we asked: Does MLN ablation induce or exacerbate obesity-associated metabolic disease (experiment 1), Can Pirfenidone treatment attenuate obesity-induced MLN fibrosis and metabolic dysfunction (experiment 2), and Do MLNs contribute to disease reversal with Pirfenidone treatment (experiment 3). *Methods:* Male C57BL/6 mice were utilized for all experiments. Experiment 1: mice received either MLN ablation (Ablation) or sham surgery (Sham), and then were placed onto either a high-fat diet (HFD) or low-fat diet (LFD) for 8 wk. Immune cells from mesenteric (MAT) and inguinal (IAT) adipose tissue, mesenteric (MLNs) and inguinal (ILNs) lymph nodes, jejunum, and spleen were characterized by flow cytometry. Hepatic insulin sensitivity was assessed by Western blot. Experiment 2: mice received either a standard rodent chow (CH) or HFD for 6 wk, after which they either began receiving (+P) or not receiving (-P) Pirfenidone treatment in food for 4 wk. MLN fibrosis was assess by histology, and circulating markers of inflammation and metabolism were assessed by multiplex assay. Experiment 3: mice received either HFD or LFD for 10 wk, after which they

either received MLN ablation (Ablation) or sham surgery (Sham). Then mice either began receiving (+P) or not receiving (+P) Pirfenidone treatment in food for 4 wk. Glucose tolerance was assessed after a 6 hr fast followed by intraperitoneal injection of 2g/kg glucose solution. Immune cells from MAT, MLNs, liver, spleen, jejunum and ileum were characterized by flow cytometry. *Results:* We found that MLN dysfunction in HFD-induced obese mice leads to metabolic and immune alterations through the promotion of visceral adiposity and T cell infiltration, impairment of insulin signaling within the liver, and compromise of jejunal immune function. Additionally, that MLN fibrosis associated with HFD-induced obesity contributes to metabolic adaptations and that Pirfenidone treatment can attenuate this obesity-induced MLN fibrosis and metabolic dysfunction. Finally, we found that Pirfenidone treatment is unable to fully restore the MLN restricted phenotype. *Conclusions:* MLN dysfunction, either by surgical manipulation or HFD-induced obesity, significantly contributes to the development and progression of metabolic disease associated with obesity.

Introduction

Obesity is highly associated with chronic (1, 2) and infectious disease (3-5) such as cardiovascular disease, cancer, and influenza. In general, diseases associated with obesity are driven largely by deleterious adaptations which occur broadly throughout the body such as immune dysfunction (6, 7), gut dysbiosis (8, 9), dyslipidemia (10), hepatic steatosis (11), and insulin resistance (12). Recent studies highlight the essential role of systemic chronic inflammation as an underlying driver of obesity-driven health dysfunction and mortality (13-17). Normally, an inflammatory response includes the temporally restricted upregulation of inflammatory activities in response to a threat which resolve once the threat has been removed. Certain lifestyle risk factors, however, such as obesity have been shown to inhibit the resolution

of acute inflammation, in turn promoting the development of systemic chronic inflammation (17). Although, total adiposity alone does not fully predict disease risk.

The distribution of adipose tissue throughout the body highly correlates with disease susceptibility (18-20). Excess visceral adiposity, fat stored within the intra-abdominal cavity among organs, is shown to confer the greatest disease risk when compared to lower body subcutaneous adipose tissue (21-23). Visceral obesity resulting from excessive visceral fat accumulation, has been shown to accelerate aging and increase the risk for cardiometabolic diseases (17, 22, 24, 25). In humans, visceral adipose tissue (VAT) consists of the omental and mesenteric adipose depots, which surround the stomach and intestines—respectively (26, 27). The increased disease risk associated with VAT is due to inherent depot differences, namely proximity to and a shared blood supply with the liver and gastrointestinal (GI) tract (27-30), as well as tissue metabolic and immunologic activity (17, 31). Recent work highlights the role of the GI tract in VAT expansion and dysfunction (32, 33). Specifically, gut dysbiosis and epithelial barrier dysfunction have been shown to increase the translocation of inflammatory stimuli from the gut to surrounding organs including the liver and mesenteric adipose depot (27, 28, 34). Indicating that alterations within the GI tract can initiate inflammatory processes and metabolic dysfunction.

The GI tract serves as an interface for nutrient digestion and absorption, as well as protects us from our environment (35). As such, the gut is continuously exposed to both innocuous and harmful stimuli. As a result, the GI tract makes up our bodies largest immune reservoir and consists of the gut-associated lymphoid tissue (GALT) and draining lymph nodes (35). The mesenteric lymph nodes (MLNs), housed within mesenteric adipose tissue (MAT), constitute the main mesenteric lymph node chain of gut draining lymph nodes (36). Here they

play an essential role in the maintenance and protection of MAT and draining sections of the GI tract (distal duodenum, jejunum, ileum, cecum, and proximal ascending colon) (36-43), serving as inductive sites for adaptive immune responses aimed at either promoting tolerance or pathogen clearance (44, 45). As such, MLNs are critical for overall maintenance and protection of abdominal tissues (46). Despite their importance and overall vulnerability to obesity-induced changes in MAT and the GI tract, few studies have directly examined the impact of obesity on MLN physiology and function.

We have previously shown that HFD-induced obesity reduces MLN function within mice (47). Specifically, HFD fed animals displayed an increase in MLN fibrosis with a concomitant reduction in immune cell number when compared to chow fed controls. Additionally, immune cells from the MLNs of HFD fed mice showed an impaired proliferative capacity when challenged *in vitro*. We have extended this study by demonstrating several HFD-induced structural and cellular modifications within MLNs via electron microscopy, including an increase in collagen deposition, cellular debris, and damaged/dead cells (48). Thus, we speculate that excessive collagen production and deposition within MLNs impairs the flow of lymphatic fluid and disrupts cell-to-cell communication. Altogether, these data support the negative impact of MAT accumulation on MLN physiology and function. Our findings are corroborated by previous work demonstrating that lymph node fibrosis leads to lymphatic vessel obstruction and degeneration (5), as well as impairment of immune cell migration (49, 50). Collectively resulting in impairment of lymphatic flow and normal immune function.

Here we investigate the contribution of the MLNs on the pathophysiology of disease associated with HFD-induced obesity. We hypothesize that MLN dysfunction will contribute to metabolic derangements associated with obesity and that without functional MLNs obesity-

associated disease reversal will not occur. This is tested with three different experiments: experiment 1, to examine if removal of the MLNs could induce or exacerbate obesity-associated metabolic disease within mice; experiment 2, to determine if treatment with the anti-fibrotic/anti-inflammatory medication Pirfenidone could attenuate obesity-induced MLN fibrosis and metabolic dysfunction within mice; and experiment 3, to characterize the role of the MLNs in Pirfenidone-induced reversal of metabolic dysfunction associated with obesity and fibrosis. Pirfenidone is a commonly prescribed medication for the treatment of numerous disorders such as idiopathic pulmonary fibrosis (51, 52) and works by exerting broad anti-fibrotic and anti-inflammatory effects (53-57). Primary mechanisms by which Pirfenidone reduces fibrosis and inflammation include 1) the inhibition of TGF-β production and activity (58-63), and 2) inhibition of nuclear factor kappa B (NF-κB) dependent cytokine production, comprising TNF, IL-6, interferon gamma (IFNγ), and IL-1 (64-69).

Methods

Animals and Experimental Design

C57/BL6 male mice (2-3 months old) were obtained from the Jackson Laboratory. Mice were singly housed in a temperature (25°C) and humidity-controlled (50-60%) environment on a 12 h:12 h light-dark cycle. Prior to initiating experimental procedures, mice were acclimatized to the housing conditions for 1 week. All animal procedures were reviewed and approved by the Colorado State University Institutional Animal Care and Use Committee. All mice were allowed *ad libitum* access to food and water for the duration of their studies. Body weight and food intake were measured weekly.

Experiment 1 – Does MLN ablation induce or exacerbate obesity-associated metabolic disease? Mice were divided into two surgical intervention groups, MLN ablation (ablation, n=20)

and sham (sham, n=20). After 1 week of recovery, ablation and sham groups were further divided into two diet groups, purified low-fat diet (LFD) (TD.08485; ENVIGO; 13% kcal from fat, 67.9% carbohydrate, and 19.1% protein) and purified high-fat diet (HFD) (TD.88137; ENVIGO; 42% kcal from fat, 42.7% carbohydrate, and 15.2% protein) for 8 weeks. This resulted in four experimental groups: Ablation-LFD (n=10), Sham-LFD (n=10), Ablation-HFD (n=9), and Sham-HFD (n=10) (*Figure 1.1*). Prior to termination, insulin or normal saline solution was administered to mice for downstream assessment of hepatic insulin sensitivity. Tissues were collected for immune cell characterization by flow cytometry (MAT, inguinal adipose tissue (IAT), MLNs, inguinal lymph nodes (ILNs), jejunum, and spleen), and insulin sensitivity by Western blot (liver).

Figure 1.1. Study design for experiment 1.

Experiment 2 – Can Pirfenidone treatment attenuate obesity-induced MLN fibrosis and metabolic dysfunction? Mice received either standard rodent chow (CH, n=6) (2918 Irradiated Teklad Global 18% Protein Rodent Diet; ENVIGO; 6.2% kcal from fat, 44.2% kcal from carbohydrate, and 18.6% kcal from protein) or purified high-fat diet (HFD, n=6) (TD.88137; ENVIGO) for 6 weeks. After which, mice either received (+P) or did not receive (-P)

Pirfenidone (0.5% (w/w); B2288; APExBIO) in their food for 4 weeks. This resulted in four experimental groups: CH+P (n=3), CH-P (n=3), HFD+P (n=3), and HFD-P (n=3) (*Figure 1.2*). Plasma and MLNs were collected for collagen quantification by histology and cytokine analysis by magnetic bead-based multiplex assay.

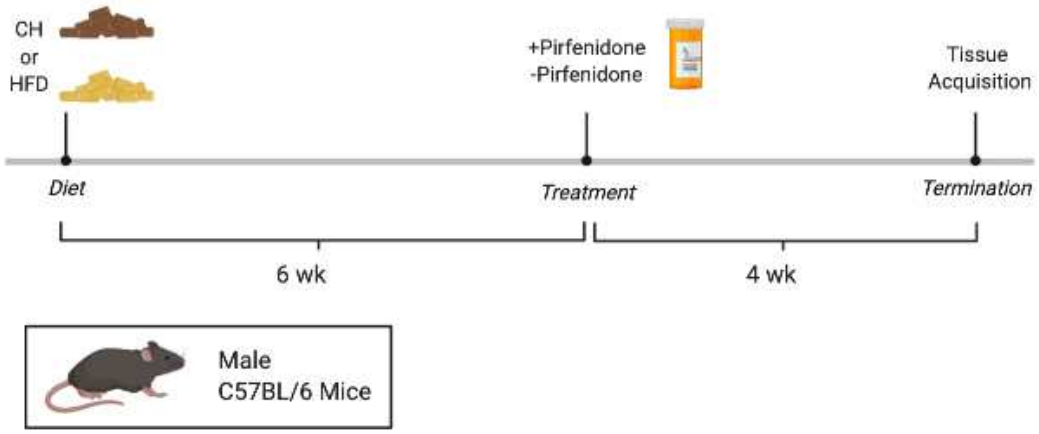

Figure 1.2. Study design for experiment 2.

Experiment 3 – Do MLNs contribute to disease reversal associated with Pirfenidone treatment? Mice received purified high-fat diet (HFD, n=30) (TD.88137; ENVIGO) for 10 weeks. Then were divided into two surgical intervention groups, MLN ablation (ablation, n=15) and sham (sham, n=15). After 1 week of recovery, mice either received (+P) or did not receive (-P) Pirfenidone (0.5% (w/w); B2288; APExBIO) in their food for 4 weeks. This resulted in four experimental groups: Ablation+P (n=6), Sham+P (n=6), Ablation-P (n=5), and Sham-P (n=7) (*Figure 1.3*). One wk prior to surgical intervention and termination, glucose tolerance tests were performed. Tissues were collected for immune cell characterization by flow cytometry (MAT, MLNs, spleen, jejunum, ileum, and liver).

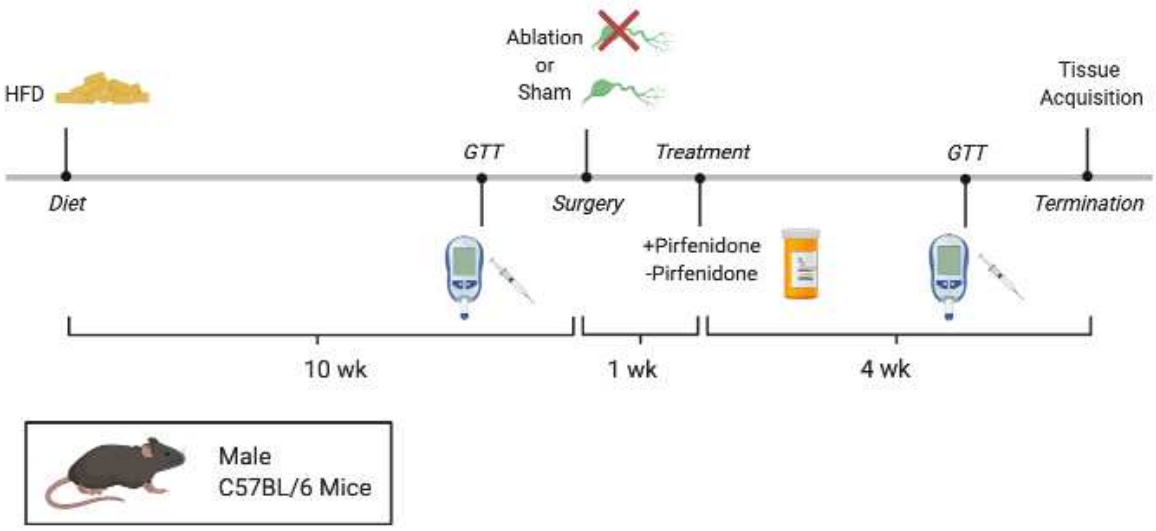

Figure 1.3. Study design for experiment 3.

Surgical Procedures

For mice in experiment 1 and 3, a small mid-ventral abdominal incision was made to visualize MLNs using a dissecting scope, while anesthetized with Fluriso™ (Isoflurane, USP; 502017; VetOne). For ablation groups, MLNs were cauterized to achieve lymph node removal. Care was taken to avoid injuring the surrounding vasculature. For sham groups, an equal area of cauterization was performed to intra-abdominal adipose tissue. Once complete, the peritoneum was sutured shut and abdominal skin was closed using wound clips. All mice received 0.03 mL of Meloxicam SR (sustained release) (2 mg/mL) subcutaneously, for 24 h post-operative pain management or as needed.

Glucose Tolerance Test (GTT)

Mice in experiment 3 were fasted for 6 h, after which baseline blood glucose concentrations were determined from tail vein blood using a glucometer (FreeStyle Lite; Abbott). Subsequently, about 100 µL of whole blood was collected into microcentrifuge tubes for serum isolation. Next mice were given an intraperitoneal (IP) injection of glucose solution (2

g of glucose/kg of body weight; D-Glucose (G 5400; Millipore Sigma)). Serial blood glucose measurements were taken post-injection at 15-, 30-, 45-, 60-, and 120-min via the tail vein. Whole blood was also collected at 15- and 30-min post-injection. Whole blood was allowed to clot at room temp for 10 min, serum was then isolated and stored at -80°C.

Insulin and Saline Injections

Mice in experiment 1 were fasted for 4 h, after which baseline blood glucose concentrations were measured as previously described. Next, mice were given an IP injection of either insulin solution (1 mU of insulin/g of body weight; Humulin R Insulin (100 U/mL, R-100; Eli Lilly)) or normal saline (for control mice). Post-injection, animals rested for 15 min and then were terminated as described below.

Termination and Tissue Collection

Mice were anesthetized with isoflurane and euthanized by rapid decapitation. Systemic whole blood was collected into microcentrifuge tubes for either serum or plasma isolation. Serum was isolated from clotted whole blood and stored at -80°C. Plasma was isolated from EDTA-treated whole blood, and stored at -80°C. Excised mesenteric and inguinal lymph nodes were placed into 1X RPMI-1640 (10-041-CV; Corning) containing 2% fetal bovine serum (FBS) (F-0050-A; Atlas Biologics) and stored on ice. Excised mesenteric, epididymal, perirenal, inguinal, and brown adipose tissue depots were weighed. Collected mesenteric and inguinal adipose depots were placed into 1X RPMI-1640 containing 2% FBS and stored on ice. Excised livers, with the gallbladder removed, were weighed and then either snap frozen in liquid nitrogen (experiment 1) or placed into MACs buffer [0.5% BSA (A7030-100G; Millipore Sigma), 10% 10X PBS, 2 mM Na_2EDTA (E5134; Millipore Sigma)] containing 2% FBS and stored on ice (experiment 3). Excised spleens where weighed and placed into 1X RPMI-1640 containing 2%

FBS, and then stored on ice. Excised portions of the jejunum and ileum were measured and then placed into 1X Phosphate-buffered saline (PBS) containing 2% FBS and stored on ice.

Preparation of Cell Lysates and Western Blotting

Frozen livers (experiment 1) were homogenized on ice in lysis buffer [10 mM Tris-HCl pH 7.4 (410901; J.T.Baker™), 150 mM NaCl (S271-500; Fisher Scientific), 5 mM Na_2EDTA (E5134; Millipore Sigma), 1% Triton™ X-100 (BP151-100; Fisher Scientific), 1% protease inhibitor cocktail (P8340; Millipore Sigma), and 1% phosphatase inhibitor cocktail 3 (P0044; Millipore Sigma)]. Samples were rotated for 30 min at 4°C, and then centrifuged at 12,000 g for 30 min. Total protein concentration was determined by the Biuret Method (Total Protein Reagent, T1949; Millipore Sigma).

Equivalent amounts of protein were subjected to capillary gel electrophoresis, using the Wes-Simple Western™ method (Protein Simple) (70) according to manufactures instructions. The 12-230 kDa Wes Separation Module (SM-W004, Protein Simple) was used for all samples. In conjunction, the Anti-Rabbit/Mouse Detection Module (DM-001 or 002, Protein Simple) was also used. The sample plate was then centrifuged at 1000 g for 10 min at room temp and run under standard conditions. Protein expression was measured by chemiluminescence and quantified as area under the curve using the Compass for Simple Western software (Protein Simple). Proteins were detected with the following primary antibodies: AKT (pan) (clone C67E7; 4691; Cell Signaling Technology), and AKT [p Ser473] (AF887-SP; Novus Biologicals).

Collagen Determination

Excised MLNs (experiment 2) were collected and then fixed in 10% neutral buffered formalin solution (HT501128-4L; Sigma) for 24 h. Lymph nodes were then embedded in

paraffin wax for Weigert's Hematoxylin staining and Picrosirius Red staining (SRS999; Scytek Laboratories Inc.) for collagen identification. Stained samples were imaged with an Olympus BX63 microscope using polarized light microscopy and analyzed using cellSens Dimension imaging software version 2.2 (Olympus). Collagen area within lymph nodes was analyzed using ImageJ software for Windows.

Blood Parameters

Serum insulin levels (experiment 3) were determined using a mouse-specific enzyme-linked immunosorbent assay (ELISA) kit (90080; Crystal Chem) per the manufacturer's instructions. Plasma insulin, leptin, resistin, monocyte chemoattractant protein-1 (MCP-1), tumor necrosis factor (TNF), plasminogen activator inhibitor-1 (PAI-1), and interleukin-6 (IL-6) concentrations (experiment 2) were determined using a magnetic bead-based multiplex assay (Millipore Sigma) per the manufacturer's instructions and analyzed on a Luminex 200™ analyzer (Millipore Sigma) with xPONENT® 3.1 software (Millipore Sigma).

Immune Cell Isolations for Flow Cytometry

All tissues taken for immune cell isolation (experiment 1 and 3) were kept on ice and immediately processed. *Spleens* were forced through 40 μm cell strainers (501050134; Fisher Scientific) using syringe plungers, with 1X RPMI-1640 containing 2% FBS. Red blood cells (RBC) in spleen suspensions were lysed using 1X RBC lysis buffer (155 mM NH_4Cl, 12 mM $NaHCO_3$, 0.1mM Na_2EDTA). Cells were then washed and resuspended with 1X PBS containing 2% FBS. *Lymph nodes* had surrounding adipose tissue removed and were then forced through 40 μm cell strainers using syringe plungers, with 1X RPMI-1640 containing 2% FBS. Cells were then washed and resuspended with 1X PBS containing 2% FBS. *Adipose tissues* were minced and then incubated with digestion solution [M199 (12340-030; Gibco) and 2 mg/mL Collagenase

type II (LS004176; Worthington Labs)]. Samples were then diluted with 1X PBS containing 2% FBS, titrated, and forced through 40 μm cell strainers. Cells were then washed and resuspended with 1X PBS containing 2% FBS. *Small intestine* segments were cut longitudinally and cleaned. Mucus was removed by washing tissues with removal solution [1X PBS, 2% FBS, 5 mM NAC (A8199; Millipore Sigma)]. Epithelial cells were then separated by washing tissues with removal solution (1X PBS, 2% FBS, 5 mM N_a2EDTA). Tissues were then minced and incubated with digestion solution [1X MEM (11090081; Gibco), 5 mg/mL Collagenase type I (LS004196; Worthington Labs), 1:40 DNAse 1 (D4263; Millipore Sigma), 1:40 Trypsin inhibitor (T6522; Millipore Sigma)]. Samples were then diluted with 1X PBS containing 2% FBS, titrated, and forced through 40 μm cell strainers. Cells then had a final wash with mucus removal solution, and then were washed and resuspended with 1X PBS containing 2% FBS. *Livers* were forced through 40 μm cell strainers using syringe plungers, with MACs buffer containing 2% FBS. Immune cells were enriched for by centrifugation with Lympholyte®-M cell separation media (CL5035, Cedarlane) and then washed with MACs buffer containing 2% FBS. Cells were then washed and resuspended with 1X PBS containing 2% FBS. Post-acquisition, cells were counted with trypan blue.

Flow Cytometry

Cell suspensions were incubated on ice in the dark for 30 min with LIVE/DEAD fixable yellow (L34967; Invitrogen) for dead cell discrimination. Nonspecific antibody binding was then blocked by incubating cells with TruStain Fc block (clone 93; 101320; Biolegend) on ice for 10 min. Cells were first stained for cell surface markers by incubating with fluorescently conjugated monoclonal antibodies at 4°C for 30 min in the dark. Then cells were prepared for intranuclear staining, using the Foxp3/Transcription Factor Staining Buffer Set (00-5523-00, eBioscience)

according to manufactures instructions. Super Bright Staining buffer (SB-4400-42; Invitrogen) was used per manufactures instructions in stain master mixes which contained more than one polymer dye.

The following fluorescent antibodies were used for cell surface staining: CD25 BV421 (clone PC61; Biolegend), CD11b eF450 (clone M1/70; eBioscience), CD45.2 BV570 (clone 104; Biolegend), TCR γ/δ BV605 (clone GL3;Biolegend), CD19 AF488 (clone 6D5; Biolegend), F4/80 PE (clone BM8; eBioscience), CD8a PE/Cy5 (clone 53-6.7; eBioscience), GR-1 PE/Cy7 (clone RB6-8C5; eBioscience), CD3ε PerCP/Cy5.5 (clone 145-2C11; Biolegend), CD4 AF647 (clone RM4-5; Biolegend), Ly6C AF700 (clone HK1.4; Biolegend), MHC2 APC (clone M5/114.15.2; eBioscience), CD11c APC/Fire750 (clone N418; Biolegend), CD103 BV510 (clone 2E7; Biolegend), integrin α4β7 PerCP/eF710 (clone DATK32; Invitrogen). The following fluorescently conjugated antibody was used for intranuclear staining: Foxp3 AF532 (clone FJK-16s; eBioscience).

All samples were analyzed using a Cytek Biosciences Aurora spectral flow cytometer and FlowJo™ Software (Becton Dickinson). Cells were gated on leukocytes based on characteristic forward and side scatter profiles. Individual cell populations were identified according to their presence of specific fluorescent-labeled antibodies.

Statistical Analysis

All statistical analysis was performed with GraphPad Prism version 8.4.2 for macOS (GraphPad Software). Data are presented as mean ± standard error of the mean (SEM). Significance was considered with a P value of < 0.05. A repeated measures two-way ANOVA with Tukey's post hoc test was used for variables measured over time. Whereas, a two-way ANOVA with Tukey's post hoc test was used for all other comparisons, with a diet × treatment

or surgery × treatment design. ANOVA assumptions were checked and if data failed to meet these assumptions the data were log transformed and then re-analyzed. To determine the magnitude of treatment effect, a Hedges' *g* effect size was calculated. A *g* equal to 0.2 is interpreted as a small effect, a *g* equal to 0.5 as a medium effect, and a *g* equal to 0.8 as a large effect.

Results

First, we sought to determine whether MLN removal would lead to metabolic dysfunction (experiment 1). Here, cauterization was used to remove the MLNs. At termination the areas of lymph node removal were well vascularized, and no necrosis was visible. We found that cauterization was able to successfully remove 80-100% of the MLNs within ablation groups. Body weight gained over the 8 wk experiment, reported as change in body weight (g), and cumulative food intake (kcals) were not found to be affected by MLN ablation (*Table 1.1*). However, both were significantly increased by HFD feeding relative to LFD controls. Similarly, we found that HFD feeding increased intrabdominal (mesenteric, epididymal, perirenal), subcutaneous (inguinal), and brown adipose depot mass (*Table 1.1*). Although MLN ablation did not significantly increase MAT mass within HFD mice (P=0.2674), using a Hedges' *g* score, it was determined that the magnitude of this effect was biologically relevant (Hedges' g=-0.81). This observation was not recapitulated within LFD mice (Hedges' g=0.16, P=0.9658).

Table 1.1. General and metabolic characteristics

	Sham-LFD	Ablation-LFD	Sham-HFD	Ablation-HFD
Change in body weight (g)	4.00 ± 0.64	3.88 ± 0.80	10.18 ± 0.35§‡	10.43 ± 0.77§‡
Cumulative food intake (kcals)	566.10 ± 12.71	569.00 ± 15.68	679.70 ± 14.44§‡	666.30 ± 11.07§‡
Mesenteric fat (g)	0.53 ± 0.05	0.49 ± 0.06	0.75 ± 0.06†	0.92 ± 0.10§‡
Inguinal fat (g)	0.71 ± 0.07	0.68 ± 0.08	1.17 ± 0.04§‡	1.12 ± 0.08§‡
Epididymal fat (g)	1.22 ± 0.15	1.00 ± 0.05	2.01 ± 0.09§‡	2.13 ± 0.15§‡
Perirenal fat (g)	0.46 ± 0.05	0.44 ± 0.06	0.74 ± 0.05§‡	0.74 ± 0.07§‡
Brown fat (g)	0.34 ± 0.03	0.34 ± 0.04	0.43 ± 0.02	0.48 ± 0.04*†

Data expressed as mean ± SEM; n=9-10/group. Statistical analysis was performed using two-way ANOVA with Tukey's post hoc test. HFD, mice fed purified high-fat diet for 8 wk; LFD, mice fed purified low-fat diet for 8 wk. Mesenteric fat, mesenteric adipose tissue; Inguinal fat, inguinal adipose tissue; Epididymal fat, epididymal adipose tissue; Perirenal fat, perirenal adipose tissue; Brown fat, brown adipose tissue.
*$P < 0.05$ and §$P < 0.01$ vs Sham-LFD
†$P < 0.05$ and ‡$P < 0.01$ vs Ablation-LFD
∫$P < 0.05$ and ∫∫$P < 0.01$ vs Sham-HFD

Hepatic insulin sensitivity, estimated by the ratio of insulin-stimulated phosphorylation of AKT to total AKT, was markedly reduced in Sham-HFD (Hedges' g=1.26, P=0.3789) and Ablation-HFD (Hedges' g=1.77, P=0.0365) mice relative to LFD controls (*Figure 1.4*). Additionally, we found that MLN ablation led to a sizable reduction in pAKT/AKT within HFD mice (Hedges' g=1.03, P=0.1866). A similar trend was also observed between LFD mice, although to a lesser extent (Hedges' g=0.52, P=0.9459).

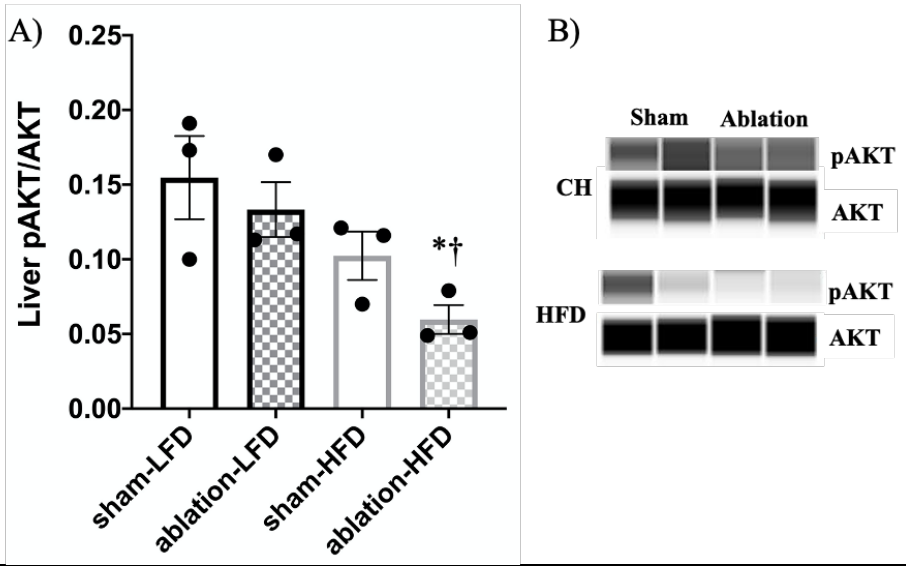

Figure 1.4. Hepatic insulin signaling. The ratio of phosphorylated to total AKT was determined in livers by Western blotting (A). Representative blots (B) are shown below. Statistical analysis was performed using two-way ANOVA with Tukey's post hoc test. Data expressed as mean ± SEM; n=3/group. *$P < 0.05$ vs Sham-LFD, †$P < 0.05$ vs Ablation-LFD, ∫$P < 0.05$ vs Sham-HFD.

To characterize immunologic changes in response to MLN ablation, we collected subcutaneous (IAT) and visceral (MAT) adipose depots, along with resident lymph nodes (ILN and MLNs—respectively). Additionally, we collected the spleen and a section of the small intestine (jejunum). All acquired tissues were digested, and cells collected. As previously

mentioned, cauterization successfully removed 80-100% of MLNs in ablation groups. Specifically, 2/5 of mice in the Ablation-LFD group and 3/5 of mice in the Ablation-HFD group had 100% removal of the MLNs (i.e. none were visible or recovered at termination). In contrast, 3/5 of mice in the Ablation-LFD group and 2/5 of mice in the Ablation-HFD group had 80% removal of the MLNs (i.e. some remained and were recovered at termination). We found that MLN ablation greatly reduced the total number of cells recovered from MLNs of Ablation-LFD (Hedges' g=1.76, P=0.0832) and Ablation-HFD (Hedges' g=2.52, P=0.0222) mice relative to Sham controls (*Figure 1.5B*). Which is in agreement with their surgical disruption via cauterization. Interestingly, we also saw a modest increase in MLN cell counts within Sham-HFD mice as compared with Sham-LFD mice (Hedges' g=-0.67, P=0.6851). This diet effect was lost in ablation groups. In contrast, neither MLN ablation nor diet had an effect on ILN cell counts (*Figure 1.5E*).

As HFD feeding increased IAT and MAT mass, total cell counts were normalized per gram of tissue. We found that Sham-HFD (Hedges' g=1.43, P=0.0803) and Ablation-HFD (Hedges' g=1.12, P=0.1839) mice had a large reduction in total cell counts within MAT relative to LFD controls (*Figure 1.5A*). A similar HFD-induced reduction in IAT cell counts was also seen in Sham-HFD (Hedges' g=2.55, P=0.0020) and Ablation-HFD (Hedges' g=2.04, P=0.0124) mice (*Figure 1.5D*). However, MLN ablation did not appear to affect either MAT or IAT total cell counts.

Within the jejunum (*Figure 1.5F*), we found that HFD feeding led to a reduction in total cell counts (Sham-LFD vs Sham-HFD Hedges' g=0.72, P=0.5999), which was exacerbated by MLN ablation (Sham-HFD vs Ablation-HFD, Hedges' g=0.66, P=0.6570). Similarly, MLN ablation reduced cell counts within LFD mice (Sham-LFD vs Ablation-LFD, Hedges' g=0.61,

P=0.7085). In opposition, within the spleen (*Figure 1.5C*), HFD feeding led to an increase splenocyte counts (Sham-LFD vs Sham-HFD, Hedges' *g*=-1.56, *P*=0.0659), which was then reduced by MLN ablation (Sham-HFD vs Ablation-HFD, Hedges' *g*=0.97, *P*=0.3608). This MLN ablation-induced reduction in splenocytes was not observed in LFD mice (Sham-LFD vs Ablation-LFD, Hedges' *g*=-0.61, *P*=0.7410).

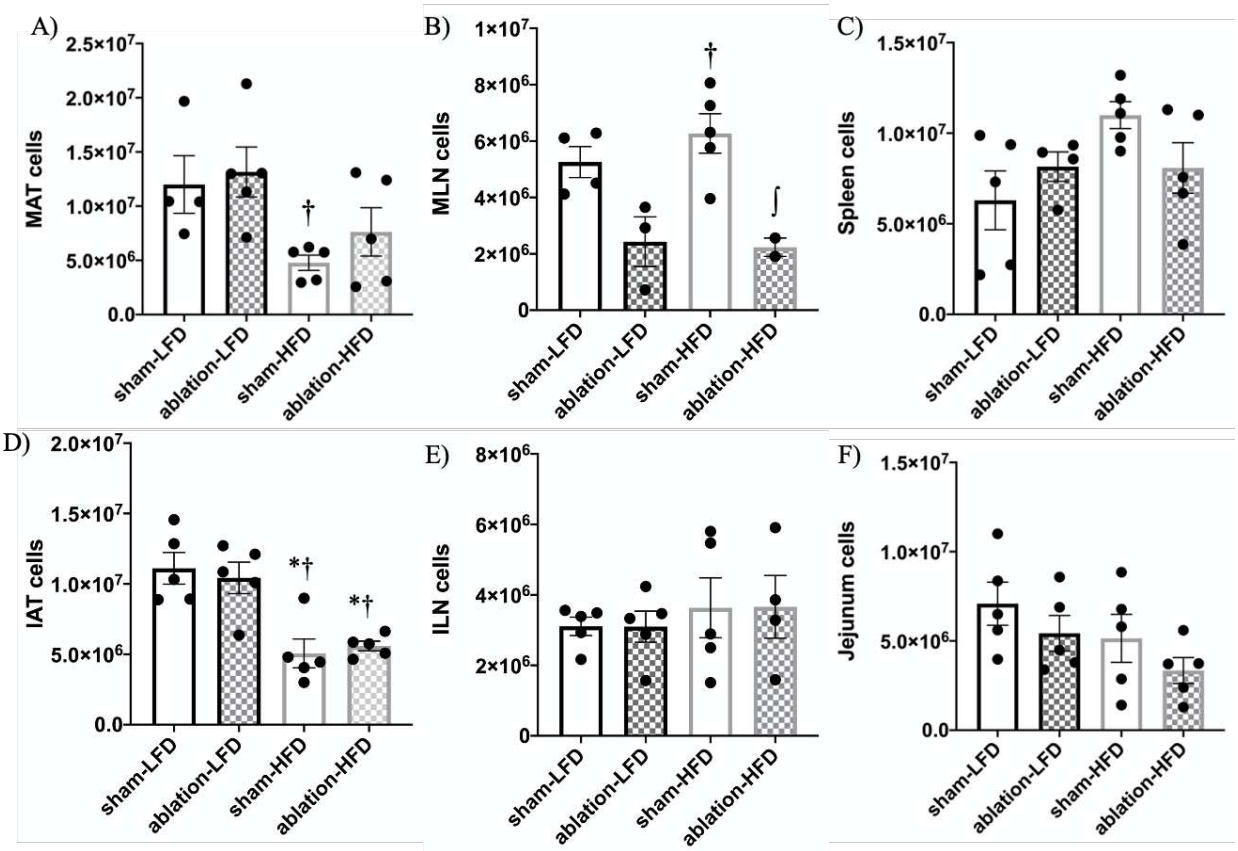

Figure 1.5. Tissue total cell counts. Immune cells were isolated from mesenteric adipose tissue (A), mesenteric lymph nodes (B), spleens (C), inguinal adipose tissue (D), inguinal lymph nodes (E), and jejunum (F). Total cell counts from MAT and IAT were normalized to tissue weight, and equal lengths of jejunum and whole spleens were used. Statistical analysis was performed using two-way ANOVA with Tukey's post hoc test. Data expressed as mean ± SEM; n=2-5/group. **P* < 0.05 vs Sham-LFD, †*P* < 0.05 vs Ablation-LFD, ∫*P* < 0.05 vs Sham-HFD.

Isolated cells were then analyzed by flow cytometry. Leukocytes were gaited with a primary gate excluding debris, a secondary gate excluding doublets, a tertiary gate on live cells (Live/Dead Yellow$^-$), and then on leukocytes (CD45.2$^+$). CD3$^+$ T cells and CD19$^+$ B cells were

then gaited off leukocytes. T cells were further analyzed for $CD4^+$ and $CD8^+$ cell subsets. Absolute numbers of cell subsets were calculated for individual mice using total cell counts.

Within MLNs, we found that the absolute number of T cells (*Figures 1.6A*) was reduced in Ablation-LFD mice (vs Sham-LFD, Hedges' g=2.53, P=0.0032). This effect was lost in Ablation-HFD mice (vs Sham-HFD, Hedges' g=0.30, P=0.8881) due to the additive reduction driven by HFD feeding (Sham-LFD vs Sham-HFD, Hedges' g=1.85, P=0.0769). Similarly, the absolute number of $CD4^+$ T cells (*Figures 1.6B*) was reduced in Ablation-LFD mice (Hedges' g=2.85, P=0.0073), as well as Ablation-HFD mice (Hedges' g=1.07, P=0.4553), relative to Sham controls. Again, with a compounded reduction by HFD feeding (Sham-LFD vs Sham-HFD, Hedges' g=1.80, P=0.0673). Further supporting their surgical disruption via cauterization. Although MLN ablation appeared to increase T cells (*Figures 1.6C*) and $CD4^+$ T cells (*Figures 1.6D*) within ILNs, no large differences were found.

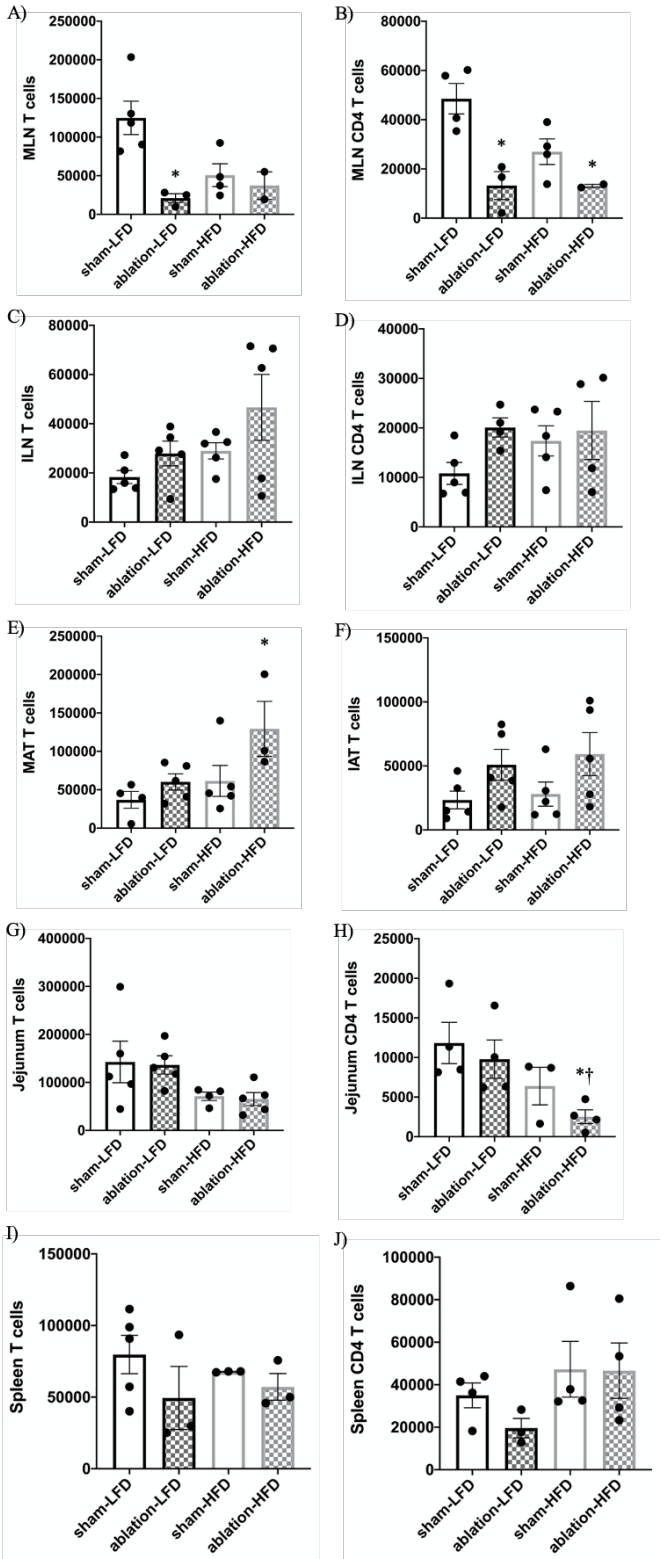

Figure 1.6. Immune cell populations. Mean ± SEM (n=2-5/group) absolute number $CD3^+$ T cells in mesenteric lymph nodes (A), inguinal lymph nodes (C), mesenteric (E) and inguinal (F) adipose tissue, jejunum (G), and spleen (I). Mean ± SEM (n=2-5/group) absolute number $CD4^+$ T cells in mesenteric lymph nodes (B), inguinal lymph nodes (D), jejunum (H), and spleen (J). Statistical analysis was performed using two-way ANOVA with Tukey's post hoc test. *$P < 0.05$ vs Sham-LFD, †$P < 0.05$ vs Ablation-LFD, ∫$P < 0.05$ vs Sham-HFD.

Within both MAT (*Figure 1.6E*) and IAT (*Figure 1.6F*), we found that MLN ablation increased the absolute number of T cells. Particularly, within MAT, Ablation-LFD (Hedges' *g*=-0.54, *P*=0.8048) and Ablation-HFD (Hedges' *g*=-1.52, *P*=0.1265) mice had an increase in T cells as compared to Sham controls (*Figure 1.6E*). Similarly, within IAT, Ablation-LFD (Hedges' *g*=-0.94, *P*=0.2708) and Ablation-HFD (Hedges' *g*=-1.06, *P*=0.3400) mice also had an increase in T cells. Interestingly, we found that HFD feeding exacerbated the ablation-induced increase in T cells within MAT (Ablation-LFD vs Ablation-HFD, Hedges' *g*=-1.55, *P*=0.1176).

Within the jejunum, we found that HFD feeding reduced the absolute number of T cells (*Figure 1.6G*) within both Sham-HFD (Hedges' *g*=1.11, *P*=0.3831) and Ablation-HFD (Hedges' *g*=1.12, *P*=0.0897) mice relative to LFD controls. Similarly, $CD4^+$ T cells (*Figure 1.6H*) were also found to be reduced within Sham-HFD (Hedges' *g*=1.09, *P*=0.5000) and Ablation-HFD (Hedges' *g*=1.50, *P*=0.0485) mice. On the other hand, we found that MLN ablation predominantly reduced $CD4^+$ T cells, in addition to total leukocytes (*Table 1.2*). Specifically, $CD4^+$ T cells were reduced within Ablation-LFD (Hedges' *g*=0.42, *P*=0.9753) and Ablation-HFD (Hedges' *g*=0.78, *P*=0.3498) mice relative to Sham controls. Comparably, total leukocytes were also reduced within Ablation-LFD (Hedges' *g*=0.83, *P*=0.7274) and Ablation-HFD (Hedges' *g*=0.33, *P*=0.9680) mice, which was further exacerbated by HFD feeding (Ablation-LFD vs Ablation-HFD, Hedges' *g*=0.21, *P*=0.8247).

With regard to the spleen, MLN ablation led to a reduction in the absolute number of T cells (*Figures 1.6I*) within Ablation-LFD mice (vs Sham-LFD, Hedges' *g*=0.99, *P*=0.4384), however this effect was minimized within Ablation-HFD mice (vs Sham-HFD, Hedges' *g*=0.32, *P*=0.9596) due to the compounded reduction driven by HFD feeding (Sham-LFD vs Sham-HFD, Hedges' *g*=0.39, *P*=0.9236). Similarly, MLN ablation led to a reduction in $CD4^+$ T cells (*Figures*

1.6J), however only within Ablation-LFD mice (vs Sham-LFD, Hedges' g=0.63, P=0.4110). In contrast, HFD feeding led to an increase in $CD4^+$ T cells within both Sham-HFD (Hedges' g=-0.52, P=0.8591) and Ablation-HFD (Hedges' g=-1.11, P=0.1746) mice relative to LFD controls. Additional immune cell population data are presented in the *Table 1.2*.

Table 1.2. Immune cell population metrics

Tissue	Population	Sham-LFD	Ablation-LFD	Sham-HFD	Ablation-HFD
Jejunum	$CD45.2^+$ Leukocytes	33.68% ± 7.31% 1.01×10^6 ± 3.77×10^5	26.50% ± 3.91% 4.50×10^5 ± 1.59×10^5	27.58% ± 6.10% 5.35×10^5 ± 3.31×10^5	30.22% ± 7.30% 3.13×10^5 ± 1.30×10^5
	$CD3^+$ T cells	2.11% ± 0.55% 1.43×10^5 ± 4.33×10^4	2.99% ± 0.72% 1.36×10^5 ± 1.91×10^4	2.39% ± 0.55% 1.05×10^5 ± 3.47×10^4	2.36% ± 0.73% 6.53×10^4 ± 1.36×10^4
	$CD4^+$ T cells	15.20% ± 3.22% 1.18×10^4 ± 2.60×10^3	11.33% ± 4.11% 9.79×10^3 ± 2.43×10^3	12.39% ± 4.19% 6.40×10^3 ± 2.38×10^3	6.84% ± 2.15% 2.52×10^3 ± 8.73×10^3*†
	$\gamma\delta$T cells	5.25% ± 1.73% 9.29×10^3 ± 6.12×10^3	6.88% ± 1.76% 8.92×10^3 ± 2.32×10^3	4.88% ± 2.41% 6.44×10^3 ± 3.59×10^3	4.79% ± 1.40% 3.12×10^3 ± 1.13×10^3
	$CD19^+$ B cells	0.13% ± 0.04% 9.29×10^3 ± 2.74×10^3	0.09% ± 0.04% 5.10×10^3 ± 2.72×10^3	0.08% ± 0.02% 4.85×10^3 ± 2.30×10^3	0.14% ± 0.07% 5.01×10^3 ± 2.84×10^3
MAT	$CD45.2^+$ Leukocytes	27.37% ± 6.20% 4.69×10^5 ± 1.89×10^5	32.64% ± 7.49% 9.21×10^5 ± 3.89×10^5	21.65% ± 5.24% 2.24×10^5 ± 7.69×10^4	17.43% ± 6.57% 2.57×10^5 ± 1.35×10^5
	$CD3^+$ T cells	3.11% ± 2.02% 3.68×10^4 ± 1.10×10^4	1.03% ± 0.20% 6.02×10^4 ± 1.06×10^4	1.72% ± 0.47% 6.14×10^4 ± 2.01×10^4	4.61% ± 3.03% 1.29×10^5 ± 3.58×10^4*
	$CD4^+$ T cells	21.27% ± 5.26% 5.15×10^4 ± 4.45×10^4	35.42% ± 6.32% 2.01×10^4 ± 3.90×10^3	17.68% ± 1.73% 1.15×10^4 ± 4.90×10^3	14.09% ± 6.51% 2.11×10^4 ± 1.53×10^4
	$\gamma\delta$T cells	8.28% ± 1.09% 1.23×10^6 ± 8.90×10^5	14.34% ± 8.95% 6.74×10^5 ± 3.47×10^5	19.20% ± 3.87% 1.45×10^6 ± 8.1×10^5	23.91% ± 10.65% 6.73×10^6 ± 4.28×10^6
	$CD19^+$ B cells	0.36% ± 0.12% 1.72×10^4 ± 6.81×10^3	0.31% ± 0.11% 1.91×10^4 ± 8.36×10^3	0.41% ± 0.30% 1.53×10^4 ± 1.17×10^4	0.92% ± 0.70% 7.34×10^4 ± 6.46×10^4
MLNs	$CD45.2^+$ Leukocytes	37.96% ± 2.19% 1.64×10^6 ± 5.06×10^5	33.47% ± 6.58% 5.80×10^5 ± 3.13×10^5	42.44% ± 1.61% 2.27×10^6 ± 2.84×10^5	24.25% ± 0.15% 4.67×10^5 ± 8.54×10^4
	$CD3^+$ T cells	2.22% ± 0.42% 1.25×10^5 ± 2.16×10^4	0.99% ± 0.18% 2.10×10^4 ± 5.70×10^3§	1.45% ± 0.58% 5.07×10^4 ± 1.48×10^4	1.83% ± 1.07% 3.72×10^4 ± 1.79×10^4
	$CD4^+$ T cells	52.24% ± 9.06% 4.85×10^4 ± 6.18×10^3	54.17% ± 16.26% 1.32×10^4 ± 5.67×10^3§	53.88% ± 9.87% 2.70×10^4 ± 5.20×10^3	46.90% ± 24.30% 1.31×10^4 ± 6.64×10^2*
	$\gamma\delta$T cells	9.95% ± 2.93%	4.97% ± 4.19%	11.10% ± 0.90%	18.60% ± 2.20%

		$7.74\times10^3 \pm 4.44\times10^3$	$1.28\times10^3 \pm 9.43\times10^2$	$4.05\times10^3 \pm 1.14\times10^3$	$2.42\times10^3 \pm 1.64\times10^2$
	$CD19^+$ B cells	$5.87\% \pm 1.96\%$ $8.28\times10^3 \pm 4.35\times10^3$	$3.39\% \pm 0.73\%$ $7.40\times10^2 \pm 3.12\times10^2$	$3.14\% \pm 0.84\%$ $2.38\times10^3 \pm 1.05\times10^3$	$2.93\% \pm 0.15\%$ $1.06\times10^3 \pm 4.69\times10^2$
IAT	$CD45.2^+$ Leukocytes	$13.98\% \pm 1.32\%$ $2.22\times10^5 \pm 3.16\times10^4$	$15.78\% \pm 0.89\%$ $2.53\times10^5 \pm 2.50\times10^4$	$13.08\% \pm 0.55\%$ $1.44\times10^5 \pm 1.24\times10^4$	$12.66\% \pm 0.68\%$ $1.38\times10^5 \pm 6.10\times10^3$
	$CD3^+$ T cells	$0.40\% \pm 0.15\%$ $2.34\times10^4 \pm 6.92\times10^3$	$0.74\% \pm 0.16\%$ $5.09\times10^4 \pm 1.21\times10^4$	$0.52\% \pm 0.17\%$ $2.80\times10^4 \pm 9.42\times10^3$	$1.08\% \pm 0.32\%$ $5.93\times10^4 \pm 1.68\times10^4$
	$CD4^+$ T cells	$9.74\% \pm 6.30\%$ $9.13\times10^3 \pm 9.09\times10^2$	$17.77\% \pm 7.02\%$ $6.07\times10^3 \pm 5.98\times10^2$	$6.53\% \pm 3.55\%$ $2.58\times10^3 \pm 4.12\times10^2$	$12.95\% \pm 4.05\%$ $9.01\times10^3 \pm 4.72\times10^3$
	$\gamma\delta$T cells	$8.30\% \pm 5.99\%$ $7.48\times10^3 \pm 2.55\times10^3$	$17.86\% \pm 7.19\%$ $7.33\times10^3 \pm 2.71\times10^3$	$22.46\% \pm 8.51\%$ $5.28\times10^3 \pm 6.63\times10^2$	$22.68\% \pm 11.62\%$ $2.30\times10^4 \pm 1.75\times10^4$
	$CD19^+$ B cells	$0.05\% \pm 0.02\%$ $5.07\times10^3 \pm 1.20\times10^3$	$0.12\% \pm 0.06\%$ $9.59\times10^3 \pm 4.38\times10^3$	$0.05\% \pm 0.02\%$ $2.88\times10^3 \pm 8.49\times10^2$	$0.11\% \pm 0.06\%$ $8.19\times10^3 \pm 4.71\times10^3$
ILNs	$CD45.2^+$ Leukocytes	$31.42\% \pm 3.10\%$ $8.07\times10^5 \pm 6.92\times10^4$	$35.34\% \pm 4.84\%$ $9.46\times10^5 \pm 1.80\times10^5$	$31.30\% \pm 3.47\%$ $1.69\times10^6 \pm 6.42\times10^5$	$36.70\% \pm 4.32\%$ $1.07\times10^6 \pm 3.18\times10^5$
	$CD3^+$ T cells	$0.59\% \pm 0.07\%$ $1.83\times10^4 \pm 2.62\times10^3$	$0.88\% \pm 0.10\%$ $2.79\times10^4 \pm 5.03\times10^3$	$0.96\% \pm 0.19\%$ $2.90\times10^4 \pm 3.30\times10^3$	$1.00\% \pm 0.26\%$ $4.67\times10^4 \pm 1.34\times10^4$
	$CD4^+$ T cells	$57.66\% \pm 4.98\%$ $1.08\times10^4 \pm 2.22\times10^3$	$57.66\% \pm 5.87\%$ $1.68\times10^4 \pm 3.59\times10^3$	$59.28\% \pm 7.78\%$ $1.74\times10^4 \pm 3.05\times10^3$	$58.68\% \pm 5.97\%$ $2.59\times10^4 \pm 7.88\times10^3$
	$\gamma\delta$T cells	$16.90\% \pm 2.35\%$ $1.87\times10^3 \pm 5.06\times10^2$	$17.62\% \pm 3.24\%$ $3.07\times10^3 \pm 1.04\times10^3$	$12.58\% \pm 1.00\%$ $2.25\times10^3 \pm 5.08\times10^2$	$13.82\% \pm 3.35\%$ $3.59\times10^3 \pm 1.19\times10^3$
	$CD19^+$ B cells	$6.09\% \pm 1.28\%$ $1.10\times10^5 \pm 2.35\times10^4$	$4.49\% \pm 0.74\%$ $1.26\times10^5 \pm 2.99\times10^4$	$3.25\% \pm 0.78\%$ $9.61\times10^4 \pm 2.63\times10^4$	$5.60\% \pm 1.34\%$ $2.47\times10^5 \pm 1.14\times10^5$
Spleen	$CD45.2^+$ Leukocytes	$39.72\% \pm 5.75\%$ $1.70\times10^6 \pm 7.47\times10^5$	$33.42\% \pm 7.45\%$ $1.98\times10^6 \pm 8.11\times10^5$	$47.72\% \pm 1.19\%$ $3.53\times10^6 \pm 9.09\times10^5$	$43.52\% \pm 6.65\%$ $2.80\times10^6 \pm 8.74\times10^5$
	$CD3^+$ T cells	$2.10\% \pm 0.83\%$ $7.97\times10^4 \pm 1.34\times10^4$	$9.82\% \pm 7.39\%$ $2.45\times10^5 \pm 1.21\times10^5$	$1.12\% \pm 0.30\%$ $1.23\times10^5 \pm 3.39\times10^4$	$6.53\% \pm 5.45\%$ $3.02\times10^5 \pm 2.01\times10^5$
	$CD4^+$ T cells	$48.50\% \pm 8.18\%$ $3.50\times10^4 \pm 5.81\times10^3$	$57.50\% \pm 8.79\%$ $1.68\times10^5 \pm 9.18\times10^4$	$52.90\% \pm 5.19\%$ $6.69\times10^4 \pm 2.21\times10^4$	$53.48\% \pm 6.57\%$ $1.54\times10^5 \pm 1.08\times10^5$
	$\gamma\delta$T cells	$3.69\% \pm 1.44\%$ $1.19\times10^3 \pm 5.13\times10^2$	$2.18\% \pm 0.48\%$ $3.64\times10^3 \pm 3.18\times10^3$	$3.10\% \pm 0.77\%$ $1.48\times10^3 \pm 4.90\times10^2$	$3.22\% \pm 1.25\%$ $1.16\times10^3 \pm 3.31\times10^2$
	$CD19^+$ B cells	$5.22\% \pm 0.81\%$ $3.66\times10^5 \pm 4.51\times10^4$	$4.40\% \pm 0.83\%$ $9.56\times10^5 \pm 4.24\times10^5$	$3.41\% \pm 0.29\%$ $4.22\times10^5 \pm 1.25\times10^5$	$8.78\% \pm 3.34\%$ $1.78\times10^6 \pm 1.10\times10^6$

Data expressed as mean ± SEM; n=2-5/group. Statistical analysis was performed using two-way ANOVA with Tukey's post hoc test. Immune cell population percent gaited and absolute number for MAT, mesenteric adipose tissue; MLNs, mesenteric lymph nodes; IAT, inguinal adipose tissue; ILNs, inguinal lymph nodes; Jejunum; Spleen.
*$P < 0.05$ and §$P < 0.01$ vs Sham-LFD
†$P < 0.05$ and ‡$P < 0.01$ vs Ablation-LFD
∫$P < 0.05$ and ∫∫$P < 0.01$ vs Sham-HFD

Second, we sought to investigate if treatment with the anti-fibrotic/anti-inflammatory medication Pirfenidone could attenuate obesity-induced MLN fibrosis and metabolic dysfunction (experiment 2). At the end of the study, we found that HFD fed mice had a greater overall body weight (*Figure 1.7A*) and cumulative food intake (*Figure 1.7B*) than their CH fed counterparts. However, after 4 wk of Pirfenidone treatment, HFD+P mice had a reduction in total body weight compared to HFD-P controls (Hedges' g=2.86, P=0.3324). Despite these differences in body weight, Pirfenidone treatment did not affect cumulative food intake (HFD-P vs HFD+P, Hedges' g=0.31, P=0.9114).

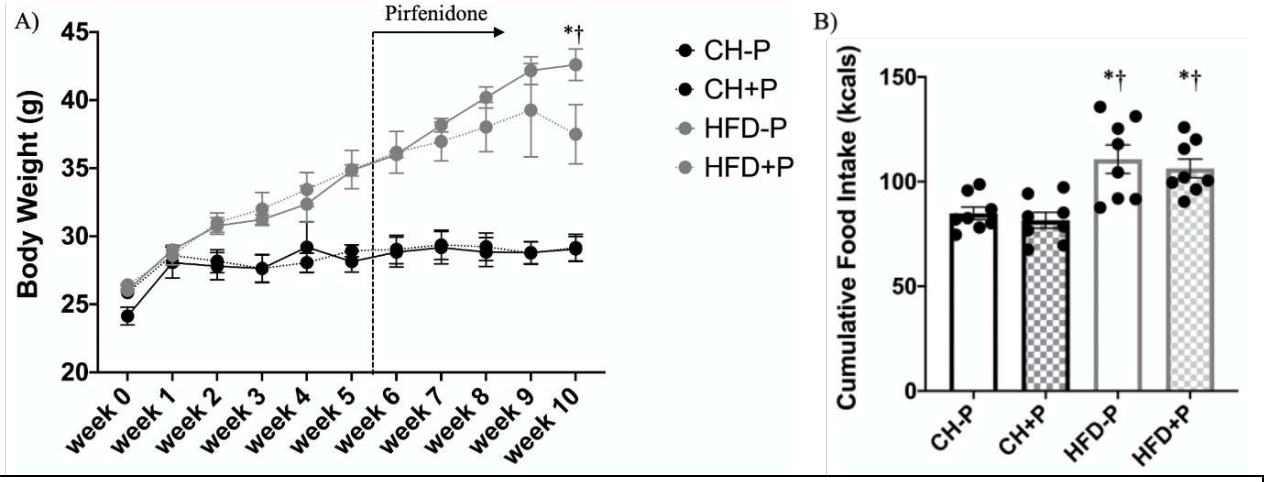

Figure 1.7. Body weight and cumulative food intake. Body weight (g) over the study period (A). Cumulative food intake (kcals) over the last 4 wk of the study period, during Pirfenidone treatment (B). Statistical analysis was performed using repeated measures two-way ANOVA with Tukey's post hoc test (A) and two-way ANOVA with Tukey's post hoc test (B). Data expressed as mean ± SEM; n=3/group. †$P < 0.05$ vs CH-P, *$P < 0.05$ vs CH+P, ∫$P < 0.05$ vs HFD-P.

An increase in inflammation is associated with obesity and metabolic dysfunction. We found that 10 wk of HFD feeding led to a broad increase in the concentration of circulating pro-

inflammatory cytokines (monocyte chemoattractant protein-1 (MCP-1), tumor necrosis factor (TNF), interleukin-6 (IL-6)) and pro-inflammatory adipokines (resistin, plasminogen activator inhibitor-1 (PAI-1), leptin), as well as insulin relative to CH fed counterparts (*Figure 1.8*). However, Pirfenidone treatment was able to reduce the increase of resistin (Hedges' g=2.73, P=0.0184), leptin (Hedges' g=2.35, P=0.1166), TNF (Hedges' g=4.52, P=0.0020), MCP-1 (Hedges' g=1.45, P=0.2157), and insulin (Hedges' g=1.21, P=0.2467) driven by HFD feeding. Interestingly, Pirfenidone treatment also exacerbated HFD-induced increases in IL-6 (Hedges' g=-4.93, P=0.0323) and PAI-1 (Hedges' g=-1.44, P=0.1697).

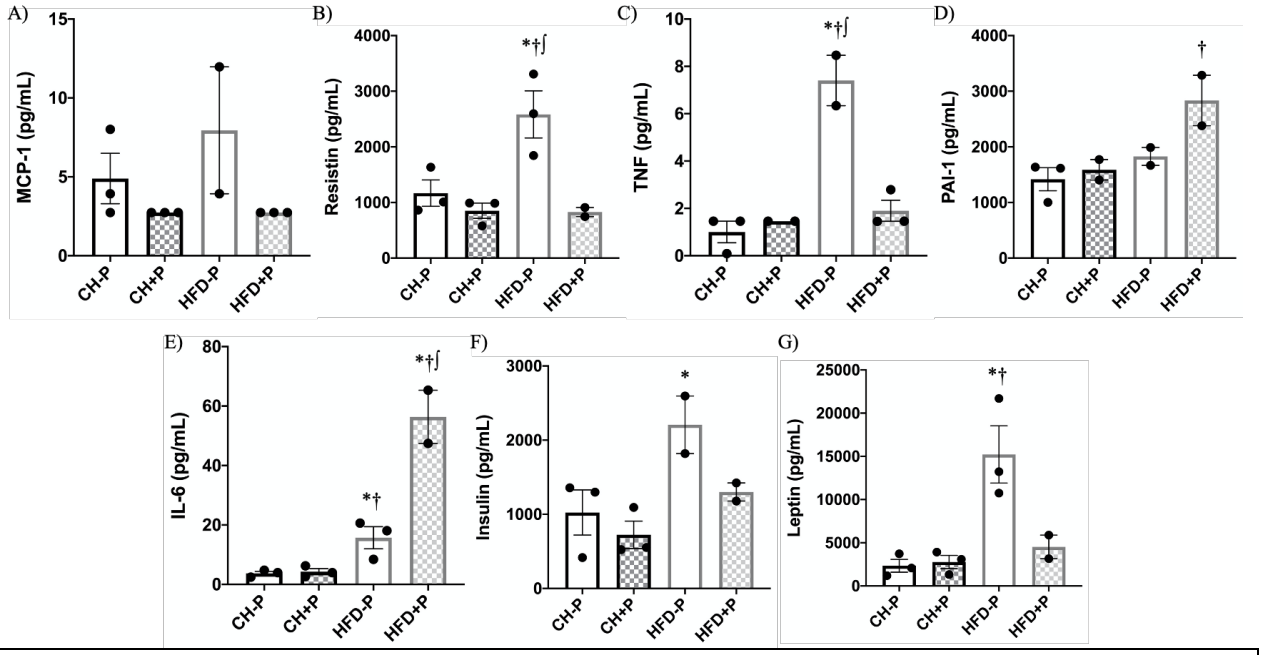

Figure 1.8. Circulating markers of inflammation and metabolic dysfunction. Plasma monocyte chemoattractant protein-1 (MCP-1) (A), resistin (B), tumor necrosis factor (TNF) (C), plasminogen activator inhibitor-1 (D), interlukin-6 (IL-6) (E), insulin (F), leptin (G) were determined via bead-based multiplex assay. Statistical analysis was performed using two-way ANOVA with Tukey's post hoc test. Data expressed as mean ± SEM; n=3/group. †$P < 0.05$ vs CH-P, *$P < 0.05$ vs CH+P, ∫$P < 0.05$ vs HFD-P.

Fibrosis results from chronic inflammatory processes, and promotes tissue damage and dysfunction (71). To evaluate the effect of Pirfenidone treatment on diet-induced MLN fibrosis (47) we used Picrosirius Red to stain collagen fibers (*Figure 1.9*). We found that HFD-P mice

had an increase in collagen accretion within MLNs (vs CH-P, Hedges' *g*=-2.13, *P*=0.0456), which was attenuated by Pirfenidone treatment (vs HFD+P, Hedges' *g*=2.34, *P*=0.0295).

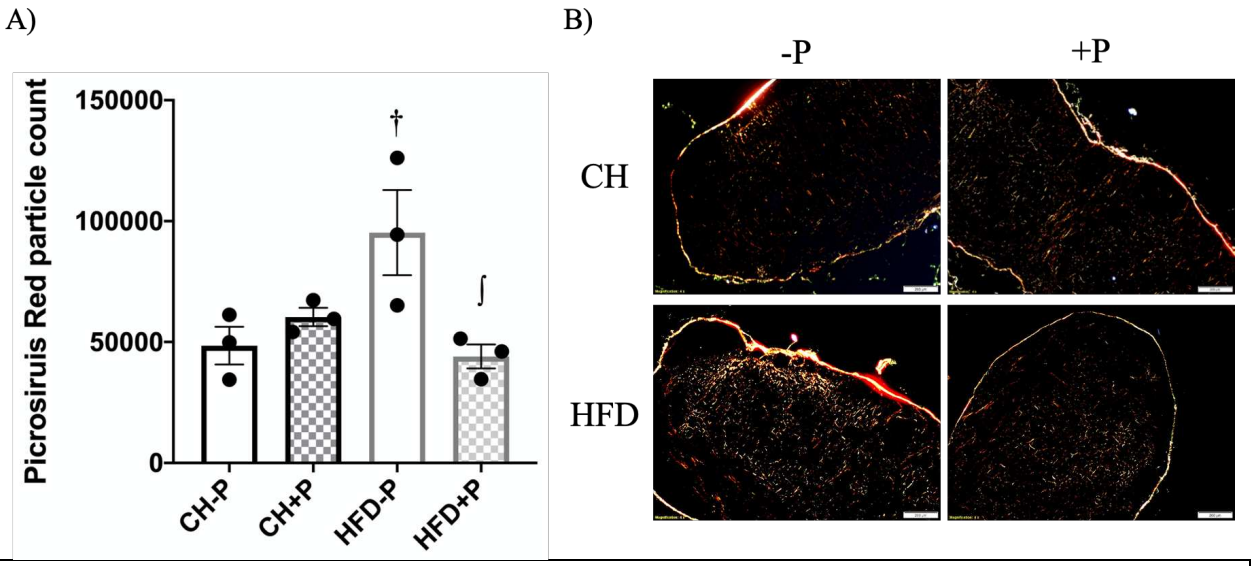

Figure 1.9. Collagen staining and quantification within MLNs. Collagen fiber quantification in MLNs (A). Representative picrosirius stained MLNs visualized by polarized light microscopy (B). Statistical analysis was performed using two-way ANOVA with Tukey's post hoc test. Data expressed as mean ± SEM; n=3/group. †$P < 0.05$ vs CH-P, *$P < 0.05$ vs CH+P, ∫$P < 0.05$ vs HFD-P.

Finally, we sought to examine whether or not the MLNs are required for disease reversal associated with Pirfenidone treatment. Again, using cauterization, we successfully removed 80-100% of the MLNs within ablation groups. We found that body weight gained over the 16 wk experiment, reported as change in body weight (g), and cumulative food intake (kcals) were modestly affected by both MLN ablation and Pirfenidone treatment (*Table 1.3*). Specifically, MLN ablation led to an increase in body weight (Sham-P vs Ablation-P, Hedges' *g*=-0.39, *P*=0.8886) despite Ablation-P mice consuming less calories overall (vs Sham-P, Hedges' *g*=0.65, *P*=0.6764). This ablation-induced increase in body weight was attenuated by Pirfenidone treatment (Ablation-P vs Ablation+P, Hedges' *g*=0.41, *P*=0.8947) in spite of Ablation+P mice consuming more calories than Ablation-P mice (Hedges' *g*=-0.45, *P*=0.8759). In contrast, Pirfenidone treatment led to an increase in body weight in Sham mice (Hedges' *g*=-0.52,

P=0.8656), coupled with an increase in total calories (Hedges' *g*=-0.82, *P*=0.4069). In agreement with body weight data, we found that MLN ablation increased intra-abdominal adipose tissue (MAT: Hedges' *g*=-0.39, *P*=0.9013; EAT: Hedges' *g*=-0.30, *P*=0.9556; PAT: Hedges' *g*=-0.87, *P*=0.4479), subcutaneous adipose tissue (IAT: Hedges' *g*=-0.64, *P*=0.6893), and spleen (Hedges' *g*=-1.22, *P*=0.1571) mass, whereas reduced BAT mass (Hedges' *g*=0.57, *P*=0.7511), within Ablation-P mice relative to Sham-P controls (*Table 1.3*). All of which were then reduced by Pirfenidone treatment in Ablation+P mice (MAT: Hedges' *g*=1.63, *P*=0.0596; EAT: Hedges' *g*=0.59, *P*=0.7585; PAT: Hedges' *g*=1.76, *P*=0.0386; IAT: Hedges' *g*=1.60, *P*=0.0681; BAT: Hedges' *g*=0.61, *P*=0.7373; and spleen: Hedges' *g*=1.29, *P*=0.1471). Interestingly, this Pirfenidone-induced reduction in adiposity also occurred in Sham+P mice (MAT (Hedges' *g*=0.43, *P*=0.8423), PAT (Hedges' *g*=0.12, *P*=0.9961), BAT (Hedges' *g*=0.48, *P*=0.7913), and IAT (Hedges' *g*=0.86, *P*=0.4105)) despite an increase in total body weight.

Table 1.3. General and metabolic characteristics

	Sham-P	Sham+P	Ablation-P	Ablation+P
Change in body weight (g)	19.50 ± 0.85	21.24 ± 2.20	20.83 ± 0.80	19.38 ± 1.28
Cumulative food intake (kcals)	2201 ± 85.24	2352 ± 50.78	2079 ± 38.90	2165 ± 79.08
Mesenteric fat (g)	1.21 ± 0.08	1.10 ± 0.12	1.32 ± 0.08	0.86 ± 0.13
Inguinal fat (g)	1.62 ± 0.03	1.41 ± 0.11	1.78 ± 0.05	1.38 ± 0.16
Epididymal fat (g)	2.38 ± 0.11	2.37 ± 0.21	2.52 ± 0.16	2.22 ± 0.28
Perirenal fat (g)	1.20 ± 0.02	1.14 ± 0.13	1.37 ± 0.03	0.96 ± 0.11∫
Brown fat (g)	0.66 ± 0.04	0.60 ± 0.05	0.59 ± 0.03	0.51 ± 0.07
Spleen (g)	0.13 ± 0.01	0.13 ± 0.01	0.17 ± 0.02	0.13 ± 0.01

Data expressed as mean ± SEM; n=5-7/group. Statistical analysis was performed using two-way ANOVA with Tukey's post hoc test. Mice fed purified high-fat diet for total of 16 wk and received Pirfenidone during the last 4 wk. Mesenteric fat, mesenteric adipose tissue; Inguinal fat, inguinal adipose tissue; Epididymal fat, epididymal adipose tissue; Perirenal fat, perirenal adipose tissue; Brown fat, brown adipose tissue.
†$P < 0.05$ and ‡$P < 0.01$ vs Sham-P
*$P < 0.05$ and §$P < 0.01$ vs Sham+P
∫$P < 0.05$ and ∫∫$P < 0.01$ vs Ablation-P

At the end of the experiment, we found that MLN ablation did not affect the blood glucose response to intraperitoneal glucose challenge in HFD fed mice (*Figure 1.10*). Although not statistically significant, Ablation-P mice had a reduction in circulating insulin (*Figure 1.10*)

compared to Sham-P mice (Hedges' g=0.16, P=0.9414), which was worsened by Pirfenidone treatment (Hedges' g=0.14, P=0.9640).

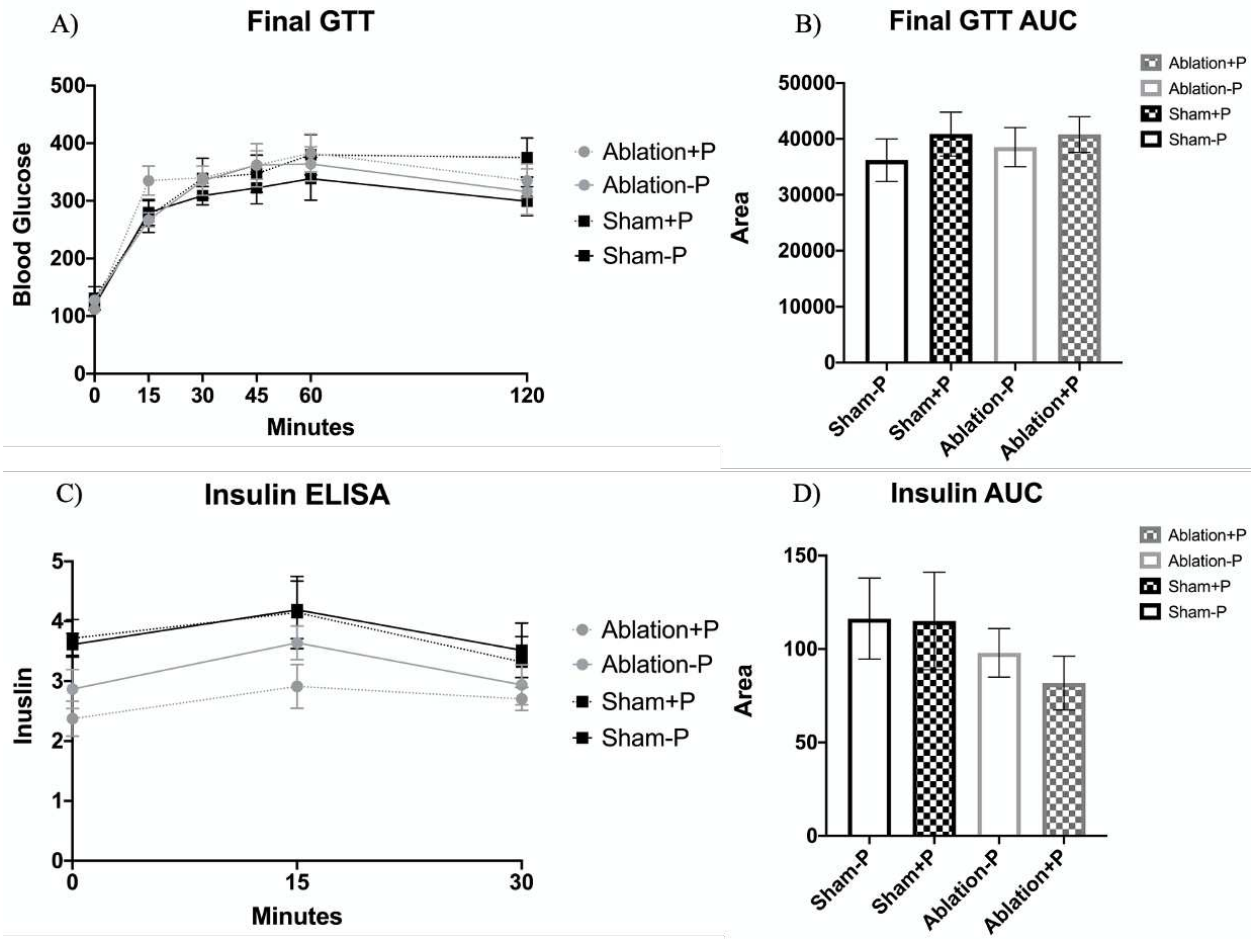

Figure 1.10. Blood glucose and insulin. Final GTT (A) and insulin response to final GTT (C). Statistical analysis of AUC data (B, D) was performed using two-way ANOVA with Tukey's post hoc test. Data expressed as mean ± SEM; n=5-7/group. †$P < 0.05$ vs Sham-P, *$P < 0.05$ vs Sham+P, ∫$P < 0.05$ vs Ablation-P.

To delineate immunologic changes in response to MLN ablation and Pirfenidone treatment, we collected MAT and MLNs, spleen, sections of the jejunum and ileum, and liver. All acquired tissues were digested and cells collected. Total cell counts from MAT and spleen were normalized per gram of tissue. As previously said, cauterization successfully removed 80-100% of MLNs in ablation groups. Specifically, 1/5 of mice in the Ablation-P group and 2/5 of mice in the Ablation+P group had 100% removal of the MLNs (i.e. none were visible or recovered at termination). In contrast, 4/5 of mice in the Ablation-P group and 3/5 of mice in the

Ablation+P group had 80% removal of the MLNs (i.e. some remained and were recovered at termination). We found that MLN ablation led to a substantial reduction in the total number of cells recovered from MLNs of Ablation-P (Hedges' *g*=2.50, *P*=0.0075) and Ablation+P (Hedges' *g*=1.60, *P*=0.1022) mice relative to Sham controls (*Figure 1.11A*). This agrees with their surgical disruption by cauterization. Additionally, we found that Pirfenidone treatment exacerbated this ablation-induced reduction in cell counts within Sham+P (vs Sham-P, Hedges' *g*=1.60, *P*=0.0537) and Ablation+P (vs Ablation-P, Hedges' *g*=0.63, *P*=0.7747) mice. Within the surrounding MAT (*Figure 1.11B*), we found that MLN ablation (Sham-P vs Ablation-P, Hedges' *g*=-0.16, *P*=0.9998) and Pirfenidone treatment (Ablation-P vs Ablation+P, Hedges' *g*=-0.84, *P*=0.4443) led to an accumulative increase in total cell numbers.

Nearby in the liver (*Figure 1.11C*), we found that MLN ablation increased the total number of cells within Ablation-P mice (vs Sham-P, Hedges' *g*=-2.41, *P*=0.0037), which was then attenuated by Pirfenidone treatment (vs Ablation+P, Hedges' *g*=2.26, *P*=0.0087). This Pirfenidone-induced reduction was not seen in Sham mice. Interestingly, we saw that within the ileum (*Figure 1.11D*) MLN ablation (Sham-P vs Ablation-P, Hedges' *g*=1.09, *P*=0.2774) and Pirfenidone treatment (Ablation-P vs Ablation+P, Hedges' *g*=0.38, *P*=0.9193) led to an accumulative reduction in total cells. While in the jejunum (*Figure 1.11E*), neither MLN ablation nor Pirfenidone treatment appeared to altered cell counts. Looking more systemically we saw that splenocytes (*Figure 1.11F*) were reduced by MLN ablation (Sham-P vs Ablation-P, Hedges' *g*=0.52, *P*=0.7167), however this effect was opposed by Pirfenidone treatment which led to an increase in splenocytes within both Sham+P (Hedges' *g*=-0.25, *P*=0.9677) and Ablation+P (Hedges' *g*=-0.67, *P*=0.5832) mice.

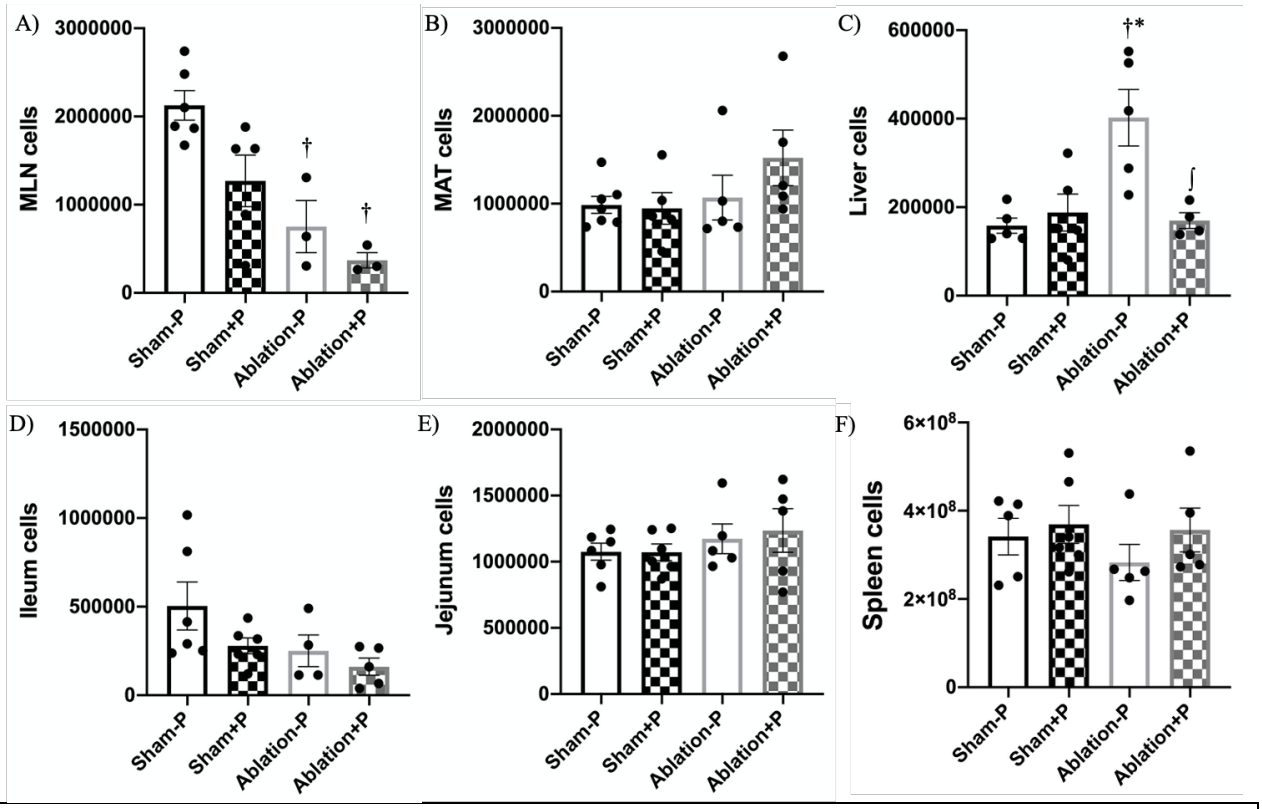

Figure 1.11. Tissue total cell counts. Immune cells were isolated from the mesenteric lymph nodes (A), mesenteric adipose tissue (B), liver (C), ileum (D), jejunum (E), and spleen (F). Total cell counts from MAT and spleen were normalized to tissue weight, equal lengths of ileum and jejunum were taken, and equal amounts of liver were used. Statistical analysis was performed using two-way ANOVA with Tukey's post hoc test. Data expressed as mean ± SEM; n=5-7/group. †$P < 0.05$ vs Sham-P, *$P < 0.05$ vs Sham+P, ∫$P < 0.05$ vs Ablation-P.

Isolated cells were analyzed by flow cytometry. Leukocytes were gaited with a primary gate excluding debris, a secondary gate excluding doublets, a tertiary gate on live cells (Live/Dead Yellow$^-$), and then on leukocytes (CD45.2$^+$). CD3$^+$ T cells and CD19$^+$ B cells were then gaited off leukocytes. T cells were further analyzed for CD4$^+$, CD8$^+$, CD25$^+$Foxp3$^+$, and $\gamma\delta$TCR$^+$ cell subsets. B cells were further analyzed for CD19$^+$LPAM-1$^+$ cell subset. Absolute numbers of cell subsets were calculated for individual mice using total cell counts.

Within MLNs (*Figure 1.12*), we found that the absolute number of B cells (Hedges' g=1.54, P=0.0800), total CD3$^+$ T cells (Hedges' g=2.23, P=0.0192), $\gamma\delta$T cells (Hedges' g=1.45, P=0.1493), CD4$^+$ T cells (Hedges' g=1.68, P=0.0864), and T_{regs} (Hedges' g=1.85, P=0.0556) were reduced in Ablation-P mice relative to Sham-P controls. This effect was compounded by

Pirfenidone treatment (Ablation-P vs Ablation+P) in B cells (Hedges' g=1.09, P=0.3651), $CD3^+$ T cells (Hedges' g=0.56, P=0.8277), $CD4^+$ T cells (Hedges' g=0.48, P=0.8800), and T_{regs} (Hedges' g=0.58, P=0.8093). Of note, this Pirfenidone-induced reduction in cell number was more prominent between Sham mice (B cells: Hedges' g=1.79, P=0.0271; $CD3^+$ T cells: Hedges' g=1.40, P=0.1206; $\gamma\delta$T cells: Hedges' g=0.68, P=0.6547; $CD4^+$ T cells: Hedges' g=1.29, P=0.1610; T_{regs}: Hedges' g=1.63, P=0.0608).

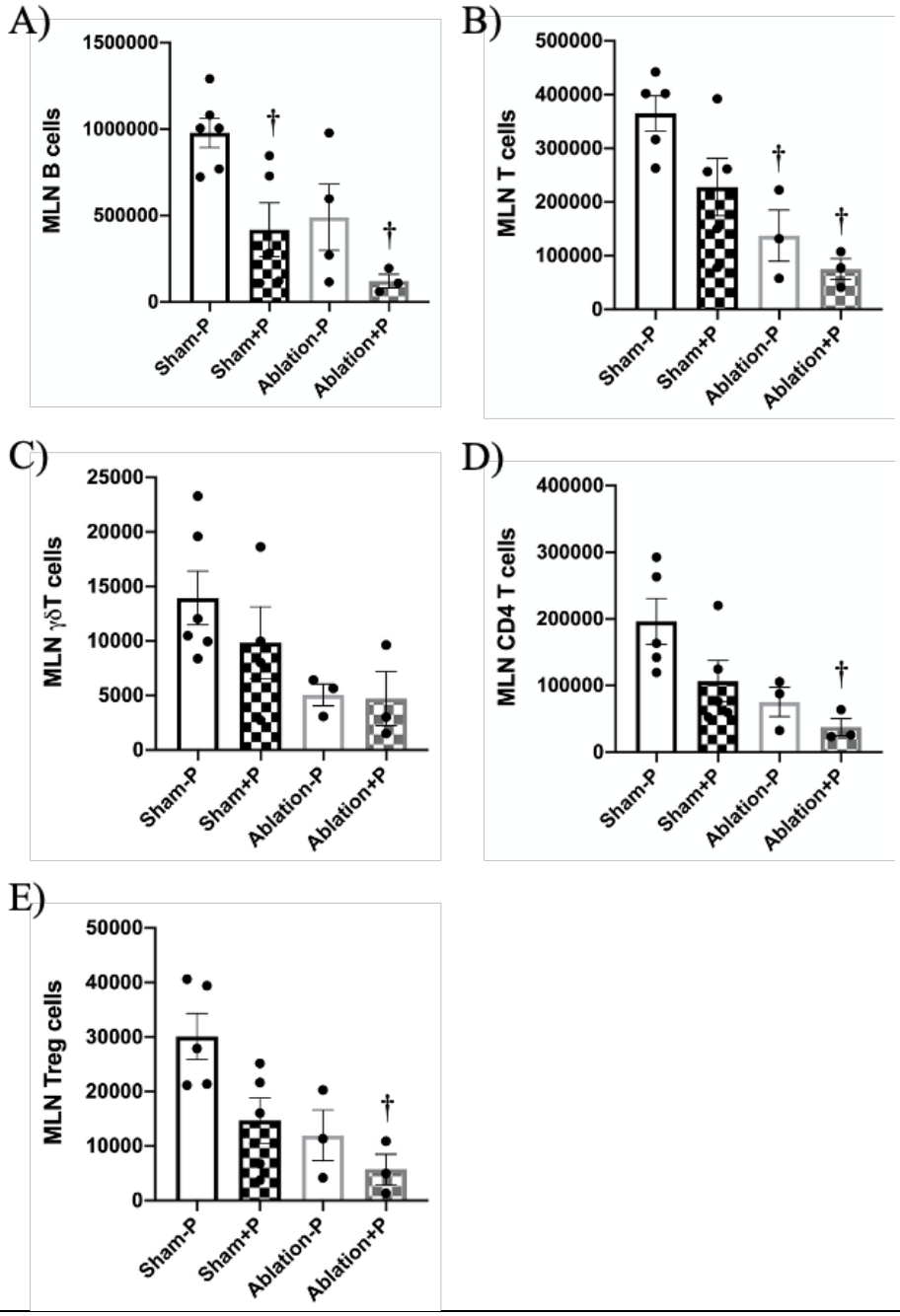

Figure 1.12. Immune cell populations within MLNs. Mean ± SEM (n=3-6/group) absolute number $CD19^+$ B cells (A), $CD3^+$ T cells (B), $\gamma\delta TCR^+$ unconventional $\gamma\delta$T cells (C), $CD4^+$ helper T cells (D), and $Foxp3^+CD25^+$ T_{regs} (E) in MLNs. Statistical analysis was performed using two-way ANOVA with Tukey's post hoc test. †$P < 0.05$ vs Sham-P, *$P < 0.05$ vs Sham+P, ∫$P < 0.05$ vs Ablation-P.

Within MAT (*Figure 1.13*), we found that Ablation-P mice had a reduction in the absolute number of B cells (vs Sham-P, Hedges' g=0.43, P=0.9021), which was exacerbated by Pirfenidone treatment (vs Ablation+P, Hedges' g=0.95, P=0.4805). Similarly, Ablation-P mice

had fewer $\gamma\delta$T cells (Hedges' g=1.70, P=0.0335) than their Sham-P counterparts. In contrast, Ablation-P mice had an increase in the absolute number of $CD4^+$ T cells (Hedges' g=-0.65, P=0.6866) and T_{regs} (Hedges' g=-0.48, P=0.8398) compared to Sham-P controls. However, Pirfenidone treatment attenuated these increases (vs Ablation+P; $CD4^+$ T cells: Hedges' g=1.60, P=0.1133; T_{regs}: Hedges' g=0.65, P=0.7446). Of note, Pirfenidone treatment led to a unanimous reduction in B cells (Hedges' g=0.78, P=0.5397), total $CD3^+$ T cells (Hedges' g=0.43, P=0.8584), $\gamma\delta$T cells (Hedges' g=0.733, P=0.5618), $CD4^+$ T cells (Hedges' g=0.84, P=0.5594) and T_{regs} (Hedges' g=0.40, P=0.9201) with Sham mice.

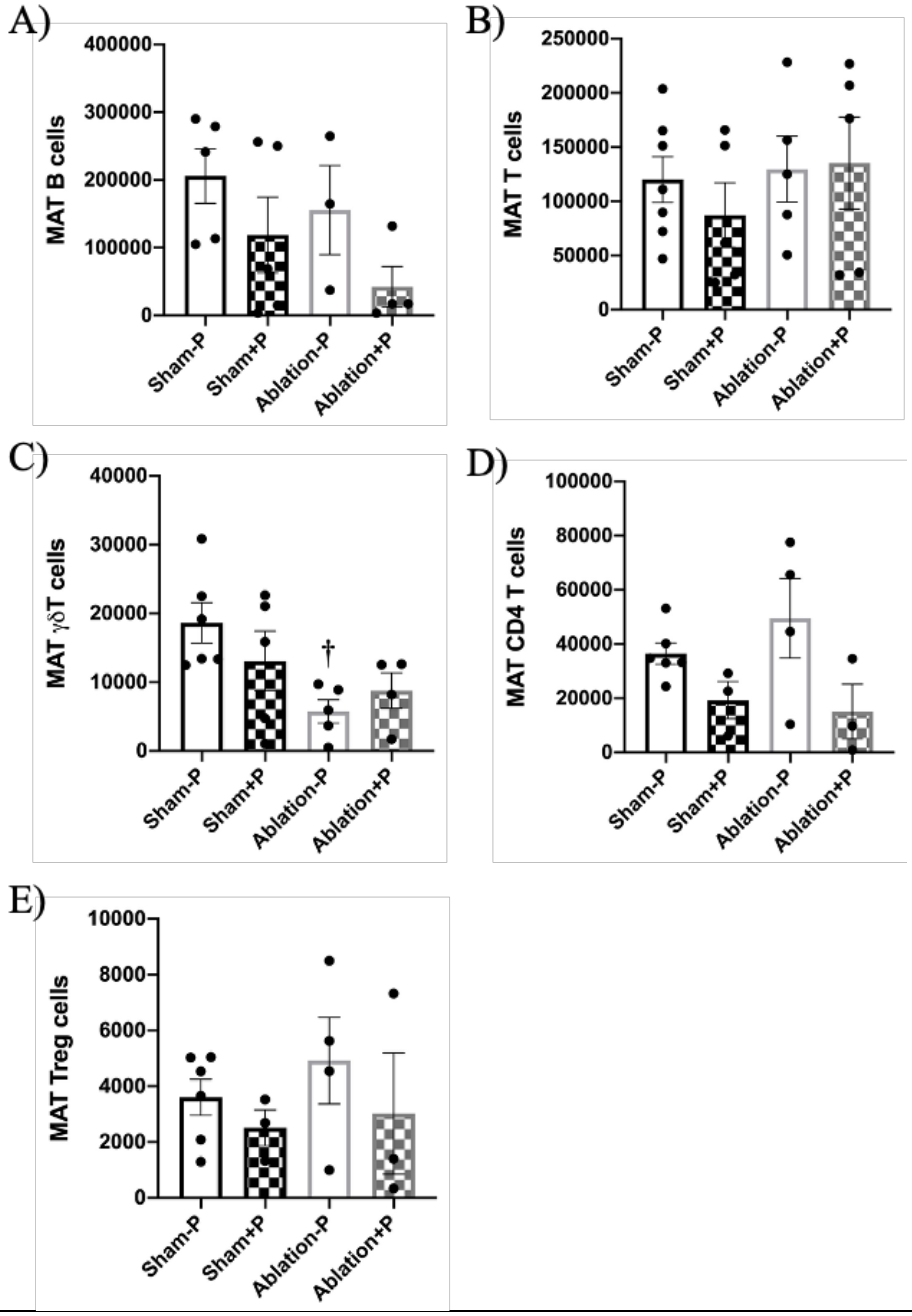

Figure 1.13. Immune cell populations within MAT. Mean ± SEM (n=3-7/group) absolute number $CD19^+$ B cells (A), $CD3^+$ T cells (B), $\gamma\delta TCR^+$ unconventional $\gamma\delta$T cells (C), $CD4^+$ helper T cells (D), and $Foxp3^+CD25^+$ T_{regs} (E) in MAT. Statistical analysis was performed using two-way ANOVA with Tukey's post hoc test. †$P < 0.05$ vs Sham-P, *$P < 0.05$ vs Sham+P, ∫$P < 0.05$ vs Ablation-P.

In the liver (*Figure 1.14*), we found that MLN ablation led to an increase in the absolute number of B cells (Hedges' g=-1.91, P=0.0284), total $CD3^+$ T cells (Hedges' g=-1.34, P=0.1240), $CD4^+$ T cells (Hedges' g=-1.76, P=0.0347), and T_{regs} (Hedges' g=-2.09, P=0.0416)

within Ablation-P mice compared to Sham-P mice. All of which were then reduced by Pirfenidone treatment in Ablation+P relative to Ablation-P controls (B cells: Hedges' g=1.26, P=0.3580; total $CD3^+$ T cells: Hedges' g=1.24, P=0.2058; $CD4^+$ T cells: Hedges' g=1.16, P=0.2510; and T_{regs}: Hedges' g=2.21, P=0.0313). Interestingly, $\gamma\delta$T cells appeared to be only affected by Pirfenidone treatment, and were reduced within both Sham+P (Hedges' g=0.36, P=0.9992) and Ablation+P (Hedges' g=0.59, P=0.8597) mice relative to untreated controls. In contrast, Pirfenidone treatment led to an increase B cells (Hedges' g=-0.27, P=0.7736), total $CD3^+$ T cells (Hedges' g=-0.77, P=0.5499), $CD4^+$ T cells (Hedges' g=-1.12, P=0.2427), and T_{regs} (Hedges' g=-0.57, P=0.8174) within Sham mice.

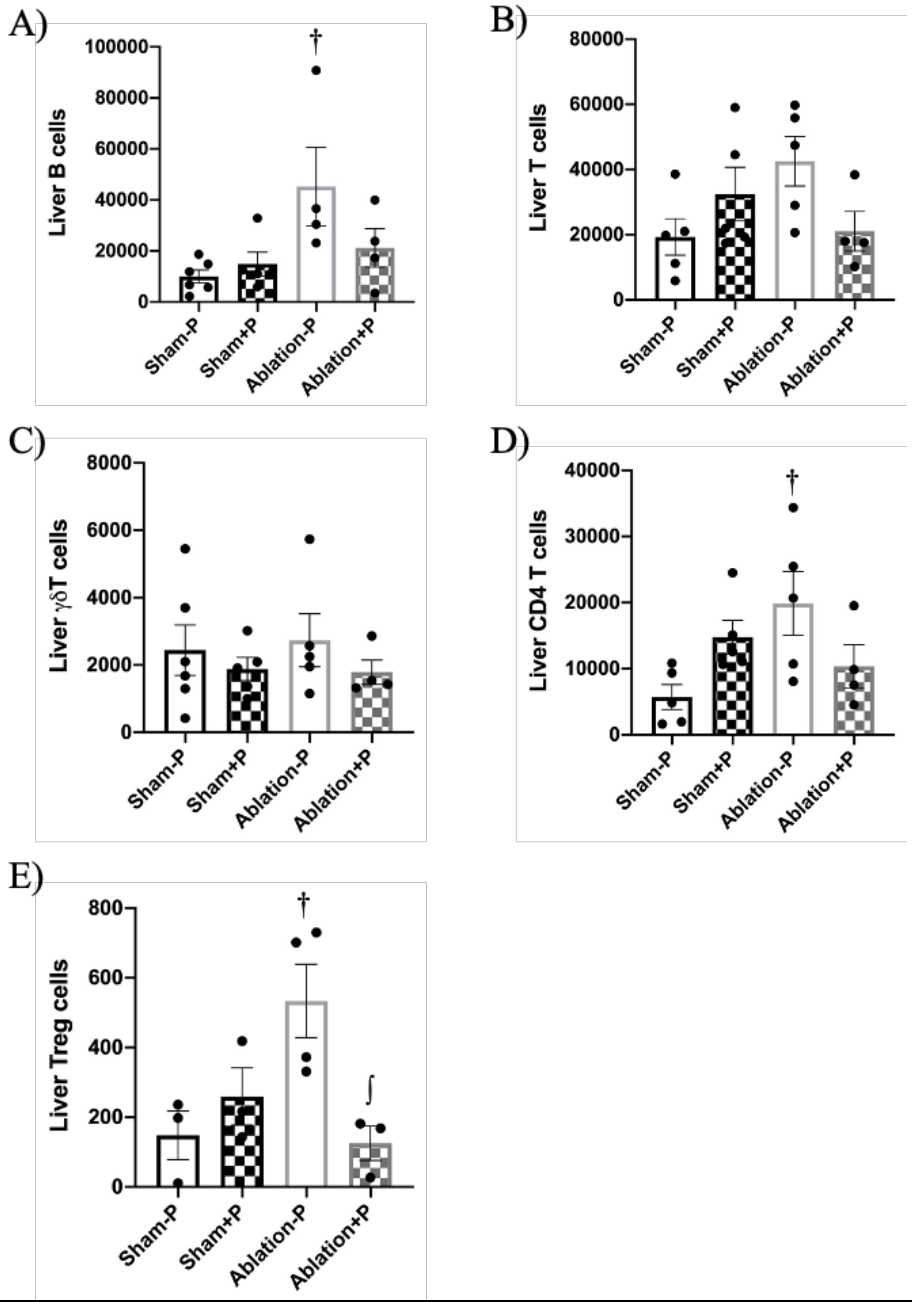

Figure 1.14. Immune cell populations within the liver. Mean ± SEM (n=3-6/group) absolute number $CD19^+$ B cells (A), $CD3^+$ T cells (B), $\gamma\delta TCR^+$ unconventional $\gamma\delta$T cells (C), $CD4^+$ helper T cells (D), and $Foxp3^+CD25^+$ T_{regs} (E) in liver. Statistical analysis was performed using two-way ANOVA with Tukey's post hoc test. †$P < 0.05$ vs Sham-P, *$P < 0.05$ vs Sham+P, ∫$P < 0.05$ vs Ablation-P.

Regarding the ileum (*Figure 1.15*), we observed that MLN ablation led to a reduction in the absolute number of total $CD3^+$ T cells (Hedges' g=0.81, P=0.5372), however did not affect B cells, $\gamma\delta$T cells or $CD4^+$ T cell numbers, in Ablation-P mice relative to Sham-P controls. In

contrast, MLN ablation led to an increase in T_{regs} (Sham-P vs Ablation-P, Hedges' g=-0.72, P=0.9365). We also found that Pirfenidone treatment led to a reduction in B cells (Hedges' g=1.12, P=0.2394), total $CD3^+$ T cells (Hedges' g=0.60, P=0.7501), $\gamma\delta$T cells (Hedges' g=0.43, P=0.8960), $CD4^+$ T cells (Hedges' g=0.75, P=0.5958), and T_{regs} (Hedges' g=1.99, P=0.0219) within Ablation+P mice relative to Ablation-P controls. As well as within Sham+P mice ($CD3^+$ T cells: Hedges' g=0.90, P=0.3952; $\gamma\delta$T cells: Hedges' g=0.50, P=0.9650; $CD4^+$ T cells: Hedges' g=0.37, P=0.9022; and T_{regs}: Hedges' g=1.25, P=0.0804).

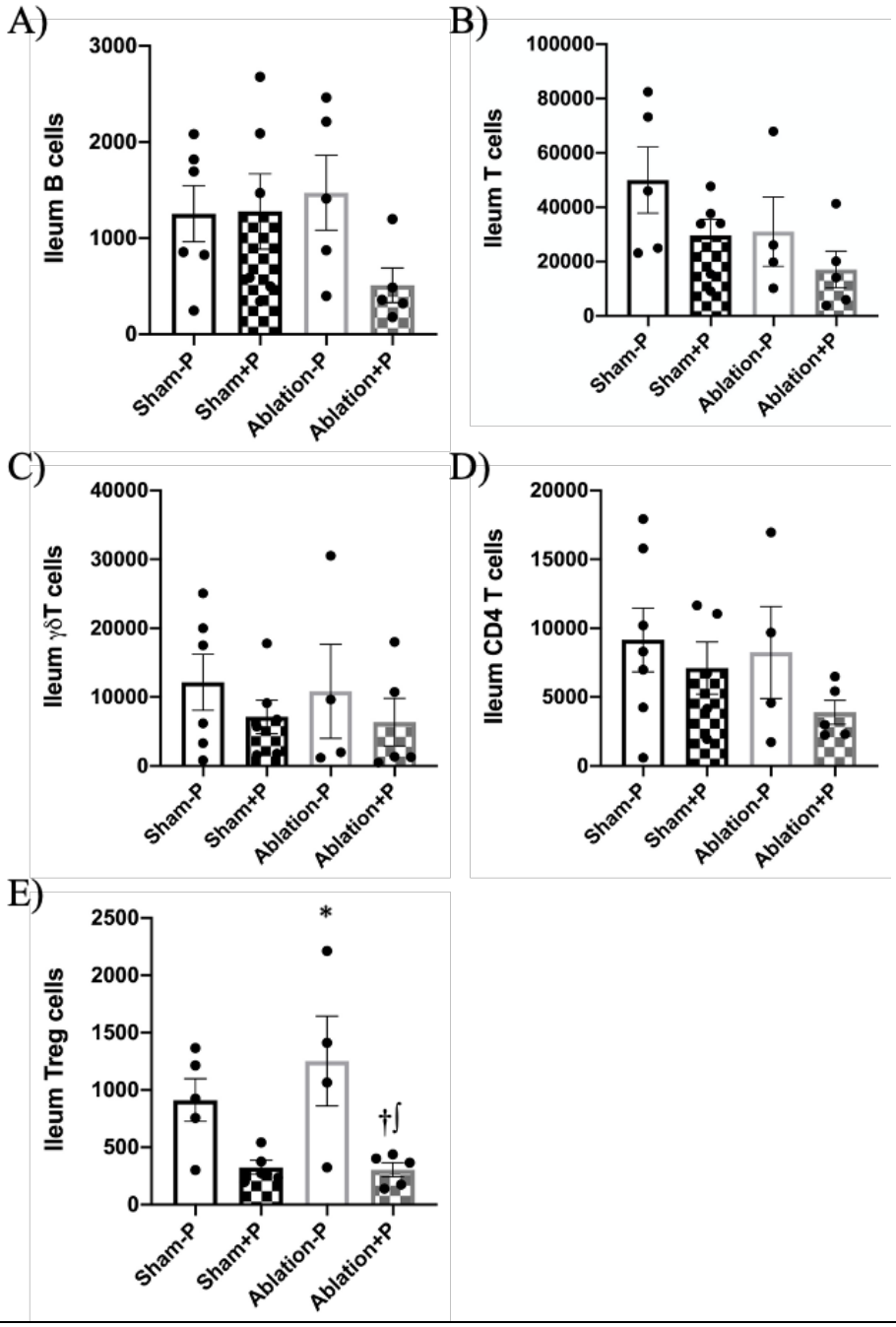

Figure 1.15. Immune cell populations within the ileum. Mean ± SEM (n=4-7/group) absolute number $CD19^+$ B cells (A), $CD3^+$ T cells (B), $\gamma\delta TCR^+$ unconventional $\gamma\delta$T cells (C), $CD4^+$ helper T cells (D), and $Foxp3^+CD25^+$ T_{regs} (E) in ileum. Statistical analysis was performed using two-way ANOVA with Tukey's post hoc test. †$P < 0.05$ vs Sham-P, *$P < 0.05$ vs Sham+P, ∫$P < 0.05$ vs Ablation-P.

In the jejunum (*Figure 1.16*), we saw that MLN ablation led to an increase in the absolute number of LPAM-1^+ B cells (Hedges' g=-1.02, P=0.4023) and total B cells (Hedges' g=-0.29,

P=0.9493) within Ablation-P mice as compared to Sham-P counterparts. This increase was further exacerbated by Pirfenidone treatment (LPAM-1$^+$ B cells: Hedges' *g*=-0.64, *P*=0.7536; B cells: Hedges' *g*=-0.27, *P*=0.9647) in Ablation+P mice. Additionally, we found that Pirfenidone treatment led to an increase in CD3$^+$ T cells (Hedges' *g*=-0.60, *P*=0.7513), CD4$^+$ T cells (Hedges' *g*=-1.29, *P*=0.1764), and T_{regs} (Hedges' *g*=-0.91, *P*=0.5229) within Ablation+P mice. As well as Sham+P mice (CD3$^+$ T cells: Hedges' *g*=-0.30, *P*=0.9455; CD4$^+$ T cells: Hedges' *g*=-0.92, *P*=0.3779; and T_{regs}: Hedges' *g*=-1.62, *P*=0.0692).

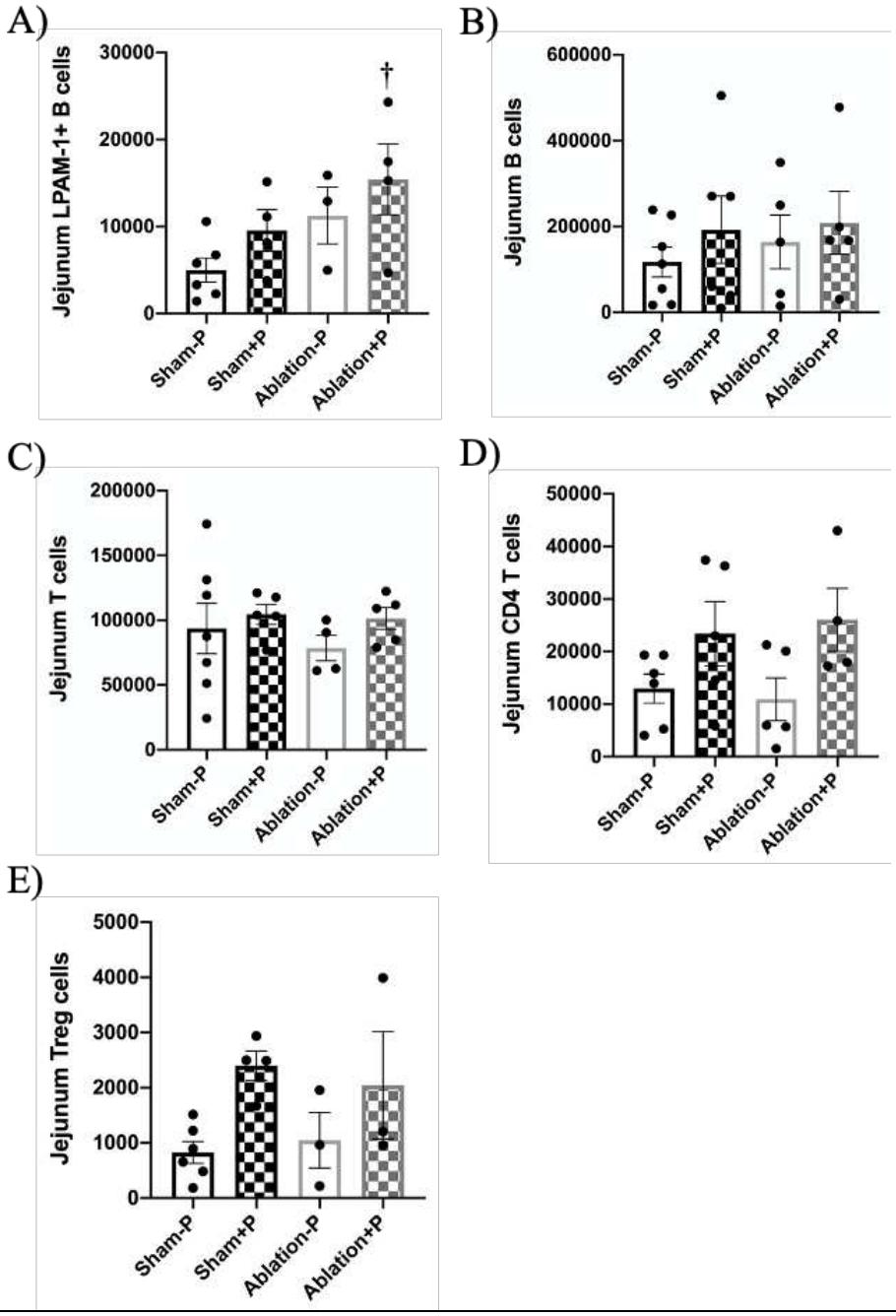

Figure 1.16. Immune cell populations within the jejunum. Mean ± SEM (n=3-7/group) absolute number LPAM-1^{+}CD19^{+} gut homing B cells (A), CD19^{+} B cells (B), CD3^{+} T cells (C), CD4^{+} helper T cells (D), and Foxp3^{+}CD25^{+} T_{regs} (E) in jejunum. Statistical analysis was performed using two-way ANOVA with Tukey's post hoc test. †P < 0.05 vs Sham-P, *P < 0.05 vs Sham+P, ∫P < 0.05 vs Ablation-P.

Within the spleen (*Figure 1.17*), we found that MLN ablation led to a reduction in the absolute number of B cells (Hedges' g=0.77, P=0.5498), CD3^{+} T cells (Hedges' g=0.68, P=0.6374), CD4^{+} T cells (Hedges' g=0.52, P=0.8024), and T_{regs} (Hedges' g=0.27, P=0.9642)

within Ablation-P mice relative to Sham-P mice. This ablation-induced reduction was further exacerbated by Pirfenidone treatment in B cells (Hedges' g=0.53, P=0.8141) and T_{regs} (Hedges' g=0.25, P=0.9719). We also saw a similar Pirfenidone-induced reduction in Sham mice (B cells: Hedges' g=0.88, P=0.4150; $CD3^+$ T cells: Hedges' g=0.45, P=0.8500; and $CD4^+$ T cells: Hedges' g=0.36, P=0.9131). Interestingly, $\gamma\delta$T cells appeared to be only affected by Pirfenidone treatment, and this was seen in both Sham+P (Hedges' g=0.71, P=0.5860) and Ablation+P (Hedges' g=0.91, P=0.4098) mice.

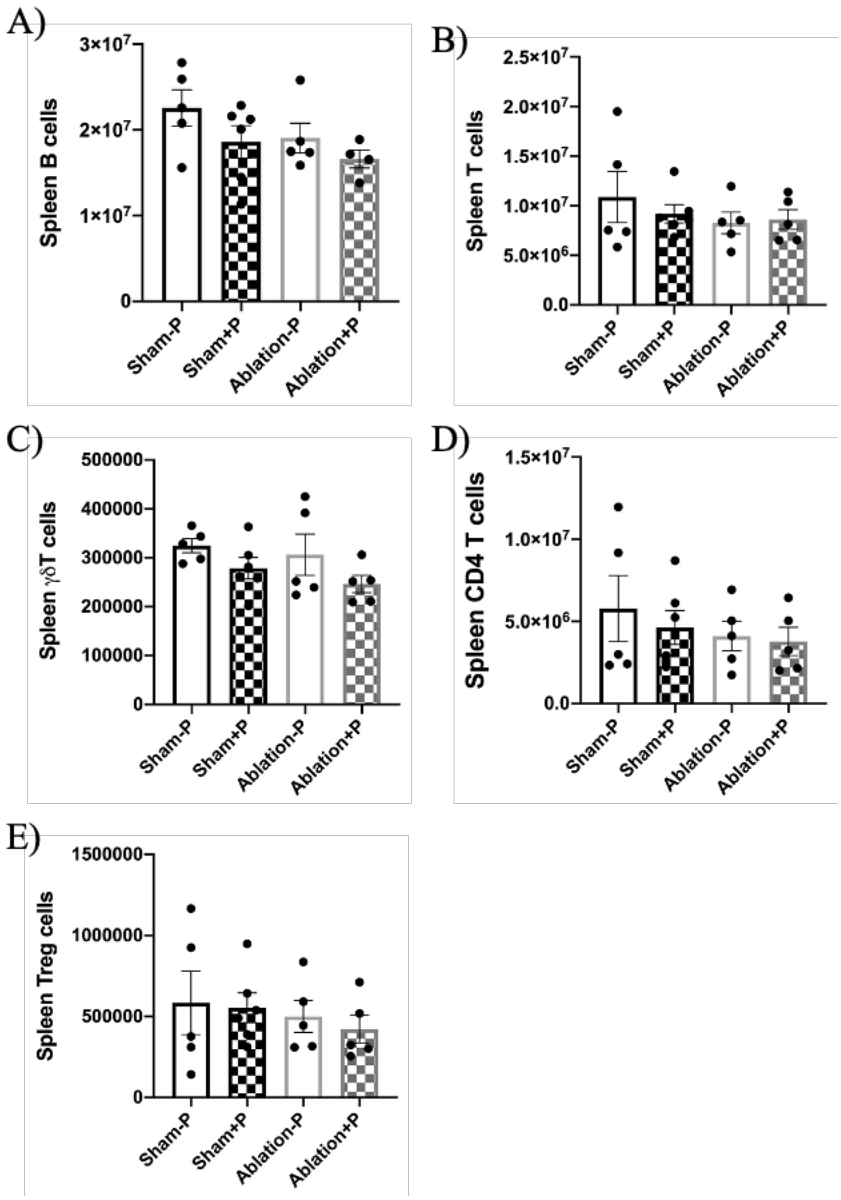

Figure 1.17. Immune cell populations within the spleen. Mean ± SEM (n=4-6/group) absolute number $CD19^+$ B cells (A), $CD3^+$ T cells (B), $\gamma\delta TCR^+$ unconventional $\gamma\delta$T cells (C), $CD4^+$ helper T cells (D), and $Foxp3^+CD25^+$ T_{regs} (E) in spleen. Statistical analysis was performed using two-way ANOVA with Tukey's post hc test. †$P < 0.05$ vs Sham-P, *$P < 0.05$ vs Sham+P, ∫$P < 0.05$ vs Ablation-P.

Discussion

Overall, the results of our studies demonstrate that MLN dysfunction, either as a result of surgical manipulation or HFD-induced obesity, promotes metabolic dysfunction. Further that functional MLNs are needed for the full restorative effects of Pirfenidone treatment. We have compared various metabolic and immune outcomes in MLN restricted (Ablation groups) and unrestricted (Sham groups) mice, consuming either obesogenic (HFD) or non-obesogenic (LFD and CH) diets. This strategy allowed us to analyze the effects of MLN dysfunction within obese and normal weight mice. To the best of our knowledge, we are the first to show that cauterization can successfully remove MLNs without significantly disrupting the surrounding tissue and vasculature. Here we reproducibly achieved 80-100% removal of the MLNs (experiment 1 and 3), generating a model of lymph node dysfunction.

In experiment 1, we aimed to investigate the ramifications of MLN removal within HFD-induced obese and non-obese mice. Lymph node dissection is a commonly used technique for the study of lymph nodes and the lymphatic system (46). MLNs constitute the main mesenteric lymph node chain of gut draining lymph nodes and are housed within MAT (36). Here they play an essential role in the maintenance and protection of MAT and draining sections of the gut (36-40). We found that MLN ablation led to alterations in general adiposity, independent of body weight and caloric intake. Within the context of HFD feeding, MLN restricted mice had an increase in MAT mass. These findings are supported by work highlighting the contribution of lymphatic function in obesity and adipose tissue metabolism, as obesity is shown to promote pathologic changes in the lymphatic system and lymphatic dysfunction is shown to promote the

development of obesity (72). Work by Escobedo et al. show that lipid-rich lymph is adipogenic, promoting adipogenesis *in vitro*, and that the fatty acid fraction of leaking lymph promotes *de novo* adipogenesis in surrounding tissue (73). Additionally, we found that MLN ablation led to a reduction in hepatic insulin-stimulated phosphorylation of AKT, which was exacerbated by HFD feeding. Assessment of AKT Ser^{473} phosphorylation is one of the most commonly used readouts of cellular insulin action (74), as activated AKT phosphorylates many downstream substrates, making it a central node in the insulin signaling cascade (75). Given the importance of insulin action in metabolic homeostasis (76) and that perturbations in the insulin signaling pathway lead to peripheral insulin resistance, a hallmark of obesity and metabolic dysfunction (76, 77), our findings suggest that MLN removal impairs hepatic insulin signaling. Numerous studies demonstrate a link between hepatic insulin resistance and inflammation within the gut and MAT, passively implicating lymphatic dysfunction within MAT (9, 78). However, to date, no studies have directly examined the role of the MLNs on hepatic insulin sensitivity. We speculate that removal of the MLNs promotes hepatic insulin resistance through 1) an increase in portal flux of effluent from the gut and MAT (i.e. fatty acids, cytokines, and LPS) that would normally be cleared by the MLNs (79-88), and 2) through an increase in inflammation within the gut and MAT (89-92). Furthermore, we found that MLN ablation led to substantial alterations in tissue immune cell populations and frequency, many of which were worsened in the context of HFD feeding. MLN restricted mice displayed reductions in total immune cells and T cell populations within the jejunum, while showed increases in T cell number within MAT. The lymphatic 'vascular' system is a unidirectional conduit responsible for an array of critical biological functions, including fluid homeostasis, absorption of dietary fat in the gastrointestinal tract, transport of antigen presenting cells (APCs) to lymph nodes, and management of immune cell

trafficking and inflammation (72). Thus, lymph nodes are essential for normal immune function (46). Our data suggests that removal of the MLNs impairs jejunal immune integrity and promotes MAT dysfunction and inflammation, which is in line with their importance in maintaining gut and MAT homeostasis (43, 93-97). Taken together, results from experiment 1 demonstrate that MLN dysfunction, simulated by removal of the MLNs, in HFD-induced obese mice leads to metabolic and immune alterations through 1) the promotion of visceral adiposity and T cell infiltration, 2) impairment of insulin signaling within the liver, and 3) compromise of jejunal immune function.

Given the above observations, and previous work from our lab demonstrating that chronic HFD consumption provokes MLN fibrosis (47, 48), in experiment 2 we aimed to investigate the effect of Pirfenidone treatment on MLNs within HFD-induced obese and non-obese mice. It is well established that inflammation associated with chronic disease facilitates tissue fibrosis, eventually leading to tissue dysfunction (51, 52). Pirfenidone is a commonly used anti-fibrotic and anti-inflammatory medication that acts through inhibiting TGF-β (58-63) and NF-κB (64-69). We found that Pirfenidone treatment led to a modest reduction in total body weight within HFD fed mice only, which occurred independent of caloric intake. Pirfenidone has previously been reported to induce anorexia, although in a dose-dependent manner (98, 99). However, as total caloric intake was comparable between groups, a separate mechanism likely explains this observation. Work by Sandoval-Rodriguez A et al. shows that Pirfenidone is a ligand for PPAR-α, increasing its expression as well as other enzymes involved in fatty acid metabolism, resulting in an overall increase in fatty acid oxidation (100). Additionally, we found that HFD-induced obese mice displayed elevated circulating levels of pro-inflammatory cytokines (MCP-1, TNF, IL-6) (101, 102) and adipokines (leptin, PAI-1, resistin) (103-106), as

well as insulin. However, Pirfenidone treatment was able to attenuate these HFD-induced increases in circulating markers, apart from IL-6 and PAI-1. These data are largely in agreement with the literature and known mechanisms of Pirfenidone action (64-69, 107). However, the observed increases in IL-6 and PAI-1 by Pirfenidone are more controversial as a limited number of studies report an increase in circulating IL-6 (65) or weak suppression of IL-6 (68), and none report an increase in PAI-1. The discrepancy in findings may result from sample type (i.e. tissue, serum) analyzed, Pirfenidone dosage and rout of administration, or study sample size. Nevertheless, further follow-up is needed. Finally, we found that HFD-induced obese mice had an increase in collagen deposition within the MLNs, evidencing MLN fibrosis, which was then rescued by Pirfenidone treatment. Collectively, results from experiment 2 support and extend previous work, highlighting the contribution of MLN fibrosis to obesity-induced metabolic adaptions. As well as demonstrate that Pirfenidone treatment can attenuate obesity-induced MLN fibrosis, and improve markers of metabolic function and inflammation.

As we have established that Pirfenidone treatment can rescue obesity-induced MLN fibrosis, in experiment 3 we aimed to determine the requirement of the MLNs in Pirfenidone-induced reversal of disease associated with obesity. As Pirfenidone is known to exert is anti-fibrotic and anti-inflammatory effects broadly throughout the body, we removed the MLNs via cauterization to determine their requirement. We found that MLN ablation led to a modest increase in body weight independent of caloric intake, which was reflected by an increase in general adiposity. Pirfenidone treatment normalized this effect in MLN restricted mice and reduced overall adiposity in unrestricted mice. These changes are in agreement with results from experiment 1 and 2, although the MLN-ablation induced increase in body weight was more prominent here in experiment 3. Surprisingly, we found that neither MLN ablation nor

Pirfenidone treatment altered glucose tolerance. Despite this, both MLN ablation and Pirfenidone treatment led to a small reduction in glucose-stimulated insulin secretion. These data may suggest impairments in insulin production and secretion. Pirfenidone treatment has previously been shown to improve pancreatic fibrosis within mice, yet not increase glucose tolerance or pancreatic insulin content (108). Overall, these findings in combination with the MLN ablation-induced impairment in hepatic insulin signaling observed in experiment 1, suggest that removal of the MLNs disrupts glucose homeostasis. Again, we found that immune cell populations were substantially altered by MLN ablation. MLN restricted mice displayed increases in several immune cell populations within the liver and MAT, suggesting tissue inflammation (109-111), while concomitantly showing reductions in splenic and ileal immune populations indicating immune cell recruitment from the spleen (112) and depletion within the ileum (113). Pirfenidone treatment of MLN restricted animals resulted in global reductions within immune cell populations, apart from in the jejunum. Similar reductions were also observed in unrestricted mice treated with Pirfenidone, however interestingly these mice also displayed increases within several jejunal and hepatic immune cell subsets. The asymmetric effect of Pirfenidone on immune cell populations is likely several fold. Previous work demonstrates that Pirfenidone can directly inhibit the activation and proliferation of T lymphocytes, dendritic cells, and B cells (114-116), whereas enhance the activity of regulatory T cells (114, 117). Observed reductions in T_{reg} populations within the present study like result from depletion of the $CD4^+$ T cell pool. These data also highlight a tissue-specific effect of Pirfenidone action (i.e. within the small intestine) that is not well discussed in the literature. As such, these findings warrant further study to better understand the tissue-specific and immune cell-specific effects of Pirfenidone treatment. Although differences in study design and tissues sampled exist between experiments 1 and 3,

these findings are largely in agreement. In general, we found that MLN ablation led to 1) a reduction in total splenocytes, which was partially reflected by a reduction in $CD3^+$ T cells and $CD4^+$ T cells; 2) a reduction in total immune cells within the jejunum (the absolute number of leukocytes not shown for experiment 3), coinciding with reductions in T cell subsets; and 3) an increase in immune cell numbers within MAT, largely constituting T cell expansion. Collectively, results from experiment 3 support a critical role for the MLNs in the regulation of metabolic and immune homeostasis and demonstrate that Pirfenidone treatment does not fully restore the MLN restricted phenotype.

Although our study is not without limitation, results presented here substantiate previous work and extend our knowledge of obesity and associated pathologies, providing new insight into the role of the MLNs. Our work poses many new questions to answer in future studies regarding the distinct effects of Pirfenidone on immune cell subsets and elucidating mechanisms of crosstalk between the gut, liver, MAT, and MLNs. We expect that future studies will confirm results shown here and shed light on how mechanisms of crosstalk affect metabolic homeostasis. Altogether it can be concluded that the MLNs play an active role in the maintenance of metabolic homeostasis and without functional MLNs disease treatment is likely to be less effective.

REFERENCES

1. Lauby-Secretan B, Scoccianti C, Loomis D, Grosse Y, Bianchini F, Straif K, Group IAfRoCHW. Body Fatness and Cancer--Viewpoint of the IARC Working Group. N Engl J Med. 2016 Aug;375:794-8.
2. Bhaskaran K, Douglas I, Forbes H, dos-Santos-Silva I, Leon DA, Smeeth L. Body-mass index and risk of 22 specific cancers: a population-based cohort study of 5·24 million UK adults. Lancet. 2014 Aug;384:755-65.
3. Green WD, Beck MA. Obesity altered T cell metabolism and the response to infection. Curr Opin Immunol. 2017 Jun;46:1-7.
4. Green WD, Beck MA. Obesity Impairs the Adaptive Immune Response to Influenza Virus. Ann Am Thorac Soc. 2017 Nov;14:S406-S9.
5. Weitman ES, Aschen SZ, Farias-Eisner G, Albano N, Cuzzone DA, Ghanta S, Zampell JC, Thorek D, Mehrara BJ. Obesity impairs lymphatic fluid transport and dendritic cell migration to lymph nodes. PLoS One. 2013;8:e70703.
6. Tagliabue C, Principi N, Giavoli C, Esposito S. Obesity: impact of infections and response to vaccines. Eur J Clin Microbiol Infect Dis. 2016 Mar;35:325-31.
7. Frasca D, Ferracci F, Diaz A, Romero M, Lechner S, Blomberg BB. Obesity decreases B cell responses in young and elderly individuals. Obesity (Silver Spring). 2016 Mar;24:615-25.
8. Tagliabue A, Elli M. The role of gut microbiota in human obesity: recent findings and future perspectives. Nutr Metab Cardiovasc Dis. 2013 Mar;23:160-8.
9. Winer DA, Luck H, Tsai S, Winer S. The Intestinal Immune System in Obesity and Insulin Resistance. Cell Metab. 2016 Mar;23:413-26.
10. Fuster JJ, Ouchi N, Gokce N, Walsh K. Obesity-Induced Changes in Adipose Tissue Microenvironment and Their Impact on Cardiovascular Disease. Circ Res. 2016 May;118:1786-807.
11. Said A, Ghufran A. Epidemic of non-alcoholic fatty liver disease and hepatocellular carcinoma. World J Clin Oncol. 2017 Dec;8:429-36.
12. Hernández E, Kahl S, Seelig A, Begovatz P, Irmler M, Kupriyanova Y, Nowotny B, Nowotny P, Herder C, et al. Acute dietary fat intake initiates alterations in energy metabolism and insulin resistance. J Clin Invest. 2017 Feb;127:695-708.
13. Monteiro R, Azevedo I. Chronic inflammation in obesity and the metabolic syndrome. Mediators Inflamm. 2010;2010.
14. Ji Y, Sakata Y, Tso P. Nutrient-induced inflammation in the intestine. Curr Opin Clin Nutr Metab Care. 2011 Jul;14:315-21.
15. Kirpich IA, Marsano LS, McClain CJ. Gut-liver axis, nutrition, and non-alcoholic fatty liver disease. Clin Biochem. 2015 Sep;48:923-30.
16. de Heredia FP, Gómez-Martínez S, Marcos A. Obesity, inflammation and the immune system. Proc Nutr Soc. 2012 May;71:332-8.
17. Furman D, Campisi J, Verdin E, Carrera-Bastos P, Targ S, Franceschi C, Ferrucci L, Gilroy DW, Fasano A, et al. Chronic inflammation in the etiology of disease across the life span. Nat Med. 2019 12;25:1822-32.

18. Blüher M, Laufs U. New concepts for body shape-related cardiovascular risk: role of fat distribution and adipose tissue function. Eur Heart J. 2019 Sep;40:2856-8.
19. Bjorntorp P. Metabolic implications of body fat distribution. Diabetes Care. 1991 Dec;14:1132-43.
20. Shuster A, Patlas M, Pinthus JH, Mourtzakis M. The clinical importance of visceral adiposity: a critical review of methods for visceral adipose tissue analysis. Br J Radiol. 2012 Jan;85:1-10.
21. Despres JP. Abdominal obesity and cardiovascular disease: is inflammation the missing link? Can J Cardiol. 2012 Nov-Dec;28:642-52.
22. Sato F, Maeda N, Yamada T, Namazui H, Fukuda S, Natsukawa T, Nagao H, Murai J, Masuda S, et al. Association of Epicardial, Visceral, and Subcutaneous Fat With Cardiometabolic Diseases. Circ J. 2018 01;82:502-8.
23. Gruzdeva O, Borodkina D, Uchasova E, Dyleva Y, Barbarash O. Localization of fat depots and cardiovascular risk. Lipids Health Dis. 2018 Sep;17:218.
24. Ferrucci L, Fabbri E. Inflammageing: chronic inflammation in ageing, cardiovascular disease, and frailty. Nat Rev Cardiol. 2018 09;15:505-22.
25. Pérez LM, Pareja-Galeano H, Sanchis-Gomar F, Emanuele E, Lucia A, Gálvez BG. 'Adipaging': ageing and obesity share biological hallmarks related to a dysfunctional adipose tissue. J Physiol. 2016 06;594:3187-207.
26. Palmer BF, Clegg DJ. The sexual dimorphism of obesity. Mol Cell Endocrinol. 2015 Feb;402:113-9.
27. Lam YY, Mitchell AJ, Holmes AJ, Denyer GS, Gummesson A, Caterson ID, Hunt NH, Storlien LH. Role of the gut in visceral fat inflammation and metabolic disorders. Obesity (Silver Spring). 2011 Nov;19:2113-20.
28. Kredel LI, Siegmund B. Adipose-tissue and intestinal inflammation - visceral obesity and creeping fat. Front Immunol. 2014;5:462.
29. Paeschke A, Erben U, Kredel LI, Kühl AA, Siegmund B. Role of visceral fat in colonic inflammation: from Crohn's disease to diverticulitis. Curr Opin Gastroenterol. 2017 01;33:53-8.
30. Eder P, Adler M, Dobrowolska A, Kamhieh-Milz J, Witowski J. The Role of Adipose Tissue in the Pathogenesis and Therapeutic Outcomes of Inflammatory Bowel Disease. Cells. 2019 06;8.
31. Macdougall CE, Wood EG, Loschko J, Scagliotti V, Cassidy FC, Robinson ME, Feldhahn N, Castellano L, Voisin MB, et al. Visceral Adipose Tissue Immune Homeostasis Is Regulated by the Crosstalk between Adipocytes and Dendritic Cell Subsets. Cell Metab. 2018 03;27:588-601.e4.
32. Boulange CL, Neves AL, Chilloux J, Nicholson JK, Dumas ME. Impact of the gut microbiota on inflammation, obesity, and metabolic disease. Genome Med. 2016 Apr 20;8:42.
33. Saltiel AR, Olefsky JM. Inflammatory mechanisms linking obesity and metabolic disease. J Clin Invest. 2017 Jan 3;127:1-4.
34. Kostic AD, Xavier RJ, Gevers D. The microbiome in inflammatory bowel disease: current status and the future ahead. Gastroenterology. 2014 May;146:1489-99.
35. Chistiakov DA, Bobryshev YV, Kozarov E, Sobenin IA, Orekhov AN. Intestinal mucosal tolerance and impact of gut microbiota to mucosal tolerance. Front Microbiol. 2014;5:781.
36. Esterházy D, Canesso MCC, Mesin L, Muller PA, de Castro TBR, Lockhart A, ElJalby M, Faria AMC, Mucida D. Compartmentalized gut lymph node drainage dictates adaptive immune responses. Nature. 2019 05;569:126-30.

37. Liu LM, MacPherson GG. Antigen acquisition by dendritic cells: intestinal dendritic cells acquire antigen administered orally and can prime naive T cells in vivo. J Exp Med. 1993 May;177:1299-307.
38. Yrlid U, Cerovic V, Milling S, Jenkins CD, Zhang J, Crocker PR, Klavinskis LS, MacPherson GG. Plasmacytoid dendritic cells do not migrate in intestinal or hepatic lymph. J Immunol. 2006 Nov;177:6115-21.
39. Milling SW, Jenkins CD, Yrlid U, Cerovic V, Edmond H, McDonald V, Nassar M, Macpherson G. Steady-state migrating intestinal dendritic cells induce potent inflammatory responses in naive CD4+ T cells. Mucosal Immunol. 2009 Mar;2:156-65.
40. Hahn A, Thiessen N, Pabst R, Buettner M, Bode U. Mesenteric lymph nodes are not required for an intestinal immunoglobulin A response to oral cholera toxin. Immunology. 2010 Mar;129:427-36.
41. Houston SA, Cerovic V, Thomson C, Brewer J, Mowat AM, Milling S. The lymph nodes draining the small intestine and colon are anatomically separate and immunologically distinct. Mucosal Immunol. 2016 Mar;9:468-78.
42. Miller MJ, McDole JR, Newberry RD. Microanatomy of the intestinal lymphatic system. Ann N Y Acad Sci. 2010 Oct;1207 Suppl 1:E21-8.
43. Macpherson AJ, Smith K. Mesenteric lymph nodes at the center of immune anatomy. J Exp Med. 2006 Mar;203:497-500.
44. Mowat AM, Agace WW. Regional specialization within the intestinal immune system. Nat Rev Immunol. 2014 Oct;14:667-85.
45. Tanoue T, Umesaki Y, Honda K. Immune responses to gut microbiota-commensals and pathogens. Gut Microbes. 2010 Jul;1:224-33.
46. Buettner M, Bode U. Lymph node dissection--understanding the immunological function of lymph nodes. Clin Exp Immunol. 2012 Sep;169:205-12.
47. Magnuson AM, Regan DP, Booth AD, Fouts JK, Solt CM, Hill JL, Dow SW, Foster MT. High-fat diet induced central adiposity (visceral fat) is associated with increased fibrosis and decreased immune cellularity of the mesenteric lymph node in mice. Eur J Nutr. 2019 Jun.
48. Solt CM, Hill JL, Vanderpool K, Foster MT. Obesity-induced immune dysfunction and immunosuppression: TEM observation of visceral and subcutaneous lymph node microarchitecture and immune cell interactions. Horm Mol Biol Clin Investig. 2019 May;39.
49. Smith AG, Sheridan PA, Tseng RJ, Sheridan JF, Beck MA. Selective impairment in dendritic cell function and altered antigen-specific CD8+ T-cell responses in diet-induced obese mice infected with influenza virus. Immunology. 2009 Feb;126:268-79.
50. Worbs T, Bode U, Yan S, Hoffmann MW, Hintzen G, Bernhardt G, Forster R, Pabst O. Oral tolerance originates in the intestinal immune system and relies on antigen carriage by dendritic cells. J Exp Med. 2006 Mar 20;203:519-27.
51. Cho ME, Kopp JB. Pirfenidone: an anti-fibrotic therapy for progressive kidney disease. Expert Opin Investig Drugs. 2010 Feb;19:275-83.
52. Margaritopoulos GA, Vasarmidi E, Antoniou KM. Pirfenidone in the treatment of idiopathic pulmonary fibrosis: an evidence-based review of its place in therapy. Core Evid. 2016;11:11-22.
53. Armendáriz-Borunda J, Rincón AR, Muñoz-Valle JF, Bueno-Topete M, Oregón-Romero E, Islas-Carbajal MC, Medina-Preciado D, González-García I, Bautista CA, et al. Fibrogenic polymorphisms (TGF-beta, PAI-1, AT) in Mexican patients with established liver fibrosis. Potential correlation with pirfenidone treatment. J Investig Med. 2008 Oct;56:944-53.

54. Rockey DC. Current and future anti-fibrotic therapies for chronic liver disease. Clin Liver Dis. 2008 Nov;12:939-62, xi.
55. RamachandraRao SP, Zhu Y, Ravasi T, McGowan TA, Toh I, Dunn SR, Okada S, Shaw MA, Sharma K. Pirfenidone is renoprotective in diabetic kidney disease. J Am Soc Nephrol. 2009 Aug;20:1765-75.
56. Azuma A, Nukiwa T, Tsuboi E, Suga M, Abe S, Nakata K, Taguchi Y, Nagai S, Itoh H, et al. Double-blind, placebo-controlled trial of pirfenidone in patients with idiopathic pulmonary fibrosis. Am J Respir Crit Care Med. 2005 May;171:1040-7.
57. Raghu G, Johnson WC, Lockhart D, Mageto Y. Treatment of idiopathic pulmonary fibrosis with a new antifibrotic agent, pirfenidone: results of a prospective, open-label Phase II study. Am J Respir Crit Care Med. 1999 Apr;159:1061-9.
58. Yamagami K, Oka T, Wang Q, Ishizu T, Lee JK, Miwa K, Akazawa H, Naito AT, Sakata Y, Komuro I. Pirfenidone exhibits cardioprotective effects by regulating myocardial fibrosis and vascular permeability in pressure-overloaded hearts. Am J Physiol Heart Circ Physiol. 2015 Aug;309:H512-22.
59. Iyer SN, Gurujeyalakshmi G, Giri SN. Effects of pirfenidone on transforming growth factor-beta gene expression at the transcriptional level in bleomycin hamster model of lung fibrosis. J Pharmacol Exp Ther. 1999 Oct;291:367-73.
60. Iyer SS, Cheng G. Role of interleukin 10 transcriptional regulation in inflammation and autoimmune disease. Crit Rev Immunol. 2012;32:23-63.
61. Tada S, Nakamuta M, Enjoji M, Sugimoto R, Iwamoto H, Kato M, Nakashima Y, Nawata H. Pirfenidone inhibits dimethylnitrosamine-induced hepatic fibrosis in rats. Clin Exp Pharmacol Physiol. 2001 Jul;28:522-7.
62. Nakayama S, Mukae H, Sakamoto N, Kakugawa T, Yoshioka S, Soda H, Oku H, Urata Y, Kondo T, et al. Pirfenidone inhibits the expression of HSP47 in TGF-beta1-stimulated human lung fibroblasts. Life Sci. 2008 Jan;82:210-7.
63. Hewitson TD, Kelynack KJ, Tait MG, Martic M, Jones CL, Margolin SB, Becker GJ. Pirfenidone reduces in vitro rat renal fibroblast activation and mitogenesis. J Nephrol. 2001 2001 Nov-Dec;14:453-60.
64. Chen G, Ni Y, Nagata N, Xu L, Zhuge F, Nagashimada M, Kaneko S, Ota T. Pirfenidone prevents and reverses hepatic insulin resistance and steatohepatitis by polarizing M2 macrophages. Lab Invest. 2019 Sep;99:1335-48.
65. Hale ML, Margolin SB, Krakauer T, Roy CJ, Stiles BG. Pirfenidone blocks the in vitro and in vivo effects of staphylococcal enterotoxin B. Infect Immun. 2002 Jun;70:2989-94.
66. Iyer SN, Hyde DM, Giri SN. Anti-inflammatory effect of pirfenidone in the bleomycin-hamster model of lung inflammation. Inflammation. 2000 Oct;24:477-91.
67. Arumugam TV, Shiels IA, Margolin SB, Taylor SM, Brown L. Pirfenidone attenuates ischaemia-reperfusion injury in the rat small intestine. Clin Exp Pharmacol Physiol. 2002 Nov;29:996-1000.
68. Nakazato H, Oku H, Yamane S, Tsuruta Y, Suzuki R. A novel anti-fibrotic agent pirfenidone suppresses tumor necrosis factor-alpha at the translational level. Eur J Pharmacol. 2002 Jun;446:177-85.
69. Nakanishi H, Kaibori M, Teshima S, Yoshida H, Kwon AH, Kamiyama Y, Nishizawa M, Ito S, Okumura T. Pirfenidone inhibits the induction of iNOS stimulated by interleukin-1beta at a step of NF-kappaB DNA binding in hepatocytes. J Hepatol. 2004 Nov;41:730-6.

70. Schiattarella GG, Altamirano F, Tong D, French KM, Villalobos E, Kim SY, Luo X, Jiang N, May HI, et al. Nitrosative stress drives heart failure with preserved ejection fraction. Nature. 2019 04;568:351-6.
71. Wynn TA. Cellular and molecular mechanisms of fibrosis. J Pathol. 2008 Jan;214:199-210.
72. Escobedo N, Oliver G. The Lymphatic Vasculature: Its Role in Adipose Metabolism and Obesity. Cell Metab. 2017 Oct;26:598-609.
73. Escobedo N, Proulx ST, Karaman S, Dillard ME, Johnson N, Detmar M, Oliver G. Restoration of lymphatic function rescues obesity in Prox1-haploinsufficient mice. JCI Insight. 2016 Feb;1.
74. Sarbassov DD, Guertin DA, Ali SM, Sabatini DM. Phosphorylation and regulation of Akt/PKB by the rictor-mTOR complex. Science. 2005 Feb;307:1098-101.
75. Petersen MC, Shulman GI. Mechanisms of Insulin Action and Insulin Resistance. Physiol Rev. 2018 10;98:2133-223.
76. Boucher J, Kleinridders A, Kahn CR. Insulin receptor signaling in normal and insulin-resistant states. Cold Spring Harb Perspect Biol. 2014 Jan;6.
77. Santoleri D, Titchenell PM. Resolving the Paradox of Hepatic Insulin Resistance. Cell Mol Gastroenterol Hepatol. 2019;7:447-56.
78. Konrad D, Wueest S. The gut-adipose-liver axis in the metabolic syndrome. Physiology (Bethesda). 2014 Sep;29:304-13.
79. Iqbal J, Hussain MM. Intestinal lipid absorption. Am J Physiol Endocrinol Metab. 2009 Jun;296:E1183-94.
80. Item F, Konrad D. Visceral fat and metabolic inflammation: the portal theory revisited. Obes Rev. 2012 Dec;13 Suppl 2:30-9.
81. Amar J, Chabo C, Waget A, Klopp P, Vachoux C, Bermúdez-Humarán LG, Smirnova N, Bergé M, Sulpice T, et al. Intestinal mucosal adherence and translocation of commensal bacteria at the early onset of type 2 diabetes: molecular mechanisms and probiotic treatment. EMBO Mol Med. 2011 Sep;3:559-72.
82. Deitch EA. Bacterial translocation or lymphatic drainage of toxic products from the gut: what is important in human beings? Surgery. 2002 Mar;131:241-4.
83. Macpherson AJ, Uhr T. Induction of protective IgA by intestinal dendritic cells carrying commensal bacteria. Science. 2004 Mar;303:1662-5.
84. Peyrin-Biroulet L, Gonzalez F, Dubuquoy L, Rousseaux C, Dubuquoy C, Decourcelle C, Saudemont A, Tachon M, Béclin E, et al. Mesenteric fat as a source of C reactive protein and as a target for bacterial translocation in Crohn's disease. Gut. 2012 Jan;61:78-85.
85. Sansonetti PJ, Di Santo JP. Debugging how bacteria manipulate the immune response. Immunity. 2007 Feb;26:149-61.
86. Deitch EA. Role of the gut lymphatic system in multiple organ failure. Curr Opin Crit Care. 2001 Apr;7:92-8.
87. Dixon JB. Lymphatic lipid transport: sewer or subway? Trends Endocrinol Metab. 2010 Aug;21:480-7.
88. Lynch PM, Delano FA, Schmid-Schönbein GW. The primary valves in the initial lymphatics during inflammation. Lymphat Res Biol. 2007;5:3-10.
89. Sun CM, Hall JA, Blank RB, Bouladoux N, Oukka M, Mora JR, Belkaid Y. Small intestine lamina propria dendritic cells promote de novo generation of Foxp3 T reg cells via retinoic acid. J Exp Med. 2007 Aug;204:1775-85.

90. Worthington JJ, Czajkowska BI, Melton AC, Travis MA. Intestinal dendritic cells specialize to activate transforming growth factor-β and induce Foxp3+ regulatory T cells via integrin αvβ8. Gastroenterology. 2011 Nov;141:1802-12.
91. Hadis U, Wahl B, Schulz O, Hardtke-Wolenski M, Schippers A, Wagner N, Müller W, Sparwasser T, Förster R, Pabst O. Intestinal tolerance requires gut homing and expansion of FoxP3+ regulatory T cells in the lamina propria. Immunity. 2011 Feb;34:237-46.
92. Ilan Y, Maron R, Tukpah AM, Maioli TU, Murugaiyan G, Yang K, Wu HY, Weiner HL. Induction of regulatory T cells decreases adipose inflammation and alleviates insulin resistance in ob/ob mice. Proc Natl Acad Sci U S A. 2010 May;107:9765-70.
93. Wang Q, Wu H. T Cells in Adipose Tissue: Critical Players in Immunometabolism. Front Immunol. 2018;9:2509.
94. Tchernof A, Despres JP. Pathophysiology of human visceral obesity: an update. Physiol Rev. 2013 Jan;93:359-404.
95. Pellegrinelli V, Carobbio S, Vidal-Puig A. Adipose tissue plasticity: how fat depots respond differently to pathophysiological cues. Diabetologia. 2016 06;59:1075-88.
96. Frasca D, Blomberg BB, Paganelli R. Aging, Obesity, and Inflammatory Age-Related Diseases. Front Immunol. 2017;8:1745.
97. Grant RW, Dixit VD. Adipose tissue as an immunological organ. Obesity (Silver Spring). 2015 Mar;23:512-8.
98. Ikeda S, Sekine A, Baba T, Katano T, Tabata E, Shintani R, Sadoyama S, Yamakawa H, Oda T, et al. Negative impact of anorexia and weight loss during prior pirfenidone administration on subsequent nintedanib treatment in patients with idiopathic pulmonary fibrosis. BMC Pulm Med. 2019 Apr;19:78.
99. Okuda R, Hagiwara E, Baba T, Kitamura H, Kato T, Ogura T. Safety and efficacy of pirfenidone in idiopathic pulmonary fibrosis in clinical practice. Respir Med. 2013 Sep;107:1431-7.
100. Sandoval-Rodriguez A, Monroy-Ramirez HC, Meza-Rios A, Garcia-Bañuelos J, Vera-Cruz J, Gutiérrez-Cuevas J, Silva-Gomez J, Staels B, Dominguez-Rosales J, et al. Pirfenidone Is an Agonistic Ligand for PPARα and Improves NASH by Activation of SIRT1/LKB1/pAMPK. Hepatol Commun. 2020 Mar;4:434-49.
101. Kang YE, Kim JM, Joung KH, Lee JH, You BR, Choi MJ, Ryu MJ, Ko YB, Lee MA, et al. The Roles of Adipokines, Proinflammatory Cytokines, and Adipose Tissue Macrophages in Obesity-Associated Insulin Resistance in Modest Obesity and Early Metabolic Dysfunction. PLoS One. 2016;11:e0154003.
102. Pirola L, Ferraz JC. Role of pro- and anti-inflammatory phenomena in the physiopathology of type 2 diabetes and obesity. World J Biol Chem. 2017 May;8:120-8.
103. Bilgic Gazioglu S, Akan G, Atalar F, Erten G. PAI-1 and TNF-α profiles of adipose tissue in obese cardiovascular disease patients. Int J Clin Exp Pathol. 2015;8:15919-25.
104. Garg MK, Dutta MK, Mahalle N. Adipokines (adiponectin and plasminogen activator inhhibitor-1) in metabolic syndrome. Indian J Endocrinol Metab. 2012 Jan;16:116-23.
105. Jamaluddin MS, Weakley SM, Yao Q, Chen C. Resistin: functional roles and therapeutic considerations for cardiovascular disease. Br J Pharmacol. 2012 Feb;165:622-32.
106. Ambroszkiewicz J, Chełchowska M, Rowicka G, Klemarczyk W, Strucińska M, Gajewska J. Anti-Inflammatory and Pro-Inflammatory Adipokine Profiles in Children on Vegetarian and Omnivorous Diets. Nutrients. 2018 Sep;10.
107. Ghosh AK, Vaughan DE. PAI-1 in tissue fibrosis. J Cell Physiol. 2012 Feb;227:493-507.

108. Lee E, Ryu GR, Ko SH, Ahn YB, Song KH. A role of pancreatic stellate cells in islet fibrosis and β-cell dysfunction in type 2 diabetes mellitus. Biochem Biophys Res Commun. 2017 04;485:328-34.
109. Freitas-Lopes MA, Mafra K, David BA, Carvalho-Gontijo R, Menezes GB. Differential Location and Distribution of Hepatic Immune Cells. Cells. 2017 Dec;6.
110. Robinson MW, Harmon C, O'Farrelly C. Liver immunology and its role in inflammation and homeostasis. Cell Mol Immunol. 2016 05;13:267-76.
111. Guzik TJ, Skiba DS, Touyz RM, Harrison DG. The role of infiltrating immune cells in dysfunctional adipose tissue. Cardiovasc Res. 2017 Jul;113:1009-23.
112. Bronte V, Pittet MJ. The spleen in local and systemic regulation of immunity. Immunity. 2013 Nov;39:806-18.
113. Winer DA, Winer S, Dranse HJ, Lam TK. Immunologic impact of the intestine in metabolic disease. J Clin Invest. 2017 01;127:33-42.
114. Visner GA, Liu F, Bizargity P, Liu H, Liu K, Yang J, Wang L, Hancock WW. Pirfenidone inhibits T-cell activation, proliferation, cytokine and chemokine production, and host alloresponses. Transplantation. 2009 Aug;88:330-8.
115. Bizargity P, Liu K, Wang L, Hancock WW, Visner GA. Inhibitory effects of pirfenidone on dendritic cells and lung allograft rejection. Transplantation. 2012 Jul;94:114-22.
116. Du J, Paz K, Flynn R, Vulic A, Robinson TM, Lineburg KE, Alexander KA, Meng J, Roy S, et al. Pirfenidone ameliorates murine chronic GVHD through inhibition of macrophage infiltration and TGF-β production. Blood. 2017 05;129:2570-80.
117. Oku H, Nakazato H, Horikawa T, Tsuruta Y, Suzuki R. Pirfenidone suppresses tumor necrosis factor-alpha, enhances interleukin-10 and protects mice from endotoxic shock. Eur J Pharmacol. 2002 Jun;446:167-76.

CHAPTER 3: CHRONIC LOW-DOSE DSS TREATMENT PROVOKES GASTROINTESTINAL INFLAMMATION WHILE RESHAPING THE IMMUNE LANDSCAPE

Overview

Background: Gastrointestinal (GI) inflammation is associated with generalized metabolic and immune dysfunction and can be characterized by alterations in hepatic lipid metabolism, insulin resistance, and visceral adipose tissue inflammation. Obesity and a high-fat diet (HFD) are well known contributors to GI dysfunction and inflammation. Previously, we have reported that HFD-induced obesity leads to mesenteric lymph node (MLN) fibrosis and immunologic dysfunction. Further, that MLN removal is associated with impaired hepatic insulin signaling and compromised GI integrity. However, the role of GI inflammation independent of diet and obesity on hepatic insulin sensitivity and immune function remains unclear. We propose that GI inflammation promotes MLN dysfunction, resulting in intestinal hyperpermeability and hepatic insulin resistance. *Methods:* Male C57BL/6 mice (n=22) were fed a low-fat diet (LFD) for the duration of the 12 wk study. GI inflammation was established by administration of 0.3% (w/v) dextran sulfate sodium (DSS) in drinking water (LFD+DSS, n=12) for the last 8 wk of study, control mice received only water (LFD-DSS, n=9). Glucose homeostasis was assessed by glucose tolerance test; hepatic insulin sensitivity was assessed by Western blot; and immune cells from mesenteric adipose tissue (MAT), MLNs, spleen, liver, jejunum, and ileum were characterized by flow cytometry. *Results:* Non-obese mice treated with low-dose DSS for 8 wk had a modest reduction in body weight and MAT mass, as well as broad alterations within tissue-

specific immune cell populations. Despite these adaptations, DSS treatment did not alter systemic glucose homeostasis. *Conclusions:* Chronic administration of low-dose DSS led to tissue level markers of inflammation within local and peripheral sites yet was unable to induce glucose intolerance.

Introduction

The immune system and inflammation are involved in a wide variety of physical health problems that dominate current morbidity and mortality worldwide (1-5). Chronic inflammatory diseases, such as heart disease, type 2 diabetes, and cancer, account for more than 50% of all deaths globally (6). Normally, an inflammatory response involves the temporally restricted upregulation of inflammatory activities in response to a threat, which resolve once the threat has been removed (7-9). However, certain lifestyle risk factors such as obesity, poor diet, and gut dysbiosis have been shown to inhibit the resolution of acute inflammation and in turn promote the development of systemic chronic inflammation (2, 8, 10). Shifts in the inflammatory response from acute to chronic lead to a breakdown of immune tolerance, which incites cell and tissue level damage (7, 9) and impairs normal immune function leading to an increased susceptibility for infection (11-14).

The gastrointestinal (GI) tract has considerable influence on immune homeostasis as it is our bodies largest immune reservoir (15-18), consisting of the gut-associated lymphoid tissue (GALT) and draining lymph nodes (16, 19). Within the gut, homeostasis relies on a delicate balance between immune tolerance and protective inflammatory responses (20-22). Where immune tolerance is critical for the prevention of aberrant inflammatory responses to commensal bacteria and nutrients (23, 24), as unrestrained inflammation is shown to promote the development of inflammatory bowel disease (15, 25). While inflammation is required for

protection against infectious pathogens like parasites and viruses (26, 27). The organized structure of the GALT and gut draining lymph nodes, particularly the mesenteric lymph nodes (MLNs), serve as critical sites for priming adaptive immune responses aimed at both promoting tolerance and pathogen clearance within the GI tract (19, 20). Disruption to any part of this complex and bidirectional relationship can impact several aspects of human health and is implicated in the development of several chronic diseases (28).

It is now widely recognized that perturbations within the GI tract including gut dysbiosis, intestinal barrier hyperpermeability, and immune dysfunction can lead to broad metabolic and inflammatory changes throughout the body (29-32). Specifically, shifts in a healthy gut microbiota, or dysbiosis, can disrupt the intestinal epithelium and increase its permeability (33-40) allowing for an increase in the translocation of intestinal contents which fuel inflammatory responses (41-43). This is demonstrated to culminate in altered hepatic lipid regulation (44), glucose homeostasis (45), and visceral fat metabolism and inflammation (46-49). Microbial populations are shown to be strongly influenced by diet composition (50-58), obesity (59-64), and a sedentary lifestyle (65-67) in both humans and rodents. For example high-fat diet (HFD) consumption is reported to induce gut dysbiosis independent of obesity, resulting in intestinal barrier hyperpermeability and endotoxemia (68-75). Similarly, obesity-induced microbial changes are associated with an increase in adiposity, insulin resistance, and systemic inflammation (76-80).

Traditionally it was thought that excess visceral adiposity was the predominant driver of co-morbidities associated with obesity, in particular hepatic insulin resistance and steatosis (81-84). This is attributed to the proximity and shared blood supply (i.e. portal vein) with the liver, as well as inflammatory phenotype of visceral adipose tissue (85, 86). However, as described

above, the GI tract also significantly contributes to the development and progression of metabolic disease. More importantly, gut-induced dysfunction and inflammation can occur independent of visceral obesity (75). Taken together, the above studies emphasize the ability of GI dysfunction to both initiate and maintain inflammation associated with obesity, resulting in systemic chronic inflammation.

We have previously demonstrated that HFD-induced obesity results in MLN dysfunction (87). Specifically, we found that HFD feeding led to MLN fibrosis and impairment of localized immunologic function, which was attributed to a reduction in immune cell number and activation. Additionally, we have shown that MLN dysfunction, simulated by the surgical removal of MLNs, was associated with impaired hepatic insulin signaling and compromised immunologic integrity in the gut (88). However, the metabolic ramifications of GI inflammation on MLN function remain unclear. We propose that inflammation localized within the gut can drive MLN dysfunction, exacerbating intestinal barrier hyperpermeability and promoting hepatic insulin resistance. To examine this, we utilized a model of GI inflammation independent of diet and obesity. This was accomplished with dextran sulfate sodium (DSS), a commonly used chemical to generate mouse models of colitis (89). The aim of the present study was to examine the effect of chemically induced GI inflammation on hepatic insulin sensitivity in male C57BL/6 mice.

Methods

Animals and Experimental Design

C57BL/6 male mice (2-3 months old) were obtained from the Jackson Laboratory. Mice were singly housed in a temperature (25°C) and humidity-controlled (50-60%) environment on a

12 h:12 h light-dark cycle. Prior to initiating experimental procedures, mice were acclimatized to the housing conditions for 1 wk. All animal procedures were reviewed and approved by the Colorado State University Institutional Animal Care and Use Committee. Mice received purified low-fat diet (LFD, n=22) (TD.08485; ENVIGO; 13% kcal from fat, 67.9% carbohydrate, and 19.1% protein) for the 12 wk duration of the study. After 4 wk on diet mice were split into two groups, those receiving (+DSS; LFD+DSS (n=12)) and not receiving (-DSS; LFD-DSS (n=9)) dextran sulfate sodium (DSS) treatment (*Figure 2.1*). Typically DSS is given at doses that lead to a reduction in body weight, however low-dose DSS treatment has been previously shown to induce gut and adipose tissue inflammation without a concurrent decrease in body mass (90, 91). For this experiment we wanted to characterize the outcomes of gut inflammation without the confounds of body weight change, thus we chose to use a low-dose DSS treatment. Mice received DSS (molecular weight, 40 kDa; J63606-14; Alfa Aeser) in autoclaved deionized water at a final dosage of 0.3% (w/v) for the last 8 wk of the study. Water was measured and replaced weekly, along with body weight and food intake. All mice were allowed free access to food and water for the duration of their studies.

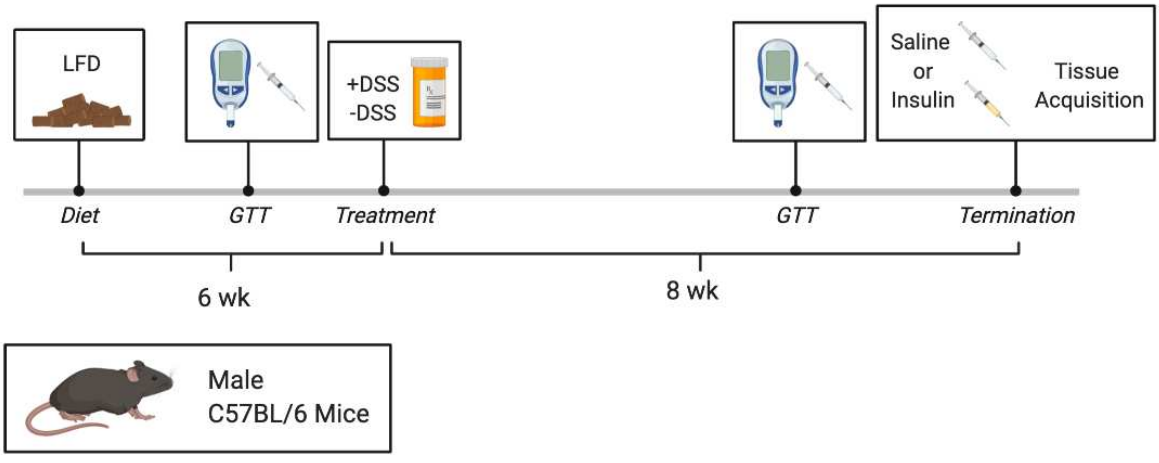

Figure 2.1. Experimental study design.

Glucose Tolerance Test (GTT)

Immediately prior to starting DSS treatment and termination, a GTT was performed. Mice were fasted for 6 h, after which baseline blood glucose concentrations were determined from tail vein blood using a glucometer (FreeStyle Lite; Abbott). Subsequently, about 100 µL of whole blood was collected into microcentrifuge tubes for serum isolation. Next mice were given an intraperitoneal (IP) injection of glucose solution (2 g of glucose/kg of body weight; D-Glucose (G 5400; Millipore Sigma)). Serial blood glucose measurements were taken post-injection at 15-, 30-, 45-, 60-, and 120-min via the tail vein. Whole blood was also collected at 15- and 30-min post-injection. Whole blood was allowed to clot at room temp for 10 min, serum was then isolated and stored at -80°C.

Insulin and Saline Injections

The day of termination, mice were fasted for 4 h. Fifteen minutes prior to termination, insulin or saline solution was administered to mice for downstream assessment of hepatic insulin sensitivity. Briefly, fasted mice were given an IP injection of either insulin solution (1 mU of insulin/g of body weight; Humulin R Insulin (100 U/mL, R-100; Eli Lilly)) or normal saline (for control mice).

Termination and Tissue Collection

Mice were anesthetized with isoflurane and euthanized by rapid decapitation. Excised MLNs were placed into 1X RPMI-1640 (10-041-CV; Corning) containing 2% fetal bovine serum (FBS) (F-0050-A; Atlas Biologics) and stored on ice. Excised mesenteric (MAT), epididymal (EAT), perirenal (PAT), inguinal (IAT), and brown (BAT) adipose tissue depots were weighed.

Collected MAT was placed into 1X RPMI-1640 containing 2% FBS and stored on ice. Excised livers, with the gallbladder removed, were weighed and then either snap frozen in liquid nitrogen or placed into MACs buffer [0.5% BSA (A7030-100G; Millipore Sigma), 10% 10X PBS, 2 mM Na_2EDTA (E5134; Millipore Sigma)] containing 2% FBS and stored on ice. Excised spleens where weighed and placed into 1X RPMI-1640 containing 2% FBS, and then stored on ice. Excised portions of the jejunum and ileum were measured and then placed into 1X Phosphate-buffered saline (PBS) containing 2% FBS and stored on ice.

Preparation of Cell Lysates and Western Blotting

Frozen liver sections were homogenized on ice in lysis buffer [10 mM Tris-HCl pH 7.4 (410901; J.T.Baker™), 150 mM NaCl (S271-500; Fisher Scientific), 5 mM Na_2EDTA (E5134; Millipore Sigma), 1% Triton™ X-100 (BP151-100; Fisher Scientific), 1% protease inhibitor cocktail (P8340; Millipore Sigma), and 1% phosphatase inhibitor cocktail 3 (P0044; Millipore Sigma)]. Samples were rotated for 30 min at 4°C, and then centrifuged at 12,000 g for 30 min. Total protein concentration was determined by the Biuret Method (Total Protein Reagent, T1949; Millipore Sigma).

Equivalent amounts of protein were subjected to capillary gel electrophoresis, using the Wes-Simple Western™ method (Protein Simple) according to manufactures instructions. The 12-230 kDa Wes Separation Module (SM-W004, Protein Simple) was used for all samples. In conjunction, the Anti-Rabbit/Mouse Detection Module (DM-001 or 002, Protein Simple) was also used. The sample plate was then centrifuged at 1000 g for 10 min at room temp and run under standard conditions. Protein expression was measured by chemiluminescence and quantified as area under the curve using the Compass for Simple Western software (Protein Simple). Proteins were detected with the following primary antibodies: AKT (pan) (clone

C67E7; 4691; Cell Signaling Technology), and AKT [p Ser473] (AF887-SP; Novus Biologicals).

Immune Cell Isolations for Flow Cytometry

All tissues taken for immune cell isolation were kept on ice and immediately processed. *MLNs* had surrounding adipose tissue removed and were then forced through 40 µm cell strainers using syringe plungers, with 1X RPMI-1640 containing 2% FBS. Cells were then washed and resuspended with 1X PBS containing 2% FBS. *MAT* was minced and then incubated with digestion solution [M199 (12340-030; Gibco) and 2 mg/mL Collagenase type II (LS004176; Worthington Labs)] for 15 min. Samples were then diluted with 1X PBS containing 2% FBS, titrated, and forced through 40 µm cell strainers. Cells were then washed and resuspended with 1X PBS containing 2% FBS. *Livers* sections were forced through 40 µm cell strainers using syringe plungers, with MACs buffer containing 2% FBS. Immune cells were then enriched for by centrifugation with Lympholyte®-M cell separation media (CL5035, Cedarlane), after which the buffy coat was removed, and then washed with MACs buffer containing 2% FBS. Finally, cells were washed and resuspended with 1X PBS containing 2% FBS. *Spleens* were forced through 40 µm cell strainers (501050134; Fisher Scientific) using syringe plungers, with 1X RPMI-1640 containing 2% FBS. Red blood cells (RBC) in spleen suspensions were lysed using 1X RBC lysis buffer (155 mM NH_4Cl, 12 mM $NaHCO_3$, 0.1mM Na_2EDTA). Cells were then washed and resuspended with 1X PBS containing 2% FBS. *Small intestine* segments were cut longitudinally and cleaned. Mucus was removed by washing tissues with removal solution [1X PBS, 2% FBS, 5 mM NAC (A8199; Millipore Sigma)]. Epithelial cells were then separated by washing tissues with removal solution (1X PBS, 2% FBS, 5 mM N_a2EDTA). Tissues were then minced and incubated with digestion solution [1X MEM (11090081; Gibco), 5

mg/mL Collagenase type I (LS004196; Worthington Labs), 1:40 DNAse 1 (D4263; Millipore Sigma), 1:40 Trypsin inhibitor (T6522; Millipore Sigma)] for 15 min. Samples were then diluted with 1X PBS containing 2% FBS, titrated, and forced through 40 μm cell strainers. Cells then had a final wash with mucus removal solution, and then were washed and resuspended with 1X PBS containing 2% FBS. Post-acquisition, cells were counted with trypan blue.

Flow Cytometry

Cell suspensions were incubated on ice in the dark for 30 min with LIVE/DEAD fixable yellow (L34967; Invitrogen) for dead cell discrimination. Nonspecific antibody binding was then blocked by incubating cells with TruStain FcX PLUS block (clone S17011E; 156604; Biolegend) on ice for 10 min. Cells were first stained for cell surface markers by incubating with fluorescently conjugated monoclonal antibodies at 4°C for 30 min in the dark. Then cells were prepared for intranuclear staining, using the Foxp3/Transcription Factor Staining Buffer Set (00-5523-00, eBioscience) according to manufactures instructions. Super Bright Complete Staining buffer (SB-4401-42; Invitrogen) was used per manufactures instructions in stain master mixes which contained more than one polymer dye.

The following fluorescent antibodies were used for cell surface staining: CD25 BV421 (clone PC61; Biolegend), CD11b eF450 (clone M1/70; eBioscience), CD45.2 BV570 (clone 104; Biolegend), TCR γ/δ BV605 (clone GL3;Biolegend), CD19 AF488 (clone 6D5; Biolegend), F4/80 PE (clone BM8; eBioscience), CD8a PE/Cy5 (clone 53-6.7; eBioscience), GR-1 PE/Cy7 (clone RB6-8C5; eBioscience), CD3ε PerCP/Cy5.5 (clone 145-2C11; Biolegend), CD4 AF647 (clone RM4-5; Biolegend), MHC2 APC (clone M5/114.15.2; eBioscience), CD11c APC/Fire750 (clone N418; Biolegend), CD103 BV510 (clone 2E7; Biolegend), integrin α4β7 PerCP/eF710

(clone DATK32; Invitrogen). The following fluorescently conjugated antibody was used for intranuclear staining: Foxp3 AF532 (clone FJK-16s; eBioscience).

All samples were analyzed using a Cytek Biosciences Aurora spectral flow cytometer and FlowJo™ Software (Becton Dickinson). Cells were gated on leukocytes based on characteristic forward and side scatter profiles. Individual cell populations were identified according to their presence of specific fluorescent-labeled antibodies.

Statistical Analysis

All statistical analysis was performed with GraphPad Prism version 8.4.2 for macOS (GraphPad Software). Data are presented as mean ± standard error of the mean (SEM). Significance was considered with a P value of < 0.05. A repeated measures two-way ANOVA with Tukey's post hoc test was used for variables measured over time. Whereas, an unpaired T test was used to compare all other group means. ANOVA and T test assumptions were checked and if data failed to meet these assumptions the data were log transformed and then re-analyzed. To determine the magnitude of treatment effect, a Hedges' g effect size was calculated. A g equal to 0.2 is interpreted as a small effect, a g equal to 0.5 as a medium effect, and a g equal to 0.8 as a large effect.

Results

Animal characteristics are shown in *Table 2.1*. We found that 8 wk of chronic low-dose DSS treatment led to a modest reduction in body weight, reported as change in body weight (g) (Hedges g=0.49, P=0.2857), despite a slightly elevated cumulative food intake (kcals) (Hedges g=-0.24, P=0.5726). No difference in water intake (mL), the vehicle for DSS treatment, was found between groups. Interestingly, we found that chronic low-dose DSS treatment led to a

moderate reduction in MAT (Hedges *g*=0.49, *P*=0.2591), IAT (Hedges *g*=1.22, *P*=0.4735), and BAT (Hedges *g*=0.40, *P*=0.3615) mass, but did not alter EAT, PAT, or spleen mass.

Table 2.1. General and metabolic characteristics

	LFD-DSS	LFD+DSS
Change in body weight (g)	3.15±0.39	2.67±0.23
Cumulative food intake (kcals)	912.40±23.45	931.30±22.32
Water intake (mL)	238.30±11.82	243.90±10.47
Mesenteric fat (g)	0.22±0.02	0.19±0.01
Inguinal fat (g)	0.46±0.03	0.43±0.03
Epididymal fat (g)	0.55±0.04	0.57±0.04
Perirenal fat (g)	0.25±0.02	0.25±0.02
Brown fat (g)	0.32±0.03	0.29±0.02
Spleen (g)	0.09±0.01	0.09±0.00

Data expressed as mean ± SEM; n=8-12/group. Statistical analysis was performed using an unpaired T test. Mice fed purified low-fat diet for 12 wk duration of the study and received DSS during the last 8 wk of study. Mesenteric fat, mesenteric adipose tissue; Inguinal fat, inguinal adipose tissue; Epididymal fat, epididymal adipose tissue; Perirenal fat, perirenal adipose tissue; Brown fat, brown adipose tissue.
**P* < 0.05 and ‡*P* < 0.01 vs LFD-DSS

It is proposed that GI inflammation independent of visceral obesity can impair hepatic glucose metabolism, which in turn can disrupt peripheral glucose homeostasis. We found that 8 wk of low-dose DSS treatment did not affect the blood glucose response (*Figure 2.2*) or glucose area under the curve (data now shown).

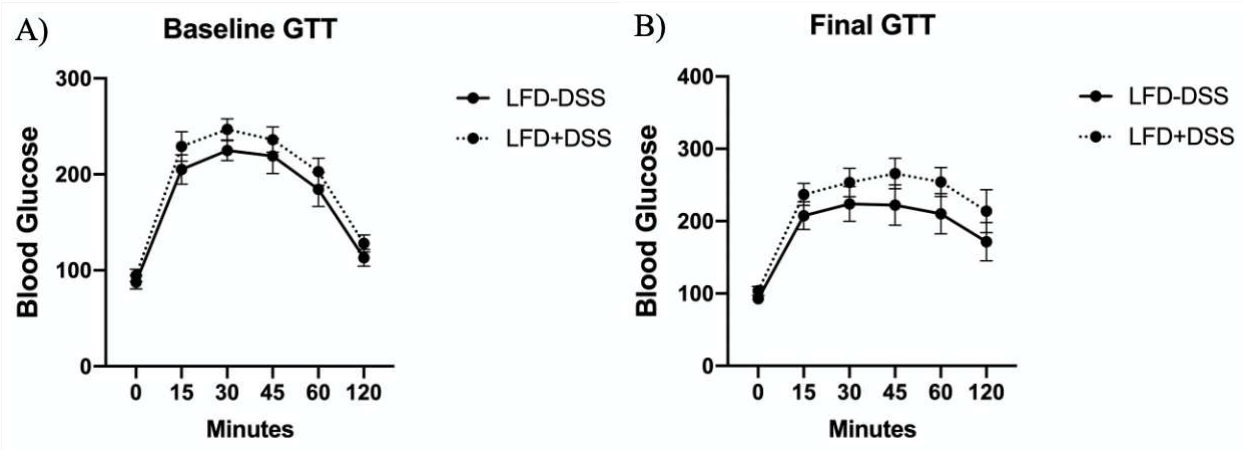

Figure 2.2. Baseline and final study blood glucose responses. Baseline GTT (A) and final GTT (B). Statistical analysis of AUC data was performed using an unpaired T test (data not shown). Data expressed as mean ± SEM; n=9-14/group. **P* < 0.05 and ‡*P* < 0.01 vs LFD-DSS.

DSS treatment leads to GI inflammation in a dose-dependent manner. To assess resultant immunologic changes, we collected portions of the small intestine (jejunum and ileum) and intra-abdominal tissues (MLNs, MAT, liver, and spleen). All acquired tissues were digested and cells collected (*Figure 2.3*). Total cell counts from MAT and spleen were normalized per gram of tissue. We found that chronic low-dose DSS treatment did not affect the total number of cells acquired from either the jejunum (*Figure 2.3A*) or ileum (*Figure 2.3B*). However, total splenocytes were substantially reduced in DSS treated mice (Hedges g=2.05, P=0.0060; *Figure 2.3C*). Additionally, we found that DSS treatment increased the total number of cells within both MAT (Hedges g=-0.27, P=0.6283; *Figure 2.3E*) and MLNs (Hedges g=-0.92, P=0.1856; *Figure 2.3F*). DSS treatment was not found to affect total cell counts within the liver (*Figure 2.3D*).

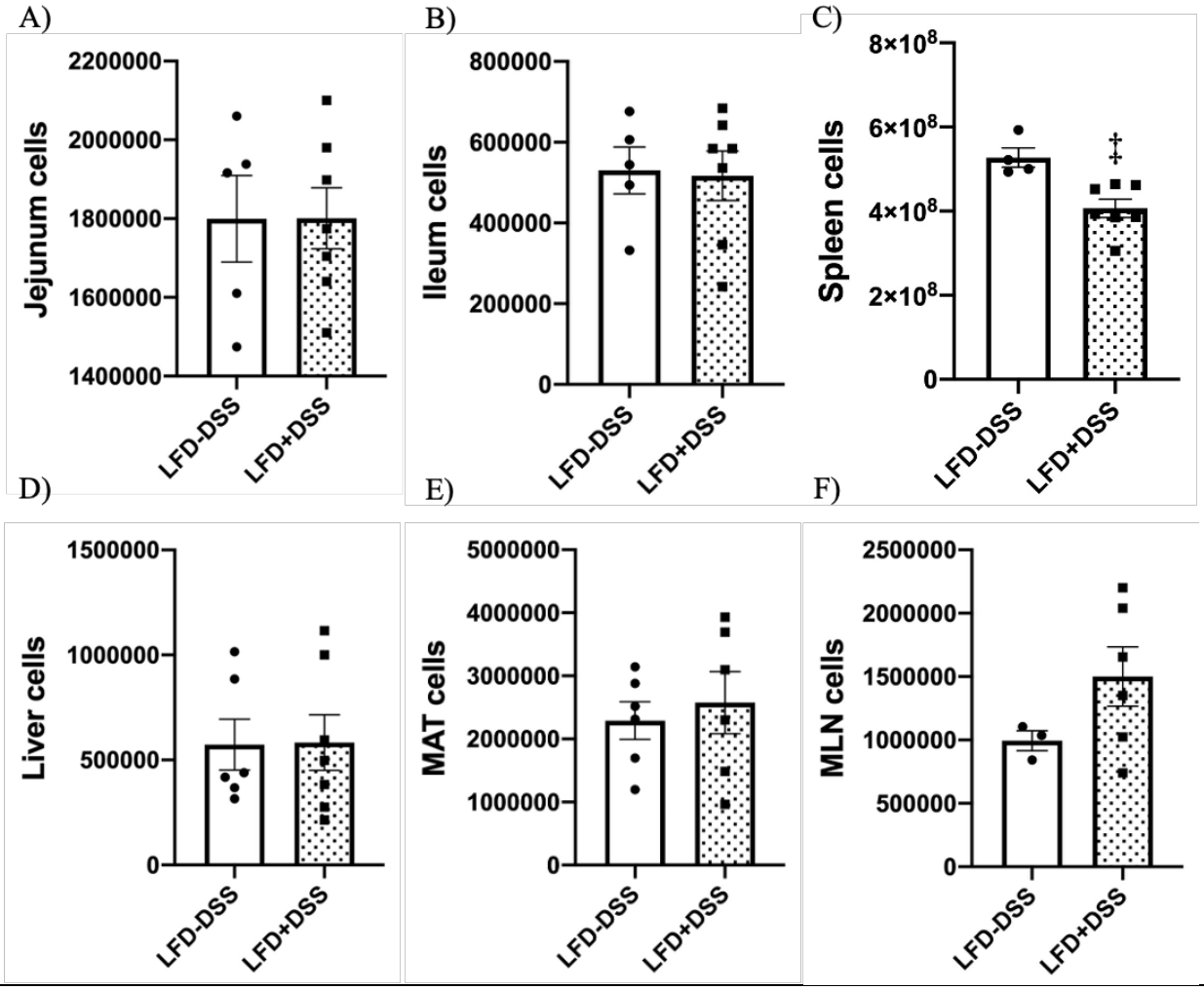

Figure 2.3. Tissue total cell counts. Immune cells were isolated from jejunum (A), ileum (B), spleen (C), liver (D), mesenteric adipose tissue (E), and mesenteric lymph nodes (F). Total cell counts from MAT and spleen were normalized to tissue weight, equal lengths of jejunum and ileum were taken, and equal sections of liver were used. Statistical analysis was performed using an unpaired T test. Data expressed as mean ± SEM; n=9-12/group. **P* < 0.05 and ‡*P* < 0.01 vs LFD-DSS.

Isolated cells were then analyzed by flow cytometry. Leukocytes were gaited with a primary gate excluding debris, secondary gate excluding doublets, tertiary gate on live cells (Live/Dead Yellow$^-$), and then on leukocytes (CD45.2$^+$). T cells (CD3$^+$), B cells (CD19$^+$), and non-lymphoid cells (CD3$^-$CD19$^-$) were gaited off leukocytes. T cells were further divided into $\gamma\delta$TCR$^+$ and $\gamma\delta$TCR$^-$ subsets, with $\gamma\delta$TCR$^-$ cells analyzed for CD8$^+$, CD4$^+$, and CD25$^+$Foxp3$^+$. Non-lymphoid cells were further divided into CD11b$^+$, CD11b$^+$CD11c$^+$, and CD11c$^+$ subsets.

$CD11b^+CD11c^+$and $CD11c^+$ cells that were $MHC2^+$ were analyzed for expression of $CD103^+$ and $CD8\alpha^+$. While $CD11b^+$ cells were analyzed for expression of GR-1^+. Absolute numbers of cell subsets were calculated for individual mice using total immune cell counts.

Within the jejunum (*Figure 2.4*), we found that chronic low-dose DSS treatment led to a sizable reduction in the absolute number of regulatory T cells ($CD25^+Foxp3^+$) (Hedges g=1.27, P=0.0712). As well as to a lesser extent unconventional $\gamma\delta$T cells ($CD3^+\gamma\delta TCR^+$) (Hedges g=1.03, P=0.1050), helper T cells ($CD4^+$) (Hedges g=0.78, P=0.2321), and $CD11b^+CD103^+$ intestinal dendritic cells ($CD11c^+MHC2^+CD11b^+CD103^+$) (Hedges g=0.77, P=0.2359). In contrast, DSS treatment increased $CD11b^+CD103^-$ dendritic cells ($CD11c^+MHC2^+CD11b^+CD103^-$) (Hedges g=-0.67, P=0.2455) and neutrophils ($CD11b^+$GR-1^+) (Hedges g=-0.80, P=0.1702). DSS was not found to affect the number of total leukocytes, B cells, T cells, $\alpha\beta$T cells ($CD3^+\gamma\delta TCR^-$) or cytotoxic T cells ($CD8^+$).

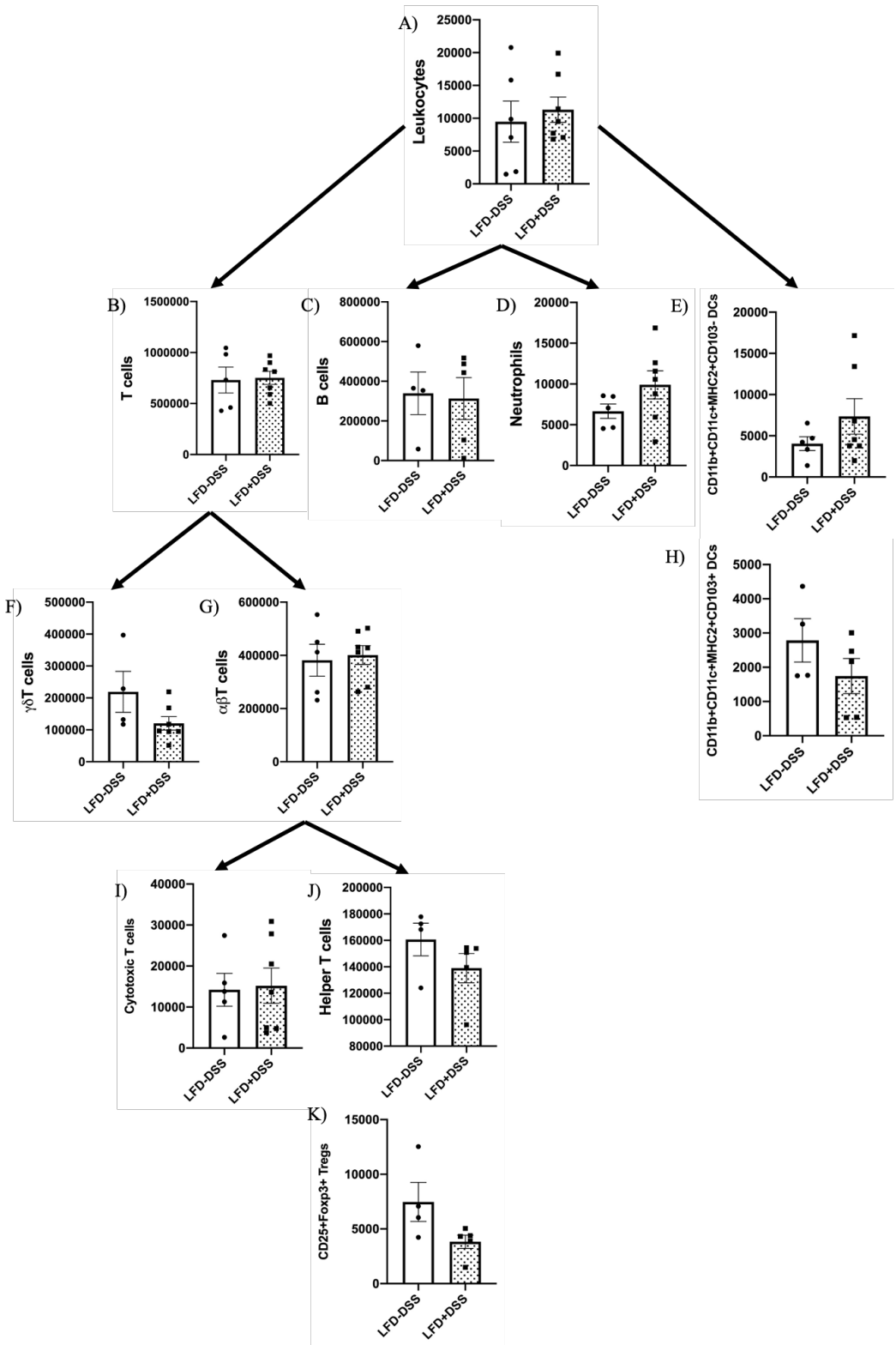

Figure 2.4. Immune cell populations within the jejunum. Mean ± SEM (n=4-7/group) absolute number leukocytes (A), T cells (B), B cells (C), neutrophils (D), $CD11c^{+}MHC2^{+}CD11b^{+}CD103^{-}$ dendritic cells (E), unconventional $\gamma\delta$T cells (F), $\alpha\beta$T cells (G), $CD11c^{+}MHC2^{+}CD11b^{+}CD103^{+}$ dendritic cells (H), cytotoxic T cells (I), helper T cells (J), $CD25^{+}Foxp3^{+}$ regulatory T cells (K). Statistical analysis was performed using an unpaired T test. *$P < 0.05$ and ‡$P < 0.01$ vs LFD-DSS.

Regarding the ileum (*Figure 2.5*), we found that chronic low-dose DSS treatment substantially reduced the absolute number of $CD11b^{-}CD103^{+}$ dendritic cells ($CD11c^{+}MHC2^{+}CD11b^{-}CD103^{+}$) (Hedges g=1.88, P=0.0121), and to a lesser extent cytotoxic T cells (Hedges g=0.56, P=0.3271) and $CD11b^{+}CD103^{+}$ intestinal dendritic cells (Hedges g=0.69, P=0.2472). Alternatively, the absolute number of regulatory T cells (Hedges g=-0.67, P=0.2961), helper T cells (Hedges g=-0.36, P=0.5619), and $CD11b^{+}CD103^{-}$ dendritic cells (Hedges g=-0.38, P=0.4992) were increased by DSS treatment. We did not find that DSS treatment affected the number of total leukocytes, B cells, T cells, $\alpha\beta$T cells, $\gamma\delta$T cells, or neutrophils.

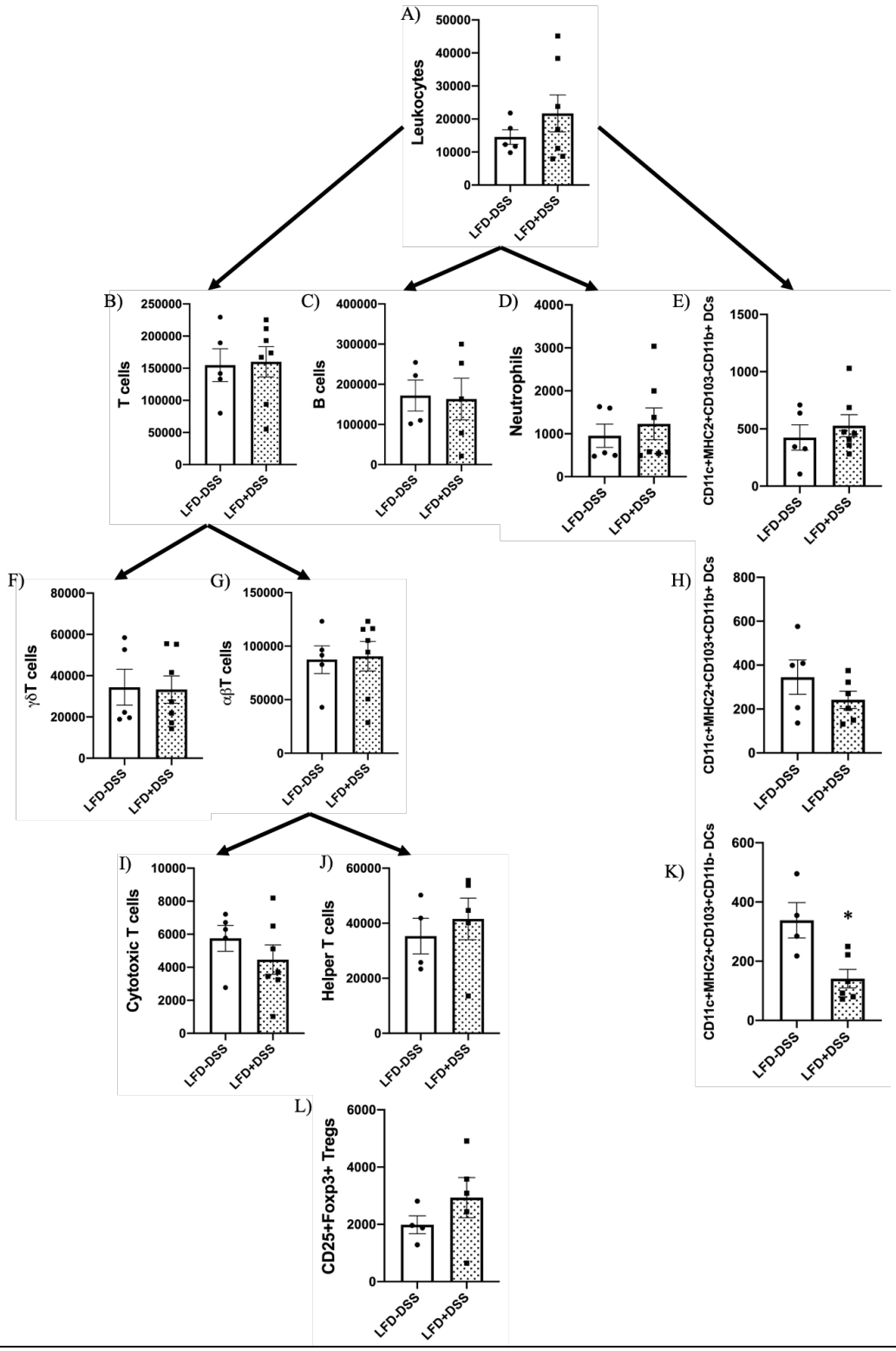

Figure 2.5. Immune cell populations within the ileum. Mean ± SEM (n=4-7/group) absolute number leukocytes (A), T cells (B), B cells (C), neutrophils (D), $CD11c^{+}MHC2^{+}CD11b^{+}CD103^{-}$ dendritic cells (E), unconventional $\gamma\delta$T cells (F), $\alpha\beta$T cells (G), $CD11c^{+}MHC2^{+}CD11b^{+}CD103^{+}$ dendritic cells (H), cytotoxic T cells (I), helper T cells (J), $CD11c^{+}MHC2^{+}CD11b^{-}CD103^{+}$ dendritic cells (K), $CD25^{+}Foxp3^{+}$ regulatory T cells (L). Statistical analysis was performed using an unpaired T test. *$P < 0.05$ and ‡$P < 0.01$ vs LFD-DSS.

In the spleen (*Figure 2.6*), we found that chronic low-dose DSS treatment considerably reduced the absolute number of $\gamma\delta$T cells (Hedges g=1.35, P=0.0351) and cytotoxic T cells (Hedges g=1.04, P=0.0823). As well as to a lesser extent total leukocytes (Hedges g=0.56, P=0.3220), T cells (Hedges g=0.87, P=0.1382), $\alpha\beta$T cells (Hedges g=0.92, P=0.1187), helper T cells (Hedges g=0.96, P=0.1525), and regulatory T cells (Hedges g=0.94, P=0.1597). DSS was not found to affect the number of B cells, $CD8^+$ dendritic cells ($CD11c^+MHC2^+CD8^+$), or $CD11b^+$ dendritic cells ($CD11c^+MHC2^+CD11b^+$).

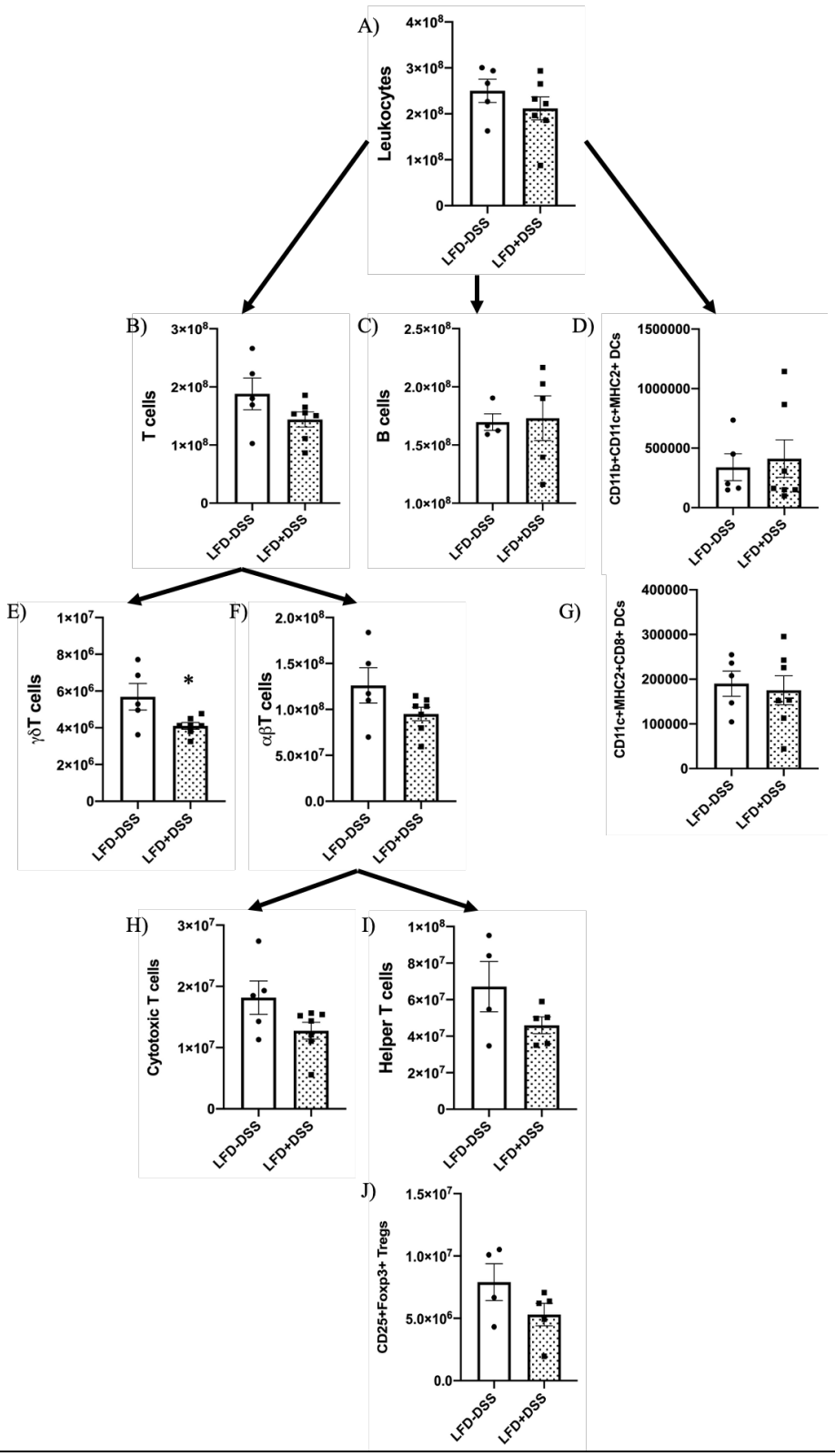

Figure 2.6. Immune cell populations within the spleen. Mean ± SEM (n=4-7/group) absolute number leukocytes (A), T cells (B), B cells (C), $CD11c^{+}MHC2^{+}CD11b^{+}$ dendritic cells (D), unconventional $\gamma\delta$T cells (E), $\alpha\beta$T cells (F), $CD11c^{+}MHC2^{+}CD8^{+}$ dendritic cells (G), cytotoxic T cells (H), helper T cells (I), $CD25^{+}Foxp3^{+}$ regulatory T cells (J). Statistical analysis was performed using an unpaired T test. *$P < 0.05$ and ‡$P < 0.01$ vs LFD-DSS.

Within the liver (*Figure 2.7*), we found that chronic low-dose DSS treatment led to a substantial increase in the absolute number of $CD8^{+}CD103^{-}$ dendritic cells (Hedges g=-2.37, P=0.0053) and to a lesser extent total leukocytes (Hedges g=-0.77, P=0.1787), B cells (Hedges g=-0.76, P=0.2455), $\gamma\delta$T cells (Hedges g=-0.69, P=0.2571), cytotoxic T cells (Hedges g=-0.60, P=0.2684), helper T cells (Hedges g=-0.25, P=0.6849), $CD11b^{+}$ dendritic cells (Hedges g=-0.92, P=0.11), and $CD8^{+}CD103^{+}$ dendritic cells ($CD11c^{+}MHC2^{+}CD8^{+}CD103^{+}$) (Hedges g=-0.81, P=0.2614). In opposition, DSS treatment reduced the number of $CD8^{-}CD103^{+}$ dendritic cells ($CD11c^{+}MHC2^{+}CD8^{-}CD103^{+}$) (Hedges g=0.30, P=0.6330). We did not find that DSS affected the absolute number of T cells, $\alpha\beta$T cells, or regulatory T cells.

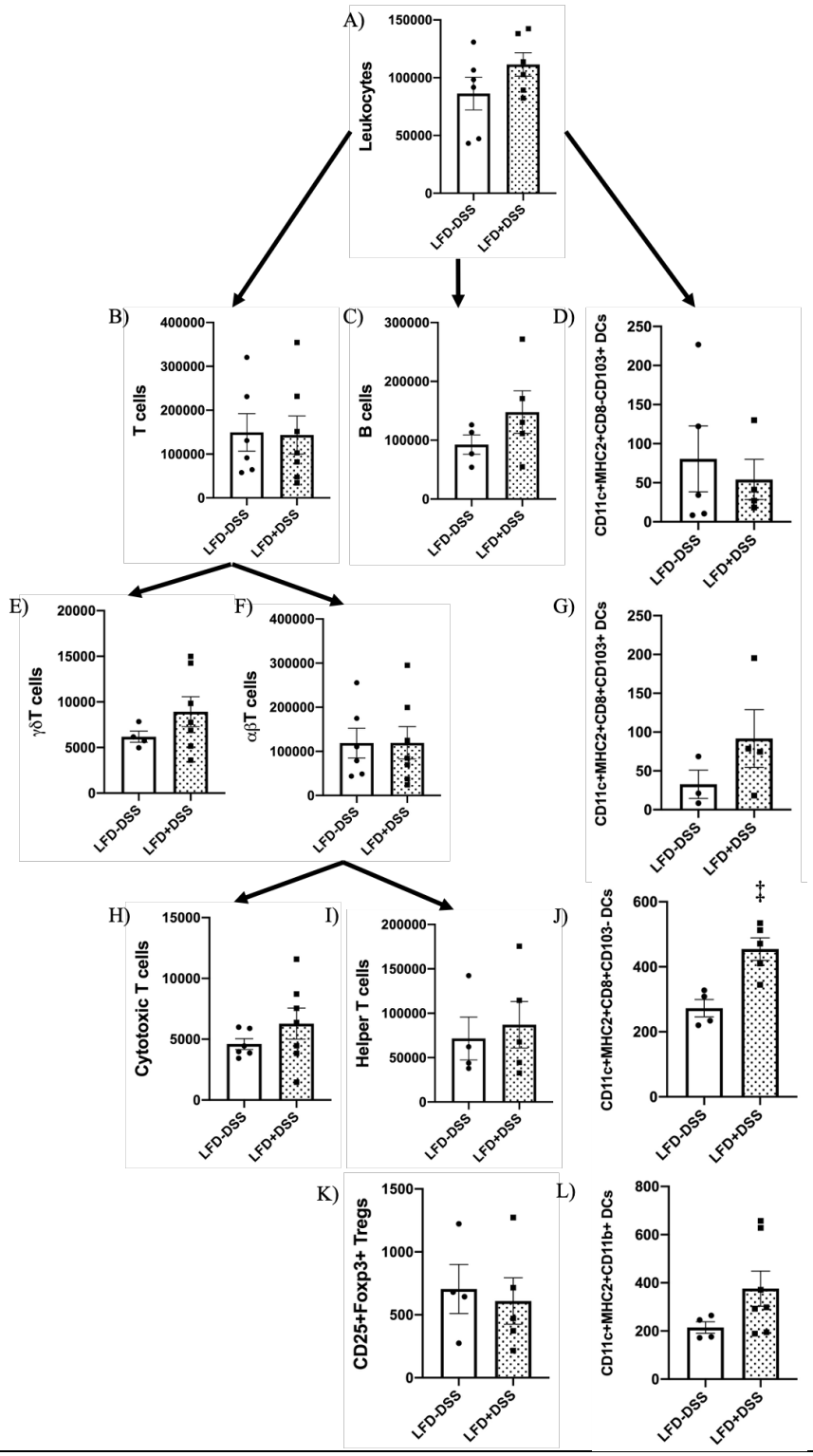

Figure 2.7. Immune cell populations within the liver. Mean ± SEM (n=3-7/group) absolute number leukocytes (A), T cells (B), B cells (C), $CD11c^{+}MHC2^{+}CD8^{-}CD103^{+}$ dendritic cells (D), unconventional $\gamma\delta$T cells (E), $\alpha\beta$T cells (F), $CD11c^{+}MHC2^{+}CD8^{+}CD103^{+}$ dendritic cells (G), cytotoxic T cells (H), helper T cells (I), $CD11c^{+}MHC2^{+}CD8^{+}CD103^{-}$ dendritic cells (J), $CD25^{+}Foxp3^{+}$ regulatory T cells (K), $CD11c^{+}MHC2^{+}CD11b^{+}$ dendritic cells (L). Statistical analysis was performed using an unpaired T test. $^{*}P < 0.05$ and ‡$P < 0.01$ vs LFD-DSS.

In MAT (*Figure 2.8*), we found that chronic low-dose DSS treatment considerably increased the absolute number of total leukocytes (Hedges g=-2.81, P=0.0022) and to a lesser extent B cells (Hedges g=-0.54, P=0.4161), T cells (Hedges g=-0.52, P=0.3514), $\alpha\beta$T cells (Hedges g=-0.48, P=0.3863), cytotoxic T cells (Hedges g=-0.24, P=0.6656), and helper T cells (Hedges g=-0.57, P=0.4006). On the contrary, DSS treatment led to a reduction in the number of $CD11b^+$ dendritic cells (Hedges g=1.03, P=0.0654), $\gamma\delta$T cells (Hedges g=0.57, P=0.3338), and regulatory T cells (Hedges g=0.36, P=0.5654).

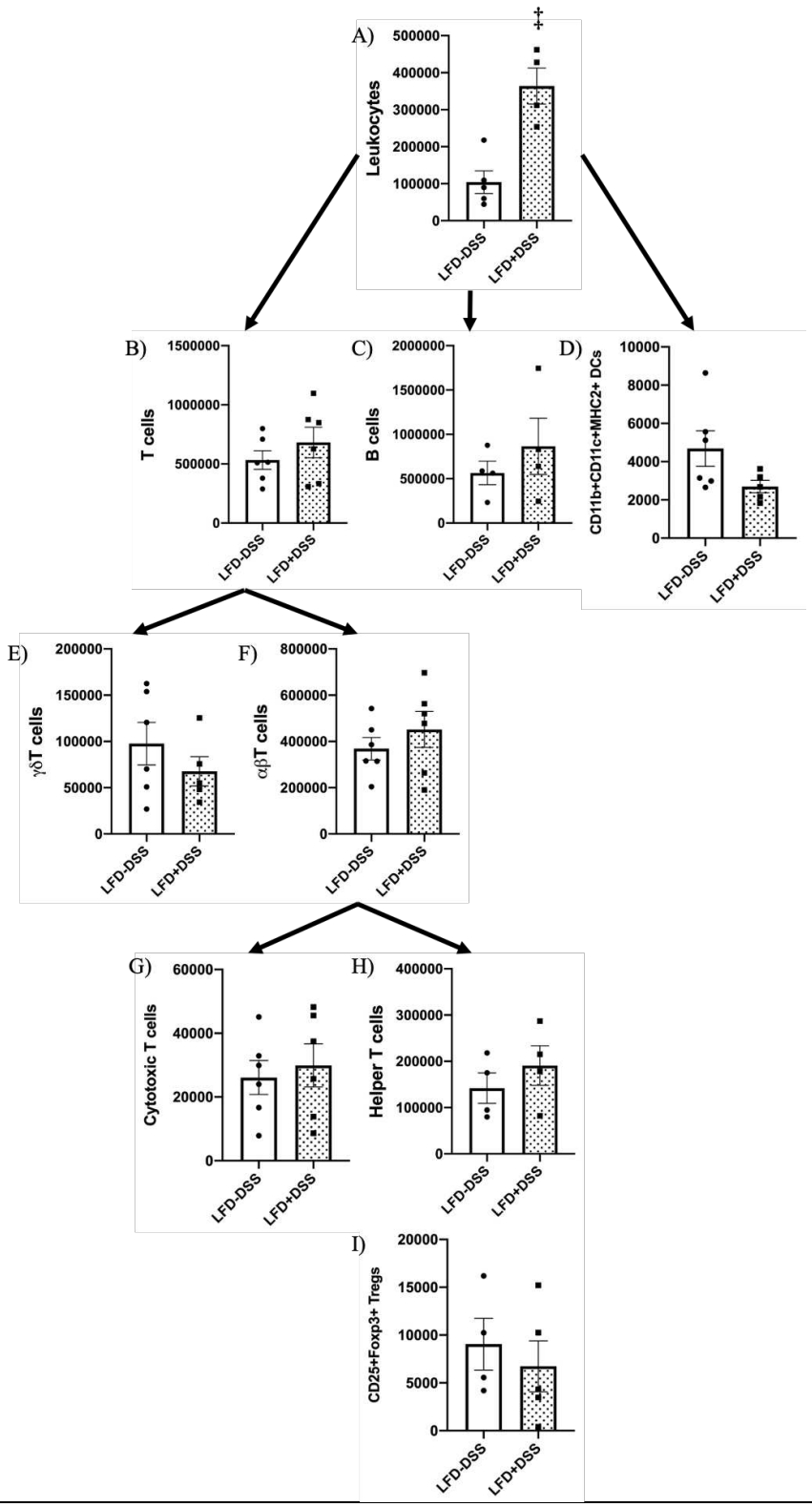

Figure 2.8. Immune cell populations within MAT. Mean ± SEM (n=4-6/group) absolute number leukocytes (A), T cells (B), B cells (C), $CD11c^{+}MHC2^{+}CD11b^{+}$ dendritic cells (D), unconventional $\gamma\delta$T cells (E), $\alpha\beta$T cells (F), cytotoxic T cells (G), helper T cells (H), $CD25^{+}Foxp3^{+}$ regulatory T cells (I). Statistical analysis was performed using an unpaired T test. $^{*}P < 0.05$ and $‡P < 0.01$ vs LFD-DSS.

Within MLNs (*Figure 2.9*), we found that chronic low-dose DSS treatment led to a sizable increase in the absolute number of total leukocytes (Hedges g=-0.36, P=0.6033), T cells (Hedges g=-0.53, P=0.3264), $\alpha\beta$T cells (Hedges g=-0.53, P=0.3919), cytotoxic T cells (Hedges g=-0.42, P=0.5270), and helper T cells (Hedges g=-0.38, P=0.6164). Alternatively, we found that DSS treatment reduced the number of $CD11b^{+}CD103^{+}$ intestinal dendritic cells (Hedges g=0.88, P=0.2285). DSS treatment was not found to affect the number of B cells or $\gamma\delta$T cells.

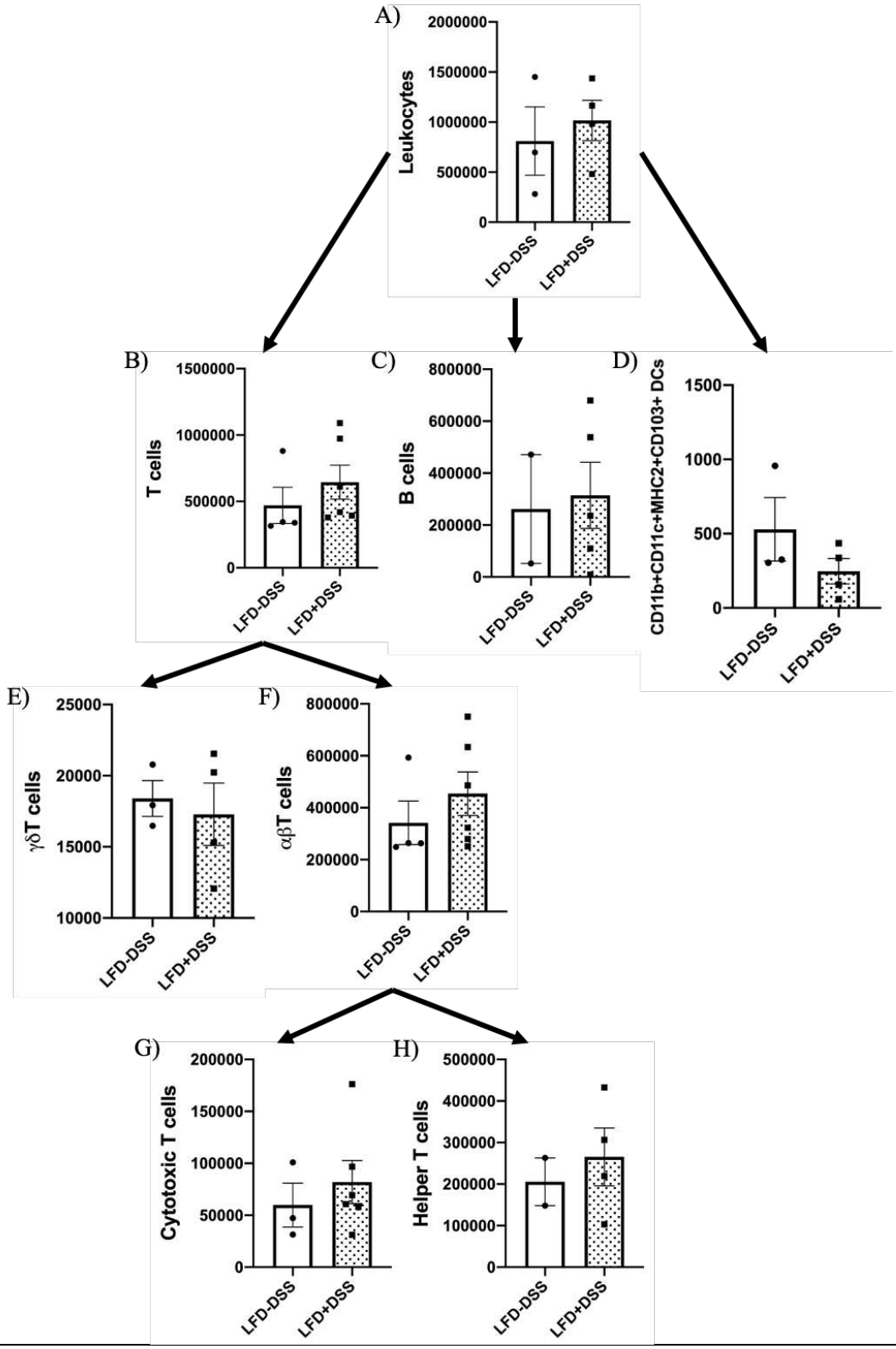

Figure 2.9. Immune cell populations within MLNs. Mean ± SEM (n=2-7/group) absolute number leukocytes (A), T cells (B), B cells (C), $CD11c^{+}MHC2^{+}CD11b^{+}CD103^{+}$ dendritic cells (D), unconventional $\gamma\delta$T cells (E), $\alpha\beta$T cells (F), cytotoxic T cells (G), helper T cells (H). Statistical analysis was performed using an unpaired T test. *$P < 0.05$ and ‡$P < 0.01$ vs LFD-DSS.

Discussion

The primary findings of the current study were that non-obese mice treated with low-dose DSS chronically for 8 wk displayed a modest reduction in total body weight and MAT mass yet showed substantial alterations in tissue immune cell populations and frequencies. These adaptations occurred without a concurrent change in glucose homeostasis. Collectively, these results indicate that the chronic low-dose DSS treatment model used here was able to induce tissue level markers of inflammation within local and peripheral sites, while insufficient to produce changes in glucose homeostasis. These results pose new questions regarding the level and type of inflammatory burden associated with metabolic dysfunction, as well as the biological relevance of observed cellular dynamics.

In the present study, we addressed the role of chronic GI inflammation independent of diet and obesity on metabolic and immune function. Typically, DSS is given at doses that lead to a reduction in body weight and adiposity (89, 92, 93). However, work by Irwin R et al. showed that 15 days of DSS treatment (1% w/v) was sufficient to induce GI inflammation without reducing body weight (91). Further, authors observed a redistribution of fat into the retroperitoneal 'visceral' adipose depot. Similarly, Mencarelli A et al. showed that 12 wk of DSS treatment (0.2% w/v) produced GI and MAT inflammation without a concurrent reduction in body weight, and led to impairments in insulin signaling within the liver and MAT (90). Here we found that 8 wk of DSS treatment (0.3% w/v) led to a modest, although not significant, reduction in total body weight and MAT mass. Discrepancies between our findings and the above mentioned may result from several experimental distinctions. First, mice used in the study by Irwin R et al. were younger in comparison to those used here and received 1% DSS solution for

15 days. Second, mice used by Mencarelli A et al. were significantly older and lacked the apolipoprotein E (ApoE) ligand ($ApoE^{-/-}$ transgenic mice). Thus, considerable variation in mouse age, disease status (94-99), and DSS treatment regimen exist between the current study and works cited. Nonetheless, our findings are in line with majority of literature which describes weight loss and reductions in organ mass upon treatment with DSS (100, 101). Taken together, the observed variation in body weight and general adiposity may be explained by the dosage of DSS used, frequency of DSS administration, and duration of DSS treatment; as the pathogenesis of DSS-induced GI inflammation is shown to vary greatly depending on these and other factors (89, 92, 102).

The regulation of glucose is largely managed by the liver (103) and skeletal muscle (104). Glucose homeostasis is generally perturbed in models of disease (105, 106) and is attributed in part to inflammation-mediated impairments in the insulin signaling cascade (107, 108). A hallmark of tissue inflammation is the recruitment and infiltration of immune cells (109). Insulin resistance within the liver and skeletal muscle is shown to coincide with immune cell accretion (110). Here we did not observe an alteration in systemic glucose homeostasis in response to chronic low-dose DSS treatment, despite a concomitant increase in immune cells within the liver. Alterations in glucose tolerance have been observed during DSS treatment, although when in combination with HFD feeding (90, 111, 112). Thus, it is possible that the inflammatory burden produced in our chronic low-dose model is insufficient to incite insulin resistance and disrupt glucose homeostasis.

Chronically inflamed tissues are characterized by an accumulation of immune cells, which maintain inflammation and promote tissue injury (109). DSS induces gastrointestinal inflammation by damaging the epithelial layer of the intestines, resulting in barrier disruption

and translocation of intestinal contents into underlying tissues (89, 93, 113-115). Although DSS has been shown to primarily affect the large intestines, its effects on the small intestine have also been characterized (113-115). We did not see a substantial increase in total leukocytes within the jejunum or ileum relative to untreated controls after 8 wk of low-dose DSS treatment. However, this is likely due to immune cell turnover in response to the chronic inflammation. In mouse models of acute DSS colitis immune cell infiltration, primarily consisting of neutrophils, is reported to occur in as little as 4-7 days after onset of treatment (113, 116). However, during chronic DSS colitis T cells are shown to predominate (92, 102, 115, 117). We found that chronic low-dose DSS treatment led to modest, yet distinct, alterations within the immune milieu of both the jejunum and ileum. Neutrophils in particular were found to be increased by DSS however primarily within the jejunum. Similar findings are reported by Yazbeck et al., who attributed this greater infiltration of neutrophils into the jejunum to an increase in vascularization relative to the ileum (113). Trafficking of neutrophils out of circulation and towards the intestines is a key component of the inflammatory response, as colitis symptoms correlate with neutrophil migration across the intestinal epithelium (116). Notably, we also found that $CD11b^{+}CD103^{+}$ dendritic cells were reduced by DSS treatment within the jejunum, ileum, and MLNs. Whereas $CD11b^{+}CD103^{-}$ dendritic cells were increased by DSS within the jejunum and ileum. In the small intestine three different populations of conventional dendritic cells can be identified based on their differential expression of the integrins CD11b and CD103 (118-120) and all three are shown to migrate to gut draining lymph nodes (121-124). The two $CD11b^{+}$ populations are closely related, as $CD11b^{+}CD103^{-}$ cells are shown to give rise to $CD11b^{+}CD103^{+}$ cells under the influence of TGFβ (125). During the steady state $CD11b^{+}CD103^{+}$ intestinal dendritic cells are required for the *in vivo* generation of T_{regs} within the small intestine (125, 126). Given that

regulatory mechanisms (i.e. IL-10 and TGFβ) are likely diminished due to the chronic inflammatory environment (127-131), we speculate that this may explain the observed reduction in $CD11b^{+}CD103^{+}$ dendritic cells. This is supported by the observed reduction in T_{regs} within the jejunum. Additionally, $CD11b^{+}CD103^{-}$ dendritic cells are shown to instruct both IL-17^{+} T_H17 cells and IFNγ^{+} T_H1 cells within the small intestine (118, 119, 132). Taken together, these findings support the development of inflammation within the jejunum and ileum in response to chronic low-dose DSS treatment. We also highlight the asymmetric effect of DSS on the jejunum and ileum which is likely several fold, supporting the significance of immunologic distinction between the segments of the small intestine during both the steady state and disease (92, 113, 133-135).

Interestingly, we also found that DSS treatment led to broad reductions in immune populations, particularly in T lymphocytes, within the spleen, which was reflected in the overall reduction in total leukocytes. This is largely supported by Hall LJ et al. who showed that T and B cells are reduced in spleens of chronically inflamed mice (136). Several studies also highlight the dynamic flux of splenocytes in response to acute and chronic DSS treatment (137-141). These data suggest that T lymphocytes are being mobilized from the spleen and are likely being redistributed to sites of antigen origination in the periphery. In agreement with this we found that total leukocytes were increased within the liver, MAT, and MLNs by DSS treatment which is indicative of inflammation (142, 143). GI inflammation associated with DSS treatment has previously been shown to promote lymphangiogenesis and dilation of collecting lymphatic vessels within the MLNs (144, 145), as well as MLN hypertrophy and recruitment of immune cells (146-150). Additionally, certain inflammatory conditions such as GI inflammation have been shown to preferentially recruit mucosal T cells into the liver, allowing them to contribute to

hepatic inflammation (151-154). Here we found parallel increases in $CD4^+$ and $CD8^+$ T cells, as well as B cells within the liver, MAT, and MLNs. Collectively, these findings indicate the presence of inflammation within the liver (155-159), MAT (160, 161), and MLNs. As well as support the considerable influence GI inflammation has on other tissues.

In sum, the present findings lend support to the tremendous importance of gut health in the maintenance of whole-body metabolic and immune function (29-32). Although we did not observe changes in systemic glucose homeostasis, the tissue-specific immune milieu was substantially reshaped by DSS treatment. These findings raise several new questions regarding 1) the required threshold of inflammation required to drive metabolic dysfunction, 2) the type of inflammatory stimuli capable of initiating metabolic dysfunction, and 3) the biological relevance of observed cellular dynamics within sampled tissues. Results reported herein should be considered in the light of some limitations including a lack of tissue cytokine and histological analysis, small sample size, and limited antibody markers used for cell characterization. As such, future studies should verify the present findings and include a more detailed analysis of tissue inflammatory status and metabolic function, as well assess intestinal barrier integrity.

REFERENCES

1. Bennett JM, Reeves G, Billman GE, Sturmberg JP. Inflammation-Nature's Way to Efficiently Respond to All Types of Challenges: Implications for Understanding and Managing "the Epidemic" of Chronic Diseases. Front Med (Lausanne). 2018;5:316.
2. Furman D, Campisi J, Verdin E, Carrera-Bastos P, Targ S, Franceschi C, Ferrucci L, Gilroy DW, Fasano A, et al. Chronic inflammation in the etiology of disease across the life span. Nat Med. 2019 12;25:1822-32.
3. Furman D, Chang J, Lartigue L, Bolen CR, Haddad F, Gaudilliere B, Ganio EA, Fragiadakis GK, Spitzer MH, et al. Expression of specific inflammasome gene modules stratifies older individuals into two extreme clinical and immunological states. Nat Med. 2017 Feb;23:174-84.
4. Netea MG, Balkwill F, Chonchol M, Cominelli F, Donath MY, Giamarellos-Bourboulis EJ, Golenbock D, Gresnigt MS, Heneka MT, et al. A guiding map for inflammation. Nat Immunol. 2017 Jul;18:826-31.
5. Slavich GM. Understanding inflammation, its regulation, and relevance for health: a top scientific and public priority. Brain Behav Immun. 2015 Mar;45:13-4.
6. Collaborators GCoD. Global, regional, and national age-sex-specific mortality for 282 causes of death in 195 countries and territories, 1980-2017: a systematic analysis for the Global Burden of Disease Study 2017. Lancet. 2018 11;392:1736-88.
7. Kotas ME, Medzhitov R. Homeostasis, inflammation, and disease susceptibility. Cell. 2015 Feb;160:816-27.
8. Straub RH. The brain and immune system prompt energy shortage in chronic inflammation and ageing. Nat Rev Rheumatol. 2017 Dec;13:743-51.
9. Fullerton JN, Gilroy DW. Resolution of inflammation: a new therapeutic frontier. Nat Rev Drug Discov. 2016 08;15:551-67.
10. Calder PC, Ahluwalia N, Albers R, Bosco N, Bourdet-Sicard R, Haller D, Holgate ST, Jönsson LS, Latulippe ME, et al. A consideration of biomarkers to be used for evaluation of inflammation in human nutritional studies. Br J Nutr. 2013 Jan;109 Suppl 1:S1-34.
11. Green WD, Beck MA. Obesity Impairs the Adaptive Immune Response to Influenza Virus. Ann Am Thorac Soc. 2017 Nov;14:S406-S9.
12. Green WD, Beck MA. Obesity altered T cell metabolism and the response to infection. Curr Opin Immunol. 2017 Jun;46:1-7.
13. Frasca D, Ferracci F, Diaz A, Romero M, Lechner S, Blomberg BB. Obesity decreases B cell responses in young and elderly individuals. Obesity (Silver Spring). 2016 Mar;24:615-25.
14. Karlsson EA, Hertz T, Johnson C, Mehle A, Krammer F, Schultz-Cherry S. Obesity Outweighs Protection Conferred by Adjuvanted Influenza Vaccination. MBio. 2016 Aug 2;7.
15. Worthington JJ, Reimann F, Gribble FM. Enteroendocrine cells-sensory sentinels of the intestinal environment and orchestrators of mucosal immunity. Mucosal Immunol. 2018 01;11:3-20.
16. Tanoue T, Umesaki Y, Honda K. Immune responses to gut microbiota-commensals and pathogens. Gut Microbes. 2010 Jul;1:224-33.

17. Battson ML, Lee DM, Weir TL, Gentile CL. The gut microbiota as a novel regulator of cardiovascular function and disease. J Nutr Biochem. 2018 06;56:1-15.
18. Shi N, Li N, Duan X, Niu H. Interaction between the gut microbiome and mucosal immune system. Mil Med Res. 2017;4:14.
19. Mowat AM, Agace WW. Regional specialization within the intestinal immune system. Nat Rev Immunol. 2014 Oct;14:667-85.
20. Chistiakov DA, Bobryshev YV, Kozarov E, Sobenin IA, Orekhov AN. Intestinal mucosal tolerance and impact of gut microbiota to mucosal tolerance. Front Microbiol. 2014;5:781.
21. Worbs T, Bode U, Yan S, Hoffmann MW, Hintzen G, Bernhardt G, Forster R, Pabst O. Oral tolerance originates in the intestinal immune system and relies on antigen carriage by dendritic cells. J Exp Med. 2006 Mar 20;203:519-27.
22. Nakajima-Adachi H, Kikuchi A, Fujimura Y, Shibahara K, Makino T, Goseki-Sone M, Kihara-Fujioka M, Nochi T, Kurashima Y, et al. Peyer's patches and mesenteric lymph nodes cooperatively promote enteropathy in a mouse model of food allergy. PLoS One. 2014;9:e107492.
23. Sun M, He C, Cong Y, Liu Z. Regulatory immune cells in regulation of intestinal inflammatory response to microbiota. Mucosal Immunol. 2015 Sep;8:969-78.
24. Sicherer SH, Sampson HA. Food allergy: Epidemiology, pathogenesis, diagnosis, and treatment. J Allergy Clin Immunol. 2014 Feb;133:291-307; quiz 8.
25. Harper JW, Zisman TL. Interaction of obesity and inflammatory bowel disease. World J Gastroenterol. 2016 Sep 21;22:7868-81.
26. Artis D, Grencis RK. The intestinal epithelium: sensors to effectors in nematode infection. Mucosal Immunol. 2008 Jul;1:252-64.
27. Alzahrani J, Hussain T, Simar D, Palchaudhuri R, Abdel-Mohsen M, Crowe SM, Mbogo GW, Palmer CS. Inflammatory and immunometabolic consequences of gut dysfunction in HIV: Parallels with IBD and implications for reservoir persistence and non-AIDS comorbidities. EBioMedicine. 2019 Aug;46:522-31.
28. Leulier F, MacNeil LT, Lee WJ, Rawls JF, Cani PD, Schwarzer M, Zhao L, Simpson SJ. Integrative Physiology: At the Crossroads of Nutrition, Microbiota, Animal Physiology, and Human Health. Cell Metab. 2017 03;25:522-34.
29. Sumida K, Kovesdy CP. The gut-kidney-heart axis in chronic kidney disease. Physiol Int. 2019 Sep;106:195-206.
30. Solas M, Milagro FI, Ramírez MJ, Martínez JA. Inflammation and gut-brain axis link obesity to cognitive dysfunction: plausible pharmacological interventions. Curr Opin Pharmacol. 2017 12;37:87-92.
31. Kirpich IA, Marsano LS, McClain CJ. Gut-liver axis, nutrition, and non-alcoholic fatty liver disease. Clin Biochem. 2015 Sep;48:923-30.
32. Munukka E, Pekkala S, Wiklund P, Rasool O, Borra R, Kong L, Ojanen X, Cheng SM, Roos C, et al. Gut-adipose tissue axis in hepatic fat accumulation in humans. J Hepatol. 2014 Jul;61:132-8.
33. Cani PD, Amar J, Iglesias MA, Poggi M, Knauf C, Bastelica D, Neyrinck AM, Fava F, Tuohy KM, et al. Metabolic endotoxemia initiates obesity and insulin resistance. Diabetes. 2007 Jul;56:1761-72.
34. de La Serre CB, Ellis CL, Lee J, Hartman AL, Rutledge JC, Raybould HE. Propensity to high-fat diet-induced obesity in rats is associated with changes in the gut microbiota and gut inflammation. Am J Physiol Gastrointest Liver Physiol. 2010 Aug;299:G440-8.

35. Hamilton MK, Boudry G, Lemay DG, Raybould HE. Changes in intestinal barrier function and gut microbiota in high-fat diet-fed rats are dynamic and region dependent. Am J Physiol Gastrointest Liver Physiol. 2015 May;308:G840-51.
36. Wang H, Zhang W, Zuo L, Dong J, Zhu W, Li Y, Gu L, Gong J, Li Q, et al. Intestinal dysbacteriosis contributes to decreased intestinal mucosal barrier function and increased bacterial translocation. Lett Appl Microbiol. 2014 Apr;58:384-92.
37. Bruce-Keller AJ, Salbaum JM, Berthoud HR. Harnessing Gut Microbes for Mental Health: Getting From Here to There. Biol Psychiatry. 2018 02;83:214-23.
38. Brun P, Castagliuolo I, Di Leo V, Buda A, Pinzani M, Palù G, Martines D. Increased intestinal permeability in obese mice: new evidence in the pathogenesis of nonalcoholic steatohepatitis. Am J Physiol Gastrointest Liver Physiol. 2007 Feb;292:G518-25.
39. Chen WY, Wang M, Zhang J, Barve SS, McClain CJ, Joshi-Barve S. Acrolein Disrupts Tight Junction Proteins and Causes Endoplasmic Reticulum Stress-Mediated Epithelial Cell Death Leading to Intestinal Barrier Dysfunction and Permeability. Am J Pathol. 2017 Dec;187:2686-97.
40. Günther C, Neumann H, Neurath MF, Becker C. Apoptosis, necrosis and necroptosis: cell death regulation in the intestinal epithelium. Gut. 2013 Jul;62:1062-71.
41. Kelly CJ, Zheng L, Campbell EL, Saeedi B, Scholz CC, Bayless AJ, Wilson KE, Glover LE, Kominsky DJ, et al. Crosstalk between Microbiota-Derived Short-Chain Fatty Acids and Intestinal Epithelial HIF Augments Tissue Barrier Function. Cell Host Microbe. 2015 May;17:662-71.
42. Peng L, Li ZR, Green RS, Holzman IR, Lin J. Butyrate enhances the intestinal barrier by facilitating tight junction assembly via activation of AMP-activated protein kinase in Caco-2 cell monolayers. J Nutr. 2009 Sep;139:1619-25.
43. Ulluwishewa D, Anderson RC, McNabb WC, Moughan PJ, Wells JM, Roy NC. Regulation of tight junction permeability by intestinal bacteria and dietary components. J Nutr. 2011 May;141:769-76.
44. Ma J, Zhou Q, Li H. Gut Microbiota and Nonalcoholic Fatty Liver Disease: Insights on Mechanisms and Therapy. Nutrients. 2017 Oct;9.
45. Maggs D, MacDonald I, Nauck MA. Glucose homeostasis and the gastrointestinal tract: insights into the treatment of diabetes. Diabetes Obes Metab. 2008 Jan;10:18-33.
46. Lam YY, Mitchell AJ, Holmes AJ, Denyer GS, Gummesson A, Caterson ID, Hunt NH, Storlien LH. Role of the gut in visceral fat inflammation and metabolic disorders. Obesity (Silver Spring). 2011 Nov;19:2113-20.
47. Gambero A, Maróstica M, Abdalla Saad MJ, Pedrazzoli J. Mesenteric adipose tissue alterations resulting from experimental reactivated colitis. Inflamm Bowel Dis. 2007 Nov;13:1357-64.
48. Kredel LI, Siegmund B. Adipose-tissue and intestinal inflammation - visceral obesity and creeping fat. Front Immunol. 2014;5:462.
49. Geurts L, Neyrinck AM, Delzenne NM, Knauf C, Cani PD. Gut microbiota controls adipose tissue expansion, gut barrier and glucose metabolism: novel insights into molecular targets and interventions using prebiotics. Benef Microbes. 2014 Mar;5:3-17.
50. Zhang C, Li S, Yang L, Huang P, Li W, Wang S, Zhao G, Zhang M, Pang X, et al. Structural modulation of gut microbiota in life-long calorie-restricted mice. Nat Commun. 2013;4:2163.

51. Ravussin Y, Koren O, Spor A, LeDuc C, Gutman R, Stombaugh J, Knight R, Ley RE, Leibel RL. Responses of gut microbiota to diet composition and weight loss in lean and obese mice. Obesity (Silver Spring). 2012 Apr;20:738-47.
52. Carmody RN, Gerber GK, Luevano JM, Gatti DM, Somes L, Svenson KL, Turnbaugh PJ. Diet dominates host genotype in shaping the murine gut microbiota. Cell Host Microbe. 2015 Jan;17:72-84.
53. Zhang C, Zhang M, Wang S, Han R, Cao Y, Hua W, Mao Y, Zhang X, Pang X, et al. Interactions between gut microbiota, host genetics and diet relevant to development of metabolic syndromes in mice. ISME J. 2010 Feb;4:232-41.
54. Voreades N, Kozil A, Weir TL. Diet and the development of the human intestinal microbiome. Front Microbiol. 2014;5:494.
55. Ley RE, Hamady M, Lozupone C, Turnbaugh PJ, Ramey RR, Bircher JS, Schlegel ML, Tucker TA, Schrenzel MD, et al. Evolution of mammals and their gut microbes. Science. 2008 Jun;320:1647-51.
56. Sonnenburg ED, Sonnenburg JL. The ancestral and industrialized gut microbiota and implications for human health. Nat Rev Microbiol. 2019 06;17:383-90.
57. Richards JL, Yap YA, McLeod KH, Mackay CR, Mariño E. Dietary metabolites and the gut microbiota: an alternative approach to control inflammatory and autoimmune diseases. Clin Transl Immunology. 2016 May;5:e82.
58. Bishehsari F, Magno E, Swanson G, Desai V, Voigt RM, Forsyth CB, Keshavarzian A. Alcohol and Gut-Derived Inflammation. Alcohol Res. 2017;38:163-71.
59. Ley RE, Bäckhed F, Turnbaugh P, Lozupone CA, Knight RD, Gordon JI. Obesity alters gut microbial ecology. Proc Natl Acad Sci U S A. 2005 Aug;102:11070-5.
60. Gill SR, Pop M, Deboy RT, Eckburg PB, Turnbaugh PJ, Samuel BS, Gordon JI, Relman DA, Fraser-Liggett CM, Nelson KE. Metagenomic analysis of the human distal gut microbiome. Science. 2006 Jun;312:1355-9.
61. Turnbaugh PJ, Hamady M, Yatsunenko T, Cantarel BL, Duncan A, Ley RE, Sogin ML, Jones WJ, Roe BA, et al. A core gut microbiome in obese and lean twins. Nature. 2009 Jan;457:480-4.
62. Franceschi C, Garagnani P, Parini P, Giuliani C, Santoro A. Inflammaging: a new immune-metabolic viewpoint for age-related diseases. Nat Rev Endocrinol. 2018 10;14:576-90.
63. Sturgeon C, Fasano A. Zonulin, a regulator of epithelial and endothelial barrier functions, and its involvement in chronic inflammatory diseases. Tissue Barriers. 2016;4:e1251384.
64. Jayashree B, Bibin YS, Prabhu D, Shanthirani CS, Gokulakrishnan K, Lakshmi BS, Mohan V, Balasubramanyam M. Increased circulatory levels of lipopolysaccharide (LPS) and zonulin signify novel biomarkers of proinflammation in patients with type 2 diabetes. Mol Cell Biochem. 2014 Mar;388:203-10.
65. Bressa C, Bailén-Andrino M, Pérez-Santiago J, González-Soltero R, Pérez M, Montalvo-Lominchar MG, Maté-Muñoz JL, Domínguez R, Moreno D, Larrosa M. Differences in gut microbiota profile between women with active lifestyle and sedentary women. PLoS One. 2017;12:e0171352.
66. Estaki M, Pither J, Baumeister P, Little JP, Gill SK, Ghosh S, Ahmadi-Vand Z, Marsden KR, Gibson DL. Cardiorespiratory fitness as a predictor of intestinal microbial diversity and distinct metagenomic functions. Microbiome. 2016 08;4:42.

67. Clarke SF, Murphy EF, O'Sullivan O, Lucey AJ, Humphreys M, Hogan A, Hayes P, O'Reilly M, Jeffery IB, et al. Exercise and associated dietary extremes impact on gut microbial diversity. Gut. 2014 Dec;63:1913-20.
68. Cani PD, Bibiloni R, Knauf C, Waget A, Neyrinck AM, Delzenne NM, Burcelin R. Changes in gut microbiota control metabolic endotoxemia-induced inflammation in high-fat diet-induced obesity and diabetes in mice. Diabetes. 2008 Jun;57:1470-81.
69. Cândido FG, Valente FX, Grześkowiak Ł, Moreira APB, Rocha DMUP, Alfenas RCG. Impact of dietary fat on gut microbiota and low-grade systemic inflammation: mechanisms and clinical implications on obesity. Int J Food Sci Nutr. 2018 Mar;69:125-43.
70. Hildebrandt MA, Hoffmann C, Sherrill-Mix SA, Keilbaugh SA, Hamady M, Chen YY, Knight R, Ahima RS, Bushman F, Wu GD. High-fat diet determines the composition of the murine gut microbiome independently of obesity. Gastroenterology. 2009 Nov;137:1716-24.e1-2.
71. Lerner A, Matthias T. Changes in intestinal tight junction permeability associated with industrial food additives explain the rising incidence of autoimmune disease. Autoimmun Rev. 2015 Jun;14:479-89.
72. Pendyala S, Walker JM, Holt PR. A high-fat diet is associated with endotoxemia that originates from the gut. Gastroenterology. 2012 May;142:1100-1 e2.
73. Chassaing B, Van de Wiele T, De Bodt J, Marzorati M, Gewirtz AT. Dietary emulsifiers directly alter human microbiota composition and gene expression ex vivo potentiating intestinal inflammation. Gut. 2017 08;66:1414-27.
74. Araujo JR, Tomas J, Brenner C, Sansonetti PJ. Impact of high-fat diet on the intestinal microbiota and small intestinal physiology before and after the onset of obesity. Biochimie. 2017 Oct;141:97-106.
75. Hernández E, Kahl S, Seelig A, Begovatz P, Irmler M, Kupriyanova Y, Nowotny B, Nowotny P, Herder C, et al. Acute dietary fat intake initiates alterations in energy metabolism and insulin resistance. J Clin Invest. 2017 Feb;127:695-708.
76. Turnbaugh PJ, Ley RE, Mahowald MA, Magrini V, Mardis ER, Gordon JI. An obesity-associated gut microbiome with increased capacity for energy harvest. Nature. 2006 Dec;444:1027-31.
77. Cani PD, Jordan BF. Gut microbiota-mediated inflammation in obesity: a link with gastrointestinal cancer. Nat Rev Gastroenterol Hepatol. 2018 11;15:671-82.
78. Küme T, Acar S, Tuhan H, Çatlı G, Anık A, Gürsoy Çalan Ö, Böber E, Abacı A. The Relationship between Serum Zonulin Level and Clinical and Laboratory Parameters of Childhood Obesity. J Clin Res Pediatr Endocrinol. 2017 Mar;9:31-8.
79. Le Chatelier E, Nielsen T, Qin J, Prifti E, Hildebrand F, Falony G, Almeida M, Arumugam M, Batto JM, et al. Richness of human gut microbiome correlates with metabolic markers. Nature. 2013 Aug;500:541-6.
80. Aron-Wisnewsky J, Prifti E, Belda E, Ichou F, Kayser BD, Dao MC, Verger EO, Hedjazi L, Bouillot JL, et al. Major microbiota dysbiosis in severe obesity: fate after bariatric surgery. Gut. 2019 01;68:70-82.
81. Clarke SD. Polyunsaturated fatty acid regulation of gene transcription: a mechanism to improve energy balance and insulin resistance. Br J Nutr. 2000 Mar;83 Suppl 1:S59-66.
82. Xu J, Nakamura MT, Cho HP, Clarke SD. Sterol regulatory element binding protein-1 expression is suppressed by dietary polyunsaturated fatty acids. A mechanism for the coordinate suppression of lipogenic genes by polyunsaturated fats. J Biol Chem. 1999 Aug;274:23577-83.

83. Bevilacqua S, Bonadonna R, Buzzigoli G, Boni C, Ciociaro D, Maccari F, Giorico MA, Ferrannini E. Acute elevation of free fatty acid levels leads to hepatic insulin resistance in obese subjects. Metabolism. 1987 May;36:502-6.
84. Oakes ND, Cooney GJ, Camilleri S, Chisholm DJ, Kraegen EW. Mechanisms of liver and muscle insulin resistance induced by chronic high-fat feeding. Diabetes. 1997 Nov;46:1768-74.
85. Bashan N, Dorfman K, Tarnovscki T, Harman-Boehm I, Liberty IF, Blüher M, Ovadia S, Maymon-Zilberstein T, Potashnik R, et al. Mitogen-activated protein kinases, inhibitory-kappaB kinase, and insulin signaling in human omental versus subcutaneous adipose tissue in obesity. Endocrinology. 2007 Jun;148:2955-62.
86. Cancello R, Tordjman J, Poitou C, Guilhem G, Bouillot JL, Hugol D, Coussieu C, Basdevant A, Bar Hen A, et al. Increased infiltration of macrophages in omental adipose tissue is associated with marked hepatic lesions in morbid human obesity. Diabetes. 2006 Jun;55:1554-61.
87. Magnuson AM, Regan DP, Booth AD, Fouts JK, Solt CM, Hill JL, Dow SW, Foster MT. High-fat diet induced central adiposity (visceral fat) is associated with increased fibrosis and decreased immune cellularity of the mesenteric lymph node in mice. Eur J Nutr. 2019 Jun.
88. Hill J, Magnuson A, Solt C, McIver K, Foster M. Role of the mesenteric lymph nodes in metabolic and immune homeostasis. Manuscript in preperation; 2020.
89. Chassaing B, Aitken JD, Malleshappa M, Vijay-Kumar M. Dextran sulfate sodium (DSS)-induced colitis in mice. Curr Protoc Immunol. 2014 Feb;104:15.25.1-15.25.14.
90. Mencarelli A, Cipriani S, Renga B, Bruno A, D'Amore C, Distrutti E, Fiorucci S. VSL#3 resets insulin signaling and protects against NASH and atherosclerosis in a model of genetic dyslipidemia and intestinal inflammation. PLoS One. 2012;7:e45425.
91. Irwin R, Raehtz S, Parameswaran N, McCabe LR. Intestinal inflammation without weight loss decreases bone density and growth. Am J Physiol Regul Integr Comp Physiol. 2016 12;311:R1149-R57.
92. Wirtz S, Popp V, Kindermann M, Gerlach K, Weigmann B, Fichtner-Feigl S, Neurath MF. Chemically induced mouse models of acute and chronic intestinal inflammation. Nat Protoc. 2017 Jul;12:1295-309.
93. Eichele DD, Kharbanda KK. Dextran sodium sulfate colitis murine model: An indispensable tool for advancing our understanding of inflammatory bowel diseases pathogenesis. World J Gastroenterol. 2017 Sep;23:6016-29.
94. King VL, Hatch NW, Chan HW, de Beer MC, de Beer FC, Tannock LR. A murine model of obesity with accelerated atherosclerosis. Obesity (Silver Spring). 2010 Jan;18:35-41.
95. Pendse AA, Arbones-Mainar JM, Johnson LA, Altenburg MK, Maeda N. Apolipoprotein E knock-out and knock-in mice: atherosclerosis, metabolic syndrome, and beyond. J Lipid Res. 2009 Apr;50 Suppl:S178-82.
96. Lo Sasso G, Schlage WK, Boué S, Veljkovic E, Peitsch MC, Hoeng J. The Apoe(-/-) mouse model: a suitable model to study cardiovascular and respiratory diseases in the context of cigarette smoke exposure and harm reduction. J Transl Med. 2016 05;14:146.
97. Ishibashi S, Brown MS, Goldstein JL, Gerard RD, Hammer RE, Herz J. Hypercholesterolemia in low density lipoprotein receptor knockout mice and its reversal by adenovirus-mediated gene delivery. J Clin Invest. 1993 Aug;92:883-93.

98. Nakashima Y, Plump AS, Raines EW, Breslow JL, Ross R. ApoE-deficient mice develop lesions of all phases of atherosclerosis throughout the arterial tree. Arterioscler Thromb. 1994 Jan;14:133-40.
99. Boué S, Tarasov K, Jänis M, Lebrun S, Hurme R, Schlage W, Lietz M, Vuillaume G, Ekroos K, et al. Modulation of atherogenic lipidome by cigarette smoke in apolipoprotein E-deficient mice. Atherosclerosis. 2012 Dec;225:328-34.
100. Harris L, Senagore P, Young VB, McCabe LR. Inflammatory bowel disease causes reversible suppression of osteoblast and chondrocyte function in mice. Am J Physiol Gastrointest Liver Physiol. 2009 May;296:G1020-9.
101. Melgar S, Bjursell M, Gerdin AK, Svensson L, Michaëlsson E, Bohlooly-Y M. Mice with experimental colitis show an altered metabolism with decreased metabolic rate. Am J Physiol Gastrointest Liver Physiol. 2007 Jan;292:G165-72.
102. Perše M, Cerar A. Dextran sodium sulphate colitis mouse model: traps and tricks. J Biomed Biotechnol. 2012;2012:718617.
103. Santoleri D, Titchenell PM. Resolving the Paradox of Hepatic Insulin Resistance. Cell Mol Gastroenterol Hepatol. 2019;7:447-56.
104. Buczkowska EO, Jarosz-Chobot P. [Insulin effect on metabolism in skeletal muscles and the role of muscles in regulation of glucose homeostasis]. Przegl Lek. 2001;58:782-7.
105. Sun Q, Li J, Gao F. New insights into insulin: The anti-inflammatory effect and its clinical relevance. World J Diabetes. 2014 Apr;5:89-96.
106. de Rekeneire N, Peila R, Ding J, Colbert LH, Visser M, Shorr RI, Kritchevsky SB, Kuller LH, Strotmeyer ES, et al. Diabetes, hyperglycemia, and inflammation in older individuals: the health, aging and body composition study. Diabetes Care. 2006 Aug;29:1902-8.
107. Petersen MC, Shulman GI. Mechanisms of Insulin Action and Insulin Resistance. Physiol Rev. 2018 10;98:2133-223.
108. de Luca C, Olefsky JM. Inflammation and insulin resistance. FEBS Lett. 2008 Jan;582:97-105.
109. Chen L, Deng H, Cui H, Fang J, Zuo Z, Deng J, Li Y, Wang X, Zhao L. Inflammatory responses and inflammation-associated diseases in organs. Oncotarget. 2018 Jan;9:7204-18.
110. Liu J, Liu Z. Muscle Insulin Resistance and the Inflamed Microvasculature: Fire from Within. Int J Mol Sci. 2019 Jan;20.
111. Teixeira LG, Leonel AJ, Aguilar EC, Batista NV, Alves AC, Coimbra CC, Ferreira AV, de Faria AM, Cara DC, Alvarez Leite JI. The combination of high-fat diet-induced obesity and chronic ulcerative colitis reciprocally exacerbates adipose tissue and colon inflammation. Lipids Health Dis. 2011 Nov;10:204.
112. Ma X, Torbenson M, Hamad AR, Soloski MJ, Li Z. High-fat diet modulates non-CD1d-restricted natural killer T cells and regulatory T cells in mouse colon and exacerbates experimental colitis. Clin Exp Immunol. 2008 Jan;151:130-8.
113. Yazbeck R, Howarth GS, Butler RN, Geier MS, Abbott CA. Biochemical and histological changes in the small intestine of mice with dextran sulfate sodium colitis. J Cell Physiol. 2011 Dec;226:3219-24.
114. Ohtsuka Y, Sanderson IR. Dextran sulfate sodium-induced inflammation is enhanced by intestinal epithelial cell chemokine expression in mice. Pediatr Res. 2003 Jan;53:143-7.
115. Kiesler P, Fuss IJ, Strober W. Experimental Models of Inflammatory Bowel Diseases. Cell Mol Gastroenterol Hepatol. 2015 Mar;1:154-70.

116. Fournier BM, Parkos CA. The role of neutrophils during intestinal inflammation. Mucosal Immunol. 2012 Jul;5:354-66.
117. Dieleman LA, Palmen MJ, Akol H, Bloemena E, Peña AS, Meuwissen SG, Van Rees EP. Chronic experimental colitis induced by dextran sulphate sodium (DSS) is characterized by Th1 and Th2 cytokines. Clin Exp Immunol. 1998 Dec;114:385-91.
118. Mayer JU, Demiri M, Agace WW, MacDonald AS, Svensson-Frej M, Milling SW. Different populations of CD11b. Nat Commun. 2017 06;8:15820.
119. Liang J, Huang HI, Benzatti FP, Karlsson AB, Zhang JJ, Youssef N, Ma A, Hale LP, Hammer GE. Inflammatory Th1 and Th17 in the Intestine Are Each Driven by Functionally Specialized Dendritic Cells with Distinct Requirements for MyD88. Cell Rep. 2016 10;17:1330-43.
120. Stagg AJ. Intestinal Dendritic Cells in Health and Gut Inflammation. Front Immunol. 2018;9:2883.
121. Bogunovic M, Ginhoux F, Helft J, Shang L, Hashimoto D, Greter M, Liu K, Jakubzick C, Ingersoll MA, et al. Origin of the lamina propria dendritic cell network. Immunity. 2009 Sep;31:513-25.
122. Cerovic V, Houston SA, Scott CL, Aumeunier A, Yrlid U, Mowat AM, Milling SW. Intestinal CD103(-) dendritic cells migrate in lymph and prime effector T cells. Mucosal Immunol. 2013 Jan;6:104-13.
123. Scott CL, Bain CC, Wright PB, Sichien D, Kotarsky K, Persson EK, Luda K, Guilliams M, Lambrecht BN, et al. CCR2(+)CD103(-) intestinal dendritic cells develop from DC-committed precursors and induce interleukin-17 production by T cells. Mucosal Immunol. 2015 Mar;8:327-39.
124. Varol C, Vallon-Eberhard A, Elinav E, Aychek T, Shapira Y, Luche H, Fehling HJ, Hardt WD, Shakhar G, Jung S. Intestinal lamina propria dendritic cell subsets have different origin and functions. Immunity. 2009 Sep;31:502-12.
125. Bain CC, Montgomery J, Scott CL, Kel JM, Girard-Madoux MJH, Martens L, Zangerle-Murray TFP, Ober-Blöbaum J, Lindenbergh-Kortleve D, et al. TGFβR signalling controls CD103. Nat Commun. 2017 09;8:620.
126. Welty NE, Staley C, Ghilardi N, Sadowsky MJ, Igyártó BZ, Kaplan DH. Intestinal lamina propria dendritic cells maintain T cell homeostasis but do not affect commensalism. J Exp Med. 2013 Sep;210:2011-24.
127. Collison LW, Workman CJ, Kuo TT, Boyd K, Wang Y, Vignali KM, Cross R, Sehy D, Blumberg RS, Vignali DA. The inhibitory cytokine IL-35 contributes to regulatory T-cell function. Nature. 2007 Nov;450:566-9.
128. Rubtsov YP, Rasmussen JP, Chi EY, Fontenot J, Castelli L, Ye X, Treuting P, Siewe L, Roers A, et al. Regulatory T cell-derived interleukin-10 limits inflammation at environmental interfaces. Immunity. 2008 Apr;28:546-58.
129. Takeda K, Clausen BE, Kaisho T, Tsujimura T, Terada N, Förster I, Akira S. Enhanced Th1 activity and development of chronic enterocolitis in mice devoid of Stat3 in macrophages and neutrophils. Immunity. 1999 Jan;10:39-49.
130. Huber S, Gagliani N, Esplugues E, O'Connor W, Huber FJ, Chaudhry A, Kamanaka M, Kobayashi Y, Booth CJ, et al. Th17 cells express interleukin-10 receptor and are controlled by $Foxp3^-$ and Foxp3+ regulatory CD4+ T cells in an interleukin-10-dependent manner. Immunity. 2011 Apr;34:554-65.

131. Chaudhry A, Rudra D, Treuting P, Samstein RM, Liang Y, Kas A, Rudensky AY. CD4+ regulatory T cells control TH17 responses in a Stat3-dependent manner. Science. 2009 Nov;326:986-91.
132. Troy AE, Zaph C, Du Y, Taylor BC, Guild KJ, Hunter CA, Saris CJ, Artis D. IL-27 regulates homeostasis of the intestinal CD4+ effector T cell pool and limits intestinal inflammation in a murine model of colitis. J Immunol. 2009 Aug;183:2037-44.
133. Denning TL, Norris BA, Medina-Contreras O, Manicassamy S, Geem D, Madan R, Karp CL, Pulendran B. Functional specializations of intestinal dendritic cell and macrophage subsets that control Th17 and regulatory T cell responses are dependent on the T cell/APC ratio, source of mouse strain, and regional localization. J Immunol. 2011 Jul;187:733-47.
134. Peuhkuri K, Vapaatalo H, Korpela R. Even low-grade inflammation impacts on small intestinal function. World J Gastroenterol. 2010 Mar;16:1057-62.
135. Stephens M, Liao S, von der Weid PY. Mesenteric Lymphatic Alterations Observed During DSS Induced Intestinal Inflammation Are Driven in a TLR4-PAMP/DAMP Discriminative Manner. Front Immunol. 2019;10:557.
136. Hall LJ, Faivre E, Quinlan A, Shanahan F, Nally K, Melgar S. Induction and activation of adaptive immune populations during acute and chronic phases of a murine model of experimental colitis. Dig Dis Sci. 2011 Jan;56:79-89.
137. Sainathan SK, Hanna EM, Gong Q, Bishnupuri KS, Luo Q, Colonna M, White FV, Croze E, Houchen C, et al. Granulocyte macrophage colony-stimulating factor ameliorates DSS-induced experimental colitis. Inflamm Bowel Dis. 2008 Jan;14:88-99.
138. Weinhage T, Däbritz J, Brockhausen A, Wirth T, Brückner M, Belz M, Foell D, Varga G. Granulocyte Macrophage Colony-Stimulating Factor-Activated CD39. Cell Mol Gastroenterol Hepatol. 2015 Jul;1:433-49.e1.
139. Zhang R, Ito S, Nishio N, Cheng Z, Suzuki H, Isobe KI. Dextran sulphate sodium increases splenic Gr1(+)CD11b(+) cells which accelerate recovery from colitis following intravenous transplantation. Clin Exp Immunol. 2011 Jun;164:417-27.
140. Bodammer P, Maletzki C, Waitz G, Emmrich J. Prophylactic application of bovine colostrum ameliorates murine colitis via induction of immunoregulatory cells. J Nutr. 2011 Jun;141:1056-61.
141. Bodammer P, Zirzow E, Klammt S, Maletzki C, Kerkhoff C. Alteration of DSS-mediated immune cell redistribution in murine colitis by oral colostral immunoglobulin. BMC Immunol. 2013 Feb;14:10.
142. Freitas-Lopes MA, Mafra K, David BA, Carvalho-Gontijo R, Menezes GB. Differential Location and Distribution of Hepatic Immune Cells. Cells. 2017 Dec;6.
143. Robinson MW, Harmon C, O'Farrelly C. Liver immunology and its role in inflammation and homeostasis. Cell Mol Immunol. 2016 05;13:267-76.
144. Rehal S, Stephens M, Roizes S, Liao S, von der Weid PY. Acute small intestinal inflammation results in persistent lymphatic alterations. Am J Physiol Gastrointest Liver Physiol. 2018 03;314:G408-G17.
145. D'Alessio S, Correale C, Tacconi C, Gandelli A, Pietrogrande G, Vetrano S, Genua M, Arena V, Spinelli A, et al. VEGF-C-dependent stimulation of lymphatic function ameliorates experimental inflammatory bowel disease. J Clin Invest. 2014 Sep;124:3863-78.
146. Heitman B, Irizarry A. Infectious disease causes of lymphadenopathy: localized versus diffuse. Lippincotts Prim Care Pract. 1999 1999 Jan-Feb;3:19-38.

147. Jang MH, Sougawa N, Tanaka T, Hirata T, Hiroi T, Tohya K, Guo Z, Umemoto E, Ebisuno Y, et al. CCR7 is critically important for migration of dendritic cells in intestinal lamina propria to mesenteric lymph nodes. J Immunol. 2006 Jan;176:803-10.
148. Seth S, Oberdörfer L, Hyde R, Hoff K, Thies V, Worbs T, Schmitz S, Förster R. CCR7 essentially contributes to the homing of plasmacytoid dendritic cells to lymph nodes under steady-state as well as inflammatory conditions. J Immunol. 2011 Mar;186:3364-72.
149. Kumar V, Scandella E, Danuser R, Onder L, Nitschké M, Fukui Y, Halin C, Ludewig B, Stein JV. Global lymphoid tissue remodeling during a viral infection is orchestrated by a B cell-lymphotoxin-dependent pathway. Blood. 2010 Jun;115:4725-33.
150. Gregory JL, Walter A, Alexandre YO, Hor JL, Liu R, Ma JZ, Devi S, Tokuda N, Owada Y, et al. Infection Programs Sustained Lymphoid Stromal Cell Responses and Shapes Lymph Node Remodeling upon Secondary Challenge. Cell Rep. 2017 01;18:406-18.
151. Murai M, Yoneyama H, Ezaki T, Suematsu M, Terashima Y, Harada A, Hamada H, Asakura H, Ishikawa H, Matsushima K. Peyer's patch is the essential site in initiating murine acute and lethal graft-versus-host reaction. Nat Immunol. 2003 Feb;4:154-60.
152. Petrovic A, Alpdogan O, Willis LM, Eng JM, Greenberg AS, Kappel BJ, Liu C, Murphy GJ, Heller G, van den Brink MR. LPAM (alpha 4 beta 7 integrin) is an important homing integrin on alloreactive T cells in the development of intestinal graft-versus-host disease. Blood. 2004 Feb;103:1542-7.
153. Grant AJ, Lalor PF, Hübscher SG, Briskin M, Adams DH. MAdCAM-1 expressed in chronic inflammatory liver disease supports mucosal lymphocyte adhesion to hepatic endothelium (MAdCAM-1 in chronic inflammatory liver disease). Hepatology. 2001 May;33:1065-72.
154. Eksteen B, Grant AJ, Miles A, Curbishley SM, Lalor PF, Hübscher SG, Briskin M, Salmon M, Adams DH. Hepatic endothelial CCL25 mediates the recruitment of CCR9+ gut-homing lymphocytes to the liver in primary sclerosing cholangitis. J Exp Med. 2004 Dec;200:1511-7.
155. Shen X, Wang Y, Gao F, Ren F, Busuttil RW, Kupiec-Weglinski JW, Zhai Y. CD4 T cells promote tissue inflammation via CD40 signaling without de novo activation in a murine model of liver ischemia/reperfusion injury. Hepatology. 2009 Nov;50:1537-46.
156. Endig J, Buitrago-Molina LE, Marhenke S, Reisinger F, Saborowski A, Schütt J, Limbourg F, Könecke C, Schreder A, et al. Dual Role of the Adaptive Immune System in Liver Injury and Hepatocellular Carcinoma Development. Cancer Cell. 2016 08;30:308-23.
157. Ochel A, Cebula M, Riehn M, Hillebrand U, Lipps C, Schirmbeck R, Hauser H, Wirth D. Effective intrahepatic CD8+ T-cell immune responses are induced by low but not high numbers of antigen-expressing hepatocytes. Cell Mol Immunol. 2016 11;13:805-15.
158. Racanelli V, Sansonno D, Piccoli C, D'Amore FP, Tucci FA, Dammacco F. Molecular characterization of B cell clonal expansions in the liver of chronically hepatitis C virus-infected patients. J Immunol. 2001 Jul;167:21-9.
159. Curry MP, Golden-Mason L, Doherty DG, Deignan T, Norris S, Duffy M, Nolan N, Hall W, Hegarty JE, O'Farrelly C. Expansion of innate CD5pos B cells expressing high levels of CD81 in hepatitis C virus infected liver. J Hepatol. 2003 May;38:642-50.
160. Mustain WC, Starr ME, Valentino JD, Cohen DA, Okamura D, Wang C, Evers BM, Saito H. Inflammatory cytokine gene expression in mesenteric adipose tissue during acute experimental colitis. PLoS One. 2013;8:e83693.

161. Peyrin-Biroulet L, Chamaillard M, Gonzalez F, Beclin E, Decourcelle C, Antunes L, Gay J, Neut C, Colombel JF, Desreumaux P. Mesenteric fat in Crohn's disease: a pathogenetic hallmark or an innocent bystander? Gut. 2007 Apr;56:577-83.

CHAPTER 4: ALTERED PBMC RESPONSE TO CONCONAVALIN A IN OBESE ADULTS

Overview

Background: Obese adults are at greater risk for both chronic and infectious diseases. Systemic chronic inflammation that occurs in obesity is shown to drive premature immunosenescence, leading to an increased susceptibility for disease. The objective of the present study was to characterize immunologic parameters within a normal weight and obese human population, otherwise free of disease, through the *ex vivo* challenge of peripheral blood mononuclear cells (PBMCs) with the T lymphocyte mitogen Concanavalin A (ConA). We hypothesized that PBMCs isolated from obese individuals would display a lower level of cell proliferation and cytokine secretion, as well as distinct expansion of immune cells upon acute *ex vivo* challenge with ConA relative to their normal weight counterparts. *Methods:* We isolated PBMCs from normal weight (n=7; 22.14$\pm$0.27 kg/m^2) and obese (n=7; 30.46$\pm$0.44 kg/m^2) male and female adults, and then stimulated them *ex vivo* with ConA (5 μg/mL) for 72 hr. After which we measured cell proliferation and immune cell populations by flow cytometry, and cytokine concentrations by ELISA. *Results:* We found that PBMCs isolated from obese adults had a modest increase in cell number (Hedges' *g*=-0.61, *P*=0.6495) and IFNγ secretion (Hedges' *g*=-0.35, *P*=0.9028) upon stimulation with ConA relative to their normal weight controls. Additionally, we found a distinct expansion of $CD4^+CD8^+$ T cells (Hedges' *g*=-1.40, *P*=0.0690), $CD16^+$ monocytes (Hedges' *g*=-1.79, *P*=0.0165), and NK cells (Hedges' *g*=-1.51, *P*=0.0488) within ConA stimulated PBMCs from obese adults. *Conclusions:* These results support an altered response of PBMCs within obese individuals and provide new insight into obesity-driven

immune alterations. Future studies in a larger population of obese adults with a range of body mass indexes may be warranted.

Introduction

Obesity has long been associated with higher risks for chronic diseases, including type 2 diabetes, cancer, and cardiovascular disease (1-3). This is especially concerning because more than 40% of adults in the United States are currently obese (4). And estimates predict this number will increase to 50% by 2030 (5). There is substantial evidence to support that underlying systemic chronic inflammation mediates this obesity-associated disease risk (6-9). In particular, visceral obesity strongly correlates with metabolic dysfunction as a result of inflammation that develops within visceral adipose tissue (9-14). This is shown to occur following the excessive hypertrophy of adipocytes, which results in cell stress and the recruitment of immune cells (3, 11-13). Although normally protective (15, 16), recurrent or prolonged inflammation can lead to pathology as a result of cell and tissue damage (17-19). We now know that obesity, in addition to poor diet and gut dysbiosis, impairs the resolution of acute inflammation, in turn promoting the development of systemic chronic inflammation (6, 7, 20). Collectively, these events lead to a breakdown of immune tolerance and impede normal immune function, driving pathologic inflammation and an increase in disease susceptibility (7, 15-17, 21-24). Recent data now also highlights the association of obesity with an increased risk for infectious diseases (6, 25-27), such as urinary tract infections (28-30), gastric infection by *Helicobacter pylori* (31), surgical infections (32-35), and respiratory infections (36-39). Taken together, it is clear that obesity is not only a high-risk group for chronic disease but also infectious disease.

Studies investigating seasonal influenza exemplify the association between obesity and immune dysfunction. During the 2009 H1N1 swine flu pandemic obesity was identified as an independent risk factor for increased morbidity and mortality (40), with the risk of contracting seasonal influenza and hospitalization increasing in parallel to body mass index (BMI) (37). Considering these observations data on vaccine efficacy among obese persons is somewhat variable, as antibody production appears impaired to vaccines such as hepatitis B (41-44), tetanus (45), and rabies (46) yet not to others. Sheridan, PA et al. found no difference in influenza-specific serological response to flu vaccine between healthy-weight, overweight, and obese individuals at 30 days post-vaccination, however found a greater decline in antibody titers at one year among overweight and obese individuals (47). Follow up studies have demonstrated that peripheral blood mononuclear cells (PBMCs) from flu vaccinated obese and overweight adults express fewer activation markers on $CD4^+$ and $CD8^+$ T cells (48), and produce less cytokines (IFNγ, granzyme B) needed for influenza clearance (49) when challenged *ex vivo* with H1N1 influenza virus relative to normal weight controls. Additionally, no differences in dendritic cell activation or function were observed suggesting that obesity independently affects T cell activation and function (49). These findings are in agreement with previously mentioned work (40) and corroborate the increased risk of influenza or influenza-like illness in obese adults relative to healthy-weight counterparts despite similar influenza-specific antibody responses to vaccination (50).

The prevalence of obesity is still on the rise, with obese adults now outnumbering underweight adults worldwide (26, 51). This creates a serious public health problem given that obesity is a high-risk group for chronic and infectious disease. In light of the above data, the purpose of the current study is to characterize immunologic parameters within a normal weight

and obese human population otherwise free of disease, through the *ex vivo* challenge of PBMCs with the T lymphocyte mitogen Concanavalin A (ConA). Primary outcome measures include the quantification of PBMC phenotype and proliferation, in addition to cytokine secretion. We hypothesized that PBMCs isolated from obese individuals will display a lower level of cell proliferation and cytokine secretion, as well as distinct expansion of immune cells upon acute *ex vivo* challenge with ConA relative to their normal weight counterparts.

Methods

Participants and study design

Healthy male and female adults, aged 18-65 years of age, with a body mass index (BMI) of 20 to 34.9 kg/m^2 were recruited into the randomized, double-blind, parallel arm, placebo-controlled clinical trial by Trotter, RE et al. (52). The study protocol was approved by the Colorado State University Institutional Review Board for Human Subjects (Protocol #19-9145H), and details of the trial design are provided elsewhere (52). For clinical sessions, study participants were asked to fast for 12 hr prior to arrival in the clinic (including no caffeine, soda, tea, etc.), to abstain from exercise within 12 hr prior to their visit, and to delay consumption of any medication or dietary supplements for 24 hr prior until conclusion of the study visit. Study participants were asked to visit the Food and Nutrition Clinical Research Laboratory (FNCRL) at visit one (Day 0) to undergo baseline sample collection (whole blood) and assessment procedures. For the current study, a subset of study participants (n=14) recruited into the clinical trial by Trotter, RE et al. were used and baseline whole blood collected (*Figure 4.1*).

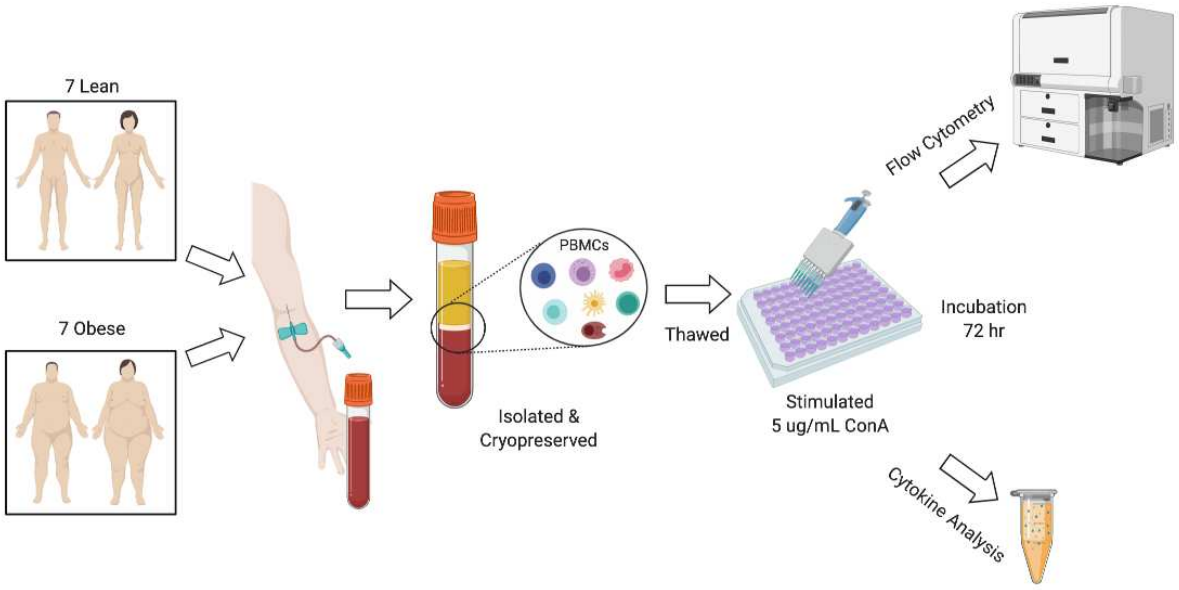

Figure 4.1. Experimental study design.

Isolation of peripheral blood mononuclear cells

Approximately 10 mL of whole blood was collected from antecubital veins into ethylenediaminetetraacetic acid (EDTA) treated vacutainer tubes. Peripheral blood mononuclear cells (PBMCs) were isolated from whole blood within 6 hr of collection by density centrifugation and a series of washes. Initially, whole blood was diluted 1:1 with 1X Phosphate Buffer Solution (PBS) containing 2% Fetal Bovine Serum (FBS) (F-0050-A; Atlas Biologics) and transferred into 50 mL SepMate™ Tubes (85450; StemCell tech.) with 17 mL Lymphoprep™ density gradient medium (07851; StemCell tech). Tubes were centrifuged for 10 min at 1200 g at room temperature. The separated plasma and PBMCs were poured off and diluted with equivalent volume of 1X PBS containing 2% FBS and centrifuged at 300 g for 8 min. Tubes were decanted and then pelleted cells were resuspended in equivalent volume of 1X PBS containing 2% FBS for final wash and centrifugation. Cells were counted using cell counting chambers (CHT4-SD100-002; Nexcelom Bioscience) and a Cellometer Mini automated

cell counter (Nexcelom Bioscience) to calculate the appropriate volume of CryoStor CS10 freeze media (210102; Biolife Solutions). Pelleted cells were re-suspended in CryoStor CS10 freeze media and placed into a Nalgene® Mr. Frosty® freezing container (ThermoFisher Scientific) container at -80°C for 24 hr before final storage in liquid nitrogen.

Peripheral blood mononuclear cell culture and stimulation

All cell processing was performed aseptically in a laminar flow hood. A complete culture medium (cMedia) containing 1X RPMI-1640 (10-041-CV; Corning), 10% FBS, 1% penicillin/streptomycin (100 U/mL penicillin and 100 µg/mL streptomycin, SV30010; HyClone) was warmed to 37°C in a water bath. Frozen human PBMCs were rapidly thawed in a 37°C water bath. Samples were added to 15 mL conical tubes and then warm cMedia was added at a rate of 1 mL/5 seconds to a final volume of 10 mL. Cells were then centrifuged (25°C, 300g, 8 min) and washed twice with cMedia. Cells were then plated at 2×10^6 cells/mL for a 24 hr recovery period. After the rest period, cells were recounted and seeded at 5×10^6 cells/well in replicate into U-bottom, 96-well, untreated plate. Sample wells were then labeled with 1 µM of 5-(and 6)-Carboxyfluorescein diacetate succinimidyl ester (CFSE) (423801; Biolegend), according to manufacture instructions, to mark cell division. After labeling, appropriate wells (i.e. treated vs untreated) were spiked with Concanavalin A (ConA) (C5275-5MG; Millipore Sigma) for a final concentration of 5 µg/mL. Finally, samples were incubated for 72 hr at 37°C and 5% CO2. Post incubation, cells were pelleted by centrifugation (400 g, 5 min, 4°C), and supernatants removed and frozen at -80°C for downstream analysis. Cells were then washed and resuspended with 1X PBS containing 2% FBS, and then stored on ice for downstream antibody staining.

Flow cytometric analysis

PBMCs were incubated on ice in the dark for 30 min with LIVE/DEAD fixable yellow (L34967; Invitrogen) for dead cell discrimination. Nonspecific antibody binding was then blocked by incubating cells with Human TruStain FcX Receptor blocking solution (422302; Biolegend) for 10 min at 4°C. Cells were first stained for cell surface markers by incubating with fluorescently conjugated monoclonal antibodies at 4°C for 30 min in the dark. Then cells were prepared for intranuclear staining, using the Foxp3/Transcription Factor Staining Buffer Set (00-5523-00, eBioscience) according to manufactures instructions. Super Bright Complete Staining Buffer (SB-4401-42; eBiosience) was used per manufactures instructions in stain master mixes which contained more than one polymer dye.

The following fluorescent antibodies were used for cell surface staining: CD25 APC (clone M-A251), CD3 BV570 (clone UCHT1), CD4 Pac Blue (clone SK3), CD8 BV750 (clone SK1), CD19 BV605 (clone HIB19), CD14 AF700 (clone HCD14), CD16 BV785 (clone 3G8), CD56 PE (clone 5.1H11), and LPAM-1 AF647 (clone Hu117; R&D). The following fluorescently conjugated antibody was used for intranuclear staining: FoxP3 BV421 (clone 206D). All antibodies were purchased from Biolegend, with the exception of LPAM-1.

All samples were analyzed using a Cytek Biosciences Aurora spectral flow cytometer and FlowJo™ Software (Becton Dickinson). Cells were gated on leukocytes based on characteristic forward and side scatter profiles. Individual cell populations were identified according to their presence of specific fluorescent-labeled antibodies.

Cytokine quantification

Human interferon gamma (IFNγ) levels were determined in cell culture supernatants using an enzyme-linked immunosorbent assays (ELISA) kit per the manufacturer's instructions (KAC1231; Invitrogen).

Statistics

All statistical analysis was performed with GraphPad Prism version 8.4.2 for macOS (GraphPad Software). Data are presented as mean ± standard error of the mean (SEM). Significance was considered with a P value of < 0.05. An unpaired T test was used when comparing two groups. Whereas, a two-way ANOVA with Tukey's post hoc test was used for all other comparisons, with a group × treatment design. ANOVA and T test assumptions were checked, if data failed to meet these assumptions the data were log transformed and then re-analyzed. To determine the magnitude of treatment effect, a Hedges' g effect size was calculated. A g equal to 0.2 is interpreted as a small effect, a g equal to 0.5 as a medium effect, and a g equal to 0.8 as a large effect.

Results

A total of 14 persons were included in the study. Participant characteristics are presented in *Table 4.1*. Both normal weight and obese groups contained 5 females and 2 males. The average BMI for persons in the normal weight group was 22.14 kg/m^2. Whereas 30.46 kg/m^2 for those in the obese group. Compared to the normal weight group, the obese group had a significantly greater BMI (Hedges' g=-7.98, P<0.0001) because of a significantly greater body weight (Hedges' g=-2.86, P<0.0001). Participants in the study did not differ appreciably by age.

Table 4.1. Participant characteristics

Group	Male	Female	Height (m)	Weight (kg)	BMI	Age
Normal	2	5	1.67±0.04	62.13±2.53	22.14±0.27	38.43±3.46
Obese	2	5	1.66±0.03	84.90±3.07‡	30.46±0.44‡	35.29±3.11

Data expressed as mean ± SEM. Statistical analysis was performed using an unpaired T test.
†$P < 0.05$ and ‡$P < 0.01$ vs Normal

For PBMC cultures, samples were plated as 5×10^6 cells/well and then incubated with (+ConA) or without (-ConA) the T lymphocyte mitogen ConA for 72 hr, and subsequently counted. The average total cell count for unstimulated and stimulated replicates (*Figure 4.2A*), and the average difference between unstimulated and stimulated replicates (*Figure 4.2B*) from normal weight and obese donors were analyzed. We found that ConA stimulation significantly increased total cell counts (*Figure 4.2A*) within the normal+ConA (Hedges' g=-2.66, P=0.0002) and obese+ConA (Hedges' g=-3.13, P<0.0001) groups relative to unstimulated controls. Additionally, we found that cell counts were greater, albeit not significantly, within the unstimulated (Hedges' g=-0.15, P=0.9902) and stimulated (Hedges' g=-0.61, P=0.6495) samples of the obese cohort relative to their normal weight controls. This was reflected by a non-significant but moderate increase in the average difference of total cells (*Figure 4.2B*) within the obese cohort as compared to their normal weight counterparts (Hedges' g=-0.39, P=0.4653).

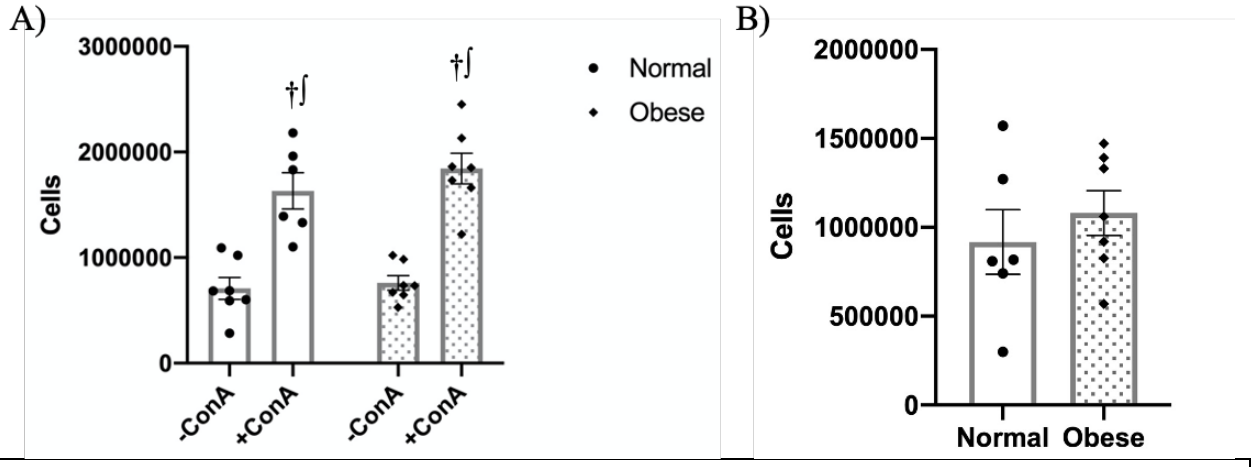

Figure 4.2. Cell counts after 72 hr incubation. Average total number of cells for unstimulated (-ConA) and stimulated (+ConA) samples from normal weight and obese donors (A). Average difference in total number of cells between unstimulated and stimulated samples from normal weight and obese donors (B). Statistical analysis was performed using a two-way ANOVA with Tukey's post hoc test (A) and an unpaired T test (B). Data expressed as mean ± SEM; n=6-7/group. †$P < 0.05$ vs Normal-ConA, *$P < 0.05$ vs Normal+ConA, ∫$P < 0.05$ vs Obese-ConA.

T lymphocyte stimulation with ConA was provided for 72 hr prior to supernatant harvest. Supernatants from stimulated and unstimulated replicates were pooled and then analyzed for IFNγ by ELISA. The average concentration of IFNγ for unstimulated and stimulated samples (*Figure 4.3A*) and the average difference between unstimulated and stimulated samples (*Figure 4.3B*) from normal weight and obese donors were analyzed. We found that ConA stimulation significantly increased IFNγ secretion (*Figure 4.3A*) within the normal+ConA (Hedges' g=-12.63, P<0.0001) and obese+ConA (Hedges' g=-12.90, P<0.0001) groups relative to unstimulated controls. We also found that IFNγ concentrations were higher, although not significantly, within obese+ConA samples relative to normal+ConA samples (Hedges' g=-0.35, P=0.9028). This was reflected by a non-significant but moderate increase in the average difference of IFNγ concentration (*Figure 4.3B*) within the obese cohort as compared to their normal weight counterparts (Hedges' g=-0.68, P=0.2345).

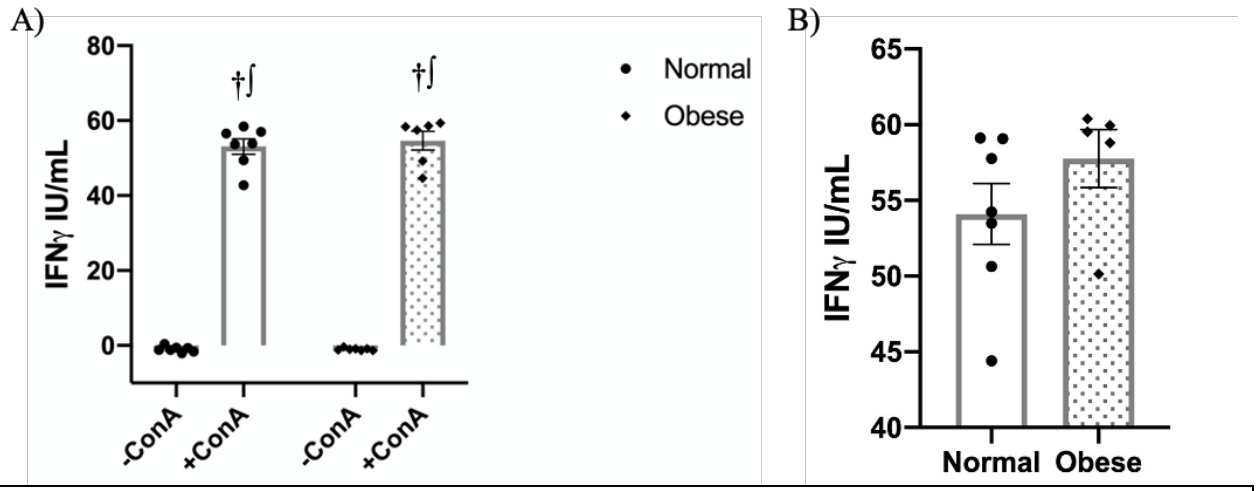

Figure 4.3. IFNγ concentrations from cultured PBMC supernatants. Average concentration of IFNγ for unstimulated (-ConA) and stimulated (+ConA) samples from normal weight and obese donors (A). Average difference in IFNγ concentration between unstimulated and stimulated samples from normal weight and obese donors (B). Statistical analysis was performed using a two-way ANOVA with Tukey's post hoc test (A) and an unpaired T test (B). Data expressed as mean ± SEM; n=5-7/group. †P < 0.05 vs Normal-ConA, *P < 0.05 vs Normal+ConA, ∫P < 0.05 vs Obese-ConA.

After the 72 hr incubation, PBMCs were immunophenotyped and cell proliferation quantified by flow cytometry (*Figures 4.4-4.6*). Leukocytes were gaited with a primary gate excluding debris, secondary gate excluding doublets, and a tertiary gate on live cells (Live/Dead Yellow^{-}). Leukocytes were then divided into T cells (CD3^{+}), B cells (CD19^{+}), and non-lymphoid cells (CD3^{-}CD19^{-}). T cells were further analyzed for changes in CD8^{+}, CD4^{+}CD8^{+}, CD4^{+}, CD25^{+}, CD25^{+}Foxp3^{+}, and CD16^{+}CD56^{+} cell subsets. Non-lymphoid cells were further analyzed for changes in CD16^{+} and CD16^{+}CD56^{+} cell subsets. All populations were analyzed for CFSE expression as a marker for cell proliferation. Absolute numbers of cell subsets were calculated for individual samples using average total cell counts.

We found that ConA stimulation had a ubiquitous effect on T lymphocyte subsets within both normal weight and obese groups. The absolute number of CD3^{+} T cells (*Figure 4.4A*) were found to be significantly increased in normal+ConA (Hedges' *g*=-2.10, *P*=0.0028) and obese+ConA (Hedges' *g*=-1.68, *P*=0.0178) groups relative to unstimulated controls. Additionally, we found that obese-ConA (Hedges' *g*=0.31, *P*=0.9267) and obese+ConA (Hedges' *g*=0.71, *P*=0.5503) groups had fewer total CD3^{+} T cells relative to their normal weight controls. A similar trend was also seen in the absolute number of CD3^{+} T cells that proliferated (*Figure 4.4B*).

The absolute number of CD8^{+} cytotoxic T cells (*Figure 4.4C*) displayed a less robust increase in response to ConA stimulation, within both normal+ConA (Hedges' *g*=-0.79, *P*=0.4797) and obese+ConA (Hedges' *g*=-0.96, *P*=0.2781) groups relative to unstimulated controls. This trend was mirrored, although slightly more prominent, in the absolute number of CD8^{+} T cells that proliferated (*Figure 4.4D*). No substantial differences between weight groups were found.

The absolute number of $CD4^+CD8^+$ T cells (*Figure 4.4E*) was significantly increased within the normal+ConA group (Hedges' *g*=-1.91, *P*=0.0064) and to a greater extent within the obese+ConA group (Hedges' *g*=-3.23, *P*<0.0001) relative to unstimulated controls. Additionally, we found that obese+ConA group had substantially more $CD4^+CD8^+$ T cells as compared to their normal weight controls (Hedges' *g*=-1.40, *P*=0.0690). A similar yet more pronounced trend was also observed within the absolute number of $CD4^+CD8^+$ T cells that proliferated (*Figure 4.4F*).

The absolute number of $CD4^+$ helper T cells (*Figure 4.4G*) were found to be significantly increased within normal+ConA (Hedges' *g*=-2.27, *P*=0.0013) and obese+ConA (Hedges' *g*=-1.82, *P*=0.0097) groups relative to unstimulated controls. We also found that the obese-ConA (Hedges' *g*=0.36, *P*=0.8917) and obese+ConA (Hedges' *g*=0.79, *P*=0.4624) groups had fewer total $CD4^+$ helper T cells relative to their normal weight controls. These trends were similarly observed within the absolute number of $CD4^+$ T cells that proliferated (*Figure 4.4H*).

The absolute number of $CD25^+$ regulatory T cells (T_{regs}) (*Figure 4.4I*) was significantly increased within the obese+ConA group (Hedges' *g*=-1.76, *P*=0.0089) and to a lesser extent within the normal+ConA group (Hedges' *g*=-1.21, *P*=0.1020) relative to unstimulated controls. Additionally, we found that the obese+ConA group had more total $CD25^+$ T_{regs} as compared with their normal weight controls (Hedges' *g*=-0.43, *P*=0.8223). Identical trends were found among groups in the absolute number of $CD25^+$ T_{regs} that proliferated (*Figure 4.4J*). On the other hand, the absolute number of $CD25^+Foxp3^+$ T_{regs} (*Figure 4.4K*) were significantly increased within the normal+ConA group (Hedges' *g*=-3.34, *P*<0.0001) and to a lesser extent in the obese+ConA group (Hedges' *g*=-2.54, *P*=0.0004) relative to unstimulated controls. We also found that the obese+ConA group had fewer total $CD25^+Foxp3^+$ T_{regs} as compared with their normal+ConA

controls (Hedges' g=0.80, P=0.4583). A similar trend was also seen in the absolute number of $CD25^{+}Foxp3^{+}$ T_{regs} that proliferated (*Figure 4.4L*).

The absolute number of $CD16^{+}CD56^{+}$ NKT cells (*Figure 4.4M*) were significantly increased within both normal+ConA (Hedges' g=-4.39, P<0.0001) and obese+ConA (Hedges' g=-3.53, P<0.0001) groups as compared with unstimulated controls. Additionally, we found that the obese-ConA (Hedges' g=0.36, P=0.9111) and obese+ConA (Hedges' g=1.34, P=0.1513) groups had fewer total $CD16^{+}CD56^{+}$ NKT cells than their normal weight counterparts. Comparable yet less prominent trends were also observed in the absolute number of $CD16^{+}CD56^{+}$ NKT cells that proliferated (*Figure 4.4N*).

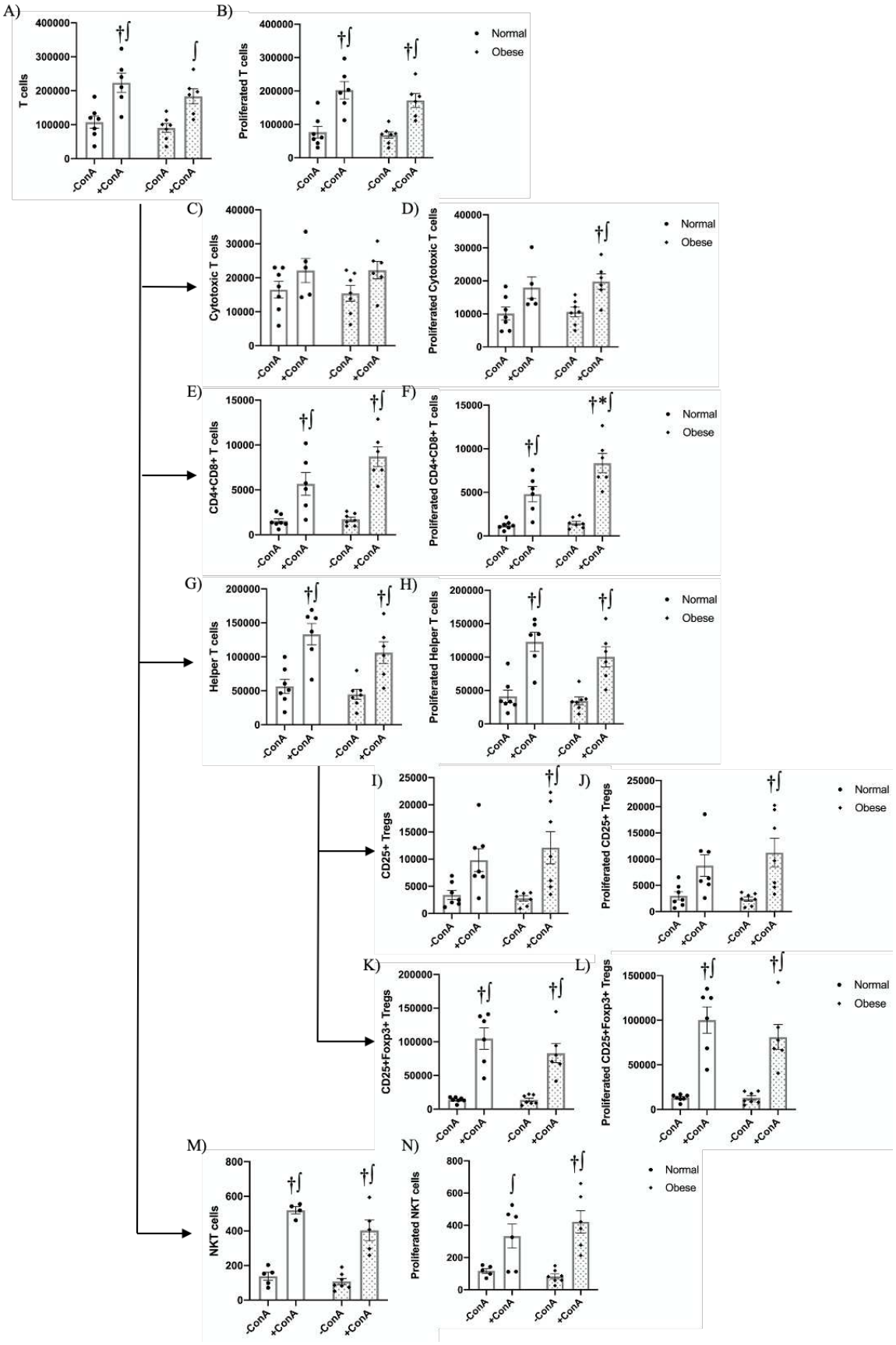
A)
T cells
B)
Proliferated T cells
Normal
Obese
C)
Cytotoxic T cells
D)
Proliferated Cytotoxic T cells
E)
CD4+CD8+ T cells
F)
Proliferated CD4+CD8+ T cells
G)
Helper T cells
H)
Proliferated Helper T cells
I)
CD25+ Tregs
J)
Proliferated CD25+ Tregs
K)
CD25+Foxp3+ Tregs
L)
Proliferated CD25+Foxp3+ Tregs
M)
NKT cells
N)
Proliferated NKT cells
-ConA
+ConA

Figure 4.4. T lymphocyte populations. Mean ± SEM (n=4-7/group) absolute number $CD3^+$ T cells (A), proliferated $CD3^+$ T cells (B), $CD8^+$ cytotoxic T cells (C), proliferated $CD8^+$ cytotoxic T cells (D), $CD4^+CD8^+$ T cells (E), proliferated $CD4^+CD8^+$ T cells (F), $CD4^+$ helper T cells (G), proliferated $CD4^+$ helper T cells (H), $CD4^+CD25^+$ T_{regs} (I), proliferated $CD4^+CD25^+$ T_{regs} (J), $CD25^+Foxp3^+$ T_{regs} (K), proliferated $CD25^+Foxp3^+$ T_{regs} (L), $CD16^+CD56^+$ NKT cells (M), proliferated $CD16^+CD56^+$ NKT cells (N). Statistical analysis was performed using a two-way ANOVA with Tukey's post hoc test. †$P < 0.05$ vs Normal-ConA, *$P < 0.05$ vs Normal+ConA, ∫$P < 0.05$ vs Obese-ConA.

Within B lymphocytes, we found that the absolute number of $CD19^+$ B cells (*Figure 4.5A*) were significantly reduced in the normal+ConA group (Hedges' g=2.51, P=0.0013) and to a lesser extent in the obese+ConA group (Hedges' g=1.17, P=0.1865) relative to unstimulated controls. We also found that the obese-ConA group had fewer total $CD19^+$ B cells than the normal-ConA group (Hedges' g=0.67, P=0.5997), however after stimulation the obese+ConA group had retained more $CD19^+$ B cells than their normal+ConA controls (Hedges' g=-0.67, P=0.6482). A similar trend was also seen among groups in the absolute number of $CD19^+$ B cells that proliferated (*Figure 4.5B*).

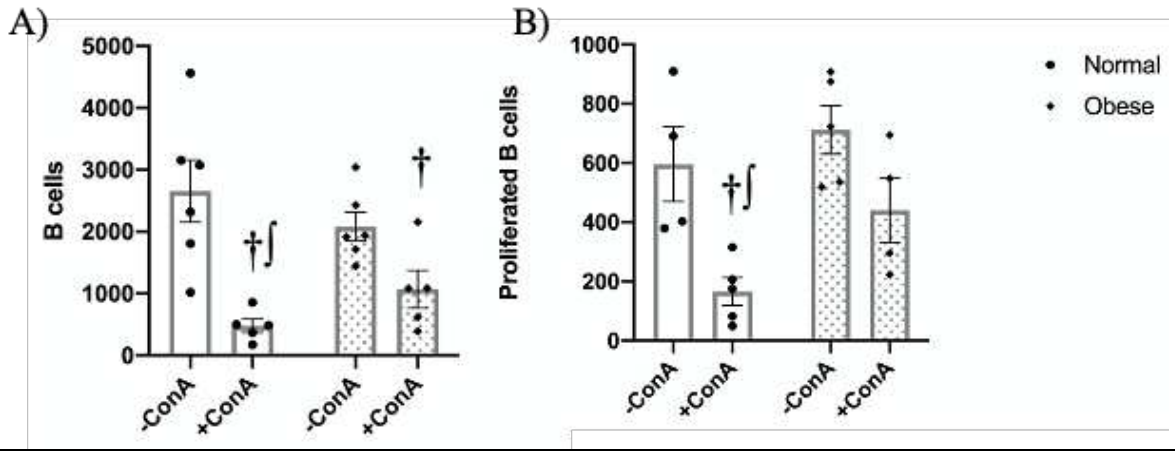

Figure 4.5. B lymphocytes. Mean ± SEM (n=4-7/group) absolute number $CD19^+$ B cells (A), proliferated $CD19^+$ B cells (B). Statistical analysis was performed using a two-way ANOVA with Tukey's post hoc test. †$P < 0.05$ vs Normal-ConA, *$P < 0.05$ vs Normal+ConA, ∫$P < 0.05$ vs Obese-ConA.

In general, myeloid cells from obese donors appeared more responsive to ConA stimulation than those from normal weight counterparts. The absolute number of $CD3^-CD19^-$ cells (*Figure 4.6A*) were found to be largely increased by ConA stimulation within the

obese+ConA group (Hedges' *g*=-1.46, *P*=0.0602) and to a lesser extent within the normal+ConA group (Hedges' *g*=-0.76, *P*=0.4772) as compared to unstimulated controls. Additionally, we found that the obese+ConA group had substantially more total $CD3^{-}CD19^{-}$ cells than their normal+ConA controls (Hedges' *g*=-0.72, *P*=0.5729). These trends were comparable yet more robust in the absolute number of $CD3^{-}CD19^{-}$ cells that proliferated (*Figure 4.6B*).

Similarly, the absolute number of $CD16^{+}$ monocytes (*Figure 4.6C*) were substantially increased within the obese+ConA group (Hedges' *g*=-1.42, *P*=0.0787), whereas only minimally within the normal+ConA group (Hedges' *g*=-0.29, *P*=0.9354), as compared to their respective controls. We also found that the obese+ConA group had significantly more $CD16^{+}$ monocytes than their normal weight controls (Hedges' *g*=-1.79, *P*=0.0165), which also occurred to a lesser degree in the obese-ConA group (vs normal-ConA; Hedges' *g*=-0.65, *P*=0.6045). A similar but more pronounced trend was observed among groups in the number of $CD16^{+}$ monocytes that proliferated (*Figure 4.6D*).

Likewise, the absolute number of $CD16^{+}CD56^{+}$ NK cells (*Figure 4.6E*) were significantly increased within the obese+ConA (Hedges' *g*=-1.60, *P*=0.0343), as well as to a lesser extent in the normal+ConA group (Hedges' *g*=-0.34, *P*=0.9029), relative to normal weight controls. Additionally, we found that the obese+ConA group (Hedges' *g*=-1.51, *P*=0.0488) had significantly more $CD16^{+}CD56^{+}$ NK cells than their normal weight counterparts, which occurred to a lesser degree in the obese-ConA group (vs normal-ConA; Hedges' *g*=-0.25, *P*=0.9580). These trends were also observed in the absolute number of $CD16^{+}CD56^{+}$ NK cells that proliferated (*Figure 4.6F*).

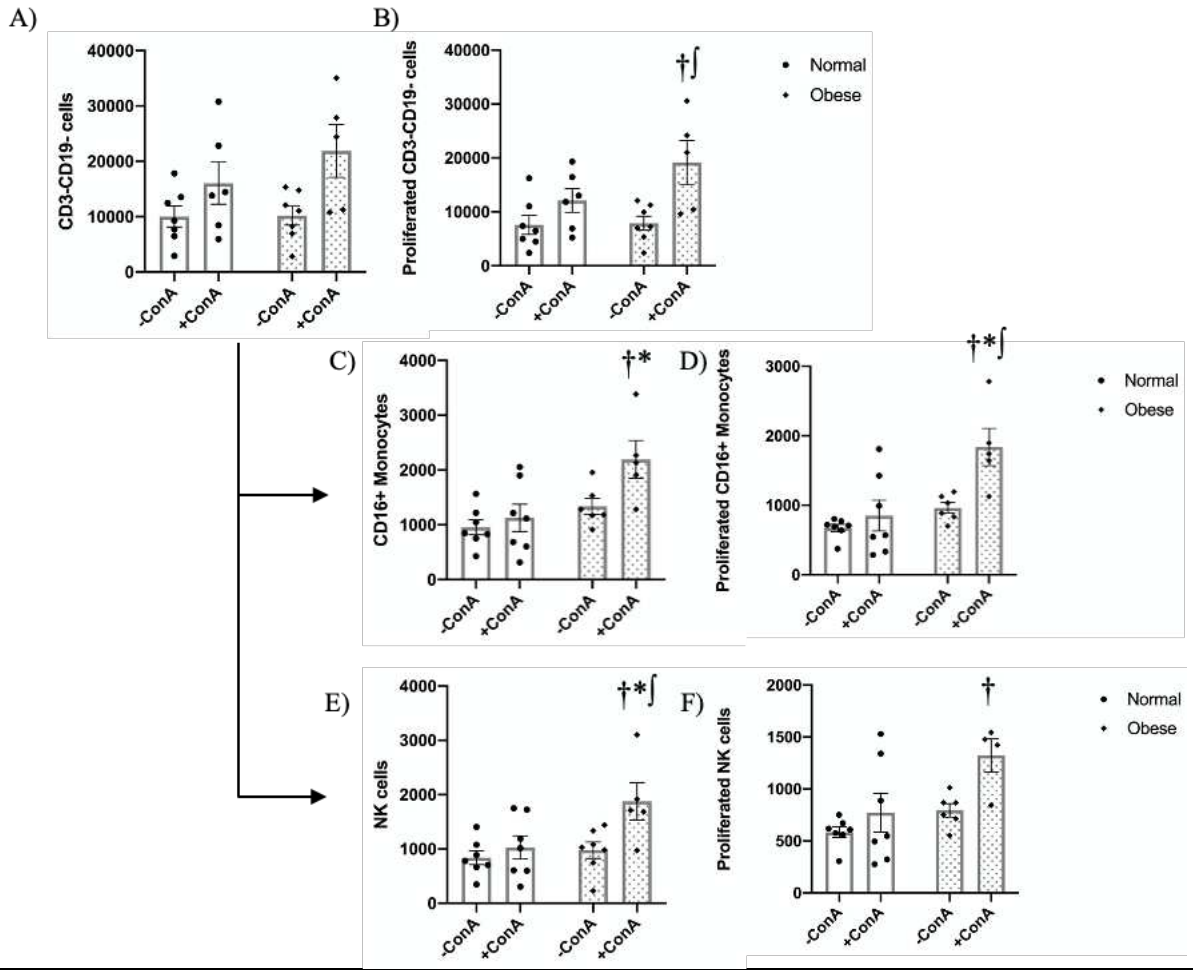

Figure 4.6. Myeloid cell populations. Mean ± SEM (n=4-7/group) absolute number $CD3^{-}CD19^{-}$ cells (A), proliferated $CD3^{-}CD19^{-}$ cells (B), $CD16^{+}$ monocytes (C), proliferated $CD16^{+}$ monocytes (D), $CD16^{+}CD56^{+}$ NK cells (E), proliferated $CD16^{+}CD56^{+}$ NK cells (F). Statistical analysis was performed using a two-way ANOVA with Tukey's post hoc test. †$P < 0.05$ vs Normal-ConA, *$P < 0.05$ vs Normal+ConA, ∫$P < 0.05$ vs Obese-ConA.

Discussion

The purpose of the present study was to characterize various immunologic parameters within a normal weight and obese human population that was otherwise free of disease. It is now well accepted that obesity is a high-risk group for both chronic and infectious diseases and given the continued increase in obesity prevalence worldwide this poses a serious public health problem. In the present study we observed the effects of *ex vivo* Concanavalin A (ConA) stimulation for 72 hr on PBMC immunocompetence and phenotype. To the best of our

knowledge, we are the first to investigate differences between obese and normal weight donor PBMCs in response to the T lymphocyte mitogen ConA.

We found that obesity had an overall effect on cellular activation and proliferation in response to ConA. Specifically, we saw a modest increase in cell number within ConA stimulated obese samples. Normally during an immune response activated immune cells undergo rapid expansion, however this is shown to be impaired in obesity due to the development of premature immunosenescence. Our findings are in contrast with previous clinical (53, 54) and pre-clinical (55, 56) work demonstrating a reduction in cell activation and proliferation in obesity. This discrepancy may result from differences in study participant characteristics, such as body weight, gender, and health status. Here, we recruited otherwise healthy male and female adults with a mean BMI of 30.46 kg/m^2. Whereas work by Parisi, MM et al., used only male subjects who were morbidly obese (50.03 kg/m^2). The aforementioned difference in BMI and gender are reasonably associated with biologically relevant confounders (57), such as inflammatory burden, that may explain the observed differences in data. Alternatively, our findings are supported by work from Paich et al. who showed no difference in influenza-stimulated proliferation of PBMCs between health weight (18.5-24.9 kg/m^2), overweight (25.0-29.9 kg/m^2), or obese ($\geq$30.0 kg/m^2) groups (48). Thus, it is clear that further work is needed to clarify differences in PBMC function across the ranges of obesity in adults.

Similarly, we found that obesity influenced interferon gamma (IFNγ) secretion from PBMCs, as there was a moderate increase in total IFNγ concentration within the supernatants of ConA stimulated obese samples. Cytokine production and secretion are instrumental for immune cell communication and eliciting an effective and accurate immune response (58). IFNγ is primarily secreted by activated T cells and natural killer (NK) cells (59), and serves a diverse

array of functions within the body such as promoting macrophage activation, mediating antiviral and antibacterial immunity, enhancing antigen presentation, orchestrating activation of the innate immune system, regulating T_H1/T_H2 balance, and controlling cellular proliferation and apoptosis (60-62). Our results somewhat contrast previous findings, as Paich et al. found that IFNγ levels trended lower in obese PBMCs relative to healthy weight controls, however authors found no difference in IFNγ secretion between healthy weight and overweight adult PBMCs (48). Discrepancies between our results may arise in part from differences in study sample size, subject characteristics, and the nature of the stimulation. Given our studies exclusive assessment of IFNγ, we cannot ascertain the full effect of obesity on the PBMC secretome. Further, we are limited in our inference as we did not specifically characterize cell types responsible for IFNγ production.

Additionally, we found that obesity had a substantial effect on the ConA stimulated *ex vivo* expansion of PBMCs. ConA is a widely used plant lectin that binds to glycoproteins expressed on the T cell surface and can mimic T cell receptor activation by cross-linking the T cell receptor (63-65). We found that all T lymphocyte subsets were significantly increased by ConA stimulation within both normal weight and obese groups, apart from $CD8^+$ T cells and $CD25^+$ T_{regs}. $CD25^+$ T_{regs} in particular were found to be only significantly increased within the obese group. Interestingly, we saw that $CD4^+CD8^+$ T cells were significantly increased by ConA within the obese group compared to the normal weight group. $CD4^+CD8^+$ T cells represent a small (~1-2%) but distinct circulating lymphocyte population that is not fully characterized (66). They are, however, shown to be elevated within various disease states including cancer and aging (67, 68). Clenet ML et al. has demonstrated that $CD4^+CD8^+$ T lymphocytes constitute a heterogenous population of activated/memory T cells which have the capacity to produce

effector molecules associated with a T_H1 profile (66). The lineage of these double positive cells is still unclear, but evidence suggests that they may arise from the transcriptional reprogramming of mature single positive T cells leaving the thymus (69-71). Given that our understanding of $CD4^+CD8^+$ T cells is still developing and they have yet to be studied within the obese cohort we can only speculate on the meaning of this finding. Be that as it may, these cells may play a role in pathology associated with obesity and thus warrant further investigation. Additionally, we found that total $CD3^+$ T cells, $CD4^+$ T cells, and NKT cells were lower, although not significantly, within both unstimulated and stimulated obese groups relative to their normal weight controls. While, $CD25^+Foxp3^+$ T_{regs} were lower only within the stimulated obese group compared to their respective control, although again not significantly. These findings are somewhat controversial. In a comparative analysis between healthy weight, overweight, and obese donor PBMCs challenged *ex vivo*, authors found no difference in total $CD4^+$ or $CD8^+$ T cell number between BMI groups within either unstimulated or stimulated samples (48). Alternatively, baseline characterization of the human peripheral blood T cell compartment between morbidly obese (>40 kg/m^2) and lean (<25 kg/m^2) individuals has previously shown that total T cell numbers were greater within morbidly obese subjects (72). This was found to be primarily due to an increase in $CD4^+$ T cells, including $CD25^+Foxp3^+$ T_{regs}, T_H1 and T_H2 cell subsets. Interestingly, authors concluded that these obesity-related differences in cell number were due to homeostatic proliferation rather than an antigen driven increase, as they found little difference in effector memory or effector populations. However, our observed reductions in $CD25^+Foxp3^+$ T_{regs} (73-76) and NKT cells (77) are largely in agreement with the literature. These discrepancies pose an interesting point in regard to immune cell numbers relative to body size, as proportional increases are likely homeostatic as mentioned above however this is not

typically discussed within the literature. Taken together, the observed alterations within T lymphocyte subsets support the obesity-induced impairment of immune function and highlight new populations for future research.

On the other hand, we found that B lymphocytes were significantly reduced by ConA stimulation within both normal weight and obese groups, however this effect was more pronounced within the normal weight group. We attribute this difference to the fact that B cells were lower, although not significantly, within the unstimulated obese group as compared to the unstimulated normal weight group. These findings are in agreement with the literature, which collectively show a decline in B cell function within the obese and aged populations (78-82). This includes reductions in antigen-stimulated activation and antibody production, as well as cytokine secretion. Hence, we speculate that the diminished loss of B cells within the stimulated obese group may be due to a reduction in overall B cell activation.

Interestingly, we found that myeloid cells were significantly increased by ConA only within the obese group. Specifically, the stimulated obese group had significantly more $CD16^{+}$ monocytes and NK cells than their normal weight controls. It is also worth noting that the unstimulated obese group had slightly more $CD16^{+}$ monocytes and NK cells, although these increases were not significant. Peripheral blood monocytes are not homogenous and three major subpopulations are described, classical ($CD14^{Hi}CD16^{-}$), intermediate ($CD14^{Hi}CD16^{+}$), and non-classical ($CD14^{Low}CD16^{+}$) (83). A number of studies have shown associations between these peripheral monocyte populations and obesity (84-87). Here we characterized the non-classical monocyte population and our findings support the work of others, showing an enhanced activation of non-classical monocytes within stimulated PBMCs from obese donors. To date, a limited number of studies have investigated differences in *ex vivo* activation and proliferation

among NK cells from various BMI donors. Several studies report a reduction in NK cell frequency and functionality within both obese human and rodent models (77, 88-90), which is in contrast to our findings. Nevertheless, the role of NK cells in obesity and how they may contribute to obesity-associated pathology remains unclear. Interestingly, a role for leptin in NK cell activation and IFNγ production has previously been shown (77). Thus, we speculate that the robust increase in NK cells within the stimulated obese group may have substantially contributed to IFNγ production and possibly compensated for a reduction in other IFNγ producing cell types (i.e. activated T cells subsets). Although further study into the contribution of NK cells in obesity is needed. Taken together, the observed alterations within $CD16^{+}$ monocytes and NK cells also support the impairment of normal immune function within obese individuals.

In sum, we found that obesity affected PBMC immunocompetence when challenged *ex vivo* with ConA, as evidenced by a modest increase in cell proliferation and IFNγ secretion relative to normal weight controls. Additionally, we found that obesity affected *ex vivo* expansion of PBMCs, as distinct immune cell populations were observed among obese and normal weight groups. Collectively, these results support an altered response of PBMCs within obese individuals and provide new insight into obesity-driven immune alterations. However, results reported herein should be taken in light of some study limitations. Our study is limited in both sample size and representation of BMI ranges, as such verification of our findings in a larger cohort is warranted. Be that as it may, our preliminary results are promising. Additionally, our study is limited in the characterization of secreted cytokines and immune cell markers, both of which limit our biologic inference of the data. Finally, *ex vivo* models are inherently limited in comparison to *in vivo* models, however they are often the only available option. Nonetheless, our

study emphasizes the need for further work in exploring differences among the ranges of obesity, as well as a more detailed characterization of the human peripheral compartment.

REFERENCES

1. O'Neill S, O'Driscoll L. Metabolic syndrome: a closer look at the growing epidemic and its associated pathologies. Obes Rev. 2015 Jan;16:1-12.
2. De Pergola G, Silvestris F. Obesity as a major risk factor for cancer. J Obes. 2013;2013:291546.
3. Guarner V, Rubio-Ruiz ME. Low-grade systemic inflammation connects aging, metabolic syndrome and cardiovascular disease. Interdiscip Top Gerontol. 2015;40:99-106.
4. Hales CM, Carroll MD, Fryar CD, Ogden CL. Prevalence of Obesity and Severe Obesity Among Adults: United States, 2017-2018. NCHS Data Brief. 2020 Feb:1-8.
5. Ward ZJ, Bleich SN, Cradock AL, Barrett JL, Giles CM, Flax C, Long MW, Gortmaker SL. Projected U.S. State-Level Prevalence of Adult Obesity and Severe Obesity. N Engl J Med. 2019 12;381:2440-50.
6. Furman D, Campisi J, Verdin E, Carrera-Bastos P, Targ S, Franceschi C, Ferrucci L, Gilroy DW, Fasano A, et al. Chronic inflammation in the etiology of disease across the life span. Nat Med. 2019 12;25:1822-32.
7. Calder PC, Ahluwalia N, Albers R, Bosco N, Bourdet-Sicard R, Haller D, Holgate ST, Jönsson LS, Latulippe ME, et al. A consideration of biomarkers to be used for evaluation of inflammation in human nutritional studies. Br J Nutr. 2013 Jan;109 Suppl 1:S1-34.
8. de Heredia FP, Gómez-Martínez S, Marcos A. Obesity, inflammation and the immune system. Proc Nutr Soc. 2012 May;71:332-8.
9. Bilecik NA, Tuna S, Samancı N, Balcı N, Akbaş H. Prevalence of metabolic syndrome in women with rheumatoid arthritis and effective factors. Int J Clin Exp Med. 2014;7:2258-65.
10. Bjorntorp P. Metabolic implications of body fat distribution. Diabetes Care. 1991 Dec;14:1132-43.
11. Thijssen E, van Caam A, van der Kraan PM. Obesity and osteoarthritis, more than just wear and tear: pivotal roles for inflamed adipose tissue and dyslipidaemia in obesity-induced osteoarthritis. Rheumatology (Oxford). 2015 Apr;54:588-600.
12. Esser N, Legrand-Poels S, Piette J, Scheen AJ, Paquot N. Inflammation as a link between obesity, metabolic syndrome and type 2 diabetes. Diabetes Res Clin Pract. 2014 Aug;105:141-50.
13. Mraz M, Haluzik M. The role of adipose tissue immune cells in obesity and low-grade inflammation. J Endocrinol. 2014 Sep;222:R113-27.
14. Lee CG, Lee JK, Kang YS, Shin S, Kim JH, Lim YJ, Koh MS, Lee JH, Kang HW. Visceral abdominal obesity is associated with an increased risk of irritable bowel syndrome. Am J Gastroenterol. 2015 Feb;110:310-9.
15. Kotas ME, Medzhitov R. Homeostasis, inflammation, and disease susceptibility. Cell. 2015 Feb;160:816-27.
16. Fullerton JN, Gilroy DW. Resolution of inflammation: a new therapeutic frontier. Nat Rev Drug Discov. 2016 08;15:551-67.

17. Calder PC, Albers R, Antoine JM, Blum S, Bourdet-Sicard R, Ferns GA, Folkerts G, Friedmann PS, Frost GS, et al. Inflammatory disease processes and interactions with nutrition. Br J Nutr. 2009 May;101 Suppl 1:S1-45.
18. Sun S, Ji Y, Kersten S, Qi L. Mechanisms of inflammatory responses in obese adipose tissue. Annu Rev Nutr. 2012 Aug;32:261-86.
19. Serhan CN, Savill J. Resolution of inflammation: the beginning programs the end. Nat Immunol. 2005 Dec;6:1191-7.
20. Straub RH. The brain and immune system prompt energy shortage in chronic inflammation and ageing. Nat Rev Rheumatol. 2017 Dec;13:743-51.
21. Shen-Orr SS, Furman D, Kidd BA, Hadad F, Lovelace P, Huang YW, Rosenberg-Hasson Y, Mackey S, Grisar FA, et al. Defective Signaling in the JAK-STAT Pathway Tracks with Chronic Inflammation and Cardiovascular Risk in Aging Humans. Cell Syst. 2016 10;3:374-84.e4.
22. Verschoor CP, Lelic A, Parsons R, Evelegh C, Bramson JL, Johnstone J, Loeb MB, Bowdish DME. Serum C-Reactive Protein and Congestive Heart Failure as Significant Predictors of Herpes Zoster Vaccine Response in Elderly Nursing Home Residents. J Infect Dis. 2017 07;216:191-7.
23. Fourati S, Cristescu R, Loboda A, Talla A, Filali A, Railkar R, Schaeffer AK, Favre D, Gagnon D, et al. Pre-vaccination inflammation and B-cell signalling predict age-related hyporesponse to hepatitis B vaccination. Nat Commun. 2016 Jan;7:10369.
24. McDade TW, Adair L, Feranil AB, Kuzawa C. Positive antibody response to vaccination in adolescence predicts lower C-reactive protein concentration in young adulthood in the Philippines. Am J Hum Biol. 2011 2011 May-Jun;23:313-8.
25. Green WD, Beck MA. Obesity Impairs the Adaptive Immune Response to Influenza Virus. Ann Am Thorac Soc. 2017 Nov;14:S406-S9.
26. Huttunen R, Syrjänen J. Obesity and the outcome of infection. Lancet Infect Dis. 2010 Jul;10:442-3.
27. Milner JJ, Beck MA. The impact of obesity on the immune response to infection. Proc Nutr Soc. 2012 May;71:298-306.
28. Basu JK, Jeketera CM, Basu D. Obesity and its outcomes among pregnant South African women. Int J Gynaecol Obstet. 2010 Aug;110:101-4.
29. Usha Kiran TS, Hemmadi S, Bethel J, Evans J. Outcome of pregnancy in a woman with an increased body mass index. BJOG. 2005 Jun;112:768-72.
30. Perdichizzi G, Bottari M, Pallio S, Fera MT, Carbone M, Barresi G. Gastric infection by Helicobacter pylori and antral gastritis in hyperglycemic obese and in diabetic subjects. New Microbiol. 1996 Apr;19:149-54.
31. Suvan J, D'Aiuto F, Moles DR, Petrie A, Donos N. Association between overweight/obesity and periodontitis in adults. A systematic review. Obes Rev. 2011 May;12:e381-404.
32. Waisbren E, Rosen H, Bader AM, Lipsitz SR, Rogers SO, Eriksson E. Percent body fat and prediction of surgical site infection. J Am Coll Surg. 2010 Apr;210:381-9.
33. Di Leo A, Piffer S, Ricci F, Manzi A, Poggi E, Porretto V, Fambri P, Piccini G, Patrizia T, et al. Surgical site infections in an Italian surgical ward: a prospective study. Surg Infect (Larchmt). 2009 Dec;10:533-8.
34. Beldi G, Bisch-Knaden S, Banz V, Mühlemann K, Candinas D. Impact of intraoperative behavior on surgical site infections. Am J Surg. 2009 Aug;198:157-62.

35. Dupuy A, Benchikhi H, Roujeau JC, Bernard P, Vaillant L, Chosidow O, Sassolas B, Guillaume JC, Grob JJ, Bastuji-Garin S. Risk factors for erysipelas of the leg (cellulitis): case-control study. BMJ. 1999 Jun;318:1591-4.
36. Van Kerkhove MD, Vandemaele KA, Shinde V, Jaramillo-Gutierrez G, Koukounari A, Donnelly CA, Carlino LO, Owen R, Paterson B, et al. Risk factors for severe outcomes following 2009 influenza A (H1N1) infection: a global pooled analysis. PLoS Med. 2011 Jul;8:e1001053.
37. Kwong JC, Campitelli MA, Rosella LC. Obesity and respiratory hospitalizations during influenza seasons in Ontario, Canada: a cohort study. Clin Infect Dis. 2011 Sep;53:413-21.
38. Akiyama N, Segawa T, Ida H, Mezawa H, Noya M, Tamez S, Urashima M. Bimodal effects of obesity ratio on disease duration of respiratory syncytial virus infection in children. Allergol Int. 2011 Sep;60:305-8.
39. Jedrychowski W, Maugeri U, Flak E, Mroz E, Bianchi I. Predisposition to acute respiratory infections among overweight preadolescent children: an epidemiologic study in Poland. Public Health. 1998 May;112:189-95.
40. Louie JK, Acosta M, Samuel MC, Schechter R, Vugia DJ, Harriman K, Matyas BT, Group CPHNW. A novel risk factor for a novel virus: obesity and 2009 pandemic influenza A (H1N1). Clin Infect Dis. 2011 Feb;52:301-12.
41. Weber DJ, Rutala WA, Samsa GP, Santimaw JE, Lemon SM. Obesity as a predictor of poor antibody response to hepatitis B plasma vaccine. JAMA. 1985 Dec;254:3187-9.
42. Weber DJ, Rutala WA, Samsa GP, Bradshaw SE, Lemon SM. Impaired immunogenicity of hepatitis B vaccine in obese persons. N Engl J Med. 1986 May;314:1393.
43. Roome AJ, Walsh SJ, Cartter ML, Hadler JL. Hepatitis B vaccine responsiveness in Connecticut public safety personnel. JAMA. 1993 1993 Dec 22-29;270:2931-4.
44. Wood RC, MacDonald KL, White KE, Hedberg CW, Hanson M, Osterholm MT. Risk factors for lack of detectable antibody following hepatitis B vaccination of Minnesota health care workers. JAMA. 1993 1993 Dec 22-29;270:2935-9.
45. Eliakim A, Schwindt C, Swindt C, Zaldivar F, Casali P, Cooper DM. Reduced tetanus antibody titers in overweight children. Autoimmunity. 2006 Mar;39:137-41.
46. Banga N, Guss P, Banga A, Rosenman KD. Incidence and variables associated with inadequate antibody titers after pre-exposure rabies vaccination among veterinary medical students. Vaccine. 2014 Feb;32:979-83.
47. Sheridan PA, Paich HA, Handy J, Karlsson EA, Hudgens MG, Sammon AB, Holland LA, Weir S, Noah TL, Beck MA. Obesity is associated with impaired immune response to influenza vaccination in humans. Int J Obes (Lond). 2012 Aug;36:1072-7.
48. Paich HA, Sheridan PA, Handy J, Karlsson EA, Schultz-Cherry S, Hudgens MG, Noah TL, Weir SS, Beck MA. Overweight and obese adult humans have a defective cellular immune response to pandemic H1N1 influenza A virus. Obesity (Silver Spring). 2013 Nov;21:2377-86.
49. Milner JJ, Wang J, Sheridan PA, Ebbels T, Beck MA, Saric J. 1H NMR-based profiling reveals differential immune-metabolic networks during influenza virus infection in obese mice. PLoS One. 2014;9:e97238.
50. Neidich SD, Green WD, Rebeles J, Karlsson EA, Schultz-Cherry S, Noah TL, Chakladar S, Hudgens MG, Weir SS, Beck MA. Increased risk of influenza among vaccinated adults who are obese. Int J Obes (Lond). 2017 09;41:1324-30.

51. (NCD-RisC) NRFC. Trends in adult body-mass index in 200 countries from 1975 to 2014: a pooled analysis of 1698 population-based measurement studies with 19·2 million participants. Lancet. 2016 Apr;387:1377-96.
52. Trotter R, Vazquez A, Grubb D, Freedman K, Grabos L, Jones S, Gentile C, Melby C, Johnson S, Weir T. ***Bacillus subtilis*** **DE111 intake may improve blood lipids and endothelial function in healthy adults**. Manuscript submitted for publication; 2020.
53. Parisi MM, Grun LK, Lavandoski P, Alves LB, Bristot IJ, Mattiello R, Mottin CC, Klamt F, Jones MH, et al. Immunosenescence Induced by Plasma from Individuals with Obesity Caused Cell Signaling Dysfunction and Inflammation. Obesity (Silver Spring). 2017 09;25:1523-31.
54. Alshahrani A, AlDubayee M, Zahra M, Alsebayel FM, Alammari N, Alsudairy F, Almajed M, Aljada A. Differential Expression of Human N-Alpha-Acetyltransferase 40 (hNAA40), Nicotinamide Phosphoribosyltransferase (NAMPT) and Sirtuin-1 (SIRT-1) Pathway in Obesity and T2DM: Modulation by Metformin and Macronutrient Intake. Diabetes Metab Syndr Obes. 2019;12:2765-74.
55. De La Fuente MDC, NM. Obesity as a Model of Premature Immunosenescence. Current Immunology Reviews; 2012. p. 63-75.
56. Hunsche C, Hernandez O, De la Fuente M. Impaired Immune Response in Old Mice Suffering from Obesity and Premature Immunosenescence in Adulthood. J Gerontol A Biol Sci Med Sci. 2016 08;71:983-91.
57. Lee J, Lee H. Effects of risk factor numbers on the development of the metabolic syndrome. J Exerc Rehabil. 2020 Apr;16:183-8.
58. Altan-Bonnet G, Mukherjee R. Cytokine-mediated communication: a quantitative appraisal of immune complexity. Nat Rev Immunol. 2019 04;19:205-17.
59. Tau G, Rothman P. Biologic functions of the IFN-gamma receptors. Allergy. 1999 Dec;54:1233-51.
60. Billiau A. Interferon-gamma: biology and role in pathogenesis. Adv Immunol. 1996;62:61-130.
61. Boehm U, Klamp T, Groot M, Howard JC. Cellular responses to interferon-gamma. Annu Rev Immunol. 1997;15:749-95.
62. Zha Z, Bucher F, Nejatfard A, Zheng T, Zhang H, Yea K, Lerner RA. Interferon-γ is a master checkpoint regulator of cytokine-induced differentiation. Proc Natl Acad Sci U S A. 2017 08;114:E6867-E74.
63. Rüdiger H, Gabius HJ. Plant lectins: occurrence, biochemistry, functions and applications. Glycoconj J. 2001 Aug;18:589-613.
64. Weiss A, Shields R, Newton M, Manger B, Imboden J. Ligand-receptor interactions required for commitment to the activation of the interleukin 2 gene. J Immunol. 1987 Apr;138:2169-76.
65. Lijnen P, Saavedra A, Petrov V. In vitro proliferative response of human peripheral blood mononuclear cells to concanavalin A. Clin Chim Acta. 1997 Aug;264:91-101.
66. Clénet ML, Gagnon F, Moratalla AC, Viel EC, Arbour N. Peripheral human CD4. Sci Rep. 2017 09;7:11612.
67. Overgaard NH, Jung JW, Steptoe RJ, Wells JW. CD4+/CD8+ double-positive T cells: more than just a developmental stage? J Leukoc Biol. 2015 Jan;97:31-8.
68. Nascimbeni M, Pol S, Saunier B. Distinct CD4+ CD8+ double-positive T cells in the blood and liver of patients during chronic hepatitis B and C. PLoS One. 2011;6:e20145.

69. Mucida D, Husain MM, Muroi S, van Wijk F, Shinnakasu R, Naoe Y, Reis BS, Huang Y, Lambolez F, et al. Transcriptional reprogramming of mature CD4$^+$ helper T cells generates distinct MHC class II-restricted cytotoxic T lymphocytes. Nat Immunol. 2013 Mar;14:281-9.
70. Luhtala M, Lassila O, Toivanen P, Vainio O. A novel peripheral CD4+ CD8+ T cell population: inheritance of CD8alpha expression on CD4+ T cells. Eur J Immunol. 1997 Jan;27:189-93.
71. Sullivan YB, Landay AL, Zack JA, Kitchen SG, Al-Harthi L. Upregulation of CD4 on CD8+ T cells: CD4dimCD8bright T cells constitute an activated phenotype of CD8+ T cells. Immunology. 2001 Jul;103:270-80.
72. van der Weerd K, Dik WA, Schrijver B, Schweitzer DH, Langerak AW, Drexhage HA, Kiewiet RM, van Aken MO, van Huisstede A, et al. Morbidly obese human subjects have increased peripheral blood CD4+ T cells with skewing toward a Treg- and Th2-dominated phenotype. Diabetes. 2012 Feb;61:401-8.
73. Wagner NM, Brandhorst G, Czepluch F, Lankeit M, Eberle C, Herzberg S, Faustin V, Riggert J, Oellerich M, et al. Circulating regulatory T cells are reduced in obesity and may identify subjects at increased metabolic and cardiovascular risk. Obesity (Silver Spring). 2013 Mar;21:461-8.
74. Agabiti-Rosei C, Trapletti V, Piantoni S, Airò P, Tincani A, De Ciuceis C, Rossini C, Mittempergher F, Titi A, et al. Decreased circulating T regulatory lymphocytes in obese patients undergoing bariatric surgery. PLoS One. 2018;13:e0197178.
75. Eller K, Kirsch A, Wolf AM, Sopper S, Tagwerker A, Stanzl U, Wolf D, Patsch W, Rosenkranz AR, Eller P. Potential role of regulatory T cells in reversing obesity-linked insulin resistance and diabetic nephropathy. Diabetes. 2011 Nov;60:2954-62.
76. Taams LS, Palmer DB, Akbar AN, Robinson DS, Brown Z, Hawrylowicz CM. Regulatory T cells in human disease and their potential for therapeutic manipulation. Immunology. 2006 May;118:1-9.
77. Laue T, Wrann CD, Hoffmann-Castendiek B, Pietsch D, Hübner L, Kielstein H. Altered NK cell function in obese healthy humans. BMC Obes. 2015;2:1.
78. Frasca D, Diaz A, Romero M, Thaller S, Blomberg BB. Metabolic requirements of human pro-inflammatory B cells in aging and obesity. PLoS One. 2019;14:e0219545.
79. Kosaraju R, Guesdon W, Crouch MJ, Teague HL, Sullivan EM, Karlsson EA, Schultz-Cherry S, Gowdy K, Bridges LC, et al. B Cell Activity Is Impaired in Human and Mouse Obesity and Is Responsive to an Essential Fatty Acid upon Murine Influenza Infection. J Immunol. 2017 06;198:4738-52.
80. Parmigiani A, Alcaide ML, Freguja R, Pallikkuth S, Frasca D, Fischl MA, Pahwa S. Impaired antibody response to influenza vaccine in HIV-infected and uninfected aging women is associated with immune activation and inflammation. PLoS One. 2013;8:e79816.
81. Frasca D, Diaz A, Romero M, Landin AM, Blomberg BB. High TNF-α levels in resting B cells negatively correlate with their response. Exp Gerontol. 2014 Jun;54:116-22.
82. Frasca D, Ferracci F, Diaz A, Romero M, Lechner S, Blomberg BB. Obesity decreases B cell responses in young and elderly individuals. Obesity (Silver Spring). 2016 Mar;24:615-25.
83. Friedrich K, Sommer M, Strobel S, Thrum S, Blüher M, Wagner U, Rossol M. Perturbation of the Monocyte Compartment in Human Obesity. Front Immunol. 2019;10:1874.
84. Rogacev KS, Ulrich C, Blömer L, Hornof F, Oster K, Ziegelin M, Cremers B, Grenner Y, Geisel J, et al. Monocyte heterogeneity in obesity and subclinical atherosclerosis. Eur Heart J. 2010 Feb;31:369-76.

85. Mattos RT, Medeiros NI, Menezes CA, Fares RC, Franco EP, Dutra WO, Rios-Santos F, Correa-Oliveira R, Gomes JA. Chronic Low-Grade Inflammation in Childhood Obesity Is Associated with Decreased IL-10 Expression by Monocyte Subsets. PLoS One. 2016;11:e0168610.
86. Poitou C, Dalmas E, Renovato M, Benhamo V, Hajduch F, Abdennour M, Kahn JF, Veyrie N, Rizkalla S, et al. CD14dimCD16+ and CD14+CD16+ monocytes in obesity and during weight loss: relationships with fat mass and subclinical atherosclerosis. Arterioscler Thromb Vasc Biol. 2011 Oct;31:2322-30.
87. Schipper HS, Nuboer R, Prop S, van den Ham HJ, de Boer FK, Kesmir Ç, Mombers IMH, van Bekkum KA, Woudstra J, et al. Systemic inflammation in childhood obesity: circulating inflammatory mediators and activated CD14++ monocytes. Diabetologia. 2012 Oct;55:2800-10.
88. Smith AG, Sheridan PA, Harp JB, Beck MA. Diet-induced obese mice have increased mortality and altered immune responses when infected with influenza virus. J Nutr. 2007 May;137:1236-43.
89. Lynch LA, O'Connell JM, Kwasnik AK, Cawood TJ, O'Farrelly C, O'Shea DB. Are natural killer cells protecting the metabolically healthy obese patient? Obesity (Silver Spring). 2009 Mar;17:601-5.
90. Bähr I, Spielmann J, Quandt D, Kielstein H. Obesity-Associated Alterations of Natural Killer Cells and Immunosurveillance of Cancer. Front Immunol. 2020;11:245.

CHAPTER 5: SUMMARY AND FUTURE DIRECTONS

The prevalence of obesity is continuing to rise worldwide. In the United States, current estimates show that roughly 40% of adults and 20% of children (ages 2-19 years old) are considered obese. Obese individuals are at greater risk for chronic and infectious diseases due to underlying systemic chronic inflammation and premature immunosenescence. Lifestyle risk factors such as obesity, poor diet, and gut dysbiosis can inhibit the resolution of acute inflammation, in turn promoting the development of systemic chronic inflammation and immunosenescence. However, total adiposity alone does not fully predict disease risk. Rather, adipose tissue distribution throughout the body is a more accurate estimator of disease susceptibility. Excessive visceral adiposity confers the greatest disease risk due to inherent depot differences, such as proximity to and a shared blood supply with the liver and gastrointestinal (GI) tract, as well as tissue metabolic and immunologic activity. Recent work highlights the considerable influence gut physiology has over local and systemic metabolic homeostasis. While the mechanisms that mediate this inter-organ crosstalk continue to be elucidated, several studies suggest that inflammation originating from the gut triggers these broad metabolic and immunologic changes found in obesity. Thus, it is critical to understand mechanisms which promote GI dysfunction and how these signals resonate to surrounding tissues.

The studies conducted as a part of this dissertation research examined 1) the relationship between mesenteric lymph nodes (MLNs) and GI inflammation on metabolic and immune outcomes, and 2) characterized immunologic changes associated with models of chronic inflammation. First, we tested the hypothesis that MLN dysfunction would contribute to

metabolic derangements associated with high-fat diet (HFD) induced obesity and that without functional MLNs obesity-associated disease reversal would not occur. Results from this study showed that MLN dysfunction, simulated by removal of the MLNs, in HFD-induced obese mice leads to metabolic and immune alterations through 1) the promotion of visceral adiposity and T cell infiltration, 2) impairment of insulin signaling within the liver, and 3) compromise of jejunal immune function. Additionally, that HFD-induced obesity leads to MLN fibrosis and is associated with systemic markers of metabolic and immune dysfunction, which were then rescued by Pirfenidone treatment. Finally, that Pirfenidone treatment does not fully restore the MLN restricted phenotype, supporting a critical role for the MLNs in the regulation of metabolic and immune homeostasis. Future studies should focus on elucidating mechanisms of crosstalk between the gut, liver, MAT, and MLNs, as well as investigating how these mechanisms affect metabolic homeostasis.

Next, we hypothesized that GI inflammation independent of diet and obesity would drive MLN dysfunction resulting in hepatic insulin resistance in low-fat diet (LFD) fed mice. Utilizing a chronic low-dose model of dextran sulfate sodium (DSS) induced GI inflammation, we found that DSS treated mice had a modest reduction in total body weight and MAT mass. As well as broad alterations in local (jejunum, ileum, MLNs, MAT, and liver) and peripheral (spleen) tissue immune cell populations and frequencies. This included immune cell infiltration within all tissues apart from the spleen, and perturbation of dendritic cell and T lymphocyte populations. We also found that these DSS-induced adaptations occurred without a concurrent change in glucose homeostasis. Further research is needed to extend the current study and elucidate mechanisms of GI inflammation-mediated metabolic dysfunction without the confounds of obesity and diet.

Lastly, utilizing peripheral blood mononuclear cells (PBMCs) from normal weight and obese adults we tested the hypothesis that PBMCs isolated from obese individuals would display a lower level of cell proliferation and cytokine secretion, as well as distinct expansion of immune cells upon acute ex vivo challenge within Concanavalin A (ConA) relative to their normal weight counterparts. Results from this study showed that PBMCs isolated from obese adults had a modest increase in cell proliferation and IFNγ secretion upon stimulation with ConA relative to their normal weight controls. Additionally, we found a distinct expansion of $CD4^+CD8^+$ T cells, $CD16^+$ monocytes, and NK cells within ConA stimulated PBMCs from obese adults. These results support an altered response of PBMCs within obese individuals and provide new insight into obesity-driven immune alterations. Future studies in a larger population of obese adults within a range of body mass indexes is warranted to verify and extend these preliminary findings.

Collectively, the studies from this dissertation research provide insight into the contribution of the MLNs in metabolic homeostasis. As well as, the impact of chronic inflammation on metabolic and immune function within pre-clinical and clinical models. Published data from our lab have demonstrated the impact of HFD-induced obesity on MLN function (1-3). The second chapter of this dissertation research provides new insights into the role of the MLNs in metabolic homeostasis within HFD-induced obese mice. While the third chapter questions the effect of GI inflammation on metabolic and immune function within non-obese, LFD fed mice. Finally, the fourth chapter supports and extends the body of knowledge by providing novel data on human immune function within obese adults who are otherwise free of disease.

In chapter 2, we found that MLN dysfunction, either due to surgical manipulation or obesity-induced fibrosis, promotes metabolic and immune dysfunction. We observed an increase in visceral adiposity and T cell infiltration, impairment of insulin signaling within the liver, and compromise of jejunal immune function within obese MLN restricted mice. Additionally, we found that HFD-induced obese mice had an increase in collagen deposition within the MLNs, which was associated with an increase of systemic markers of metabolic and immune dysfunction. However, Pirfenidone treatment was able to attenuate obesity-induced MLN fibrosis and improve markers of metabolic function and inflammation. Finally, we found that Pirfenidone treatment was unable to fully restore the MLN restricted phenotype in HFD-induced obese mice, supporting a critical role of the MLNs in metabolic homeostasis. Disruption to lymphatic vasculature integrity and flow coincide with an impairment of normal lymphatic function (4). Dysfunctional lymphatics are observed in and cause several diseases such as obesity and lymphedema—respectively (5). Features of lymphatic dysfunction include tissue fibrosis, susceptibility to infections, and accumulation of fat in the surrounding tissue (6-10). We now know that obesity actively contributes to lymphatic dysfunction (11-13), subsequently exacerbating metabolic impairments (12, 14, 15). Visceral adipose tissue accumulation and inflammation are associated with a reduction in hepatic insulin sensitivity (16-18). More recently, alterations in GI homeostasis are shown to incite and exacerbate metabolic dysfunction, including hepatic insulin resistance and visceral adipose tissue inflammation (19-22). While mechanisms that mediate this inter-organ crosstalk are incompletely understood, our results support a critical role of the MLNs in this process. This is substantiated by several studies which demonstrate the importance of MLNs in maintaining gut and mesenteric ‘visceral’ adipose depot homeostasis (23-29), and that MLN dysfunction is implicated in GI inflammation (30, 31).

Collectively, these results provide new insight into the contribution of the MLNs in metabolic homeostasis and their potential requirement for disease reversal.

GI inflammation is now strongly implicated in driving metabolic impairments associated with obesity (22, 32) and a poor diet (33-35). In chapter 3, we investigated the effect of chronic low-dose DSS-induced GI inflammation, independent of diet and obesity, on metabolic and immune function. We found that non-obese mice treated with DSS had a modest reduction in total body weight and MAT mass. Additionally, DSS treatment led to broad alterations in local (jejunum, ileum, MLNs, MAT, and liver) and peripheral (spleen) tissue immune cell populations and frequencies. This included immune cell infiltration within all tissues apart from the spleen, where we speculate that cells were recruited into peripheral tissues. As well as perturbation of dendritic cell and T lymphocyte populations. We also found that these DSS-induced adaptations occurred without a concurrent change in glucose homeostasis. The regulation of glucose is largely managed by the liver (36) and skeletal muscle (37). Glucose homeostasis is commonly perturbed in models of disease (38, 39) and is attributed in part to inflammation-mediated impairments in the insulin signaling cascade (40, 41). A hallmark of tissue inflammation is the recruitment and infiltration of immune cells (42). In support, insulin resistance within the liver and skeletal muscle are shown to coincide with immune cell accretion (43). However, we did not observe alterations in systemic glucose homeostasis despite a concomitant increase in immune cells within the liver. Thus, it is possible that the inflammatory burden produced in our chronic, low-dose model was insufficient to incite insulin resistance. Nevertheless, these results pose new questions regarding the level and type of inflammatory burden associated with metabolic dysfunction, as well as the biological relevance of observed cellular dynamics.

In chapter 4, we show the impact of obesity on immune function through the assessment of isolated PBMCs from otherwise healthy male and female donors challenged *ex vivo*. Our data highlight distinct obesity-induced alterations in the PBMC response to acute challenge, as well as emphasize the need for further work in exploring differences among the ranges of obesity and a more detailed characterization of the human peripheral compartment. Several studies demonstrate the broad health consequences associated with obesity such as immune dysfunction (44-46). As such, obesity is considered a high-risk group for chronic and infectious diseases (47-50). Nevertheless, findings on circulating immune cell frequencies within the obese population, as well as their clinical relevance are controversial. This emphasizes the need for further study and characterization among the ranges of obesity.

Collectively, the studies conducted in this dissertation research further our understanding of obesity and chronic inflammation within clinical and pre-clinical models. Although the number of studies examining obesity-associated disease pathophysiology in relation to the gut and MLNs has risen exponentially, there are still many unknowns. This is partly due to the limited sampling within human populations, as well as a lack of translation between pre-clinical and clinical findings. More importantly, characterization of the immune system is subject to great biologic and operator-related variability. Future studies from our lab could employ more detailed analytic approaches when studying disease processes, to help elucidate underlying mechanisms and more definitively answer scientific questions. In conclusion, the studies included in this dissertation research provide evidence in support of obesity-induced immune dysfunction. Future studies characterizing the functional differences in immune cell populations among the obese cohort will provide greater understanding of the relationship between obesity and immune function, which carries substantial public health implications.

REFERENCES

1. Magnuson AM, Regan DP, Fouts JK, Booth AD, Dow SW, Foster MT. Diet-induced obesity causes visceral, but not subcutaneous, lymph node hyperplasia via increases in specific immune cell populations. Cell Prolif. 2017 Oct;50.
2. Magnuson AM, Regan DP, Booth AD, Fouts JK, Solt CM, Hill JL, Dow SW, Foster MT. High-fat diet induced central adiposity (visceral fat) is associated with increased fibrosis and decreased immune cellularity of the mesenteric lymph node in mice. Eur J Nutr. 2019 Jun.
3. Solt CM, Hill JL, Vanderpool K, Foster MT. Obesity-induced immune dysfunction and immunosuppression: TEM observation of visceral and subcutaneous lymph node microarchitecture and immune cell interactions. Horm Mol Biol Clin Investig. 2019 May;39.
4. Escobedo N, Oliver G. The Lymphatic Vasculature: Its Role in Adipose Metabolism and Obesity. Cell Metab. 2017 Oct;26:598-609.
5. Rockson SG. Lymphedema. Am J Med. 2001 Mar;110:288-95.
6. Aschen S, Zampell JC, Elhadad S, Weitman E, De Brot M, Mehrara BJ. Regulation of adipogenesis by lymphatic fluid stasis: part II. Expression of adipose differentiation genes. Plast Reconstr Surg. 2012 Apr;129:838-47.
7. Brorson H. Liposuction in Lymphedema Treatment. J Reconstr Microsurg. 2016 Jan;32:56-65.
8. Witte MH, Bernas MJ, Martin CP, Witte CL. Lymphangiogenesis and lymphangiodysplasia: from molecular to clinical lymphology. Microsc Res Tech. 2001 Oct;55:122-45.
9. Tavakkolizadeh A, Wolfe KQ, Kangesu L. Cutaneous lymphatic malformation with secondary fat hypertrophy. Br J Plast Surg. 2001 Jun;54:367-9.
10. Wang Y, Oliver G. Current views on the function of the lymphatic vasculature in health and disease. Genes Dev. 2010 Oct;24:2115-26.
11. Weitman ES, Aschen SZ, Farias-Eisner G, Albano N, Cuzzone DA, Ghanta S, Zampell JC, Thorek D, Mehrara BJ. Obesity impairs lymphatic fluid transport and dendritic cell migration to lymph nodes. PLoS One. 2013;8:e70703.
12. Arngrim N, Simonsen L, Holst JJ, Bülow J. Reduced adipose tissue lymphatic drainage of macromolecules in obese subjects: a possible link between obesity and local tissue inflammation? Int J Obes (Lond). 2013 May;37:748-50.
13. Savetsky IL, Torrisi JS, Cuzzone DA, Ghanta S, Albano NJ, Gardenier JC, Joseph WJ, Mehrara BJ. Obesity increases inflammation and impairs lymphatic function in a mouse model of lymphedema. Am J Physiol Heart Circ Physiol. 2014 Jul;307:H165-72.
14. Rutkowski JM, Markhus CE, Gyenge CC, Alitalo K, Wiig H, Swartz MA. Dermal collagen and lipid deposition correlate with tissue swelling and hydraulic conductivity in murine primary lymphedema. Am J Pathol. 2010 Mar;176:1122-9.
15. Lim HY, Rutkowski JM, Helft J, Reddy ST, Swartz MA, Randolph GJ, Angeli V. Hypercholesterolemic mice exhibit lymphatic vessel dysfunction and degeneration. Am J Pathol. 2009 Sep;175:1328-37.

16. Wiedemann MS, Wueest S, Item F, Schoenle EJ, Konrad D. Adipose tissue inflammation contributes to short-term high-fat diet-induced hepatic insulin resistance. Am J Physiol Endocrinol Metab. 2013 Aug;305:E388-95.
17. Rytka JM, Wueest S, Schoenle EJ, Konrad D. The portal theory supported by venous drainage-selective fat transplantation. Diabetes. 2011 Jan;60:56-63.
18. Kabir M, Catalano KJ, Ananthnarayan S, Kim SP, Van Citters GW, Dea MK, Bergman RN. Molecular evidence supporting the portal theory: a causative link between visceral adiposity and hepatic insulin resistance. Am J Physiol Endocrinol Metab. 2005 Feb;288:E454-61.
19. Konrad D, Wueest S. The gut-adipose-liver axis in the metabolic syndrome. Physiology (Bethesda). 2014 Sep;29:304-13.
20. Munukka E, Pekkala S, Wiklund P, Rasool O, Borra R, Kong L, Ojanen X, Cheng SM, Roos C, et al. Gut-adipose tissue axis in hepatic fat accumulation in humans. J Hepatol. 2014 Jul;61:132-8.
21. Ding S, Lund PK. Role of intestinal inflammation as an early event in obesity and insulin resistance. Curr Opin Clin Nutr Metab Care. 2011 Jul;14:328-33.
22. Lam YY, Mitchell AJ, Holmes AJ, Denyer GS, Gummesson A, Caterson ID, Hunt NH, Storlien LH. Role of the gut in visceral fat inflammation and metabolic disorders. Obesity (Silver Spring). 2011 Nov;19:2113-20.
23. Amar J, Chabo C, Waget A, Klopp P, Vachoux C, Bermúdez-Humarán LG, Smirnova N, Bergé M, Sulpice T, et al. Intestinal mucosal adherence and translocation of commensal bacteria at the early onset of type 2 diabetes: molecular mechanisms and probiotic treatment. EMBO Mol Med. 2011 Sep;3:559-72.
24. Deitch EA. Bacterial translocation or lymphatic drainage of toxic products from the gut: what is important in human beings? Surgery. 2002 Mar;131:241-4.
25. Dixon JB. Lymphatic lipid transport: sewer or subway? Trends Endocrinol Metab. 2010 Aug;21:480-7.
26. Lynch PM, Delano FA, Schmid-Schönbein GW. The primary valves in the initial lymphatics during inflammation. Lymphat Res Biol. 2007;5:3-10.
27. Macpherson AJ, Uhr T. Induction of protective IgA by intestinal dendritic cells carrying commensal bacteria. Science. 2004 Mar;303:1662-5.
28. Peyrin-Biroulet L, Gonzalez F, Dubuquoy L, Rousseaux C, Dubuquoy C, Decourcelle C, Saudemont A, Tachon M, Béclin E, et al. Mesenteric fat as a source of C reactive protein and as a target for bacterial translocation in Crohn's disease. Gut. 2012 Jan;61:78-85.
29. Sansonetti PJ, Di Santo JP. Debugging how bacteria manipulate the immune response. Immunity. 2007 Feb;26:149-61.
30. Rehal S, von der Weid PY. TNFΔARE Mice Display Abnormal Lymphatics and Develop Tertiary Lymphoid Organs in the Mesentery. Am J Pathol. 2017 Apr;187:798-807.
31. Wu TF, Carati CJ, Macnaughton WK, von der Weid PY. Contractile activity of lymphatic vessels is altered in the TNBS model of guinea pig ileitis. Am J Physiol Gastrointest Liver Physiol. 2006 Oct;291:G566-74.
32. Winer DA, Luck H, Tsai S, Winer S. The Intestinal Immune System in Obesity and Insulin Resistance. Cell Metab. 2016 Mar;23:413-26.
33. Pendyala S, Walker JM, Holt PR. A high-fat diet is associated with endotoxemia that originates from the gut. Gastroenterology. 2012 May;142:1100-1.e2.
34. Ji Y, Sakata Y, Tso P. Nutrient-induced inflammation in the intestine. Curr Opin Clin Nutr Metab Care. 2011 Jul;14:315-21.

35. Araújo JR, Tomas J, Brenner C, Sansonetti PJ. Impact of high-fat diet on the intestinal microbiota and small intestinal physiology before and after the onset of obesity. Biochimie. 2017 Oct;141:97-106.
36. Santoleri D, Titchenell PM. Resolving the Paradox of Hepatic Insulin Resistance. Cell Mol Gastroenterol Hepatol. 2019;7:447-56.
37. Buczkowska EO, Jarosz-Chobot P. [Insulin effect on metabolism in skeletal muscles and the role of muscles in regulation of glucose homeostasis]. Przegl Lek. 2001;58:782-7.
38. Sun Q, Li J, Gao F. New insights into insulin: The anti-inflammatory effect and its clinical relevance. World J Diabetes. 2014 Apr;5:89-96.
39. de Rekeneire N, Peila R, Ding J, Colbert LH, Visser M, Shorr RI, Kritchevsky SB, Kuller LH, Strotmeyer ES, et al. Diabetes, hyperglycemia, and inflammation in older individuals: the health, aging and body composition study. Diabetes Care. 2006 Aug;29:1902-8.
40. Petersen MC, Shulman GI. Mechanisms of Insulin Action and Insulin Resistance. Physiol Rev. 2018 10;98:2133-223.
41. de Luca C, Olefsky JM. Inflammation and insulin resistance. FEBS Lett. 2008 Jan;582:97-105.
42. Chen L, Deng H, Cui H, Fang J, Zuo Z, Deng J, Li Y, Wang X, Zhao L. Inflammatory responses and inflammation-associated diseases in organs. Oncotarget. 2018 Jan;9:7204-18.
43. Liu J, Liu Z. Muscle Insulin Resistance and the Inflamed Microvasculature: Fire from Within. Int J Mol Sci. 2019 Jan;20.
44. Louie JK, Acosta M, Samuel MC, Schechter R, Vugia DJ, Harriman K, Matyas BT, Group CPHNW. A novel risk factor for a novel virus: obesity and 2009 pandemic influenza A (H1N1). Clin Infect Dis. 2011 Feb;52:301-12.
45. Sheridan PA, Paich HA, Handy J, Karlsson EA, Hudgens MG, Sammon AB, Holland LA, Weir S, Noah TL, Beck MA. Obesity is associated with impaired immune response to influenza vaccination in humans. Int J Obes (Lond). 2012 Aug;36:1072-7.
46. Paich HA, Sheridan PA, Handy J, Karlsson EA, Schultz-Cherry S, Hudgens MG, Noah TL, Weir SS, Beck MA. Overweight and obese adult humans have a defective cellular immune response to pandemic H1N1 influenza A virus. Obesity (Silver Spring). 2013 Nov;21:2377-86.
47. O'Neill S, O'Driscoll L. Metabolic syndrome: a closer look at the growing epidemic and its associated pathologies. Obes Rev. 2015 Jan;16:1-12.
48. De Pergola G, Silvestris F. Obesity as a major risk factor for cancer. J Obes. 2013;2013:291546.
49. Guarner V, Rubio-Ruiz ME. Low-grade systemic inflammation connects aging, metabolic syndrome and cardiovascular disease. Interdiscip Top Gerontol. 2015;40:99-106.
50. Furman D, Campisi J, Verdin E, Carrera-Bastos P, Targ S, Franceschi C, Ferrucci L, Gilroy DW, Fasano A, et al. Chronic inflammation in the etiology of disease across the life span. Nat Med. 2019 12;25:1822-32.